

Supersymmetry in a Sector of Higgsless Electroweak Symmetry Breaking

Dissertation zur Erlangung des
naturwissenschaftlichen Doktorgrades
der Julius-Maximilians-Universität Würzburg



vorgelegt von

Alexander Karl Knochel
aus Gleisweiler

Würzburg, 2009

Eingereicht am: 01.04.2009

bei der Fakultät für Physik und Astronomie

1. Gutachter: _____

2. Gutachter: _____

3. Gutachter: _____

der Dissertation

1. Prüfer: _____

2. Prüfer: _____

3. Prüfer: _____

im Promotionskolloquium

Tag des Promotionskolloquiums: _____

We wish to find the truth, no matter where it lies. But to find the truth we need imagination and skepticism both. We will not be afraid to speculate, but we will be careful to distinguish speculation from fact.

- *Carl Sagan*

Zusammenfassung

Der Einsatz von gekrümmten Raumzeithintergründen mit Extradimensionen, vor allem des AdS_5 , hat seit der viel beachteten Arbeit von Randall/Sundrum (RS) vor 10 Jahren, insbesondere in Verbindung mit der AdS/CFT -Korrespondenz, sehr an Popularität gewonnen und gilt seither als eine der fruchtbarsten neuen Ideen bei der Suche nach Modellen jenseits des Standardmodells (SM). Dieser Ansatz brachte nicht nur frische Einsichten in die Physik stark wechselwirkender Feldtheorien, die zuvor störungstheoretischen Methoden verschlossen waren, sondern schaffte auch einen faszinierenden neuen Zusammenhang zwischen phänomenologischen Modellen an der TeV-Skala und der Gravitation. Dies hat unter anderem auch das Interesse an Modellen der elektroschwachen Symmetriebrechung ohne physikalische Skalarfelder (“Higgslose Modelle”) in diesem Kontext mit dem Ziel neu aufleben lassen, Alternativen zu dem im Standardmodell der Teilchenphysik enthaltenen Higgs-Mechanismus zu finden. Bei der Umsetzung dieser Ideen lag das Hauptaugenmerk meisst auf potentiellen neuen Beiträgen zu elektroschwachen Präzisionsobservablen. Gleichzeitig gibt es jedoch sehr starke astrophysikalische Indizien dafür, dass die Antwort auf die Frage nach dem Ursprung der beobachteten dunklen Materie in Teilchenmodellen jenseits des Standardmodells zu finden ist. Die Natur der elektroschwachen Symmetriebrechung und der dunklen Materie gehören zu den zentralen Fragen, deren Beantwortung dank aktueller und anstehender Experimente z.B. an Beschleunigern wie dem Tevatron, wie auch in naher Zukunft am LHC, in greifbare Nähe rückt. Diese Situation legt nahe, dass neue Szenarien jenseits des Standardmodells beide Fragestellungen gleichermaßen thematisieren sollten. In der vorliegenden Arbeit untersuchen wir die phänomenologischen Implikationen einer Erweiterung Higgsloser Modelle in 5D um Supersymmetrie mit erhaltener R -Parität im elektroschwachen Symmetriebrechungssektor. Das Ziel war, eine möglichst einfache Erweiterung zu finden, die ein realistisches leichtes Spektrum aufweist und gleichzeitig einen guten Kandidaten für kalte dunkle Materie enthält, ohne zu viele freie Parameter einzuführen. Um dies zu bewerkstelligen, bot sich der gleiche Mechanismus an, der bereits für die Brechung der Eichsymmetrien zum Einsatz kommt, nämlich die Brechung durch Randbedingungen. Während Supersymmetrie in 5D vier Superladungen beinhaltet und somit eng mit $\mathcal{N} = 2$ Supersymmetrie in 4D verwandt ist, wird allein durch den RS-Hintergrund die Hälfte der Symmetrien gebrochen, so dass nach der Kaluza-Klein-Reduktion lediglich eine erhaltene Supersymmetrie verbleibt. Davon ausgehend war das einfachste gangbare Sze-

nario, die Brechung der verbleibenden Generatoren effektiv durch Randbedingungen auf der UV-Brane der RS-Raumzeit zu beschreiben. Obwohl hierdurch Teile des leichten SUSY-Spektrums, insb. die Superpartner der Fermionen, ausprojiziert werden, verbleibt die reichhaltige Phänomenologie von vollständigen $\mathcal{N} = 2$ -Multiplets im Kaluza-Klein-Sektor. Das leichte erweiterte Spektrum besteht aus den Superpartnern der elektroschwachen Eichbosonen, die Massen um $\mathcal{O}(100 \text{ GeV})$ erhalten. Die Neutralinos als Masseneigenzustände des neutralen Bino-Wino-Sektors sind automatisch die leichtesten supersymmetrischen Teilchen (LSP) und damit natürliche Kandidaten für kalte dunkle Materie. Ihre Reliktdichte kann ohne exzessive Feineinstellung von Parametern in Einklang mit Beobachtungen gebracht werden. Das Modell sagt somit eine leichte NLSP-Masse im Bereich $m_{\chi^+} \approx 100 \dots 110 \text{ GeV}$ und einen LSP bei etwa $m_{\chi} \approx 90 \text{ GeV}$ voraus. Am LHC hat der nicht-supersymmetrische Teilcheninhalt des Modells weitestgehend die gleichen phänomenologischen Konsequenzen wie sie bereits von Studien Higgsloser Modelle bekannt sind. Wir haben uns daher auf die Produktion des LSP und NLSP am LHC als typische Signatur des erweiterten Modells konzentriert, und insbesondere Monte-Carlo-Simulationen mit O'Mega/WHIZARD zur Beobachtung von fehlender transversaler Energie (\cancel{p}_T) in Assoziation mit schweren Quarks durchgeführt. Wir diskutieren geeignete Schnitte auf Winkel, invariante Massen und Impulse, und erhalten Hadronische Produktionsquerschnitte von $\sigma > 100 \text{ fb}$ bei 14 TeV, welche charakteristische \cancel{p}_T -Verteilungen im $\chi\chi t\bar{t}$ Endzustand aufweisen. Der Nachweis über die Produktion von b -Paaren erweist sich als schwieriger. Unsere Ergebnisse legen nahe, dass die Entdeckung dieses Typs von dunkler Materie in Higgslosen Modellen am LHC über fehlende transversale Energie mit wenigen fb^{-1} bei 14 TeV möglich ist, insofern eine zuverlässige Identifikation schwerer Quarks gegeben ist.

Abstract

Since its popularization due to Randall and Sundrum (RS) one decade ago, and in connection with the *AdS/CFT* correspondence in particular, 5D warped background spacetime has been one of the most fruitful new ideas in physics beyond the standard model (SM), leading to new insights into symmetry breaking and the properties of strongly interacting theories inaccessible to direct perturbative calculations, while at the same time relating gravity to phenomenological model building. This has, among others, led to a renewed interest in models of electroweak symmetry breaking without physical scalar fields in the guise of so-called 'warped higgsless' models, which could provide an alternative to the famed Higgs mechanism of electroweak symmetry breaking which is part of the Standard Model of particle physics. However, little emphasis was put on reconciling these models with the strong evidence from astrophysical observations that one or several new, as yet unknown, stable particle species exist which form the cold dark matter content of the universe. The nature of dark matter and electroweak symmetry breaking are among the most prominent puzzles subject to experimental scrutiny at the Tevatron, direct search experiments, and in the near future at the LHC, which compels us to believe that both issues should be addressed together in any alternative scenario beyond the Standard Model. In this thesis we have investigated phenomenological implications which arise for cosmology and collider physics when the electroweak symmetry breaking sector of warped higgsless models is extended to include warped supersymmetry with conserved R parity. The goal was to find the simplest supersymmetric extension of these models which still has a realistic light spectrum including a viable dark matter candidate. To accomplish this, we have used the same mechanism which is already at work for symmetry breaking in the electroweak sector to break supersymmetry as well, namely symmetry breaking by boundary conditions. While supersymmetry in five dimensions contains four supercharges and is therefore directly related to 4D $\mathcal{N} = 2$ supersymmetry, half of them are broken by the background leaving us with ordinary $\mathcal{N} = 1$ theory in the massless sector after Kaluza-Klein expansion. We thus use boundary conditions to model the effects of a breaking mechanism for the remaining two supercharges. The simplest viable scenario to investigate is a supersymmetric bulk and IR brane without supersymmetry on the UV brane. Even though parts of the light spectrum are effectively projected out by this mechanism, we retain the rich phenomenology of complete $\mathcal{N} = 2$ supermultiplets in the Kaluza-Klein sector. While the light supersymmet-

ric spectrum consists of electroweak gauginos which get their $\mathcal{O}(100 \text{ GeV})$ masses from IR brane electroweak symmetry breaking, the light gluinos and squarks are projected out on the UV brane. The neutralinos, as mass eigenstates of the neutral bino-wino sector, are automatically the lightest gauginos, making them LSP dark matter candidates with a relic density that can be brought to agreement with WMAP measurements without extensive tuning of parameters. For chargino masses close to the experimental lower bounds at around $m_{\chi^+} \approx 100 \dots 110 \text{ GeV}$, the dark matter relic density points to LSP masses of around $m_{\chi} \approx 90 \text{ GeV}$. At the LHC, the standard particle content of our model shares most of the key features of known warped higgsless models. We have performed Monte Carlo simulations of warped higgsless LSP and NLSP production at a benchmark point using O'Mega/WHIZARD, concentrating on \cancel{p}_T in association with third generation quarks. After background reduction cuts on the quark momenta and angles, we get hadronic cross sections of $\sigma > 100 \text{ fb}$ at 14 TeV with characteristic \cancel{p}_T distributions for $\chi\chi t\bar{t}$ final states, while the final states with $b\bar{b}$ pairs have much lower event rates and shapes which are hard to discern in experiments. Our results suggest that the discovery of warped higgsless LSP dark matter at the LHC via missing energy is within reach for the first few fb^{-1} at 14 TeV if b and in particular t identification is reliable.

Contents

1	Introduction	1
2	Extra Dimensions	5
2.1	A Short Introduction to Quantum Fields in Extra Dimensions . . .	5
2.1.1	Motivation	5
2.1.2	The Kaluza-Klein Approach for a Scalar Field	7
2.1.3	An Algorithm for Solving KK Towers with Many Fields . .	11
2.1.4	Gauge Theory	13
2.1.5	A Note on Nonrenormalizability	14
2.2	The Randall/Sundrum Scenario and Warped Space	15
2.2.1	Christoffel Symbols and Spin Connections	16
2.3	Scalars, Spinors and Gauge Fields in Warped Space	17
2.3.1	Scalars	17
2.3.2	Spinors	17
2.3.3	Nonabelian Gauge Theory in Warped Space	19
2.3.4	The Impact of UV and IR Boundary Conditions	21
3	Higgsless Electroweak Symmetry Breaking	24
3.1	Symmetries, Unitarity and Boundary Conditions	25
3.1.1	Perturbative Unitarity and Massive Vector Bosons	25
3.2	Warped Higgsless Models	26
3.3	Why do We Need to Extend Higgsless Models	32
4	Supersymmetry in Warped Space	34
4.1	Killing Spinors and Global SUSY in Warped Space	34
4.2	Formulating Warped Supersymmetry Using 4D $\mathcal{N} = 1$ Superfields	36
4.3	Boundary Conditions for Supersymmetry	41
5	A Toy Model: Warped sQED	43
5.1	The Supersymmetric Spectrum	43
5.2	A Broken Spectrum	45
5.3	Effective Couplings	46

6	Building the Extended Higgsless Model	48
6.1	The Superfield Content	48
6.2	Supersymmetric Boundary Conditions and Spectrum	49
6.3	The Action in 4D Fields	50
6.3.1	Chargino Interactions with Matter	50
6.3.2	Neutralino Interactions with Matter	53
6.3.3	Gluino Interactions with Matter	54
6.3.4	The Strong Quark Yukawa Coupling	54
6.3.5	The Gluino Yukawa Interaction	55
6.3.6	The Strong Squark Gauge Scalar Coupling	55
6.3.7	The Electroweak Matter Gauge Coupling	56
6.3.8	The Strong Quark Gauge Coupling	56
6.3.9	The Gaugino Charged Current Interaction	57
6.3.10	The Gaugino Neutral Current Interaction	57
7	Breaking Supersymmetry	58
7.1	Supersymmetry Breaking by Boundary Conditions	59
7.1.1	Gauginos	59
7.1.2	Scalars	61
7.1.3	Gravitinos	62
7.2	A Benchmark Point	64
7.2.1	The Spectrum	64
8	Phenomenology	67
8.1	General Features	67
8.2	Tree Level Contributions to Precision Observables	68
8.3	The LSP and its Relic Density	71
8.4	Properties of the Physical Scalars	75
8.4.1	Yukawa Couplings	76
8.4.2	Mass Corrections from UV Brane Breaking	78
8.5	Decays of Heavy Resonances	79
8.6	Production of the LSP	83
8.6.1	Heavy Quarks and Missing Energy at the LHC	83
8.6.2	Simulation of Warped Higgsless LSP Production at the LHC	86
8.6.3	Production of $t\bar{t} + \cancel{E}_T$	89
8.6.4	Production of $b\bar{b} + \cancel{E}_T$	95
8.6.5	Production of the NLSPs	96
8.7	Discussion and Further Issues	97
9	Conclusions	105
A	Conventions	108
A.1	Coordinate Systems and Lorentz Structure	108
A.2	Overlap Integrals for Effective Coupling Constants	110

B	The Action of 5D SYM + Matter in 5D Component Fields	112
B.1	Derivation	112
B.1.1	Integrating out the Auxiliary Fields	114
B.1.2	Many Flavors	116
B.2	Summary of the 5D Onshell Action	117
B.2.1	Action from the Gauge Superfields	117
B.2.2	Interaction with Matter	117
B.2.3	Matter Coupling to the Chiral Part of the Vector	118
B.2.4	The F Term	118
B.2.5	The Vector F Term	118
B.2.6	The D Term	119
C	Boundary Conditions and Linear Algebra	120
D	Useful Properties of the Warped KK expansion	123
D.1	Remarks about Majorana Spinors	125
E	Implementation of the Model	130
E.1	Fortran/Mathematica	130
E.2	O'Mega/WHIZARD	132
E.2.1	O'Mega	132
E.2.2	WHIZARD	135
E.3	FeynArts/FormCalc	137
E.4	FORM	140

Chapter 1

Introduction

As the Large Hadron Collider (LHC) at CERN will commence operation in 2009, some of the most pressing questions in fundamental physics that have arisen during the past decades might finally be answered as more and more data will be collected by the associated experiments in the months and years to come. Two of them in particular, ATLAS and CMS, have the potential to either vindicate or bring to an end the decades-long rule of the so-called Electroweak Standard Model of particle physics (SM) and the standard Higgs mechanism of electroweak symmetry breaking employed therein as the favoured model of fundamental particle interactions. The SM has earned this status through three decades of astonishing experimental successes which range from discoveries of theoretically predicted particles (most recently the τ neutrino in 2000 at Fermilab) to successful non-trivial precision tests at the LEP experiments and B factories among others. Despite all this, we now know that the picture of fundamental interactions as described by the SM is incomplete, inviting theorists to speculate about extensions or alternatives.

The most obvious shortcoming of the SM is the complete lack of an explanation for the lion's share of the matter in the universe dubbed *dark matter* (DM) which, according to the combined evidence of observations of the cosmological microwave background and direct observations of gravitational lensing, is most readily explained by the presence of one or several species of massive particles permeating the cosmos at nonrelativistic speeds which neither carry electrical charge nor participate in the strong interaction and, most importantly, must be stable on cosmological time scales. Indeed, recent results of the WMAP experiment confirm that nonrelativistic DM makes up roughly 20% of the energy density of the universe, as compared to ordinary baryonic matter such as atoms and their nuclei which contributes about 5%. The remaining $\approx 70\%$ of the energy density appears to have the equation of state of vacuum energy and thus raises deep questions about quantum field theory and gravity in its own right.

In contrast, on the side of yet to be verified predictions, the Higgs boson is the last and only particle species predicted by the SM which has so far eluded experimental detection, and has therefore become one of the central topics to be addressed at the LHC, along with precision measurements for example of mesons and the

top quark, which are the basis for a deeper understanding of the structure of flavour and symmetry breaking. One should keep in mind that the version of the Higgs mechanism for electroweak symmetry breaking used in the SM is not unique but merely the simplest in a whole family of models. It is minimal in the sense that it, as far as we know today, represents the smallest possible particle content required to achieve electroweak symmetry breaking in a way that is compatible with experiments while at the same time being renormalizable, meaning that the model can, even after the inclusion of quantum corrections, be parametrized completely using a finite set of input parameters. The fields it introduces to do the job are one physical Higgs boson whose theoretical significance will be discussed in more detail later, and three unphysical “would-be” Goldstone bosons needed to obtain the three currently known massive vector bosons W^+ , W^- and Z .

Apart from the absence of evidence for Higgs bosons and the lack of DM candidates in the SM, there is another theoretical reason why alternatives to the minimal Higgs mechanism are considered, namely the hierarchy problem. It can be stated as follows: defining the SM with a weak scale ($m_H < \text{TeV}$) Higgs boson via a renormalization prescription is unproblematic. However, as soon as the SM is to be embedded in a larger theory involving higher scales (for example quantum gravity), quantum corrections of the Higgs potential will include the contributions up to this scale. Unfortunately, the SM contributions to the Higgs self energy are quadratically divergent in the cutoff scale, leading to a natural¹ Higgs mass of $m_H \approx 10^{19}$ GeV which can only be brought down to the theoretically acceptable sub-TeV scale by introducing a counterterm which has to be dialed to many digits accuracy in order to cancel this huge mass shift. This is very unappealing and compels many theorists to believe that some mechanism might set in not too far above currently observable energies to tame this quadratic divergence, the classic (and to date still the only renormalizable) example being supersymmetry (SUSY), or the composite Higgs and little Higgs models. A yet more radical approach leads us to abandon the notion of symmetry breaking from a physical scalar Higgs particle - fundamental or composite - altogether while introducing vector resonances to unitarize scattering amplitudes in its stead. Historically, such models were already proposed only a few years after the introduction of the SM. In this class of models a new strong interaction, called Technicolor (TC), effects EWSB in analogy to chiral symmetry breaking in QCD, but at the TEV scale. While they do a good job giving the W^\pm and Z their masses, it turned out to be much more challenging to implement fermion masses, in particular for the third generation of quarks. In order to generate these masses, the twelve known fermions had to participate in the new strong interaction (extended Technicolor or ETC), introducing severe flavour changing neutral currents and large corrections to LEP precision observables. Even though progress has been made since the first introduction of TC and ETC, for example by considering different choices of representations for the fermions, these models remain strongly coupled and thus uncalculable in perturbation theory.

¹if, for example, the Planck scale is assumed to be the cutoff scale where new physics appears to provide a consistent completion of the SM at high energies

One particularly fruitful new approach was developed during the past 5 years which has led to a renewed interest in “higgsless” models, namely electroweak symmetry breaking (EWSB) in extra dimensions, and in particular in a slice of AdS_5 (“warped space”). Warped EWSB has all the properties to be a dual description of Technicolor in the sense of the AdS/CFT correspondence, and even reproduces some of the problems mentioned above. However, it has two great advantages which make it worthwhile to consider as an alternative to the standard Higgs mechanism: The 5D picture is weakly coupled well above LHC energies and valid beyond the perturbative unitarity cutoff of the SM in the limit $m_H \rightarrow \infty$ which is at around 1 . . . 1.5 TeV. They can therefore be said to provide a weakly coupled description of the symmetry breaking physics. On the other hand, properties and parameters which have before been hard to control, such as the scaling behaviour of operators, now become accessible through mass parameters and boundary terms of the extra dimensional gauge theory. By virtue of appropriate fermion representations under the 5D gauge theory corresponding to global symmetries of the 4D theory, and slight tuning of the 5D mass parameters, the first realistic higgsless models could be constructed. That is, they are realistic up to their lack of DM, and it is the main subject of this work to construct a well-motivated extension to provide them with a candidate particle which exhibits the right properties to account for the missing matter density in the universe that so far went unexplained.

There are many ways to extend the particle spectrum of any model, and we would therefore like to use a construction principle which is at the same time predictive and well motivated. As we will explain in the chapter on symmetry breaking, the well-known mechanism of Kaluza-Klein parity which is employed to generate stable particles in so-called models of “Universal Extra Dimensions” (UED), is not available in the warped higgsless setting. We instead consider a supersymmetric extension of higgsless models in a slice of AdS_5 with R parity, and show how the boundary conditions in the extra dimension can be used to obtain a realistic sparticle spectrum and a viable DM candidate without additional fine tuning of input parameters. Many of the features of the extended model are imposed by 5D SUSY, leading to several interesting predictions concerning its low energy phenomenology, including the nature of DM and its signatures at the LHC.

This thesis is structured as follows: In the second chapter we give a general introduction to field theory in extra dimensions and spend some time on the technical details of assigning boundary conditions and boundary operators, calculating the spectrum and the treatment of gauge theories. We furthermore present the concept of warped space, discuss how fields of different spin behave in a slice of AdS_5 , and present the action of Yang-Mills theory. The third chapter is devoted to higgsless electroweak symmetry breaking. In this context, the notion of perturbative unitarity is introduced, and the full model of higgsless electroweak symmetry breaking in warped space is presented upon which the following work will be based. The fourth chapter provides some theoretical background which is necessary to formulate supersymmetric theories in AdS_5 , in particular we discuss

a useful formalism using $\mathcal{N} = 1$ superfields in $D > 4$. In the fifth chapter we illustrate its use with an abelian toy model. The chapters six and seven connect the different concepts which were introduced in the preceding chapters and present in detail the construction of a warped supersymmetric higgsless model, the resulting particle spectrum and their interactions, first for the $\mathcal{N} = 1$ supersymmetric case followed by a scenario with broken supersymmetry. Finally, the phenomenological properties of the model are investigated in chapter eight. We calculate the relic density of the lightest superpartner (LSP) DM candidate and discuss some striking features of the extended particle spectrum. We identify promising channels for observing missing energy signatures of LSP and next-to-lightest superpartner (NLSP) production at the LHC, propose kinematical cuts, and perform the corresponding Monte Carlo simulations using O'Mega/WHIZARD. Chapter nine summarizes our results. Finally, conventions, further details about the software implementations of the model and some background on mathematical methods are given in the Appendix.

Chapter 2

Extra Dimensions

Ham' se welche gesehen?

- *Ernst Mach's answer when being asked whether atoms exist*

In this chapter, the basics of extra dimensional models in flat and warped space are introduced. The beginning of the first section presents some motivation to consider such scenarios. The remainder is dedicated to the task of making sense of extra dimensional models as a description of 4D physics. In doing so, some formalism and terminology is introduced.

2.1 A Short Introduction to Quantum Fields in Extra Dimensions

2.1.1 Motivation

The notion that our world might have more than four spacetime dimensions dates back to at least 1921 and 1926 when Theodor Kaluza and Oskar Klein published their work on the unification of gravity and electromagnetism in five dimensions [1, 2]. Since in the meantime, many new forces and particles have been discovered, generating Maxwell's equations from higher dimensional Einstein's equations is, though elegant, not sufficient any more. The idea of extra dimensions in particle physics has become popular again many years later through String Theory. When it turned out that Superstring Theory requires 6 additional spacetime dimensions for internal consistency, there was initially no reason to think of them as being visible at low energy scales accessible to experiments, but in the late nineties, with the advent of D-branes in String Theory, warped space [3] and the ADD scenario [4, 5] among others, having extra dimensions at the scale of current colliders suddenly became an option that was considered seriously, sparking renewed interest in phenomenological model building in this direction.

Considering the existence of additional dimensions is interesting due to various reasons of different origins. The first and most obvious is that, though quantum field theories in four dimensions have rather special properties, there is no a

priori reason why extra space dimensions should not exist in nature¹, suggesting the search for and theoretical modeling of extra dimensions in the context of upcoming experiments such as the LHC.

As will be discussed in section 3 there are good reasons to expect that within the energy range accessible to the LHC experiments, new effects have to appear which are connected to the origin of gauge boson masses. Since the kinetic energy component of a particle in the direction of an extra dimension has the same phenomenological consequences in four dimensions as a mass, it is intriguing to consider this mechanism as an alternative or extension of the standard Higgs mechanism. In such a scenario extra dimensions would exist which are somehow related to the generation of masses of the W and Z particles.

We will see in section 2.1.5 that it is a general property of quantum field theories in $D > 4$ that they are valid only up to a certain energy called the cut-off scale above which the descriptive power of the model breaks down. In this sense an extra dimension is only a metaphor, providing a construction principle for a set of particles and their interactions. This idea lead to an approach dubbed “deconstructed extra dimensions” [6]. One of the most exciting theoretical developments in quantum field theory and string theory in recent years, the celebrated *AdS/CFT* correspondence, gives us reason to believe that certain field theories with a curved extra dimension might be closely related or even equivalent to a class of four-dimensional theories which have so far been virtually inaccessible to known mathematical techniques², namely strongly coupled gauge theories with an approximate conformal symmetry. The Technicolor and Composite Higgs models mentioned in the introduction are important examples of this. Therefore, one further motivation for considering extra dimensions in particle physics phenomenology is that they might provide a calculable framework to model the dynamics of bound states present in this class of models, shedding new light on the properties of Technicolor and the Composite Higgs. However, regardless of whether the models discussed in this work have an exact strongly coupled dual via the *AdS/CFT* correspondence, they can still provide an interesting description of symmetry breaking and DM in their own right.

It is clear that any additional spacelike dimensions, since so far observable indirectly at best, have to differ in nature from the three known ones to escape direct detection. This is easily imaginable if either

1. the extra dimension is of finite extent with a size R corresponding to energies $\hbar c/R$ hitherto unreached by experiments. Here R is typically around $\hbar c/R \approx 1$ TeV corresponding to the energy range of past and current experiments such as LEP and the Tevatron.
2. the number of particle species allowed to propagate in the higher dimensional volume is restricted. In particular in the case of extra dimensions in

¹Extra timelike dimensions are a significantly more problematic subject that will not be treated in this work

²With the exception of lattice calculations, which so far only capture static properties of strongly interacting particles rather than their dynamics

which only geometry and thus gravitons themselves are present, the bounds on R are greatly loosened to the order of microns.

3. the extra dimension is strongly curved as proposed by Randall and Sundrum [7], locating low energy physics sufficiently towards the boundary of the space and thus making it appear effectively four dimensional even though it does not have to be compact.

The scenario investigated in this work contains a variation of the latter. The curved background geometry and brane setup is that of Randall and Sundrum [7]. While the possibility of mode localization in the warped background is used to some extent and plays an important role, every field in the model is allowed to propagate in the volume of the extra dimension.

2.1.2 The Kaluza-Klein Approach for a Scalar Field

Kaluza-Klein Decomposition

For definiteness, let us consider the simplest case of Minkowski space extended by one flat compact extra dimension. Such a space can be represented as the direct product of Minkowski space and an interval

$$(x^\mu, y) \equiv x^M \in \mathbb{R}^4 \times [0, \pi R] \quad (2.1)$$

with the metric $g_{MN} = \text{diag}(1, -1, -1, -1, -1)$ where now $M, N = 0 \dots 3, 5$. Fields now depend on x and y ,

$$\phi(x) \longrightarrow \phi(x, y)$$

In the present case of a compact space, Fourier analysis teaches us that we can represent the y dependence using a complete, countably infinite set of functions $g^n(y)$ and an equal number of coefficients $\phi^n(x)$,

$$\phi(x, y) = \sum_{n=0}^{\infty} \phi^n(x) g^n(y) \quad (2.2)$$

The key point is now the choice of functions $g^n(y)$ and it turns out that it will be dictated to us by the dynamics. Consider the free action of such a real scalar field

$$S = \frac{1}{2} \int d^4x \int dy \left[\partial_M \phi \partial^M \phi \right] \quad (2.3)$$

Substituting (2.2) and integrating by parts with respect to y , we obtain

$$S = \frac{1}{2} \sum_{n,m} \int d^4x \left[\mathcal{I}_{mn} \partial_\mu \phi^n \partial^\mu \phi^m - \mathcal{M}_{mn} \phi^n \phi^m \right] \quad (2.4)$$

where $\mathcal{I}_{mn} = \int dy g^n g^m$ and $\mathcal{M}_{mn} = - \int dy g^n \partial_y^2 g^m$. It becomes obvious that the action takes a particularly simple form if the functions g are chosen orthonormal with respect to the scalar product,

$$\mathcal{I}_{mn} = \delta_{mn} \quad (2.5)$$

and even more so if they are eigenfunctions of the operator $\hat{O} = \partial_y^2$, satisfying $\hat{O}g^n = -m_n^2 g^n$ and thus

$$\mathcal{M}_{mn} = \delta_{mn} m_n^2 \quad (\text{no sum}) \quad (2.6)$$

Once boundary conditions for the field are specified, this is a Sturm-Liouville problem of which we know that it is solvable with orthonormal solutions. In section 2.2 where curvature is introduced, the operator and the scalar product will become more complicated, but this particular point remains unchanged. In either case, we are left with

$$S = \frac{1}{2} \sum_n \int d^4x \left[\partial_\mu \phi^n \partial^\mu \phi^n - m_n^2 \phi^n \phi^n \right] \quad (2.7)$$

This is the action of an infinite tower of scalar fields with masses m_n ! The particles springing from the quantization of the coefficient fields $\phi^n(x)$ will henceforth be called *Kaluza-Klein modes*, and the functions $g^n(y)$ *Kaluza-Klein wave functions*. The Fourier expansion (2.2) in mass eigenmodes and substitution into the action (2.7) is consequently dubbed *Kaluza-Klein decomposition*.

Boundary Terms and the Choice of Boundary Conditions

In the above example we have ignored the boundary term from the partial integration,

$$S_{\text{bnd}} = \frac{1}{2} \int d^4x \left[-\phi(x, y) \partial_y \phi(x, y) \right] \Big|_{y=0}^{y=\pi R} = \frac{1}{2} \sum_{n,m} \mathcal{B}_{nm} \int d^4x \phi^n \phi^m \quad (2.8)$$

where

$$\mathcal{B}_{nm} = [g^n \partial_y g^m] \Big|_{y=0}^{y=\pi R}$$

which will do two things if present. If $\mathcal{B}_{nm} \neq 0$ for $n \neq m$ the diagonality of the free action is spoiled, whereupon the particles associated with ϕ^n will not be physical mass eigenstates. This is not in and of itself a problem, but has to be taken into account carefully. Furthermore, if $\mathcal{B}_{nm} \neq 0$, solving the equations of motion on the boundary will give additional constraints, thus modifying the effective boundary conditions. In this case it is said that the original boundary conditions are “not compatible” with the variation of the action.

Thus $\mathcal{B}_{nm} = 0$ is a condition we can use to restrict the choice of boundary conditions. In the case of one 5D field, this is rather trivial. Excluding the cases

where the two boundaries cancel by some nonlocal constraint or where the field takes some constant nonzero value, two possibilities remain,

$$\phi|_{y_0} = 0 \quad \text{or} \quad \partial_y \phi|_{y_0} = 0 \quad (2.9)$$

independently for $y_0 = 0, \pi R$ corresponding to Dirichlet or Neumann boundary conditions on either boundary of the interval. This becomes more interesting if several fields are coupled on the boundary, an essential ingredient of the models described in this work. Consider n flavors of scalars,

$$S = \frac{1}{2} \sum_{f=1}^n \int d^4x \int dy \left[\partial_M \phi_f \partial^M \phi_f \right] \quad (2.10)$$

The resulting boundary term is (writing $\vec{\phi}' \equiv \partial_y \vec{\phi}$)

$$\mathcal{L}_{\text{bnd}} = \frac{1}{2} \sum_f \phi_f \partial_y \phi_f \Big|_0^{\pi R} = \frac{1}{2} \langle \vec{\phi}, \vec{\phi}' \rangle \Big|_0^{\pi R} \quad (2.11)$$

which has the form of a scalar product. The boundary conditions we would like to impose are (at $y_0 = 0$ or $y_0 = \pi R$)

$$D\vec{\phi} + N\vec{\phi}'|_{y=y_0} = 0 \quad (2.12)$$

where $D, N \in \mathbb{R}^{n \times n}$. We are thus looking for matrices D, N which satisfy

$$\forall v, w \in \mathbb{R}^N : Dv + Nw = 0 \Rightarrow \langle v, w \rangle = 0 \quad (2.13)$$

A constructive proof (appendix C) shows that they can without loss of generality be parametrized as follows:

$$D = \begin{pmatrix} I_{d \times d} & 0 \\ 0 & 0 \end{pmatrix} V \quad N = \begin{pmatrix} \tilde{N} & 0 \\ 0 & I_{n-d \times n-d} \end{pmatrix} V \quad (2.14)$$

in which $V \in SO(N)$ and

$$\tilde{N} = \text{diag} \left(\left[\begin{array}{cc} 0 & b_1 \\ -b_1 & 0 \end{array} \right], \dots \right)$$

This corresponds to a net number of $n - d$ Neumann boundary conditions and d mixed or Dirichlet boundary conditions depending on the choice of b_i . For d odd, there is one trailing zero in \tilde{N} . The two options in the trivial case of one field are reproduced by $d = 1, 0$.

Localized Mass Terms

We have seen that it is possible to assign antisymmetric mixed boundary conditions if several fields are present. There is yet another possibility, namely via a

symmetric localized mass term. If it is situated at $y_0 = 0$ ($y_0 = \pi R$) it has the following structure

$$\mathcal{L} = \frac{1}{2}\delta(y - y_0)M_{ef}\phi_e\phi_f, \quad M = M^T \quad (2.15)$$

and contributes to the boundary action

$$\mathcal{L}_{\text{bnd}} = \frac{1}{2}\langle\vec{\phi}, \pm\vec{\phi}' + M\vec{\phi}\rangle|_{y=y_0} \quad (2.16)$$

The most general boundary conditions have the same form, except that now

$$D\vec{\phi} + N(\pm\vec{\phi}' + M\vec{\phi})|_{y=y_0} = 0 \quad (2.17)$$

In the case of just one field, we have

$$\phi|_{y=y_0} = 0 \quad \text{or} \quad (\pm\partial_y\phi + M\phi)|_{y=y_0} = 0 \quad (2.18)$$

Localized Kinetic Terms

The remaining possibility to modify the free action is through localized kinetic terms. They differ in an essential way from the things covered before because after Kaluza-Klein expansion, each mode will, according to its mass, see a different effective boundary condition. Also, the scalar product with respect to which the solutions of the eigenvalue problem are orthonormal is modified³. Consider the following action

$$S = \frac{1}{2}\int d^4x \int dy \left[\partial_M\phi\partial^M\phi \right] + \frac{1}{2}\int d^4x \kappa \partial_\mu\phi\partial^\mu\phi \Big|_{y=0} \quad (2.19)$$

The boundary term at $y = 0$ after partial integration gives

$$S_{\text{bnd}} = \frac{1}{2}\int d^4x \left[\phi\partial_y\phi - \kappa\phi\Box\phi \right] \Big|_{y=0} \quad (2.20)$$

We see that the boundary action contains a kinetic operator, which, after Kaluza-Klein expansion, turns into the 4D mass of the mode, giving a mass dependent boundary condition

$$\phi(p, y) \Big|_{y=0} = 0 \quad \text{or} \quad (\partial_y\phi(p, y) + \kappa p^2\phi(p, y)) \Big|_{y=0} = 0 \quad (2.21)$$

After Kaluza-Klein decomposition, the individual modes on their mass shell will have $p^2 = m_n^2$. If one solves the eigenvalue problem (2.6) using this prescription,

³If the kinetic term includes higher powers of fields (such as covariant derivatives), the effective couplings will also receive corrections. This will be treated later.

one notices that the solutions are not orthogonal with respect to $\langle f, g \rangle = \int dy f g$. For this type of boundary conditions, the scalar product has to be modified to

$$\langle f, g \rangle_\kappa = \int_0^{\pi R} f g dy + \kappa f g \Big|_{y=0} \quad (2.22)$$

This makes sense physically as any new kinetic term in the Lagrangian, localized or not, also contributes to the wave function normalization of the field.

There is one *caveat* when introducing this type of terms: If the coefficient κ becomes negative, the effective kinetic term can get a negative sign and the scalar product is not positive definite any more. This will result in tachyonic solutions of the eigenvalue problem (2.6) with $m^2 < 0$. If $|\kappa|$ is not too large compared to the radius, this tachyon resides at high energies beyond the cutoff scale of the model, which is maybe theoretically less severe than having one at accessible energies. We have nevertheless avoided this situation in our model.

2.1.3 An Algorithm for Solving KK Towers with Many Fields Coupled by Boundary Conditions

As long as each boundary condition on the branes only affects two fields (in a suitable basis), we can obtain the Kaluza-Klein tower and wave functions by solving the conditions step by step until we have one boundary condition left and one free parameter, the mass eigenvalue, which we can solve for numerically or in an analytic approximation. We would like to outline an algorithm which, from matrices defining the boundary conditions for a set of fields ϕ_f , gives us the complete action on a boundary and thus a compact expression which can be used to determine the Kaluza-Klein tower.

We start from the premise that the n fields $\phi_f(x, y)$, $f = 1 \dots n$ live on an interval $y \in [0, \pi]$ and obey n boundary conditions on both ends. To write mixed boundary conditions in a compact form, we define (with suppressed Kaluza-Klein indices)

$$\phi_f = \phi_f(x) g_f(y), \quad \mathfrak{G} = (g_1, \tilde{\partial} g_1, \dots, g_n, \tilde{\partial} g_n) \quad (2.23)$$

where the $\tilde{\partial}$ is a first order differential operator which is chosen such that $\tilde{\partial}\phi = 0$ is a valid modified Neumann boundary condition compatible with the variation of the boundary action as it was introduced above. In the case of scalar fields in flat space without boundary operators, it reduces to the ordinary partial derivative. Now we can write the coupled boundary conditions for n flavours as

$$A\mathfrak{G}(0) = 0 \quad B\mathfrak{G}(\pi) = 0 \quad (2.24)$$

where $A, B \in \mathbb{R}^{n \times 2n}$ should fulfil (2.14) for compatibility with the action. Since we assume second order equations of motion for ϕ , n fields should be subject to $2n$ boundary conditions, with n conditions imposed on each. This means that $\text{rk } A = \text{rk } B = n$, $\dim \ker A = \dim \ker B = n$. Furthermore, we can solve for

$\mathfrak{G}(y)$ explicitly if we fix \mathfrak{G} on one boundary and choose an eigenvalue m . This is done using the transport diffeomorphism $T_m(y_1, y_2)$, for example

$$\mathfrak{G}(0) = T_m(0, \pi)\mathfrak{G}(\pi) \quad (2.25)$$

We can use this to connect the boundary conditions on both sides as follows: We know that

$$\mathfrak{G}(\pi) \in \ker B \quad (2.26)$$

We write the kernel of B as a matrix, $K_B \in \mathbb{R}^{2n \times n}$ with the vectors as columns. For arbitrary vectors $v \in \mathbb{R}^n$ we can reach all valid configurations on the boundary

$$\mathfrak{G}(\pi) = K_B v \Leftrightarrow B\mathfrak{G}(\pi) = 0 \quad (2.27)$$

It follows from (2.25) that

$$\mathfrak{G}(0) = T_m(0, \pi)K_B v \quad (2.28)$$

We can now impose the boundary conditions at $y = 0$ and demand that v should fulfil

$$AT_m(0, \pi)K_B v = 0 \quad (2.29)$$

To find all Kaluza-Klein modes in a mass range, all we need to do is impose

$$\det(AT_m(0, \pi)K_B) = 0 \quad (2.30)$$

and determine the values of m for which it is satisfied. Drawbacks of this approach are that the expressions can get large, and that mass degeneracy of particles will result in higher order roots of (2.30) which are harder to solve for numerically. Once we have found a value m_0 which satisfies (2.30), we can automatically obtain the complete Kaluza-Klein wave functions pertaining to one particle mass eigenstate,

$$v \in \ker(AT_{m_0}(0, \pi)K_B) \Rightarrow \mathfrak{G}(y) = T_{m_0}(y, \pi)K_B v \quad (2.31)$$

The corresponding 5D fields are

$$\phi_f(x, y) = \phi^{n_0}(x)\mathfrak{G}_{2f-1}(y) \quad (2.32)$$

Note that we assign one 4D coefficient field for all $f = 1 \dots n$. If some of the flavours do not participate in a particular eigenmode, the corresponding functions in \mathfrak{G} will vanish identically. In the case of d -fold degeneracy at mass m_0 , we have

$$\dim \ker(AT_{m_0}(0, \pi)K_B) = d$$

We use this for example in appendix D.1.

2.1.4 Gauge Theory

Gauge Fixing

Gauge fields require a special treatment because unphysical degrees of freedom differ in their Kaluza-Klein expansion. For simplicity and clarity, we restrict ourselves to abelian gauge theory, and will treat the nonabelian case and the dependence on boundary conditions in the context of warped space. To proceed, we first have to implement the BRST program in 5D. For this discussion of the abelian case it is sufficient to concentrate on the gauge fixing term which decouples the 4D vector and scalar components of the gauge field in the free action. Also, we will postpone the discussion of boundary conditions in relation to gauge invariance to the section on symmetry breaking. The straightforward generalization of the Lorenz condition to five dimensions is given by

$$\mathcal{L}_{gf} = -\frac{1}{2} (\partial_M A^M)^2 \quad (2.33)$$

It is however much more convenient to be able to go to an axial gauge $A_5 \rightarrow 0$ (which turns out to be equivalent to a unitary gauge), and this can be easily implemented by

$$\mathcal{L}_{gf} = -\frac{1}{2\xi} (\partial_\mu A^\mu + \xi \partial_5 A^5)^2 \quad (2.34)$$

Now, the unitary gauge can be reached by taking the limit $\xi \rightarrow \infty$. The combined action of gauge kinetic and gauge fixing terms is

$$S = \int d^4x \int dy \left[-\frac{1}{4} F_{MN} F^{MN} - \frac{1}{2\xi} (\partial_\mu A^\mu + \xi \partial_5 A^5)^2 \right] \quad (2.35)$$

After partial integration,

$$S = \int d^4x \int dy \left[\frac{1}{2} A_\mu (\square g^{\mu\nu} - (1 - \frac{1}{\xi}) \partial^\mu \partial^\nu - \partial_5 \partial_5 g^{\mu\nu}) A_\nu - \frac{1}{2} A_5 (\square - \xi \partial_5 \partial_5) A_5 \right] \quad (2.36)$$

where the mixing terms $\partial_\mu A^\mu \partial_5 A^5$ have canceled between the gauge fixing and kinetic terms.

Kaluza-Klein Decomposition

It would complicate the expansion significantly if longitudinal, scalar and transverse modes of A_μ had different Kaluza-Klein wave functions. Luckily this is not the case due to our choice of gauge fixing through which all components share the 5D kinetic operator $\hat{O} = \partial_5 \partial_5$ and do not mix. We can thus write

$$A_\mu(x, y) = \sum_n A_\mu^n(x) g^n(y) \quad (2.37)$$

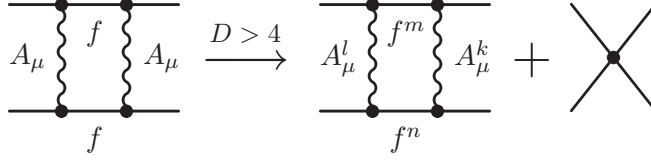


Figure 2.1: An illustration of nonrenormalizability of models in extra dimensions. The graph on the left shows a contribution to the interaction of four fermions in the SM. It is finite which means that counterterms such as the one on the right are not required in the model, thus increasing its predictivity. The graph in the middle shows the same contribution in extra dimensions. Since every propagator contains an infinite tower of particles, this contribution is in general not finite. To remove this infinity, the four fermi interaction on the right has to be introduced in the Lagrangian.

$$A_5(x, y) = \sum_l A_5^l(x) f^l(y) \quad (2.38)$$

giving us

$$S = \int d^4x \int dy \sum_n \left[\frac{1}{2} A_\mu^n \left((\square + m_n^2) g^{\mu\nu} - \left(1 - \frac{1}{\xi}\right) \partial^\mu \partial^\nu \right) A_\nu^n - \sum_l \frac{1}{2} A_5^l (\square + \xi \tilde{m}_l^2) A_5^l \right] \quad (2.39)$$

This is the action of massive scalar fields A_5^l of mass $\sqrt{\xi} \tilde{m}_l$ and massive Stückelberg vector fields A_μ^n of mass m_n . The correct choice of boundary conditions will achieve that for all modes $m_l = \tilde{m}_l$ except that either A_μ or A_5 may also have a massless mode which is projected out for the other field. This is important because exactly like in the standard Higgs mechanism, the gauge boson propagator has an unphysical pole at $\sqrt{\xi} m_n$ which must cancel with the scalar contribution.

2.1.5 A Note on Nonrenormalizability

As hinted at in the introduction, quantum field theories in four dimensions have special properties which are modified when going to $D > 4$. The key difference is the property of renormalizability. Since the first beginnings of quantum field theory in the first half of the 20th century, the major difficulty was the handling of infinities appearing in quantum corrections to the classical field theory. With the success of Quantum Electrodynamics (QED), it became clear that it was possible to remove them consistently by rescaling (renormalizing) the existing parameters of the model. This property of models has been considered an essential consistency condition, and the proof of renormalizability of the SM was a major theoretical achievement which led to the Nobel Prize for Martinus Veltman and Gerardus 't Hooft in 1999. Nevertheless, it became clear in the past decade that nonrenormalizable models can very well be a sensible description of physics in the context of low energy effective theories, with one limitation, namely the existence of a cutoff energy scale Λ_c which marks the upper limit of validity above which the predictive power of the model breaks down. This is always the case

in the extra dimensional models discussed in this work. The critical step is that infinities appear corresponding to operators with energy dimension larger than four, for example $\frac{1}{\Lambda_c^2} \bar{\Psi} \Psi \bar{\Psi} \Psi$ as illustrated in figure 2.1. Once they are introduced, an infinite number of higher operators follows. This sounds severe at first, but the predictiveness of these models lies in the fact that those operators are by dimensional analysis suppressed by increasing powers of a scale Λ_c , rendering higher contributions irrelevant at energies $E \ll \Lambda_c$ [8]. Raising Λ_c by putting as much of the physics as possible in renormalizable operators is therefore an important objective for effective theories.

2.2 The Randall/Sundrum Scenario and Warped Space

Even though the *AdS/CFT* correspondence was formulated already in 1997 [9], *AdS*₅ as a background space for particle physics models became much more popular starting with the two seminal papers by Randall and Sundrum in 1999 [7, 3]. They showed that a slice of *AdS*₅ arises dynamically as a solution to Einstein's equations in 5D if two 3-Branes are set up and suitable brane and bulk cosmological constants are chosen. Furthermore, they demonstrated that this scenario could provide a solution to the hierarchy problem of the Higgs model. We will state the results of this construction as far as they are relevant for this thesis and refer the reader to the literature for details of the derivation. We work with the "mostly -" metric convention throughout the remaining chapters. In so-called proper distance coordinates, the background metric takes the form

$$g_{\mu\nu}(x, y) = e^{-2Rky} \eta_{\mu\nu}, \quad g_{55}(x, y) = -R^2, \quad g_{5\mu}(x, y) = 0 \quad (2.40)$$

where $y \in [0, \pi]$. In these coordinates, the density factor is

$$\sqrt{g} \equiv \sqrt{\det g} = R e^{-4Rky} \quad (2.41)$$

The 5D space equipped with such a nonfactorizable background metric is generally referred to as *warped space*. We see that R gives the size of the extra dimension, while k is the RS curvature. As always for fields in a curved background, the Lagrangian has to be densitized with \sqrt{g} to make the action a scalar under general coordinate transformations,

$$S = \int d^5x \sqrt{g} \mathcal{L}_{5D}[\phi, \partial_\mu \phi, g^{\mu\nu}] \quad (2.42)$$

The 4D spaces at $y = 0$ and $y = \pi$ are referred to as the ultraviolet- or Planck brane (UV brane) and the infrared- or TeV brane (IR brane) respectively. The name hints already at the role the branes will play: If $Rk\pi \approx 37$, then

$$e^{-Rk\pi} M_{Pl} \approx 1 \text{ TeV} \quad (2.43)$$

This has an interesting consequence for the physical mass of a scalar field living on the IR brane,

$$\mathcal{L} = \int dy \sqrt{g} \left[g^{\mu\nu} \partial_\mu \phi^\dagger \partial_\nu \phi - M^2 \phi^\dagger \phi + \lambda (\phi^\dagger \phi)^2 \right] \delta(y - \pi) \quad (2.44)$$

If we evaluate this expression, it yields

$$\mathcal{L} = R e^{-4Rk\pi} \left[e^{2Rk\pi} \eta^{\mu\nu} \partial_\mu \phi^\dagger \partial_\nu \phi - M^2 \phi^\dagger \phi + \lambda (\phi^\dagger \phi)^2 \right] \quad (2.45)$$

Going to canonical normalization of the scalar field ($\phi \rightarrow e^{Rk\pi}/\sqrt{R} \phi$) to read off the physical parameters, we find

$$\mathcal{L} = \eta^{\mu\nu} \partial_\mu \phi^\dagger \partial_\nu \phi - (e^{-Rk\pi} M)^2 \phi^\dagger \phi + \lambda (\phi^\dagger \phi)^2 \quad (2.46)$$

Together with (2.43) this produces a TeV scale mass from a Planck scale mass parameter. A second important property is the profile of the massless graviton mode \bar{h} , which is $e^{-2Rky} (\eta_{\mu\nu} + \bar{h}_{\mu\nu})$. This ensures that all particle species feel the same strength of mutual gravitational attraction in the 4D Kaluza-Klein picture independent of their localization in the extra dimension.

In this work it is not the purpose of the warped background to solve the hierarchy problem for scalar particles. It instead helps to realize symmetry breaking by boundary conditions, and the hierarchy of scales which it produces separates the electroweak symmetry breaking sector with intact custodial $SU(2)$ symmetry (the IR brane and bulk) from the UV brane localized physics with broken $SU(2)_R$, leading naturally to $\rho = \cos^2 \theta_W^2 m_Z^2 / m_W^2 \approx 1$. Warped space provides a natural localization mechanism through bulk masses which can help to explain the mass hierarchy of fermions [10]. Also, it opens up interesting possibilities for SUSY breaking with a distinct low energy phenomenology.

There is a fashionable interpretation of fields in warped space which is very useful to gain an intuitive understanding of the physics which is going on, namely the dictionary provided by the *AdS/CFT* correspondence. A useful introduction to the basic concepts can be found in [11, 12].

2.2.1 Christoffel Symbols and Spin Connections

In the following sections lowercase latin indices and barred numbers $\bar{5}$ indicate “flat” indices. The coordinate frame introduced above has the advantage that g_{55} is constant and yet the $g_{\mu\nu}$ only depend on y . Therefore, the only nonvanishing Christoffel symbols are

$$\Gamma_{\mu\nu}^{\bar{5}} = -\frac{k}{R} g_{\mu\nu} \quad \Gamma_{5\nu}^\mu = \Gamma_{\nu 5}^\mu = -Rk \delta_\nu^\mu \quad (2.47)$$

The connection for “flat” indices which is used to built covariant derivatives for spinors is defined as

$$\omega_M^n{}_m = e_N^n e_m^R \Gamma_{MR}^N - (\partial_M e_N^n) e_m^N \quad (2.48)$$

where we use the fünfbein and inverse fünfbein

$$e_\mu^a = e^{-Rky} \delta_\mu^a, \quad e_a^\mu = e^{Rky} \delta_a^\mu, \quad e^{\bar{5}} = R, \quad e_{\bar{5}} = 1/R \quad (2.49)$$

After lowering the upper index with the Minkowski metric, there are two nonvanishing spin connection coefficients,

$$\omega_{\mu\bar{5}a} = -\omega_{\mu a\bar{5}} = k e^{-Rky} \eta_{\mu\nu} \delta_a^\nu \quad (2.50)$$

2.3 Scalars, Spinors and Gauge Fields in Warped Space

2.3.1 Scalars

The Lagrangian of a scalar field which can propagate in warped space is given by

$$\begin{aligned} \mathcal{L} &= \frac{1}{2} \int dy \sqrt{g} [g^{MN} \partial_N \phi \partial_M \phi - M_5^2 \phi^2] \\ &= \frac{1}{2} \int dy \sqrt{g} \left[e^{2Rky} \eta^{\mu\nu} \partial_\mu \phi \partial_\nu \phi - \frac{\partial_y \phi}{R} \frac{\partial_y \phi}{R} - M_5^2 \phi^2 \right] \end{aligned} \quad (2.51)$$

The general covariant derivatives are trivial in this case. After partial integration, we get

$$\begin{aligned} \mathcal{L} &= -\frac{1}{2} \int dy \sqrt{g} \left[e^{2Rky} \phi \square \phi - \phi \left(\frac{\partial_y \partial_y}{R^2} - 4k \frac{\partial_y}{R} - M_5^2 \right) \phi \right] \\ &\quad + \frac{1}{2} \left[-\frac{e^{-4Rky}}{R} \phi \partial_y \phi \right]_0^\pi \end{aligned} \quad (2.52)$$

The differential equation for $\phi = \phi_n(x) g_n(y)$ together with the on-shell condition $\square \rightarrow -m_n^2$ leads to a basis of solutions

$$g_n(y) = e^{2Rky} \left[a_n J_{\sqrt{4+M_5^2/k^2}} \left(\frac{m_n}{k} e^{Rky} \right) + b_n Y_{\sqrt{4+M_5^2/k^2}} \left(\frac{m_n}{k} e^{Rky} \right) \right] \quad (2.53)$$

We will see later that the scalar fields which are part of supermultiplets have to be provided with the right boundary and bulk mass terms for SUSY to be intact.

2.3.2 Spinors

Spinors in 5D are always of Dirac type, and in warped space, their behaviour under Lorentz transformations gives us a nontrivial general covariant derivative for objects with spinor indices

$$\nabla_M \Psi = \partial_M \Psi - \frac{i}{4} \omega_M \Psi, \quad \nabla_M \bar{\Psi} = \partial_M \bar{\Psi} + \frac{i}{4} \bar{\Psi} \omega_M \quad (2.54)$$

where

$$\omega_M = \omega_{Mnm} \frac{i}{2} [\bar{\gamma}^n, \bar{\gamma}^m] \quad (2.55)$$

As a generalization of metric compatibility $\nabla_K g^{MN} = 0$, it satisfies $\nabla_M \gamma^N = 0$ and allows for integration by parts under the density factor \sqrt{g} ,

$$\int d^5x \sqrt{g} \bar{\Psi} \gamma^M \nabla_M \Psi = - \int d^5x \sqrt{g} (\nabla_M \bar{\Psi}) \gamma^M \Psi \quad (2.56)$$

In our case, $\omega_5 = 0$ and

$$\gamma^\mu \nabla_\mu \Psi = \left[e^{Rky} \bar{\gamma}^\mu \partial_\mu - 2k \bar{\gamma}^5 \right] \Psi \quad (2.57)$$

and therefore,

$$\bar{\Psi} \gamma^M \nabla_M \Psi = \bar{\Psi} \left[e^{Rky} \bar{\gamma}^\mu \partial_\mu + \bar{\gamma}^5 \frac{\partial_5 - 2Rk}{R} \right] \Psi \quad (2.58)$$

It is customary to rewrite the bulk mass in units of the RS curvature k as $M_5/k = c$. Up to 5D boundary terms, the action rewritten using our conventions is therefore

$$\begin{aligned} \mathcal{L} &= \int dy \sqrt{g} \bar{\Psi} [i\gamma^M \nabla_M - M_5] \Psi \\ &= \int dy \sqrt{g} \bar{\Psi} \left[i e^{Rky} \bar{\gamma}^\mu \partial_\mu + \frac{1}{R} \begin{pmatrix} -\partial_5 + (2-c)Rk & \\ & \partial_5 + (-2-c)Rk \end{pmatrix} \right] \Psi \end{aligned} \quad (2.59)$$

Compare this for example to $\mathcal{L}_{11}, \mathcal{L}_{18}, \mathcal{L}_{20}$ (appendix B.2). One can now proceed to solve the differential equation to obtain a basis of Kaluza-Klein wave functions in analogy to the scalar case, but since we now have first order equations, there is some additional work to do. First of all, we vary $\bar{\Psi}$ and get

$$i e^{Rky} \bar{\gamma}^\mu \partial_\mu \Psi = \left(-\frac{i}{R} (\partial_5 - 2Rk) \bar{\gamma}^5 - ck \right) \Psi \quad (2.60)$$

We act on both sides with $\bar{\gamma}^\mu \partial_\mu$ and commute it to the right. After resubstituting (2.60) in the RHS we get diagonal second order equations of motion

$$\square \Psi = e^{-2Rky} \begin{bmatrix} (\partial_5/R - 5k) \partial_5/R + (6 - c^2 - c)k^2 & 0 \\ 0 & (\partial_5/R - 5k) \partial_5/R + (6 - c^2 + c)k^2 \end{bmatrix} \Psi \quad (2.61)$$

Now we again solve the differential equation for the Kaluza-Klein wave functions

$$\Psi = \begin{pmatrix} \psi_n(x) f_n(y) \\ \bar{\psi}_n^c(x) g_n(y) \end{pmatrix}$$

by assuming the on-shell condition $\square \rightarrow -m_n^2$ and get

$$\begin{aligned} f_n(y) &= e^{5Rky/2} \left[a_n J_{c+1/2} \left(\frac{m_n}{k} e^{Rky} \right) + b_n Y_{c+1/2} \left(\frac{m_n}{k} e^{Rky} \right) \right] \\ g_n(y) &= e^{5Rky/2} \left[a_n J_{c-1/2} \left(\frac{m_n}{k} e^{Rky} \right) + b_n Y_{c-1/2} \left(\frac{m_n}{k} e^{Rky} \right) \right] \end{aligned} \quad (2.62)$$

2.3.3 Nonabelian Gauge Theory in Warped Space

The flat 5D version of Yang-Mills theory is a straightforward generalization of the 4D form,

$$\mathcal{L} = \int dy \left[-\frac{1}{4} F_{MN}^a F^{aMN} - \frac{1}{2\xi} (\partial_\mu A^{a\mu} + \xi \partial_5 A^{a5})^2 - \bar{c}^a (\partial^\mu D_\mu^{ab} + \xi \partial^5 D_5^{ab}) c^b \right] \quad (2.63)$$

and substituting the metric and density factor, we get the warped version of the gauge invariant part,

$$\begin{aligned} \mathcal{L} &= \int dy \sqrt{g} \left[-\frac{1}{4} g^{MN} g^{OP} F_{MO} F_{NP} \right] \\ &= \int dy R \left[-\frac{1}{4} \eta^{\mu\nu} \eta^{\omega\rho} F_{\mu\omega} F_{\nu\rho} + \frac{1}{2R^2} e^{-2Rky} \eta^{\mu\nu} F_{\mu 5} F_{\nu 5} \right] \end{aligned} \quad (2.64)$$

The fifth component of the gauge connection has still energy dimension $[A_5] = 1/2$ because y is unitless. To furnish A_5 with the canonical normalization of a scalar, we now perform the substitution $A_5 \rightarrow R A_5$. The warped version of the R_ξ gauge fixing is

$$\mathcal{L}_{gf} = - \int dy \frac{R}{2\xi} \left(\eta^{\mu\nu} \partial_\mu A_\nu^a - \xi \frac{e^{-2Rky}}{R} (\partial_5 - 2Rk) A_5^a \right)^2 \quad (2.65)$$

which entails a BRST ghost Lagrangian

$$\mathcal{L}_{gh} = - \int dy R \bar{c}^a \left(\eta^{\mu\nu} \partial_\mu D_\nu^{ab} - \xi \frac{e^{-2Rky}}{R} (\partial_5 - 2Rk) D_5^{ab} \right) c^b \quad (2.66)$$

with

$$D_\mu^{ac} = \partial_\mu \delta^{ac} + f^{abc} A_\mu^b, \quad D_5^{ac} = \frac{\partial y}{R} \delta^{ac} + f^{abc} A_5^b \quad (2.67)$$

It is designed such that the ghosts c, \bar{c} have a Kaluza-Klein expansion which matches that of A_μ , but with unphysical Kaluza-Klein masses $\sqrt{\xi} m_n$ like A_5 . We have included them for completeness but will not need them for the bulk of this thesis. Let us state the kinetic Lagrangian in its Kaluza-Klein decomposed form:

$$\mathcal{L}_{kin}[A_\mu] = \sum_{m,n;a} \left[\frac{1}{2} A_\mu^{a,n} \left(\square \eta^{\mu\nu} - \left(1 - \frac{1}{\xi}\right) \partial^\mu \partial^\nu \right) A_\mu^{a,m} \right] \int dy R f_n^a f_m^a$$

$$\begin{aligned}
& + \sum_{m,n;a} \left[-\frac{1}{2} \eta^{\mu\nu} A_\mu^{a,n} A_\nu^{a,m} \right] \int dy \frac{1}{R} f_n^a (\partial_y e^{-2Rky} \partial_y) f_m^a \\
& + \sum_{m,n;a} \left[\frac{1}{2} \eta^{\mu\nu} A_\mu^{a,n} A_\nu^{a,m} \right] \left[\frac{1}{R} e^{-2Rky} f_n^a \partial_y f_m^a \right]_0^\pi \quad (2.68)
\end{aligned}$$

$$\begin{aligned}
\mathcal{L}_{kin}[A_5] & = \sum_{m,n;a} \left[-\frac{1}{2} A_5^{a,n} \square A_5^{a,m} \right] \int dy R e^{-2Rky} g_n^a g_m^a \\
& + \sum_{m,n;a} \left[\frac{\xi}{2} A_5^{a,n} A_5^{a,m} \right] \int dy \frac{1}{R} g_n^a (e^{-2Rky} \partial_y^2 e^{-2Rky}) g_m^a \\
& + \sum_{m,n;a} \left[\frac{\xi}{2} A_5^{a,n} A_5^{a,m} \right] \left[-\frac{1}{R} g_n^a e^{-2Rky} \partial_y e^{-2Rky} g_m^a \right]_0^\pi \quad (2.69)
\end{aligned}$$

$$\mathcal{L}_{mix}[A_M] = \sum_{m,n;a} [\eta^{\mu\nu} \partial_\mu A_\nu^{a,n} A_5^{a,m}] \left[R e^{-2Rky} f_n^a g_m^a \right]_0^\pi \quad (2.70)$$

Note the boundary terms indicated by $[\dots]_0^\pi$. As explained in section 2.1.2 they should vanish by choice of boundary conditions. Solving the equations of motion which follow from this action, the Kaluza-Klein decomposition of the vector field is given by

$$\begin{aligned}
A_\mu(x, y) & = A_\mu^0(x) \left[a_0 + b_0 e^{2Rky} \right] \\
& + \sum_n A_\mu^n(x) e^{Rky} \left[a_n J_1 \left(\frac{m_n}{k} e^{Rky} \right) + b_n Y_1 \left(\frac{m_n}{k} e^{Rky} \right) \right] \\
A_5(x, y) & = A_5^0(x) \left[\tilde{a}_0 y e^{2Rky} + \tilde{b}_0 e^{2Rky} \right] \\
& + \sum_n A_5^n(x) e^{2Rky} \left[\tilde{a}_n J_0 \left(\frac{\sqrt{\xi} \tilde{m}_n}{k} e^{Rky} \right) + \tilde{b}_n Y_0 \left(\frac{\sqrt{\xi} \tilde{m}_n}{k} e^{Rky} \right) \right] \\
c(x, y) & = c^0(x) \left[a_0 + b_0 e^{2Rky} \right] \\
& + \sum_n c^n(x) e^{Rky} \left[a_n J_1 \left(\frac{\sqrt{\xi} m_n}{k} e^{Rky} \right) + b_n Y_1 \left(\frac{\sqrt{\xi} m_n}{k} e^{Rky} \right) \right] \quad (2.71)
\end{aligned}$$

Much can be said about relations between the two groups of parameters if boundary conditions are chosen that are compatible with Ward identities. Simply speaking, it is necessary for unitarity to have ghost modes for each massless vector mode and both ghost modes and a would-be goldstone mode for each massive vector mode. We can draw two conclusions: c and \bar{c} should get the same BC as A_μ . Furthermore, looking at the 5D equation of motion which arises for the Kaluza-Klein wave function of the A_μ and A_5 fields,

$$\begin{aligned}
m^2 f(y) & = -\partial_y e^{-2Rky} \partial_y f(y) \\
m^2 g(y) & = -\partial_y \partial_y e^{-2Rky} g(y)
\end{aligned}$$

it becomes apparent that A_5 satisfies the same equation of motion as $\partial_y A_\mu$ if $m \neq 0$. This leads to an obvious choice of relative boundary conditions

$$\begin{aligned} \partial_y A_\mu|_{\partial} = 0 &\implies A_5|_{\partial} = 0 \\ A_\mu|_{\partial} = 0 &\implies \partial_y e^{-2Rky} A_5|_{\partial} = 0 \end{aligned} \quad (2.72)$$

which achieves exactly the desired spectrum and is compatible with gauge transformations. The Kaluza-Klein wave functions of the massive modes indeed satisfy

$$m_n = \tilde{m}_n, \quad a_n = \tilde{a}_n, \quad b_n = \tilde{b}_n \quad (2.73)$$

and thus

$$f'_n(y) = m_n g_n(y) \quad (2.74)$$

The existence of massless modes depends on the interplay of all boundary conditions on both branes. For now let us state that there are combinations such that A_5 contains a massless scalar physical mode, for example when two Dirichlet conditions on A_μ coincide. This is interesting for models of gauge-higgs unification. The model presented in this thesis assigns at least one Neumann boundary condition for each vector such that $b_0 = 0$ and $\tilde{a}_0 = \tilde{b}_0 = 0$ for every field. There are thus no massless physical scalars, and all massless vector modes have a flat profile $f_0(y) = a_0$. This can be restated in the language of the *AdS/CFT* dictionary: all symmetries which are broken dynamically (Dirichlet conditions on the IR brane) are also gauged (Neumann conditions on the UV brane) such that no true goldstone bosons appear.

2.3.4 The Impact of UV and IR Boundary Conditions

We have seen above that extra dimensional gauge theories result in scenarios with nonlinear gauge invariance. Which gauge symmetries are realized exactly in the effective 4D theory and which are not, depends on the choice of boundary conditions for the fields. From now on we shall designate the basic two types of boundary conditions as follows:

$\oplus\oplus$	Neumann at $y = 0$ and $y = \pi$
$\oplus\ominus$	Neumann at $y = 0$, Dirichlet at $y = \pi$
$\ominus\oplus$	Dirichlet at $y = 0$, Neumann at $y = \pi$
$\ominus\ominus$	Dirichlet at $y = 0$ and $y = \pi$

By Neumann conditions we mean the modified Neumann condition appropriate for the field as derived in chapter D, or for example in (2.18) or (2.72). It is fair to say that on 4D slices in 5D space where $A_\mu = 0$ is enforced, the 4D gauge symmetry is absent as covariant derivatives locally reduce to ordinary derivatives and gauge transformations are incompatible with this constraint. For a $U(1)$ gauge theory, there are now four possibilities which we want to recapitulate

UV\IR	$A_\mu(\oplus), A_5(\ominus)$	$A_\mu(\ominus), A_5(\oplus)$
$A_\mu(\oplus)$ $A_5(\ominus)$	Unbroken gauge theory There is a massless delocalized vector mode with massive IR localized vector resonances starting at $m = 1266$ GeV	Softly broken gauge theory There is a light almost delocalized vector mode at $m = 121$ GeV with massive IR localized vector resonances starting at $m = 2006$ GeV
$A_\mu(\ominus)$ $A_5(\oplus)$	UV broken gauge theory There is no light vector, but massive IR localized vector resonances starting at around $m = 1245$ GeV	UV+IR broken There is again no light vector, but massive IR localized vector resonances starting at $m = 1983$ GeV. In addition, a massless physical scalar mode from A_5 appears.

Table 2.1: The impact of different choices of boundary conditions on the spectrum of a $U(1)$ gauge theory in warped space. The numbers are determined using (2.75) with a typical choice of parameters, $k = 10^{19}$ GeV, $Rk\pi = 37.5$.

quickly as they are the prototypes of what happens in the full model. Let us therefore summarize the different cases in table 2.1.

The generic Kaluza-Klein wave function of vector bosons is given in (2.71). According to (2.9), we can assign a Dirichlet condition to either A_μ or A_5 , with the other field receiving the Neumann assignment. From this we directly obtain the equation which we have to solve in order to calculate the nonzero eigenvalues,

$$Y_\omega(me^{Rk\pi}/k) - \frac{Y_\delta(m/k)}{J_\delta(m/k)} J_\omega(me^{Rk\pi}/k) = 0 \quad (2.75)$$

where $\delta = 0/1$ for the UV condition $A_\mu(\oplus/\ominus)$ and $\omega = 0/1$ for the IR condition $A_\mu(\oplus/\ominus)$. The condition for A_5 has $\delta \rightarrow 1 - \delta$ and $\omega \rightarrow 1 - \omega$. Thus the massive modes of A_5 always coincide with modes of A_μ and can thus act as would-be goldstone modes. Things are a little different for massless modes. The $m = 0$ solutions for the gauge field are also given in (2.71). In the present scenario, two solutions arise, $b_0 = \tilde{a}_0 = \tilde{b}_0 = 0, a_0 \neq 0$ which is allowed for $A_\mu(\oplus\oplus)$ and $\tilde{a}_0 = a_0 = b_0 = 0, \tilde{b}_0 \neq 0$ which is allowed for $A_\mu(\ominus\ominus)$.

Solving the equations (2.75), we see that the masses of the heavy resonances are almost, but not quite, entirely unaffected by what happens on the UV brane. The UV physics contributes a ≈ 20 GeV shift while the choice of IR boundary conditions causes a large shift. The existence of light vector modes however depends crucially on the boundary condition at the UV brane, and a Dirichlet condition there pushes the zero mode out of the spectrum. This behavior is a

peculiarity of fields in warped space and will be very important in later chapters as the superpartners of vector particles do inherit it. In flat space in comparison, there is essentially no hierarchy between the two boundaries, and light modes as well as heavy modes are equally affected by both.

Chapter 3

Higgsless Electroweak Symmetry Breaking

In the minimal SM, EWSB is accomplished by the condensation of a fundamental scalar Higgs field, but the corresponding particle has, so far, eluded detection at LEP and the Tevatron. While the minimal SM with a rather light Higgs particle describes the electroweak precision data very well, any model with just a light fundamental scalar is not natural when a much higher scale exists, such as the grand unification and quantum gravity scales. As we have already pointed out in the introduction, this is a reason to believe that the minimal SM is just the low energy effective theory of an extended model in which new physics protecting the mass of the Higgs particles appears at the TeV scale. Instead of adding particles to the minimal SM in order to protect the naturalness of a light fundamental scalar, one can instead attempt to break the electroweak symmetry without invoking the condensation of fundamental scalar fields. Indeed, such models were already proposed [13] in the form of TC models a few years after the introduction of the SM. Recently a deeper understanding, based on the celebrated *AdS/CFT* duality, of such higgsless models has emerged which is inspired by EWSB in extra dimensions, particularly in warped spacetimes such as a slice of *AdS*₅ [14, 15]. Even though these approaches are nonrenormalizable and still suffer from some of the problems that plague ETC, they remain perturbatively calculable up to energies of 5 ... 10 TeV [16] while simultaneously improving the fits to electroweak precision observables [17, 18].

It is no problem at all to introduce a mass for abelian gauge fields, as Stückelberg has pointed out already in 1938 [19]. Introducing a scalar (“Stückelberg”) field B which transforms nonlinearly under gauge transformations

$$A_\mu \rightarrow A_\mu + \partial_\mu \theta, \quad B \rightarrow B + m\theta \quad (3.1)$$

one can write down an action

$$\mathcal{L} = -\frac{1}{4}F_{\mu\nu}F^{\mu\nu} + \frac{1}{2}(mA_\mu - \partial_\mu B)^2 - \frac{1}{2}(\partial_\mu A^\mu + mB)^2 \quad (3.2)$$

which closely resembles (2.39) for $\xi = 1$ if one identifies B with Kaluza-Klein modes of A_5 and applies a gauge fixing term. This simple model has many nice properties as it is unitary and even renormalizable [20] in the context of massive QED. This invites us to extend the idea to nonabelian gauge theory in order to find models of electroweak symmetry breaking without a Higgs boson. This has been tried extensively in the past three decades, but it turned out that either unitarity or renormalizability is lost. As pointed out earlier, the latter point is not so severe if we restrict ourselves to effective theory describing physics to, say, scales somewhat above LHC energies. It turns out that 5D Yang-Mills theory provides an elegant method of constructing improvements on Stückelberg models for the nonabelian case as well.

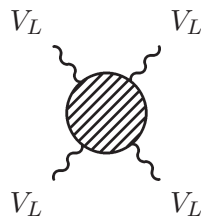
3.1 Symmetries, Unitarity and Boundary Conditions

3.1.1 Perturbative Unitarity and Massive Vector Bosons

There is a well-known consistency criterion for the S matrix due to Froissart [21] which sets limits on the growth of scattering amplitudes. The S matrix should be unitary, leading to the constraint

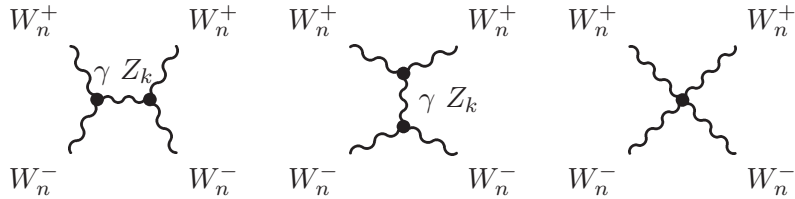
$$S^\dagger S = (1 - iT^\dagger)(1 + iT) = 1 \implies T^\dagger T = -i(T - T^\dagger) \quad (3.3)$$

It can be applied to the unitarity of the S matrix in the context of perturbation theory, for example as in the classic analyses of longitudinal massive gauge boson scattering at tree level by Lee, Quigg and Thacker [22] and the search for renormalizable massive vector theories in [23]. Massive vector bosons are important in this context because they have longitudinal modes which feature polarization vectors $\epsilon = (p/m, 0, 0, E/m)$ growing with energy. Naïvely, a scattering amplitude of four longitudinal vector bosons,



grows therefore with $\mathcal{M} \propto E^4$, and this is indeed the case if the coupling constants are not carefully chosen. Unfortunately, tree level amplitudes are real and therefore never unitary in the strict sense - they only allow to estimate how large the corrections of the next order have to be to satisfy (3.3), giving an upper bound based on perturbative calculability. While in the SM the $\mathcal{O}(E^4)$ growth cancels between the three electroweak gauge bosons, the Higgs boson plays a central role in canceling the remaining $\mathcal{O}(E^2)$ growth, giving an upper bound of the Higgs mass of $m_H \leq \text{TeV}$. One can obtain more stringent bounds for massive vector bosons and the Higgs model going to the one loop level [24], leading to $m_H \leq 350 \text{ GeV}$. If the Higgs boson is heavier, it comes in too late to tame high

energy behavior and the perturbative description breaks down, leaving us with an effective theory and a cutoff scale $\Lambda \approx \text{TeV}$. Now, how is the situation in higgsless models? Obviously, something has to take over at low scales to cancel the $\mathcal{O}(E^2)$ growth of scattering amplitudes, and it is the Kaluza-Klein resonances which can do the job. Consider the graphs of elastic $2 \rightarrow 2$ charged gauge boson scattering in extra dimensions,



with the triple and quartic coupling constants g_{nnk} and g_{nnnn} . The asymptotical expansion of scattering amplitudes for high energies is of the form

$$\mathcal{M} \approx c + bE^2 + aE^4 \quad (3.4)$$

$$a \propto g_{nnnn} - \sum_k g_{nnk}^2, \quad b \propto \frac{4}{3}M_n^2 g_{nnnn} - \sum_k g_{nnk}^2 M_k^2 \quad (3.5)$$

Many more similar, but more complicated expressions hold for the inelastic case [25]. It is surely not by chance that any model would satisfy these conditions. Fortunately, due to Ward identities and 5D BRST invariance, one can satisfy all of them at once simply by choosing appropriate boundary conditions. A detailed discussion of these connections can be found in [26]. The advantage of extra dimensional models as opposed to 4D models or deconstructed models of massive Yang-Mills theory is the absence of derivative couplings for the would-be Goldstone bosons. It is sufficient to have BRST invariance and from it Goldstone boson equivalence for high energy vector scattering, and good high energy behavior follows. Derivative couplings of A_5 as they are present for example for the link fields in deconstructed higgsless models such as in [27] only come in as effective operators at the cutoff scale and can be the more suppressed the better the unitarization from Kaluza-Klein modes works.

3.2 Warped Higgsless Models

Let us first give a short description of the higgsless models our construction is based upon, which are due to Csaki et al. [15, 10]. They feature a left-right symmetric gauge group¹

$$G = SU(3)_C \times SU(2)_L \times SU(2)_R \times U(1)_{B-L} \quad (3.6)$$

¹The general case $g_L \neq g_R$ has been studied in the literature and it turned out not to be an effective means to improve precision fits and perturbative unitarity. We therefore assume the gauge action to be LR symmetric in the bulk for simplicity.

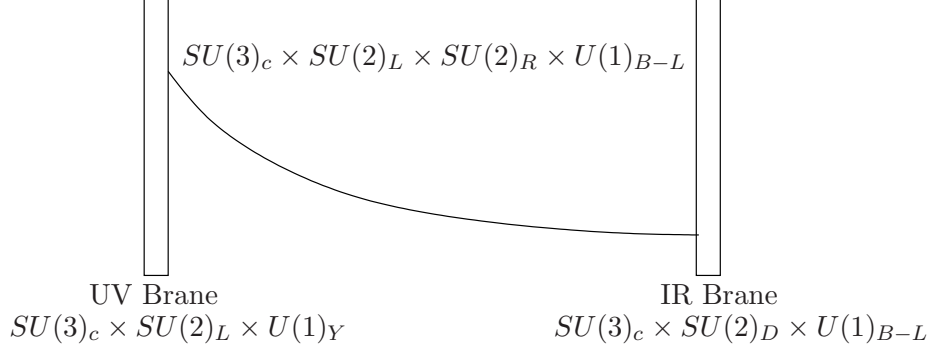


Figure 3.1: A gauge breaking scenario for warped higgsless models. The diagonal subgroups which remain unbroken in the entire space are QCD and electromagnetism, $SU(3)_c \times U(1)_Q$.

where X will be the $(B - L)/2$ quantum number which is $1/6$ for quarks and $-1/2$ for leptons. The corresponding coupling constants are g_{5s} , $g_L = g_R = g_{ew}$ and \tilde{g}_{ew} . The natural hierarchy in the warped background is used to break electroweak symmetry at an IR scale while the LR symmetry which is present in the gauge group is broken on the UV brane. This results in a breaking scheme

$$G \rightarrow \begin{cases} SU(3)_C \times SU(2)_L \times U(1)_Y & \text{on the UV brane} \\ SU(3)_C \times SU(2)_D \times U(1)_X & \text{on the IR brane} \end{cases}, \quad (3.7)$$

leaving only an overall $SU(3)_C \times U(1)_{EM}$ unbroken. This is illustrated in figure 3.1. The model exploits the fact that, in the SM, the hypercharge assignments can be “explained” using baryon and lepton number and a righthanded isospin.

$$Q = \frac{B - L}{2} + T_L^3 + T_R^3, \quad Y/2 = \frac{B - L}{2} + T_R^3 \quad (3.8)$$

The diagonal subgroup $SU(2)_D$ generated by $T_D^a = T_L^a + T_R^a$ acts as custodial symmetry.

In the most radical variety of these models which we use, all gauge symmetry breaking is done purely by boundary conditions. They can be obtained by putting Higgs doublets in the appropriate representations on the boundaries. Localized scalar VEVs can be translated into effective boundary conditions, and taking the limit $v \rightarrow \infty$ causes the localized dynamical scalar fields to decouple. For example, the scalar on the IR brane is in a fundamental representation under $SU(2)_L$ and $SU(2)_R$ and its VEV breaks $SU(2)_L \times SU(2)_R$ down to the $SU(2)_D$ which plays a role in reproducing $\rho \approx 1$. Let us analyze how this works in detail

on the Planck brane [25]. The covariant derivative of the VEV is

$$D_\mu \langle \phi \rangle = -v \frac{i}{2\sqrt{2}} \left[g_{ew} \begin{pmatrix} \sqrt{2} A_\mu^{R+} \\ -A_\mu^{R3} \end{pmatrix} + \tilde{g}_{ew} \begin{pmatrix} 0 \\ B_\mu \end{pmatrix} \right]_{y=0} \quad (3.9)$$

and the VEV-dependent non-kinetic part of the Klein-Gordon Lagrangian becomes

$$D_\mu \langle \phi \rangle^\dagger D^\mu \langle \phi \rangle = \frac{v^2}{4} g_{ew} A_\mu^{R+} A^{R-\mu} |_{y=0} + \frac{v^2}{8} (\tilde{g}_{ew} B_\mu - g_{ew} A_\mu^{R3})^2 |_{y=0} \quad (3.10)$$

The variation of this yields

$$\delta_B (D_\mu \langle \phi \rangle^\dagger D^\mu \langle \phi \rangle) = \frac{v^2}{4} \tilde{g}_{ew} (\tilde{g}_{ew} B_\mu - g_{ew} A_\mu^{R3}) |_{y=0} \quad (3.11)$$

$$\delta_{A^\pm} (D_\mu \langle \phi \rangle^\dagger D^\mu \langle \phi \rangle) = \frac{v^2}{4} g_{ew} A^\mp |_{y=0} \quad (3.12)$$

$$\delta_{A^3} (D_\mu \langle \phi \rangle^\dagger D^\mu \langle \phi \rangle) = -\frac{v^2}{4} g_{ew} (\tilde{g}_{ew} B_\mu - g_{ew} A_\mu^{R3}) |_{y=0} \quad (3.13)$$

This can already be part of a viable model of warped electroweak symmetry breaking for finite v , but taking the limit, we generate a set of Dirichlet boundary conditions,

$$\tilde{g}_{ew} B_\mu - g_{ew} A_\mu^{R3} = 0, \quad A^{R\pm} = 0 \quad (3.14)$$

which represent the higgsless limit of the breaking of

$$SU(2)_L \times SU(2)_R \times U(1)_{B-L} \rightarrow SU(2)_L \times U(1)_Y$$

The BCs for the gauge fields (and later on those of their scalar and fermionic superpartners) which can be obtained in this way are compatible with the breaking scenario and with variation of the boundary action. From now on we keep in mind the possibility to generate higgsless limits from brane Higgs models, and simply assign conditions consistent with the action, symmetries and ward identities as required. The full set of gauge sector boundary conditions for the warped higgsless model is given by [25]

$$\hat{A} \begin{pmatrix} A_\mu^L \\ A_\mu^R \\ B_\mu \end{pmatrix} = \hat{A}' \begin{pmatrix} A_5^L \\ A_5^R \\ B_5 \end{pmatrix} = \hat{B} \begin{pmatrix} A_\mu^L \\ A_\mu^{R12} \\ A_\mu^{R3} \\ B_\mu \end{pmatrix} = \hat{B}' \begin{pmatrix} A_5^L \\ A_5^{R12} \\ A_5^{R3} \\ B_5 \end{pmatrix} = 0 \quad (3.15)$$

where the boundary matrices are defined as

$$\hat{A} = \left(\begin{array}{ccc} 1 & -1 & 0 \\ \partial_y & \partial_y & 0 \\ 0 & 0 & \partial_y \end{array} \right) \Big|_{y=\pi} \quad \hat{B} = \left(\begin{array}{cccc} \partial_y & 0 & 0 & 0 \\ 0 & 1 & 0 & 0 \\ 0 & 0 & \tilde{g}_{ew}\partial_y & g_{ew}\partial_y \\ 0 & 0 & -g_{ew} & \tilde{g}_{ew} \end{array} \right) \Big|_{y=0} \quad (3.16)$$

From gauge invariance, we obtain the corresponding would-be Goldstone boundary conditions,

$$\hat{X}' = \hat{X}(\partial_y \leftrightarrow 1) e^{-2Rky} \quad (3.17)$$

By virtue of these BCs, the W^\pm is a mixture of the $SU(2)_L$ and $SU(2)_R$ gauge bosons (localized in the $SU(2)_L$ field up to one permille in order to ensure the observed $V - A$ coupling), the Z and γ are a mixture of the $SU(2)_L$, $SU(2)_R$ and $U(1)_{B-L}$ gauge bosons. For this reason, the neutral boson tower will be 3/2 as dense, with modes which can be identified as either roughly W -like or B -like. The UV brane kinetic term which we will introduce later is that of 4D $SU(2)_L$ gauge theory and has the form

$$S \rightarrow S + \kappa \int d^5x \delta(y - 0+) \pi R \left(-\frac{1}{4} \eta^{\mu\rho} \eta^{\nu\omega} L_{\mu\nu}^a L_{\rho\omega}^a \right) \quad (3.18)$$

We pull the volume factor πR out of the constants κ and β to simplify the following expressions. In addition, we will use a IR brane localized kinetic term for the $SU(2)_D$ group,

$$S \rightarrow S + \beta \int d^5x \delta(y - \pi + 0+) \pi R \left(-\frac{1}{4} \eta^{\mu\rho} \eta^{\nu\omega} (L_{\mu\nu}^a L_{\rho\omega}^a + R_{\mu\nu}^a R_{\rho\omega}^a) \right) \quad (3.19)$$

Since those are the full gauge invariant terms with interactions, adding them not only modifies the boundary conditions and the scalar product of the gauge bosons but also contributes to the effective gauge boson coupling constants. In the case of $SU(2)_L$, the canonical normalization conditions for the W^\pm , Z and photon Kaluza-Klein wave functions are affected as follows:

$$\int dy R \left(f^{L12(n)}(y)^2 + f^{R12(n)}(y)^2 \right) + \pi R \kappa f^{L12(n)}(0)^2 + \pi R \beta \left(f^{L12(n)}(\pi)^2 + f^{R12(n)}(\pi)^2 \right) = 1 \quad (3.20a)$$

$$\int dy R \left(f^{L3(n)}(y)^2 + f^{R3(n)}(y)^2 + f^{X(n)}(y)^2 \right) + \pi R \kappa f^{L3(n)}(0)^2 + \pi R \beta \left(f^{L3(n)}(\pi)^2 + f^{R3(n)}(\pi)^2 \right) = 1 \quad (3.20b)$$

$$\pi R \left((2 + \kappa + 2\beta) \left(\frac{a_0}{g_{ew}} \right)^2 + \left(\frac{a_0}{\tilde{g}_{ew}} \right)^2 \right) = 1 \quad (3.20c)$$

The Neumann BC for the 5D fields is modified to

$$\partial_y A_\mu^L(0) = 0 \rightarrow (\partial_y + m^2 \pi R^2 \kappa) A_\mu^L(0) = 0. \quad (3.21)$$

$$\partial_y (A_\mu^L + A_\mu^R)(\pi) = 0 \rightarrow (\partial_y - m^2 \pi R^2 \beta e^{2Rk\pi}) (A_\mu^L + A_\mu^R)(\pi) = 0 \quad (3.22)$$

The constants κ and β are dimensionless and naturally of $\simeq \mathcal{O}(1)$. The coupling of Kaluza-Klein modes to the β term is however so large that we will always have $\beta < 0.1$ (section 8.2). The effective 4D coupling constant of gauge bosons is now

$$g_{nml} = g_{ew} \left[\int_0^\pi dy R (f_n^L f_m^L f_l^L + f_n^R f_m^R f_l^R) + R\pi\kappa f_n^L f_m^L f_l^L(0) + R\pi\beta (f_n^L f_m^L f_l^L + f_n^R f_m^R f_l^R)(\pi) \right] \quad (3.23)$$

$$g_{nmrl} = g_{ew}^2 \left[\int_0^\pi dy (f_n^L f_m^L f_l^L f_r^L + f_n^R f_m^R f_l^R f_r^R) + R\pi\kappa f_n^L f_m^L f_l^L f_r^L(0) + R\pi\beta (f_n^L f_m^L f_l^L f_r^L + f_n^R f_m^R f_l^R f_r^R)(\pi) \right] \quad (3.24)$$

The UV localized kinetic term has two effects: it raises the Kaluza-Klein scale relative to the W mass, which is generally not conducive to perturbative unitarity, and lowers the S precision observable somewhat, which is desirable. We adopt this approach in combination with the IR brane term which affects the light modes very little but lowers the mass of Kaluza-Klein modes at the expense of a larger value for S (section 8.2). For the lightest modes of W^\pm and Z which correspond to the standard model gauge bosons, they are given approximately by²

$$m_W^2 \simeq \frac{k e^{-2Rk\pi}}{(1 + \kappa) R \pi} \quad (3.25a)$$

$$m_Z^2 \simeq \frac{(g_{ew}/\tilde{g}_{ew})^2 + \kappa + 2}{(g_{ew}/\tilde{g}_{ew})^2 + 1} m_W^2, \quad (3.25b)$$

where the brane kinetic term (3.18) contributes the κ -dependence, while the term (3.19) is neglected for small β . To leading order in m/Λ_{IR} and $(Rk\pi)^{-1}$, the radius R is therefore determined by the RS curvature k and the W mass.

The leptons and quarks are implemented as in [17]. There are two doublets

²If the ratio g_{ew}/\tilde{g}_{ew} is determined from the particle masses, the deviations from the SM are shifted to the couplings. To make the tree level corrections ‘‘oblique’’, this quantity should be defined by fixing the gauge couplings to matter first [17].

transforming under $SU(2)_L$ and $SU(2)_R$ respectively for each SM fermion

$$\Psi_L = (\psi_L^u, \overline{\psi_L^{uc}}, \psi_L^d, \overline{\psi_L^{dc}})^T \quad (3.26a)$$

$$\Psi_R = (\psi_R^u, \overline{\psi_R^{uc}}, \psi_R^d, \overline{\psi_R^{dc}})^T. \quad (3.26b)$$

The two doublets get 5D Dirac masses as defined in (2.61) and (4.34) denoted by c_L and c_R respectively which are allowed in the bulk where the theory is vectorlike. In the limit of massless fermion zero modes, we impose BCs such that ψ_L and ψ_R^c have a zero mode for which ψ_R and ψ_L^c vanish,

$$\psi_R(0) = \psi_R(\pi) = 0, \quad \psi_L^c(0) = \psi_L^c(\pi) = 0 \quad (3.27)$$

The mass of the zero modes is then lifted by a $SU(2)_D$ -invariant Dirac mass μ on the IR brane, resulting in modified effective BCs which mix Ψ_L and Ψ_R ,

$$\psi_R(\pi) = \mu\psi_L(\pi), \quad \psi_L^c(\pi) = -\mu\psi_R^c(\pi) \quad (3.28)$$

We now have degenerate massive $SU(2)$ fermion doublets. So far the treatment is the same for the quarks and leptons. They differ however in the way how the doublets are split on the UV brane where the theory is not invariant under $SU(2)_D$. Here, it is permitted to couple to localized fermions on the UV brane to split the doublets, or to add a localized kinetic term resulting in modified boundary conditions, scalar products and effective coupling constants. Consider the discussions in [10] about the different prescriptions how localized fermion terms can be converted to effective boundary conditions. We assume a localized kinetic term for the $SU(2)_R$ transforming fields on the UV brane controlled by a parameter ρ , which yields effective boundary conditions

$$f_q^R(0) = m\rho^2 f_q^R(0) \quad (3.29)$$

For neutrinos the situation is a little different than for quarks: The $SU(2)_R$ transforming neutrinos are singlets on the UV brane where $SU(2)_R \times U(1)_X$ is broken down to hypercharge, and the action of the two generators $Y/2 = T_R^3 - L/2 = 0$ exactly cancels. Thus they can receive a UV localized Majorana mass μ_r ,

$$\psi_\nu^R(0) = \frac{\mu_r}{k} \psi_\nu^{Rc}(0) \quad (3.30)$$

which for $\mu_r \gg \text{TeV}$ leads to a seesaw-like mechanism with light almost exactly lefthanded neutrinos (section D.1). To conclude, the mass of each fermion is determined by the UV splitting parameter, the IR mass and the 5D ‘‘bulk’’ masses of the doublets, c_L and c_R , which control the localization of the fermion zero modes. The resulting masses are approximately (for $c_L > 1/2$, $c_R < -1/2$)

$$m_f \simeq \frac{\sqrt{(1-2c_L)(1+2c_R)} (e^{Rk\pi})^{c_L-c_R-1} \mu}{\sqrt{1-(1+2c_R)} k \rho^2} \quad (3.31a)$$

$$m_\nu \simeq \frac{\mu^2}{\mu_r} (2c_L - 1) \left(e^{-2Rk\pi} \right)^{c_L - c_R - 1} \quad (3.31b)$$

In our implementation of the model, we do not rely entirely on approximation formulae for masses and effective coupling constants but solve the “exact” expressions numerically.

Like in Technicolor theories, the generation of Fermion masses is the most serious problem of this class of models, for many of the same reasons. The phenomenological challenges to warped higgsless models have been addressed extensively in the literature [10, 15, 28, 29, 30, 31, 32, 17, 33, 16, 34, 18, 35] from different perspectives, mainly concerning LEP precision observables STU and Zbb , perturbative unitarity and flavour changing operators.

In our implementation of flavour we restrict ourselves to generating realistic masses to limit the complexity of the model. In the work cited above, the generation of quark and lepton mixing on the UV and IR brane is discussed. The generation of flavour in the IR sector is strongly constrained and ruled out for $\Lambda_{IR} \approx \text{TeV}$ [36, 37, 38]. Thus, it seems unlikely that the mechanisms which have been devised to explain flavour using a warped background [39, 37] are transferable to warped higgsless models which are bound to have Kaluza-Klein gluons and other resonances at the TeV scale to satisfy unitarity constraints. The implementation of realistic quark and lepton mixing angles in the extended model is an interesting and challenging objective for further study.

3.3 Why do We Need to Extend Higgsless Models

Models in extra dimensions can be set up to contain stable particles without having to introduce new fields beyond the SM particle content. They are known as models of “Universal Extra Dimensions” (UED) and provide an interesting mechanism to explain the DM content of the universe [40]. This class of models very much restricts the allowed boundary conditions and boundary operators which is one of its strengths. It is owed to an exact mirror symmetry of the extra dimension, $y \rightarrow \pi/2 - y$ which all operators and boundary conditions have to obey. As a consequence, the Kaluza-Klein eigenmodes have definite parity called Kaluza-Klein parity,

$$f^n(y) = \pm f^n(\pi/2 - y) \quad (3.32)$$

Since all interactions can be chosen to be parity-even, the lightest parity-odd Kaluza-Klein mode (LKP) is automatically stable, even when radiative corrections are included. Unfortunately, this mechanism is not suitable in our case. We have seen above that higgsless models heavily rely on different physics on both boundaries to realize a realistic gauge symmetry breaking scenario. Also, the warped background is of course not even under this kind of KK parity. Still, the presence of a stable neutral particle is essential to cosmology as has been outlined in the introduction. There are now several ways how one can proceed:

- Extend the particle spectrum in some way and introduce an internal parity such as R parity, T parity etc. under which one or some of the new particles are odd [41, 42, 43].
- Extend the space, for example to two warped intervals glued together, to regain a KK-even background and thus KK parity as a good quantum number [44].
- There exists the possibility that some 5D gauge theories can contain stable Skyrminion-like topological defects [45].

We are going to follow the first approach [41]. There is an infinite number of ways to extend the particle spectrum of any theory, but one of them, SUSY, has been particularly successful and unique as it is the only nontrivial extension of the Poincaré group in four dimensions. As we will see, SUSY will provide us with the necessary particle candidate for DM once we employ an R parity, and yields an interesting and characteristic spectrum of superpartners. Before we can proceed with the extension of the models, we have to review the properties of SUSY in warped space, and introduce the tools necessary to formulate the supersymmetric action and boundary conditions.

Chapter 4

Supersymmetry in Warped Space

Interesting if true.

- *Rich Little's Head on Futurama*

4.1 Killing Spinors and Global Supersymmetry in Warped Space

It is natural to allow for supergravity in the bulk of a warped extra dimension. In terms of *AdS/CFT* language, a CFT with global supersymmetry has local supersymmetry in *AdS*₅ and will exhibit spin 3/2 and spin 2 resonances corresponding to the 5D Kaluza-Klein graviton and gravitinos. We do not want to insist on this interpretation, and it will greatly simplify the task of determining the low energy phenomenology of our model if we have a means to separate 5D gravity from matter and gauge multiplets. Therefore it is useful to introduce the notion of global supersymmetry in *AdS*₅. This can be done in two ways - either those supersymmetry transformations are determined which do not affect the gravitino, or equivalently, those which close into a Killing vector and thus leave the metric invariant.

In the case of flat extra dimensions, the SUSY algebra in Minkowski space can be generalized straightforwardly to five dimensions by using the corresponding Clifford algebra and promoting the parameters to four component spinors. The commutator of two transformations then still reads

$$[\delta_\eta, \delta_\xi] = -2(\bar{\eta}\gamma^M\xi - \bar{\xi}\gamma^M\eta)P_M, \quad (4.1)$$

where the gamma matrices are now defined such that

$$\{\gamma^M, \gamma^N\} = 2\eta^{MN}, \quad M, N = 0 \dots 3, 5. \quad (4.2)$$

Expressing the 5D $\mathcal{N} = 1$ -SUSY algebra in terms of four component generators,

$$\{Q_i, \overline{Q}_j\} = -2\gamma_{ij}^M P_M = -2\gamma_{ij}^\mu P_\mu - 2\gamma_{ij}^5 P_5, \quad (4.3)$$

a comparison with the 4D $\mathcal{N}=2$ -SUSY algebra reveals that iP_5 plays the role of a central charge in the 4D picture [46]. Since translations leave the metric η_{MN} invariant, we are dealing with a global spacetime symmetry.

Moving on to a warped background, we retain the approximation of neglecting the backreaction, as stated above. Following the approach of [47] for the treatment of a curved background, we define global SUSY transformations by demanding that these global SUSY transformations close into a Killing vector field v of the background metric. In particular

$$[\delta_\xi, \delta_\eta] = v^N P_N \quad (4.4)$$

and the Killing condition for v reads

$$v^M \partial_M g_{AB} + g_{AM} \partial_B v^M + g_{BM} \partial_A v^M = 0, \quad (4.5)$$

while the gamma matrices satisfy now

$$\{\gamma^M, \gamma^N\} = 2g^{MN}. \quad (4.6)$$

This gives us a condition for the spinor valued parameters of the SUSY transformations, and solutions (ξ, η) of (4.4) and (4.5) are called Killing spinors.

There are the usual 4D Poincaré symmetries and an additional scaling symmetry $x^M \rightarrow (1 + \delta)x^M$ which is broken only by the presence of the branes. Working out the Killing condition (4.4) and (4.5) in this background, one ends up with a set of SUSY parameters which generate SUSY transformations that close into the remaining symmetries, namely, using 2-spinor notation,

$$\xi(x, y) = e^{-Rky/2} \begin{pmatrix} \xi_\alpha^0 \\ 0 \end{pmatrix}, \quad (4.7)$$

where the space-time dependence remains confined to the warp factor. This relation fixes the KK wave functions of the superpartners. Since (4.7) is parameterized by a single Weyl-spinor, there can be at most one 4D supersymmetry left after integrating out the extra dimension. Nevertheless, we will see in the following sections, that the spectrum of the massive KK modes will formally be that of 4D $\mathcal{N} = 2$ -SUSY.

We can conclude from the above considerations that in unbroken $\mathcal{N} = 1$ SUSY, the Kaluza-Klein wave functions within one 4D multiplet should only differ by factors of $e^{-Rky/2}$. Looking at the generic solutions for Kaluza-Klein wave functions of scalars, spinors and vectors in section 2.3, it is clear that the bulk masses of scalars and spinors are constrained by supersymmetry. First of all, sfermions

belonging to a fermion with bulk mass $M_f = ck$ have to fulfil

$$\begin{aligned}\sqrt{4 + M_s^2/k^2} &= c + 1/2 & (4\text{D lefthanded}) \\ \sqrt{4 + M_s^2/k^2} &= c - 1/2 & (4\text{D righthanded})\end{aligned}\tag{4.8}$$

The Kaluza-Klein wave functions of A_μ always come with a J_1 or Y_1 while A_5 features J_0 and Y_0 , which is only consistent with the gaugino bulk mass choice

$$c(\text{Gauginos}) = 1/2\tag{4.9}$$

Further scalar partners of A_5 need to fulfil

$$\sqrt{4 + M_s^2/k^2} = 0 \Rightarrow M_s^2 = -4k^2\tag{4.10}$$

This is a negative mass squared which would certainly pose a problem in flat space. In the warped background however there are no tachyonic solutions for this choice due to the Breitenlohner-Freedman bound which holds for AdS_5 , and the mass term vanishes in the flat limit $k \rightarrow 0$. We will now review a formalism which gets all these conditions right automatically along with the supersymmetric gauge interactions.

4.2 Formulating Warped Supersymmetry Using 4D $\mathcal{N} = 1$ Superfields

Naïvely, the formalism using ordinary 4D $\mathcal{N} = 1$ superfields is not suitable to treat theories with two supercharges or, equivalently, 5D $\mathcal{N} = 1$ supersymmetry. There are developments in this direction (harmonic superspace) which will not be pursued further in this work. However, if one takes a hybrid approach which furnishes the kinetic terms ∂_μ acting on four of the five dimensions through the $\sigma^\mu \bar{\theta} \partial_\mu$ and $\theta^4 \square$ components of chiral superfields as usual while putting the remaining ones involving ∂_5 in by hand, one can use the well known and comparatively simple formalism involving 4D $\mathcal{N} = 1$ vector- and chiral superfields. By choosing a convenient coordinate frame, the dimension receiving the special treatment will coincide with the compact direction of the extra dimension which is treated separately during Kaluza-Klein reduction (and Holography, for that matter) anyhow, and there is thus no great disadvantage from the fact that neither 5D Lorentz invariance nor 5D Supersymmetry are manifest.

Using ordinary superfields for SUSY in higher dimensions was considered in detail already in 1983 by [48], where the authors extend the formalism for treating 4D $\mathcal{N} = 4$ SUSY to the maximal case of 10D $\mathcal{N} = 1$ SUSY. They also present the extended gauge and supersymmetry transformations and the action for the resulting vector- and triplet of chiral superfields. The explicit formalism in 5D and 6D was presented again more recently in [49] for flat space and then extended to a slice of AdS_5 in [50]. We shall now summarize the aspects relevant for this work in some detail and discuss the straightforward extension of the formalism

to nonabelian gauge theory in AdS_5 . Note that evaluating the larger traces of superfields including group generators as well as Berezin integrals by hand to recover the action in component fields can be cumbersome and was partly done using a FORM program outlined in appendix E.4.

The Gauge Multiplet

In order to be able to express the action for matter in a gauge invariant form right away, let us start discussing how to extend 4D Supersymmetric Yang-Mills theory to five dimensions. Our convention for the expansion in components of the vector superfield in Wess-Zumino gauge is

$$V^a = -\theta\sigma^m\bar{\theta}A_m^a - i\bar{\theta}^2\theta\lambda_1^a + i\theta^2\bar{\theta}\lambda_1^a + \frac{1}{2}\theta\theta\bar{\theta}\bar{\theta}D^a \quad (4.11)$$

In the following, $V \equiv V^a T^a$ where T^a are the generators of the gauge group in question. At this point the Yang-Mills gauge coupling is still absorbed in the fields and $[V] = 0$. There are two important objects that can be built from this, namely the superfield from the exponential and its inverse

$$e^{\pm V} \quad (4.12)$$

and a superfield

$$W_\alpha = -\frac{1}{4}\overline{DD}e^V D_\alpha e^{-V} \quad (4.13)$$

which is automatically chiral as it fulfils $\overline{D}_\beta W_\alpha = 0$ by virtue of the covariant derivative's properties. As usual, a chiral superfield $\Phi = \Phi^a T^a$

$$\Phi = \phi + i\theta\sigma^m\bar{\theta}\partial_m\phi - \frac{1}{4}\theta\theta\bar{\theta}\bar{\theta}\square\phi + \sqrt{2}\theta\omega - \frac{i}{\sqrt{2}}\theta\theta\partial_m\omega\sigma^m\bar{\theta} + \theta\theta G \quad (4.14)$$

acts as the supergauge parameter:

$$e^V \longrightarrow e^\Phi e^V e^{\bar{\Phi}} \quad (4.15)$$

We consequently have to define W_α to end on e^{-V} because then

$$W_\alpha \longrightarrow e^\Phi W_\alpha e^{-\Phi} \quad (4.16)$$

The real scalar $\alpha = -\text{Im}\phi$ can be identified with the usual bosonic gauge parameter via Baker-Campbell-Hausdorff,

$$A_\mu^a \longrightarrow A_\mu^a - 2\partial_\mu\alpha^a + f^{abc}\alpha^b A_\mu^c \quad (4.17)$$

Only after the redefinition $V \longrightarrow 2g_{YM}V$ does this take the conventional form

$$A_\mu^a \longrightarrow A_\mu^a - \frac{1}{g_{YM}}\partial_\mu\alpha^a + f^{abc}\alpha^b A_\mu^c \quad (4.18)$$

Now we would like to extend this to 5D. As a first step, we give all fields including the gauge parameter a formal dependence on a new parameter y . It is well-known that the 4D $\mathcal{N} = 2$ gauge multiplet as well as the 5D and 6D $\mathcal{N} = 1$ gauge multiplet have the same field content as one $\mathcal{N} = 1$ gauge multiplet and one $\mathcal{N} = 1$ chiral multiplet [46]. The fifth component of the vector field is a 4D scalar and should therefore be part of the complex scalar in the chiral multiplet. Since the gauge parameter is a chiral superfield with the bosonic gauge parameter as imaginary part, it is clear that the scalar in the gauge sector chiral superfield should be of the form $A = (\Sigma + iA_5)/\sqrt{2}$ with

$$\chi = A + i\theta\sigma^m\bar{\theta}\partial_m A - \frac{1}{4}\theta\theta\bar{\theta}\bar{\theta}\square A + \sqrt{2}\theta\lambda_2 - \frac{i}{\sqrt{2}}\theta\theta\partial_m\lambda_2\sigma^m\bar{\theta} + \theta\theta C \quad (4.19)$$

The real component Σ is a new scalar field which in 6D would be identified with A_6 . The vector should transform as

$$A_5^a \longrightarrow A_5^a - 2\partial_y\alpha^a + f^{abc}\alpha^b A_5^c \quad (4.20)$$

The result of the gauge transformation on χ must again be a chiral superfield, so only Φ can be involved. This leads us to the 5D supergauge transformation law

$$\chi \longrightarrow e^\Phi(\chi - \sqrt{2}\partial_y)e^{-\Phi} \quad (4.21)$$

Using the above redefinition, we get fundamental and adjoint covariant derivatives with the following sign conventions

$$D_M\Psi = (\nabla_M - ig_{YM}A_M^a T^a)\Psi \quad (4.22)$$

$$(D_M\Phi)^a = \nabla_M\Phi^a + g_{YM}f^{abc}A_M^b\Phi^c. \quad (4.23)$$

The challenging part is now to find gauge and SUSY invariant combinations which give us the complete 5D gauge theory. It can be easily checked that the expression proposed by the authors mentioned above,

$$\int d^4\theta \operatorname{tr} \left[(\sqrt{2}\partial_y + \bar{\chi})e^{-V}(-\sqrt{2}\partial_y + \chi)e^V + \partial_y e^{-V}\partial_y e^V \right] \quad (4.24)$$

satisfies this requirement. The 4D part is $\int d\theta^2 WW + h.c.$ as usual, and the normalization of generators is

$$\operatorname{tr}[T^a T^b] = N\delta^{ab} \quad (4.25)$$

Thus the 5D action is given by

$$S_g[V, \chi] = \int d^5x \int d^2\theta \frac{R}{16Ng_{YM}^2} \operatorname{tr}[W^\alpha W_\alpha] + h.c.$$

$$+ \int d^5x \int d^4\theta \frac{1}{4R N g_{YM}^2} \text{tr}[(\sqrt{2}\partial_y + \bar{\chi})e^{-V}(-\sqrt{2}\partial_y + \chi)e^V + \partial_y e^{-V} \partial_y e^V] \quad (4.26)$$

In warped space, the density e^{-4Rky} cancels with the two inverse metric tensors of F^2 , so the first part of the action is already complete. To give the vector field its correct canonical 5D kinetic term

$$\int dy \eta^{\mu\nu} R e^{-2Rky} \partial_y A_\mu \partial_y A_\nu$$

however, we need to add it in the second part of the action. The final 5D SYM action in AdS_5 reads

$$\begin{aligned} S_g[V, \chi] = & \int d^5x \int d^2\theta \frac{R}{16N g_{YM}^2} \text{tr}[W^\alpha W_\alpha] + \text{h.c.} \\ & + \int d^5x \int d^4\theta \frac{e^{-2Rky}}{4R N g_{YM}^2} \text{tr}[(\sqrt{2}\partial_y + \bar{\chi})e^{-V}(-\sqrt{2}\partial_y + \chi)e^V + \partial_y e^{-V} \partial_y e^V] \end{aligned} \quad (4.27)$$

All we have to do now is to perform field redefinitions on the remaining components of the multiplet to give them proper units and canonical kinetic terms with general covariant derivatives according to their spin:

$$\begin{aligned} A_\mu & \longrightarrow 2g_{YM} A_\mu, & \lambda_1 & \longrightarrow 2g_{YM} e^{-\frac{3}{2}Rky} \lambda_1, \\ A_5 & \longrightarrow 2g_{YM} R A_5, & \lambda_2 & \longrightarrow -2ig_{YM} R e^{-\frac{1}{2}Rky} \lambda_2, & \Sigma & \longrightarrow 2g_{YM} R \Sigma \end{aligned} \quad (4.28)$$

To have supersymmetry, the fields get bulk masses which are already encoded in this action, and boundary localized masses, which will be implemented through effective boundary conditions. More on this will be said in the section on boundary conditions and the spectrum.

The Hypermultiplet

As we have seen in the previous sections, the natural extension of the chiral multiplet to five dimensions is obtained by adding a second chiral fermion as demanded by 5D Lorentz invariance and with it the corresponding scalar partners. We then get the so-called Hypermultiplet, and it is not surprising that it can be seen as a combination of a chiral and an antichiral superfield. This shall now be made explicit. We expand the chiral superfield as follows

$$H = h + i\theta\sigma^m\bar{\theta}\partial_m h - \frac{1}{4}\theta\theta\bar{\theta}\bar{\theta}\square h + \sqrt{2}\theta\psi - \frac{i}{\sqrt{2}}\theta\theta\partial_m\psi\sigma^m\bar{\theta} + \theta\theta F \quad (4.29)$$

and in an analogous way the antichiral superfield which is basically the complex conjugate of a chiral superfield, is given by

$$\overline{H}^c = h^{c\dagger} - i\theta\sigma^m\overline{\theta}\partial_m h^{c\dagger} - \frac{1}{4}\theta\theta\overline{\theta}\overline{\theta}\square h^{c\dagger} + \sqrt{2}\overline{\theta}\psi^c + \frac{i}{\sqrt{2}}\overline{\theta}\theta\sigma^m\partial_m\overline{\psi}^c + \overline{\theta}\theta F^{c\dagger} \quad (4.30)$$

The gauge transformations are exactly like those of a hypermultiplet in 4D, namely

$$H \longrightarrow e^\Phi H, \quad \overline{H}^c \longrightarrow e^{-\overline{\Phi}}\overline{H}^c \quad (4.31)$$

such that the real superfields $\overline{H}e^{-V}H$ and $H^ce^V\overline{H}^c$ are gauge invariant, supplying us with the usual 4D kinetic terms. There are also gauge invariant chiral superfields, H^cH and $\overline{H}\overline{H}^c$ which are used to write down mass terms. Can a 5D kinetic term be constructed as well with what we have so far? The answer is yes, because χ can be used to compensate the derivative ∂_y acting on Φ in the following manner,

$$H^c(\partial_y - \frac{1}{\sqrt{2}}\chi)H \quad (4.32)$$

the θ^2 component of which gives us a 5D kinetic term for the multiplet. The complete action of a hypermultiplet of mass M_5 coupled to 5D SYM is thus

$$\begin{aligned} S_h[H, H^c, V, \chi] = & \int d^5x R \int d^4\theta \left[\overline{H}e^{-V}H + H^ce^V\overline{H}^c \right] \\ & + \int d^5x R \int d^2\theta H^c \left[\partial_y/R - \frac{1}{\sqrt{2}R}\chi - M_5 \right] H + \text{h.c.} \end{aligned} \quad (4.33)$$

Introducing the correct density factors in warped space as determined in [50], we finally obtain the offshell action of a hypermultiplet coupled to SYM in warped space,

$$\begin{aligned} S_h[H, H^c, V, \chi] = & \int d^5x R \int d^4\theta e^{-2Rky} \left[\overline{H}e^{-V}H + H^ce^V\overline{H}^c \right] \\ & + \int d^5x R \int d^2\theta e^{-3Rky} H^c \left[\partial_y/R - \frac{1}{\sqrt{2}R}\chi - \left(\frac{3}{2} - c\right)k \right] H + \text{h.c.} \end{aligned} \quad (4.34)$$

where the mass has been expressed in units of the RS curvature by introducing the bulk mass parameter c , and a shift of $3/2k$ has been added to generate the correct general covariant derivatives. The action of the fermions in the gauge multiplet corresponds to the choice $c = 1/2$. Again, a redefinition of fields has to be done in order to recover the canonical Lagrangian. In addition to (4.28), the substitution

$$\psi \longrightarrow e^{-\frac{1}{2}Rky}\psi, \quad \psi^c \longrightarrow e^{-\frac{1}{2}Rky}\psi^c \quad (4.35)$$

has to be performed.

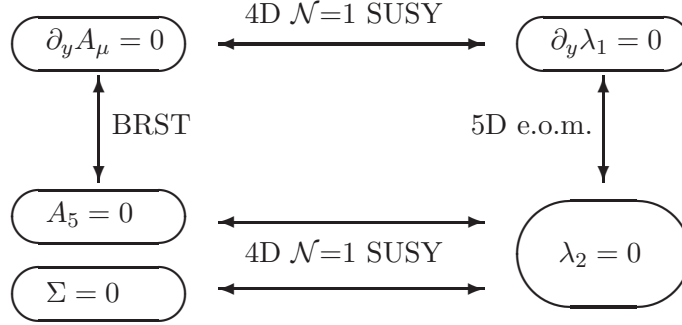


Figure 4.1: An illustration on how the boundary conditions within a 5D vector multiplet are naturally related by different consistency conditions imposed on the model.

4.3 Boundary Conditions for Supersymmetry

Before any further field redefinitions, the supersymmetric action as outlined above includes bulk mass terms to the effect that, indeed, the same bulk equations of motion and the same basis of Kaluza-Klein solutions are bestowed upon all components within each superfield. It should be noted that this is the case for the gauge sector only after a suitable gauge fixing term is introduced. There is only one Killing spinor in warped space, and consequently this kind of degeneracy is not present within entire 5D supermultiplets. This is visible already before supersymmetry is introduced since the ψ^c fermions have Kaluza-Klein wave functions which differ from those of ψ and the same is true for A_μ and A_5 . To conserve at least one supersymmetry, the boundary conditions have to fulfil the right relations to make sure that even the actual Kaluza-Klein wave solutions and corresponding mode masses are the same throughout the 4D multiplets, and this is obviously the case if the superfields themselves are assigned to boundary conditions which are shared by all coefficient fields. Let us start with the gauge sector, which consists of two real scalars, a dirac spinor and a 4D vector. First of all, we would like to have BRST invariance of the massless sector and a nonlinear realization for the massive modes. This dictates to us the boundary conditions of A_5 and therefore of the chiral superfield. Requiring one supersymmetry to remain intact fixes the boundary conditions for the remaining parts of the multiplet (figure 4.1). Assume n gauge fields $A_\mu^1 \dots A_\mu^n$ and $(n \times n)$ matrices N and D chosen such that the boundary action of A_μ^i vanishes and the symmetry breaking is consistent when

$$(N\partial_y + D)\vec{A}_\mu = 0 \quad (4.36)$$

Also, we assume that $\ker N \perp \ker D$. Then a consistent choice for the would-be Goldstone scalars is

$$(D\partial_y e^{-2Rky} + N)\vec{A}_5 = 0 \quad (4.37)$$

This translates to boundary conditions for the multiplets

$$(N\partial_y + D)\vec{V} = 0, \quad \left(D\partial_y e^{-2Rky} + N\right)\vec{\chi} = 0 \quad (4.38)$$

Similar reasoning applies for the Hypermultiplets, where

$$\psi = 0 \longrightarrow H = 0, \quad \psi^c = 0 \longrightarrow H^c = 0 \quad (4.39)$$

We now have all the tools to construct supersymmetric models of matter and gauge multiplets in warped space. In order to be able to do explicit calculations we have to determine the onshell action in terms of 5D component fields from the superfield expressions. This is done in appendix B. To illustrate the mechanism, we will first study an abelian toy model.

Chapter 5

A Toy Model: Warped sQED

The best way to see the formalism which we have introduced at work is in a simple abelian toy model, in our case an implementation of warped supersymmetric QED. There are certainly many different ways how one could embed QED in warped supersymmetry, and we do it in a way that is partly reminiscent of the full higgsless model treated later, but deviates from it in the way it implements fermions in order to discuss some challenges which will appear. We want $U(1)$ gauge theory with one fermion species, and we exploit the fact that, in contrast to electroweak theory, we do not need chiral fermions. We therefore have four superfields,

$$(V_Q, \chi_Q) \quad (H, H^c) \quad (5.1)$$

which house the “standard” fields A_μ , A_5 , ψ , ψ^c and their superpartners λ_1 , λ_2 , Σ , h and h^c . They have generic Kaluza-Klein wave functions given in (2.53), (2.62) and (2.71) using the parameters specified in (4.8), (4.9) and (4.10).

5.1 The Supersymmetric Spectrum

For unbroken electromagnetism, we assign boundary conditions $\oplus\oplus$ to V and $\ominus\ominus$ to χ . The tower of vector bosons, gauginos and gauge scalars is then determined by the eigenvalue problem

$$Y_0\left(m\frac{e^{Rk\pi}}{k}\right) = \frac{J_0\left(m\frac{e^{Rk\pi}}{k}\right)Y_0(m/k)}{J_0(m/k)} \quad (5.2)$$

There is a zero mode for the vector,

$$A_\mu(x, y) = A_\mu^0(x)\frac{g_4}{g_5} + \dots \quad (5.3)$$

and a corresponding zero mode of λ_1 ,

$$\lambda_1(x, y) = \lambda_1^0(x)e^{3/2Rky}\frac{g_4}{g_5} + \dots \quad (5.4)$$

while λ_2 , Σ and A_5 have no corresponding solution for $m = 0$ and vanish. Apart from the massless modes, the expression (5.2) is approximately satisfied when

$$J_0\left(m\frac{e^{Rk\pi}}{k}\right) \approx 0 \quad (5.5)$$

which leads to a mass spectrum of Kaluza-Klein modes

$$m_n \approx z_n k e^{-Rk\pi}, \quad z_n = 2.4, 5.52, 8.65 \dots \quad (5.6)$$

of degenerate massive photons, Dirac photinos and real scalar ‘‘sphotinos’’. Now let us construct the electron. If we assign boundary conditions $(\oplus\oplus, \ominus\ominus)$ to (ψ, ψ^c) we get a massless Weyl electron. This is certainly not satisfactory and we need to introduce a second hypermultiplet to get a complete light vectorlike electron. This is the way how it is done in the full model since there we need chiral fermion interactions anyhow, but let us try something else here: If we twist the boundary conditions on the IR brane, $(\oplus\ominus, \ominus\oplus)$, the massless electron mode is lifted to $m > 0$ and the 5D Dirac fermion provides a right-handed component. It will have a completely different Kaluza-Klein profile, but still couples universally to the massless delocalized gauge bosons. We have a free localization parameter c which we can use to dial the coupling strength of the electron to the IR brane to get realistic masses. With twisted IR boundary conditions, the electron and selectron towers are determined by the eigenvalue problem

$$Y_{c+1/2}\left(m\frac{e^{Rk\pi}}{k}\right) = \frac{J_{c+1/2}\left(m\frac{e^{Rk\pi}}{k}\right)Y_{c-1/2}(m/k)}{J_{c-1/2}(m/k)} \quad (5.7)$$

We want the electron to be much lighter than the Kaluza-Klein scale and therefore have to choose $c > 1/2$ to localize it sufficiently towards the UV brane. In this case we can, at least for the lightest modes, approximate the Bessel functions to first order using $(m/k)^{2c} \ll 1$ and $m \ll k e^{-Rk\pi}$, and get the condition

$$(1 - 4c^2) \left(\frac{m}{k}\right)^{2c-1} + \left(m\frac{e^{Rk\pi}}{k}\right)^{2c+1} = 0 \quad (5.8)$$

which further simplifies to

$$(1 - 4c^2) \frac{k^2}{m^2} + (e^{Rk\pi})^{2c+1} = 0 \quad (5.9)$$

giving us an approximation for our electron and selectron mass of

$$m^2 \approx (4c^2 - 1)k^2 e^{-(1+2c)Rk\pi} \quad (5.10)$$

The heavy Kaluza-Klein electron and selectron modes from (5.7) for $c > 1/2$ are mainly determined by the roots \tilde{z}_n of $J_{c+1/2}$ with

$$m_n \approx \tilde{z}_n k e^{-Rk\pi} \quad (5.11)$$

5.2 A Broken Spectrum

We have used warped space localization to generate a small electron mass from Dirac boundary conditions, but this comes at a price: We have used up our freedom to generate “soft” masses, and it is impossible to raise the selectron to a much larger scale purely by putting further selectron operators on the IR brane. We will be facing a similar dilemma later with electroweak and SUSY breaking. Let us therefore see what happens when we project out the light superpartners by twisting UV boundary conditions for the photino and selectrons. First we assign boundary conditions $(\ominus\oplus, \oplus\ominus)$ to (λ_1, λ_2) . The equation for the photino tower is now

$$Y_0\left(m\frac{e^{Rk\pi}}{k}\right) = \frac{J_0\left(m\frac{e^{Rk\pi}}{k}\right)Y_1(m/k)}{J_1(m/k)} \quad (5.12)$$

There is no zero mode for either λ_1 or λ_2 which is good, and no light almost-zero mode as we have it in the case of our electron, which is not so nice since SUSY is basically absent in the light sector. The above equation is again approximately satisfied when $J_0\left(m\frac{e^{Rk\pi}}{k}\right) = 0$, leading to a heavy photino spectrum which is almost degenerate with the heavy photons and sphotinos. We can now try to do the same to the selectrons by assigning $(\ominus\oplus, \ominus\oplus)$ to (h, h^c) which corresponds to twisting boundary conditions on the UV brane. This does unfortunately not work since we would get a zero mode of h^c , but unlike in the case of the fermions ψ and ψ^c , the two components h and h^c are not linked by 5D equations of motion or boundary terms and can be treated separately. This means that we are allowed to choose $(\ominus\ominus, \ominus\oplus)$, and there are no light selectrons left. We now have two separate equations from the eigenvalue problem,

$$\begin{aligned} Y_{c+1/2}\left(m\frac{e^{Rk\pi}}{k}\right) &= \frac{J_{c+1/2}\left(m\frac{e^{Rk\pi}}{k}\right)Y_{c+1/2}(m/k)}{J_{c+1/2}(m/k)} && \text{for } h \\ Y_{c+1/2}\left(m\frac{e^{Rk\pi}}{k}\right) &= \frac{J_{c+1/2}\left(m\frac{e^{Rk\pi}}{k}\right)Y_{c-1/2}(m/k)}{J_{c-1/2}(m/k)} && \text{for } h^c \end{aligned} \quad (5.13)$$

which gives us two nondegenerate selectron towers

$$m_n \approx z_n k e^{-Rk\pi} \quad (5.14)$$

where $z_n(h)$ are the positive roots of $J_{c+1/2}$ while $z_n(h^c)$ are the positive roots of $J_{c-1/2}$.

Let us plug in some numbers to check whether this works. We choose $k = 10^{19}$ GeV, $Rk\pi = 37.5$ and thus $ke^{-Rk\pi} \approx 518$ GeV which are typical values in warped EWSB models. There is of course the massless photon, and the massive photon and sphotino modes start at $m \approx 1266, 2880, 4500, \dots$ GeV. The photino tower from UV twisted boundary conditions is, apart from the missing massless mode, almost degenerate with the photons as it has $m \approx 1245, 2856, 4479, \dots$ GeV. We still have to choose the bulk Dirac mass c to fit

the electron mass. For our choice of parameters and $m_e \approx 5.11 \cdot 10^{-4}$ GeV, we need $c = 0.814$. The corresponding heavy electron resonances start at $m \approx 2200, 3863, 5500, \dots$ GeV. The “lefthanded” selectron h has the same spectrum within the accuracy shown here. The “righthanded” selectron h^c however has much lighter resonances $m \approx 1488, 3107, 4731, \dots$ GeV because it sees a Neumann boundary condition on the IR brane.

5.3 Effective Couplings

The warped gauge action for the abelian case can be derived from (4.27) by inserting the trivial generator $T = 1$. It simplifies a lot,

$$S_{abel}[V, \chi] = \int d^5x \int d^2\theta \frac{R}{16g_{YM}^2} W^\alpha W_\alpha + \text{h.c.} \\ + \int d^5x \int d^4\theta \frac{e^{-2Rky}}{4Rg_{YM}^2} \left(\partial_y V - \frac{1}{2}(\chi + \bar{\chi}) \right)^2 \quad (5.15)$$

while the gauge invariant action of the hypermultiplet essentially remains the same as (4.34),

$$S_h[H, H^c, V, \chi] = \int d^5x R \int d^4\theta e^{-2Rky} \left[\bar{H} e^{-V} H + H^c e^V \bar{H}^c \right] \\ + \int d^5x R \int d^2\theta e^{-3Rky} H^c \left[\partial_y/R - \frac{1}{\sqrt{2}R} \chi - \left(\frac{3}{2} - c \right) k \right] H + \text{h.c.} \quad (5.16)$$

The abelian gauge action contains no interactions as was to be expected, while the gauge coupling to matter gives us the following types of dimension four interactions between physical particles and auxiliary fields:

$$ee\gamma \quad \tilde{e}\tilde{e}\gamma \quad \tilde{e}\tilde{e}\gamma\gamma \quad e\tilde{e}\tilde{\gamma} \quad ee\Sigma \quad \tilde{e}\tilde{e}\Sigma\Sigma \quad D\tilde{e}\tilde{e} \quad C\tilde{e}\tilde{e} \quad F\tilde{e}\Sigma \quad (5.17)$$

Since the photon zero mode has a flat profile, it couples universally with the same strength because the overlap integral reduces to an expression proportional to the norm and can be used to set the 5D gauge coupling,

$$-g_5 \int dy Re^{-3Rky} \psi^c \sigma^\mu A_\mu \bar{\psi}^c \\ = -\psi^{c,r}(x) \sigma^\mu A_\mu^0(x) \bar{\psi}^{c,l}(x) \int dy Re^{-3Rky} g_4 f_{\psi^c}^r(y) f_{\psi^c}^l(y) + \mathcal{O}(A') \\ = -g_4 \psi^{c,r}(x) \sigma^\mu A_\mu^0(x) \bar{\psi}^{c,r}(x) + \mathcal{O}(A')$$

With this matching condition to the 4D effective coupling and the way we have defined the photon Kaluza-Klein zero mode, we get the 5D gauge coupling directly

from the canonical normalization condition for the photon,

$$\int_0^\pi dy R \left(\frac{g_4}{g_5} \right)^2 = 1 \Rightarrow g_5 = g_4 \sqrt{\pi R} \quad (5.18)$$

Now, all 4D tree level couplings are fixed as long as we do not introduce further operators (such as boundary terms). In particular, the lefthanded electron has the same coupling strength,

$$g_5 \int dy R e^{-3Rky} \frac{g_4}{g_5} f_\psi^r(y) f_\psi^l(y) = g_4 \quad (5.19)$$

In the unbroken SUSY case, there are relationships between the corresponding Kaluza-Klein wave functions given by the Killing spinor,

$$f_{\psi^c}^l = e^{1/2Rky} f_{hc}^l, \quad f_\psi^l = e^{1/2Rky} f_h^l, \quad f_{\lambda 1}^l = e^{3/2Rky} f_A^l, \quad \dots \quad (5.20)$$

from which we get identical effective couplings from supersymmetry,

$$e^{-3Rky} f_\psi^l f_\psi^r f_A^s = e^{-4Rky} f_h^l f_\psi^r f_{\lambda 1}^s \quad (5.21)$$

As a final point, let us look at the effective coupling constants of the first massive photon to left- and righthanded electrons. It is

$$g_5 \langle \psi^0 \psi^0 A^1 \rangle = -0.1871 g_4 \quad (5.22)$$

$$g_5 \langle \psi^{c,0} \psi^{c,0} A^1 \rangle = 6.55 g_4 \quad (5.23)$$

$$g_5 \langle \psi^1 \psi^1 A^1 \rangle = 5.0 g_4 \quad (5.24)$$

$$g_5 \langle \psi^{c,1} \psi^{c,1} A^1 \rangle = 3.8 g_4 \quad (5.25)$$

We notice that first of all, some couplings to light matter are suppressed while couplings between three heavy resonances can be an order of magnitude larger than the zero mode coupling. Secondly, the coupling of the righthanded electron to the heavy photon is also strongly enhanced with potentially disastrous consequences for precision tests. Realistic models avoid this problem by introducing a second electron field with $c < 0$ which is set up to contain the light righthanded fermion modes.

Chapter 6

Building the Extended Higgsless Model

Die Supersymmetrie ist viel zu schön, um sie zur Lösung des Hierarchieproblems zu verschwenden

- *Julius Wess, 2007*

6.1 The Superfield Content

Let us recapitulate the field content of the model before supersymmetrization: We have a 5D Yang-Mills theory with custodial symmetry,

$$SU(3)_c \times SU(2)_L \times SU(2)_R \times U(1)_X \quad (6.1)$$

which gives us the fields G_μ^a , G_5^a , A_μ^{Li} , A_5^{Li} , A_μ^{Ri} , A_5^{Ri} , B_μ , and B_5 . Since there are no chiral fermions in 5D, each flavor of matter gets two complete Dirac spinors. The Lepton components are in the representation

$$L_L \simeq (\mathbf{1}, \mathbf{2}, \mathbf{1}, -1) \quad L_R \simeq (\mathbf{1}, \mathbf{1}, \mathbf{2}, -1) \quad (6.2)$$

while quarks have

$$Q_L \simeq (\mathbf{3}, \mathbf{2}, \mathbf{1}, 1/3) \quad Q_R \simeq (\mathbf{3}, \mathbf{1}, \mathbf{2}, 1/3) \quad (6.3)$$

Each of the components consists of two Weyl spinors ψ_α and $\overline{\psi}^{c\dot{\alpha}}$. As was explained in Chapter 4, each 5D gauge field corresponds to one vector superfield and one chiral superfield carrying an adjoint index. Each Dirac spinor on the other hand corresponds to two chiral superfields in the fundamental containing ψ_α and ψ_α^c . This leads to the superfield content given in table 6.1 which represents the complete supersymmetric field content (up to boundary fields which can be added to modify the model further). As an example, the 4D gauge coupling

Field	Representations	Field	Representations
V^{Ca}, χ^{Ca}	8 of $SU(3)_C$	V^{Li}, χ^{Li}	3 of $SU(2)_L$
V^{Ri}, χ^{Ri}	3 of $SU(2)_R$	V^X, χ^X	$U(1)_{B-L}$
$H_{l,g}^L$	(1, 2, 1, -1)	$H_{l,g}^R$	(1, 1, 2, -1)
$H_{l,g}^{Lc}$	(1, $\bar{2}$, 1, 1)	$H_{l,g}^{Rc}$	(1, 1, $\bar{2}$, 1)
$H_{q,g}^L$	(3, 2, 1, 1/3)	$H_{q,g}^R$	(3, 1, 2, 1/3)
$H_{q,g}^{Lc}$	($\bar{3}$, $\bar{2}$, 1, -1/3)	$H_{q,g}^{Rc}$	($\bar{3}$, 1, $\bar{2}$, -1/3)

Table 6.1: The superfield content of the model and respective group representations under $SU(3)_c \times SU(2)_L \times SU(2)_R \times U(1)_X$, where $g = 1 \dots 3$ denotes the generation. The quantum numbers refer to the usual bosonic gauge transformations and it is implied that the vector fields also have the inhomogeneous transformation property.

of H_q^{Lc} is

$$\mathcal{L}_5 = \int d^4\theta H^c \exp \left[\frac{\lambda^a}{2} V_C^a + \frac{\sigma^i}{2} V_L^i + \frac{1}{2} \frac{1}{3} V_X \right] \bar{H}^c \quad (6.4)$$

6.2 Supersymmetric Boundary Conditions and Spectrum

In section 4.3 we have established explicit relations between the boundary conditions which have to be assigned to the components of a 5D supermultiplet to obtain a theory which is 4D $\mathcal{N} = 1$ SUSY and BRST invariant. From these rules and the conditions given in section 3.2 we can read off the complete set of boundary conditions for the higgsless model with supersymmetry. They are

$$\begin{bmatrix} 1 & -1 \\ \partial_y & \partial_y \end{bmatrix} \begin{bmatrix} V^L \\ V^R \end{bmatrix} \Big|_{y=\pi} = \begin{bmatrix} \partial_y & -\partial_y \\ 1 & 1 \end{bmatrix} e^{-2Rky} \begin{bmatrix} \chi^L \\ \chi^R \end{bmatrix} \Big|_{y=\pi} = 0, \quad (6.5a)$$

$$\partial_y V^X(\pi) = \chi^X(\pi) = \partial_y V^C(\pi) = \chi^C(\pi) = 0, \quad (6.5b)$$

$$H_{Lf}^c(\pi) + \mu H_{Rf}^c(\pi) = H_{Rf}(\pi) - \mu H_{Lf}(\pi) = 0 \quad (6.5c)$$

on the IR brane (i. e. $y = \pi$), where f runs over all leptons and quarks, and $\mu k e^{-Rk\pi}$ is the IR Dirac boundary mass parameter. On the UV brane (i. e. $y = 0$), we have

$$\begin{bmatrix} \tilde{g}_5 \partial_y & g_5 \partial_y \\ -g_5 & \tilde{g}_5 \end{bmatrix} \begin{bmatrix} V^{R3} \\ V^X \end{bmatrix} \Big|_{y=0} = \begin{bmatrix} \tilde{g}_5 & g_5 \\ -g_5 \partial_y & \tilde{g}_5 \partial_y \end{bmatrix} e^{-2Rky} \begin{bmatrix} \chi^{R3} \\ \chi^X \end{bmatrix} \Big|_{y=0} = 0, \quad (6.5d)$$

$$\partial_y V^L(0) = V^{R12}(0) = \partial_y V^C(0) = 0 \quad (6.5e)$$

$$\chi^L(0) = \partial_y e^{-2Rky} \chi^{R12}(0) = \chi^C(0) = 0, \quad (6.5f)$$

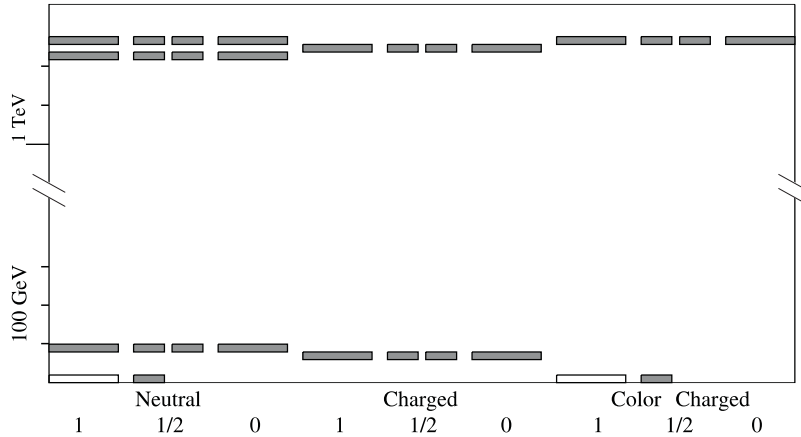


Figure 6.1: The gauge sector spectrum of the supersymmetrized warped higgsless model. Filled/unfilled boxes in the $s = 1$ column stand for three/two physical degrees of freedom. The filled boxes in the $s = 1/2$ column stand for Dirac fermions in the electrically charged sector and Majorana/Weyl fermions in the neutral and color sector. Similarly, the filled boxes in the $s = 0$ column stand for complex scalars in the electrically charged sector and real scalars in the neutral and color sector.

$$H_{Lf}^c(0) = H_{Rf}(0) = 0 \quad (6.5g)$$

The spectroscopy which follows from this after Kaluza-Klein expansion is shown in figure 6.1. It is characteristic for warped supersymmetric models and can be summarized as follows: For every massless vector in the nonsupersymmetric theory, there is one massless 4D $\mathcal{N} = 1$ vector multiplet. For each massive vector in the nonsupersymmetric theory with mass $m \neq 0$, there is a degenerate 4D $\mathcal{N} = 2$ vector multiplet with central charge m . The unphysical degrees of freedom are not shown, and are degenerate with the others for $\xi = 1$.

6.3 The Action in 4D Fields

In this section we will recast a selected number of interaction terms from the 5D Lagrangian in warped space in an explicit 4D language with 4D Vectors, Dirac and Majorana spinors and Scalars. All information about the fifth dimension is then encoded in the overlap integrals. This is done in the usual Kaluza-Klein approach which is straightforward apart from the somewhat tedious task of classifying all possible types of 4D vertex expressions in connection with their corresponding effective coupling constants.

6.3.1 Chargino Interactions with Matter

Let us start with the arguably most complicated interaction from \mathcal{L}_{16} , \mathcal{L}_{17} , \mathcal{L}_{19} , \mathcal{L}_{21} (appendix B.2) in which many of the interesting subtleties such as “clashing”

fermion lines appear. To proceed, we need the following definitions of 4D fields:

$$\Psi = (\psi_u, \bar{\psi}_u^c, \psi_d, \bar{\psi}_d^c)^T \quad H = \begin{pmatrix} h_u \\ h_d \end{pmatrix} \quad H^{c\dagger} = \begin{pmatrix} h_u^{c\dagger} \\ h_d^{c\dagger} \end{pmatrix} \quad (6.6)$$

represent any one fermion generation and the sfermion partners of the lefthanded (H) and righthanded components (H^c), while

$$\chi_a^+ = \frac{1}{\sqrt{2}} \begin{pmatrix} \lambda_1^1 - i\lambda_1^2 \\ \bar{\lambda}_2^1 - i\bar{\lambda}_2^2 \end{pmatrix} \quad \chi_b^+ = \frac{1}{\sqrt{2}} \begin{pmatrix} \lambda_2^1 - i\lambda_2^2 \\ \bar{\lambda}_1^1 - i\bar{\lambda}_1^2 \end{pmatrix} \quad (6.7)$$

$$(C\chi_a^+) = \frac{1}{\sqrt{2}} \begin{pmatrix} \lambda_2^1 + i\lambda_2^2 \\ \bar{\lambda}_1^1 + i\bar{\lambda}_1^2 \end{pmatrix} \quad (C\chi_b^+) = \frac{1}{\sqrt{2}} \begin{pmatrix} \lambda_1^1 + i\lambda_1^2 \\ \bar{\lambda}_2^1 + i\bar{\lambda}_2^2 \end{pmatrix} \quad (6.8)$$

are our choice of chargino mass eigenstates which are both positive in the standard form and negative in their charge conjugated form denoted with a prefix C . In all these the Kaluza-Klein index and the x^μ dependence are left implicit for now. Since there are no identical particles in this interaction there should be no ambiguities. Let us furthermore define the matrices for charged currents and the chirality projectors as

$$T^\pm = T^1 \mp iT^2 \quad P^+ = \begin{pmatrix} \delta_\alpha^\beta & 0 \\ 0 & 0 \end{pmatrix} \quad P^- = \begin{pmatrix} 0 & 0 \\ 0 & \delta_{\dot{\alpha}}^{\dot{\beta}} \end{pmatrix} \quad (6.9)$$

With these components we can build (up to complex conjugation) the following electrically neutral Lorentz invariants

$$\bar{\Psi}T^+P^+(C\chi_a^+)H = \frac{1}{\sqrt{2}}\psi_d^{c\alpha}(\lambda_2^1 + i\lambda_2^2)_\alpha h_u = \psi_d^c \lambda_2^- h_u \quad (6.10)$$

$$\bar{\Psi}T^+P^-(C\chi_a^+)H = \frac{1}{\sqrt{2}}\bar{\psi}_{d\dot{\alpha}}(\bar{\lambda}_1^1 + i\bar{\lambda}_1^2)^{\dot{\alpha}} h_u = \bar{\psi}_d \bar{\lambda}_1^- h_u \quad (6.11)$$

$$\bar{\Psi}T^-P^+\chi_a^+H = \frac{1}{\sqrt{2}}\psi_u^{c\alpha}(\lambda_1^1 - i\lambda_1^2)_\alpha h_d = \psi_u^c \lambda_1^+ h_d \quad (6.12)$$

$$\bar{\Psi}T^-P^-\chi_a^+H = \frac{1}{\sqrt{2}}\bar{\psi}_{u\dot{\alpha}}(\bar{\lambda}_2^1 - i\bar{\lambda}_2^2)^{\dot{\alpha}} h_d = \bar{\psi}_u \bar{\lambda}_2^+ h_d \quad (6.13)$$

where the missing 12 combinations are obtained when exchanging $\chi_a \leftrightarrow \chi_b$ and $H \leftrightarrow H^{c\dagger}$ by performing the substitutions $\lambda_1 \leftrightarrow \lambda_2$ and $h_i \leftrightarrow h_i^{c\dagger}$ respectively on the results. Luckily, only half of the possible combinations actually appear in the interaction, and the resulting structure bears some resemblance to the corresponding interaction in the MSSM. Now we can compare with the corresponding expressions in the 5D Lagrangian density where now all fields depend on x^μ and y ,

$$\mathcal{L} = \int dy \sqrt{g} g_{ew} \sqrt{2} \left[i\bar{\lambda}_1^l \bar{\psi} T^l h + i\lambda_1^l \psi^c T^l h^{c\dagger} - i\lambda_2^l \psi^c T^l h + i\bar{\lambda}_2^l \bar{\psi} T^l h^{c\dagger} \right] + h.c.$$

$$\begin{aligned}
&= \int dy \sqrt{g} g_{ew} \left[i\bar{\lambda}_1^+ \bar{\psi} T^- h + i\bar{\lambda}_1^- \bar{\psi} T^+ h + i\lambda_1^+ \psi^c T^- h^{c\dagger} + i\lambda_1^- \psi^c T^+ h^{c\dagger} \right. \\
&\quad \left. - i\lambda_2^+ \psi^c T^- h - i\lambda_2^- \psi^c T^+ h + i\bar{\lambda}_2^+ \bar{\psi} T^- h^{c\dagger} + i\bar{\lambda}_2^- \bar{\psi} T^+ h^{c\dagger} \right] \\
&\quad + h.c. + \text{neutral} \\
&= \int dy \sqrt{g} g_{ew} \left[i\bar{\lambda}_1^+ \bar{\psi}_u h_d + i\bar{\lambda}_1^- \bar{\psi}_d h_u + i\lambda_1^+ \psi_u^c h_d^{c\dagger} + i\lambda_1^- \psi_d^c h_u^{c\dagger} \right. \\
&\quad \left. - i\lambda_2^+ \psi_u^c h_d - i\lambda_2^- \psi_d^c h_u + i\bar{\lambda}_2^+ \bar{\psi}_u h_d^{c\dagger} + i\bar{\lambda}_2^- \bar{\psi}_d h_u^{c\dagger} \right] \\
&\quad + h.c. + \text{neutral} \tag{6.14}
\end{aligned}$$

By comparing the coefficients, we finally get an answer in 4D notation

$$\begin{aligned}
\mathcal{L} = & ig_{ew} \left[\bar{\Psi} T^- \left(\langle \lambda_1 u \tilde{d} \rangle P^- - \langle \lambda_2 u^c \tilde{d} \rangle P^+ \right) \chi_b^+ H \right. \\
& + \bar{\Psi} T^+ \left(\langle \lambda_1 d \tilde{u} \rangle P^- - \langle \lambda_2 d^c \tilde{u} \rangle P^+ \right) (C\chi_a^+) H \\
& + \bar{\Psi} T^- \left(\langle \lambda_1 u^c \tilde{d}^c \rangle P^+ + \langle \lambda_2 u \tilde{d}^c \rangle P^- \right) \chi_a^+ H^{c\dagger} \\
& \left. + \bar{\Psi} T^+ \left(\langle \lambda_1 d^c \tilde{u}^c \rangle P^+ + \langle \lambda_2 d \tilde{u}^c \rangle P^- \right) (C\chi_b^+) H^{c\dagger} \right] \\
& + h.c. + \text{neutral} \tag{6.15}
\end{aligned}$$

where the overlap integrals are defined as

$$\langle \lambda f \tilde{f} \rangle = \int dy Re^{-4Rky} f_\lambda(y) f_f(y) f_{\tilde{f}}(y) \tag{6.16}$$

The expression (6.15) is still incomplete: The chargino is actually a mix of $SU(2)_L$ and $SU(2)_R$ gauginos while each fermion flavour also possesses two 5D doublets Ψ_L and Ψ_R which each transform only under the group of the same name. So far we have simply written down everything as if there was only one $SU(2)$ group present, but for quarks it is simple to do the final step to the full gauge group: Let us recall that the boundary terms on the IR brane mix $\psi_L(x, y)$ with $\psi_R(x, y)$ and $\psi_L^c(x, y)$ with $\psi_R^c(x, y)$ only. Similarly, the boundary conditions mix λ_{jL}^i and λ_{jR}^i only for i, j equal. This means that it is these combinations of 5D fields which share the same 4D Kaluza-Klein coefficient field, and since the couplings are diagonal with respect to the two groups (everywhere except in the coupling of two scalars to two gauge bosons), all we have to do is to sum over the contributing overlap integrals in the Lagrangian. The final result is

$$\begin{aligned}
\mathcal{L} = & ig_{ew} \times \tag{6.17} \\
& \left[\bar{\Psi} T^- \left(\langle \lambda_{1L} u_L \tilde{d}_L + \lambda_{1R} u_R \tilde{d}_R \rangle P^- - \langle \lambda_{2L} u_L^c \tilde{d}_L + \lambda_{2R} u_R^c \tilde{d}_R \rangle P^+ \right) \chi_b^+ H \right. \\
& + \bar{\Psi} T^+ \left(\langle \lambda_{1L} d_L \tilde{u}_L + \lambda_{1R} d_R \tilde{u}_R \rangle P^- - \langle \lambda_{2L} d_L^c \tilde{u}_L + \lambda_{2R} d_R^c \tilde{u}_R \rangle P^+ \right) (C\chi_a^+) H \\
& \left. + \bar{\Psi} T^- \left(\langle \lambda_{1L} u_L^c \tilde{d}_L^c + \lambda_{1R} u_R^c \tilde{d}_R^c \rangle P^+ + \langle \lambda_{2L} u_L \tilde{d}_L^c + \lambda_{2R} u_R \tilde{d}_R^c \rangle P^- \right) \chi_a^+ H^{c\dagger} \right]
\end{aligned}$$

$$\begin{aligned}
& +\bar{\Psi}T^+\left(\langle\lambda_{1L}d_L^c\tilde{u}_L^c+\lambda_{1R}d_R^c\tilde{u}_R^c\rangle P^++\langle\lambda_{2L}d_L\tilde{u}_L^c+\lambda_{2R}d_R\tilde{u}_R^c\rangle P^-\right)(C\chi_b^+)H^{c\dagger}] \\
& +h.c.+neutral
\end{aligned} \tag{6.18}$$

Again, we have left the triple sum over all combinations of Kaluza-Klein modes implicit for clarity.

6.3.2 Neutralino Interactions with Matter

Now we turn to the neutral gauginos which we ignored in the above derivation. We define two Majorana neutralino towers

$$\chi_a^0(x)=\frac{1}{\sqrt{2}}\begin{pmatrix}\lambda_1^0+\lambda_2^0 \\ \lambda_1^0+\lambda_2^0\end{pmatrix}\quad\chi_b^0(x)=\frac{i}{\sqrt{2}}\begin{pmatrix}\lambda_1^0-\lambda_2^0 \\ \lambda_2^0-\lambda_1^0\end{pmatrix} \tag{6.19}$$

where $\lambda_i^0(x)$ is the Kaluza-Klein coefficient which pertains to the 5D fields λ_i^{L3} , λ_i^{R3} and λ_i^X after electroweak symmetry breaking. With these definitions, the full 4D neutralino-matter-smatter interaction Lagrangian takes the form

$$\mathcal{L}=h_j\bar{\Psi}_i i\Gamma_{ij}(\chi_a^0+i\chi_b^0)+h_j^{c\dagger}\bar{\Psi}_i i\Gamma_{ij}^c(\chi_a^0-i\chi_b^0)+h.c. \tag{6.20}$$

The vertices are given in terms of the projectors, overlap integrals and quantum numbers by

$$\begin{aligned}
\Gamma_{ij}&=g_{ew}T_{ij}^{3L}[P^-\langle\lambda_1^{L3}\psi_{Li}h_{Lj}\rangle-P^+\langle\lambda_2^{L3}\psi_{Li}^c h_{Lj}\rangle] \\
&\quad +g_{ew}T_{ij}^{3R}[P^-\langle\lambda_1^{R3}\psi_{Ri}h_{Rj}\rangle-P^+\langle\lambda_2^{R3}\psi_{Ri}^c h_{Rj}\rangle] \\
&\quad +\tilde{g}_{ew}X_{ij}[P^-\langle\lambda_1^X\psi_{Li}h_{Lj}\rangle-P^+\langle\lambda_2^X\psi_{Li}^c h_{Lj}\rangle] \\
&\quad +\tilde{g}_{ew}X_{ij}[P^-\langle\lambda_1^X\psi_{Ri}h_{Rj}\rangle-P^+\langle\lambda_2^X\psi_{Ri}^c h_{Rj}\rangle] \\
\Gamma_{ij}^c&=g_{ew}T_{ij}^{3L}[P^-\langle\lambda_2^{L3}\psi_{Li}h_{Lj}^c\rangle+P^+\langle\lambda_1^{L3}\psi_{Li}^c h_{Lj}^c\rangle] \\
&\quad +g_{ew}T_{ij}^{3R}[P^-\langle\lambda_2^{R3}\psi_{Ri}h_{Rj}^c\rangle+P^+\langle\lambda_1^{R3}\psi_{Ri}^c h_{Rj}^c\rangle] \\
&\quad +\tilde{g}_{ew}X_{ij}[P^-\langle\lambda_2^X\psi_{Li}h_{Lj}^c\rangle+P^+\langle\lambda_1^X\psi_{Li}^c h_{Lj}^c\rangle] \\
&\quad +\tilde{g}_{ew}X_{ij}[P^-\langle\lambda_2^X\psi_{Ri}h_{Rj}^c\rangle+P^+\langle\lambda_1^X\psi_{Ri}^c h_{Rj}^c\rangle].
\end{aligned}$$

In this expression, the brackets

$$\langle\lambda\psi h\rangle\equiv\int dy\sqrt{g}f_\lambda(y)f_\psi(y)f_h(y) \tag{6.21}$$

stand for the 5D overlaps which give us the coupling strengths of a sfermion to the corresponding matter fermion and a neutralino. The coupling constants g_{ew} and \tilde{g}_{ew} are those of the $SU(2)$ groups and $U(1)_X$ group respectively, while $T_{ij}^{3L,R}=\pm\frac{1}{2},0$ is the $SU(2)_{L,R}$ isospin and $X_{ij}=\frac{1}{2}(B-L)_i\delta_{ij}$ is the $U(1)_X$ quantum number. The structure is such that the ‘‘left handed’’ sfermion couples

to gauginos and matter fermions of the same handedness, the “right handed” one to gauginos and matter fermions of opposite handedness.

6.3.3 Gluino Interactions with Matter

The QCD analog of the above interactions are the couplings of the gluinos to quarks and squarks which of course originate from the same parts of the warped $SU(N)$ SYM Lagrangian, \mathcal{L}_{16} , \mathcal{L}_{17} , \mathcal{L}_{19} , \mathcal{L}_{21} (appendix B.2). In contrast to the charginos which one usually puts in a complex representation on purpose to obtain electrical charge eigenstates, we choose a Majorana basis of mass eigenstates for all gluinos analogous to the neutralino

$$\Lambda_a = \frac{1}{\sqrt{2}} \begin{pmatrix} \lambda_1 + \lambda_2 \\ \bar{\lambda}_1 + \bar{\lambda}_2 \end{pmatrix} \quad \Lambda_b = \frac{i}{\sqrt{2}} \begin{pmatrix} \lambda_1 - \lambda_2 \\ -\bar{\lambda}_1 + \bar{\lambda}_2 \end{pmatrix} \quad (6.22)$$

In analogy to what we have seen before, the 4D interaction has to have the structure

$$\mathcal{L} = \bar{\Psi} i\Gamma^l (\Lambda_a + i\Lambda_b)^l h + \bar{\Psi} i\Gamma^{c,l} (\Lambda_a - i\Lambda_b)^l h^{c\dagger} \quad (6.23)$$

where the vertex expression reads

$$\Gamma^l = g_{YM} T^l [P^- \langle \lambda_1 \psi_L h_L + \lambda_1 \psi_R h_R \rangle - P^+ \langle \lambda_2 \psi_L^c h_L + \lambda_2 \psi_R^c h_R \rangle] \quad (6.24)$$

$$\Gamma^{c,l} = g_{YM} T^l [P^- \langle \lambda_2 \psi_L h_L^c + \lambda_2 \psi_R h_R^c \rangle + P^+ \langle \lambda_1 \psi_L^c h_L^c + \lambda_1 \psi_R^c h_R^c \rangle] \quad (6.25)$$

where the overlap integrals are defined as

$$\langle \lambda \psi h \rangle = \int dy Re^{-4Rky} f_\lambda(y) f_\psi(y) f_h(y) \quad (6.26)$$

6.3.4 The Strong Quark Yukawa Coupling

The scalar partner of the gluon has a Yukawa type interaction with the quarks from \mathcal{L}_{18} and \mathcal{L}_{20} (appendix B.2). The KK decomposed version is straightforward,

$$\mathcal{L} = \Sigma^{(n),l} \bar{\Psi}^{(m)} T^l \Gamma^{(nmk)} \Psi^{(k)} \quad (6.27)$$

where

$$\begin{aligned} \Gamma^{(nmk)} = & g_{YM} P^+ \left[\langle \Sigma^{(n)} \psi_L^{c(m)} \psi_L^{(k)} \rangle + \langle \Sigma^{(n)} \psi_R^{c(m)} \psi_R^{(k)} \rangle \right] \\ & + g_{YM} P^- \left[\langle \Sigma^{(n)} \psi_L^{c(k)} \psi_L^{(m)} \rangle + \langle \Sigma^{(n)} \psi_R^{c(k)} \psi_R^{(m)} \rangle \right] \end{aligned} \quad (6.28)$$

and

$$\langle \Sigma \psi^c \psi \rangle \equiv \int dy \sqrt{g} f_\Sigma(y) f_{\psi^c}(y) f_\psi(y) \quad (6.29)$$

while T^l are the Gell-Mann matrices. What is special about this class of couplings is the suppression with mass and potential cancellations between the L and R sectors for $c_L = -c_R$.

6.3.5 The Gluino Yukawa Interaction

The interaction of gluinos with the same color charged gauge scalar from \mathcal{L}_8 (appendix B.2) has a similar structure,

$$\sqrt{g}g_{YM} \left[-i f^{bda} \Sigma^d (\bar{\lambda}_2^a \lambda_1^b + \lambda_2^a \lambda_1^b) \right] \quad (6.30)$$

We choose the same Majorana basis for the gluinos as above. Now, it can be easily checked, that, in order to obtain the interaction above including the color structure, we have to combine these in the following way

$$\begin{aligned} \mathcal{L} = g_{YM} \sum_{q,k,p} \langle \lambda_1^q \lambda_2^k \Sigma^p \rangle f^{mnl} \times \\ \frac{1}{2} \Sigma^{n,p} \left(\bar{\Lambda}_a^{l,k} \Lambda_b^{m,q} - \bar{\Lambda}_a^{m,q} \Lambda_b^{l,k} + i \bar{\Lambda}_a^{l,k} (-i\bar{\gamma}^5) \Lambda_a^{m,q} + i \bar{\Lambda}_b^{m,q} (-i\bar{\gamma}^5) \Lambda_b^{l,k} \right) \end{aligned} \quad (6.31)$$

where

$$\langle \Sigma \lambda \lambda \rangle \equiv \int dy \sqrt{g} f_\Sigma(y) f_\lambda(y) f_\lambda(y) \quad (6.32)$$

Note the assignment of Kaluza-Klein indices to the wavefunctions of λ_1, λ_2 and the fact that they are independent of color.

6.3.6 The Strong Squark Gauge Scalar Coupling

This interaction stems from \mathcal{L}_{24} and \mathcal{L}_{31} (appendix B.2). Since in 6D this would be the A_6 gauge coupling (but $p_6 = 0$ in this model), it is not surprising that all the 5D derivative terms ∂_y which appear in it merely form a 5D boundary term. Gathering the terms, we obtain

$$\begin{aligned} \mathcal{L} = \partial_y \left[g_{YM} e^{-4Rky} (\Sigma^l h^\dagger T^l h - \Sigma^l h^c T^l h^{c\dagger}) \right] \\ + \sqrt{g} g_{YM} k \Sigma^l \left[(2c - 1) h^\dagger T^l h + (2c + 1) h^c T^l h^{c\dagger} \right] \end{aligned} \quad (6.33)$$

The 4D version is

$$\begin{aligned} \mathcal{L} = g_{YM} \sum_{m,n,r} \Sigma^{l,n} h^{m\dagger} T^l h^r \left[(2c_L - 1) k \langle \Sigma^n h_L^m h_L^r \rangle + (2c_R - 1) k \langle \Sigma^n h_R^m h_R^r \rangle \right] + \\ g_{YM} \sum_{m,n,r} \Sigma^{l,n} h^{c,m} T^l h^{c\dagger,r} \left[(2c_L + 1) k \langle \Sigma^n h_L^{c,m} h_L^{c,r} \rangle + (2c_R + 1) k \langle \Sigma^n h_R^{c,m} h_R^{c,r} \rangle \right] \end{aligned} \quad (6.34)$$

The overlap integrals in this case are defined as

$$\langle \Sigma hh \rangle \equiv \int dy \sqrt{g} f_\Sigma(y) f_h(y) f_h(y) \quad (6.35)$$

The resulting couplings have energy dimension 1 where, similarly to A_5 , the scale is set by the masses of the particles participating in the interaction.

6.3.7 The Electroweak Matter Gauge Coupling

This is the standard gauge interaction of quarks from \mathcal{L}_{15} (appendix B.2) for the gauge groups $SU(2)^2 \times U(1)$. From this follows

$$\mathcal{L} = \sum_{nmr} \left[\bar{\Psi}^m \Upsilon^+ \Psi^r + \bar{\Psi}^m \Upsilon^- \Psi^r \right] \quad (6.36)$$

where

$$\begin{aligned} \Upsilon^+ = & \left(g_{ew} T^l A_L^{l,n} \langle A_L^n \psi_L^m \psi_L^r \rangle \right. \\ & \left. + g_{ew} T^l A_R^{l,n} \langle A_R^n \psi_R^m \psi_R^r \rangle + \tilde{g}_{ew} X \mathcal{B}^n \langle B^n \psi_L^m \psi_L^r + B^n \psi_R^m \psi_R^r \rangle \right) P^+ \end{aligned} \quad (6.37)$$

$$\begin{aligned} \Upsilon^- = & \left(g_{ew} T^l A_L^{l,n} \langle A_L^n \psi_L^{c,m} \psi_L^{c,r} \rangle \right. \\ & \left. + g_{ew} T^l A_R^{l,n} \langle A_R^n \psi_R^{c,m} \psi_R^{c,r} \rangle + \tilde{g}_{ew} X \mathcal{B}^n \langle B^n \psi_L^{c,m} \psi_L^{c,r} + B^n \psi_R^{c,m} \psi_R^{c,r} \rangle \right) P^- \end{aligned} \quad (6.38)$$

and

$$\langle A\psi\psi \rangle \equiv \int dy \sqrt{g} e^{Rky} f_A(y) f_\psi(y) f_\psi(y) \quad (6.39)$$

The matrix X contains the abelian quantum numbers $(B - L)/2$ on the diagonal which is $1/6$ for quarks and $-1/2$ for leptons.

6.3.8 The Strong Quark Gauge Coupling

This is the standard gauge interaction of quarks from \mathcal{L}_{15} (appendix B.2) for the gauge group $SU(3)_c$. From this follows

$$\begin{aligned} \mathcal{L} = g_{YM} \sum_{nmr} G_\mu^{l,n} \left[\bar{\Psi}^m \bar{\gamma}^\mu T^l P^+ \Psi^r \langle G^n \psi_L^m \psi_L^r + G^n \psi_R^m \psi_R^r \rangle + \right. \\ \left. \bar{\Psi}^m \bar{\gamma}^\mu T^l P^- \Psi^r \langle G^n \psi_L^{c,m} \psi_L^{c,r} + G^n \psi_R^{c,m} \psi_R^{c,r} \rangle \right] \end{aligned} \quad (6.40)$$

where

$$\langle G\psi\psi \rangle \equiv \int dy \sqrt{g} e^{Rky} f_G(y) f_\psi(y) f_\psi(y) \quad (6.41)$$

6.3.9 The Gaugino Charged Current Interaction

The charged current interaction Lagrangian from $\mathcal{L}_0, \mathcal{L}_6$ (appendix B.2) can again be rewritten using the definitions of 4D fields given above. It is

$$\mathcal{L} = -\frac{1}{\sqrt{2}} W_\mu^+ \left[\overline{\chi_a^+} \Gamma_a^\mu (\chi_a^0 - i\chi_b^0) + \overline{\chi_b^+} \Gamma_b^\mu (\chi_a^0 + i\chi_b^0) \right] + \text{h.c.} \quad (6.42)$$

and the corresponding vertex expressions are

$$\begin{aligned} \Gamma_a^\mu &= g_{ew} \overline{\gamma}^\mu \left[P^- (\langle W^{L\pm} \lambda_2^{L\pm} \lambda_2^{L3} \rangle + \langle W^{R\pm} \lambda_2^{R\pm} \lambda_2^{R3} \rangle) \right. \\ &\quad \left. + P^+ (\langle W^{L\pm} \lambda_1^{L\pm} \lambda_1^{L3} \rangle + \langle W^{R\pm} \lambda_1^{R\pm} \lambda_1^{R3} \rangle) \right] \\ \Gamma_b^\mu &= \Gamma_a^\mu (P^+ \leftrightarrow P^-), \end{aligned}$$

with the overlap integrals

$$\langle W \lambda_i \lambda_j \rangle \equiv \int dy \sqrt{g} e^{Rky} f_W(y) f_{\lambda_i}(y) f_{\lambda_j}(y) \quad (6.43)$$

which now have an additional factor e^{Rky} from the inverse vielbein contained in $\overline{\gamma}^\mu$.

6.3.10 The Gaugino Neutral Current Interaction

The interaction of charginos with the neutral gauge bosons comes from the same part of the Lagrangian. It is

$$\mathcal{L} = Z_\mu^k \left[\overline{\chi_a^{+,l}} \Gamma_a^{\mu,klr} \chi_a^{+,r} + \overline{\chi_b^{+,l}} \Gamma_b^{\mu,klr} \chi_b^{+,r} \right] \quad (6.44)$$

where

$$\begin{aligned} \Gamma_a^{\mu,klr} &= g_{ew} \overline{\gamma}^\mu \left[P^+ \langle W^{L3,k} \lambda_1^{L\pm,l} \lambda_1^{L\pm,r} + W^{R3,k} \lambda_1^{R\pm,l} \lambda_1^{R\pm,r} \rangle \right. \\ &\quad \left. + P^- \langle W^{L3,k} \lambda_2^{L\pm,l} \lambda_2^{L\pm,r} + W^{R3,k} \lambda_2^{R\pm,l} \lambda_2^{R\pm,r} \rangle \right] \\ \Gamma_b^{\mu,klr} &= \Gamma_a^{\mu,klr} (P^+ \leftrightarrow P^-) \end{aligned}$$

again with the overlap integrals

$$\langle W \lambda_i \lambda_j \rangle \equiv \int dy \sqrt{g} e^{Rky} f_W(y) f_{\lambda_i}(y) f_{\lambda_j}(y) \quad (6.45)$$

Chapter 7

Breaking Supersymmetry

Right from the start when supersymmetry was considered as an extension of the Poincaré group in high energy physics, it was clear that it had to be hidden or broken in nature similarly to electroweak symmetry. It is obviously not present in the known particle spectrum and as of today still remains a purely speculative endeavour. There are mass sum rules which imply that it is not possible to achieve purely spontaneous supersymmetry breaking in the minimal supersymmetric extension of the standard model (MSSM) without there being very light superpartners of matter fermions. Eventually, there was a consensus that one should remain agnostic about the origin of supersymmetry breaking by determining a maximal set of symmetry breaking operators which could be used to obtain a realistic spectrum while still retaining the most important properties of the model, in particular the absence of quadratic contribution to the Higgs potential. These operators were then dubbed “soft supersymmetry breaking” terms, and they are responsible for the proliferation of free parameters in the MSSM. Many scenarios to avoid this have been proposed in the literature which involve a so-called hidden sector where supersymmetry breaking occurs which is then mediated to the MSSM via some messenger. This has for example been implemented in approaches such as mSUGRA models which postulate relations between parameters at a high scale and exploit the renormalization group running to achieve a realistic low energy spectrum with SUSY breaking and electroweak symmetry breaking. Again, models in $D > 4$, within the limitations mentioned in the preceding chapters, offer new tools to approach SUSY breaking. More sophisticated schemes employ for example the VEV of 5D gravity fields over the interval (Wilson lines) which then lead to SUSY breaking, or brane F terms, among many others. The simplest path to implementing effective SUSY breaking in higher dimensions without introducing a plethora of breaking parameters is to assign different boundary conditions for the components of a multiplet on an interval. This approach will be used here to generate a realistic spectrum of superpartners while introducing as few new parameters as possible. First we will discuss the different possibilities on the IR and UV brane that are compatible with the gauge symmetry breaking scheme and do not violate obvious constraints. We will then give the mass spectra for different choices.

7.1 Supersymmetry Breaking by Boundary Conditions

A rather appealing implementation of SUSY breaking by boundary conditions would be to have it on the IR brane together with the breaking of electroweak symmetry. We do not follow along this path for several reasons. An obvious phenomenological constraint is that in this setup the gluino mass saturates at around $m_{\tilde{g}} \approx \sqrt{2}m_W$ while the coupling remains at α_s strength. We would therefore have to raise the scales of the extra dimension significantly to avoid the experimental bound of $m_{\tilde{g}} \gtrsim 300$ GeV. This situation becomes even more severe when we try to raise the masses of squarks and sneutrinos. The experimental limit of around $m_{\tilde{f}} \gtrsim 380$ GeV for squarks is hard to avoid. If $c_L > 1/2$ the $SU(2)_L$ doublets couple less strongly to the IR brane than gauge bosons, and at values $c_L \approx 1/2$ which are necessary to satisfy LEP precision bounds, masses saturate much below 100 GeV. The mechanisms which are used on the UV brane to split the $SU(2)$ doublets (large localized kinetic terms and localized Majorana masses) make things worse. One also has to decide what attitude one has towards the gravity sector of the model which we have excluded from our considerations as much as possible. If one allows for the gravitino on the UV brane by giving the gravitino the same boundary conditions as the graviton, there is going to be a massless gravitino mode whose couplings to the IR brane are suppressed such that it can only be raised to the sub-eV level by Dirac boundary conditions on the IR brane, resulting in a superlight gravitino whose couplings are partly only TeV suppressed. We will get back to this point later. There are some conceptual difficulties related to unitarity and consistency with supergravity in this class of models (see for example [47, 51]) which are particularly problematic for light gravitinos.

Since our goal is to study the interplay of supersymmetry and the higgsless electroweak symmetry breaking sector and its implications on DM and collider physics, the above considerations lead us to investigate the following scenario: We do not assume that there is unbroken or low energy supersymmetry on the UV brane. Something similar has been considered before in a different context, for example by [52]. We retain SUSY in the higgsless EWSB sector represented by the bulk and IR brane and study the effects that arise when it is coupled to the UV brane. We can also feel free to assign different UV Dirac boundary conditions to the gravitino. As we will see later there will still be heavy spin 3/2 resonances, but they have short lifetimes, masses above the Kaluza-Klein scale and suppressed couplings to light matter. Let us now consider the different choices for UV brane boundary conditions.

7.1.1 Gauginos

In the supersymmetric case, the gluinos (λ_1^a, λ_2^a) satisfy boundary conditions¹ ($\oplus\oplus, \ominus\ominus$). This is of course undesirable because there is a massless Weyl gluino

¹The different assignments of boundary conditions correspond to the choices outlined in section 2.3.4.

acting as superpartner to the gluon. We can “twist” the boundary conditions to $(\ominus\oplus, \oplus\ominus)$ and so completely get rid of the massless modes. Compare this to the photino in our toy model. The equation for the gluino tower is now

$$Y_0\left(m\frac{e^{Rk\pi}}{k}\right) = \frac{J_0\left(m\frac{e^{Rk\pi}}{k}\right)Y_1(m/k)}{J_1(m/k)} \quad (7.1)$$

There is again no zero mode for either λ_1 or λ_2 , and the equation is approximately satisfied when $J_0\left(m\frac{e^{Rk\pi}}{k}\right) = 0$, leading to a heavy gluino spectrum which is almost degenerate with the heavy gluons and sgluinos. Note that $(\ominus\oplus, \ominus\oplus)$ would, apart from breaking SUSY on the IR brane, reintroduce a massless Weyl gluino.

The situation is more interesting in the electroweak sector. We want our new assignments to be compatible to the gauge symmetry breaking scheme, and that means in this case that all boundary conditions should be compatible with $SU(2)_L \times U(1)_Y$ gauge symmetry. Hypercharge is generated by $T_R^3 + (B - L)/2$, which rotates λ_s^{R1} into λ_s^{R2} and vice versa, but leaves λ_s^X and λ_s^{R3} invariant. T_L^i generates arbitrary orthogonal rotations among the three λ_s^{Li} . This leaves us with several conditions: λ^X and λ^{R3} can mix, while $\lambda^{R1,2}$ and $\lambda^{L1,2,3}$ each share one type of boundary condition. There are several classes of solutions summarized in table 7.1. All models of type III feature a massless BLino. The models Ic,IIc and Id,IIId contain a massless chargino mode while model IIb contains a massless neutralino mode. Since model Ia is the unbroken case if $\theta = \theta_{w5}$ and always contains a photino-like massless mode, we are left with varieties Ib and IIa. In IIa the neutralino and chargino are degenerate at tree level and have Kaluza-Klein wave functions identical to those of the W . Furthermore, the chargino in both varieties is degenerate in mass with the W boson, which is unfortunately too low a mass to escape current detection bounds. How can we remedy this without having to introduce further SUSY breaking in the bulk or on the IR brane? One mechanism to raise the chargino mass would be a negative UV localized kinetic term, but as was hinted at in section 2.1.2, this introduces a tachyonic mode because the scalar product is no longer positive definite. The imaginary mass solution can generally be above the cutoff of our effective theory, $|m_T| \gg \Lambda_c$, but we nevertheless avoid this measure altogether in order not to jeopardize theoretical consistency. Now, the opposite strategy would be to introduce a positive localized kinetic term for the gauge fields. This was done in the literature (for example [33]), though not in detail for the case of delocalized fermions. We thus split the W^\pm and charginos by introducing the $SU(2)_L$ UV brane localized term (3.18) which is non-supersymmetric. The degeneracy is thus lifted and

$$m_{\chi^+}^2 \simeq \frac{k^2 e^{-2Rk\pi}}{Rk\pi} \simeq (1 + \kappa)m_W^2 \quad (7.2)$$

For an optimistic lower mass bound for the chargino of 95 GeV this requires $\kappa \gtrsim 0.4$. The neutralinos differ between Ib and IIa, in that

$$\text{Ib:} \quad m_{\chi^0} \simeq \cos\theta m_{\chi^+} \simeq \sqrt{1 + \kappa} \cos\theta m_W$$

	λ_1^{Li}	$\lambda_1^{R1,2}$	λ_1^{R3}	λ_1^X
Ia.	\oplus	\ominus	$\cos \theta \lambda_1^{R3} = \sin \theta \lambda_1^X$	
Ib.	\ominus	\oplus	$\cos \theta \lambda_1^{R3} = \sin \theta \lambda_1^X$	
Ic.	\oplus	\oplus	$\cos \theta \lambda_1^{R3} = \sin \theta \lambda_1^X$	
Id.	\ominus	\ominus	$\cos \theta \lambda_1^{R3} = \sin \theta \lambda_1^X$	
IIa.	\oplus	\ominus	\ominus	\ominus
IIb.	\ominus	\oplus	\ominus	\ominus
IIc.	\oplus	\oplus	\ominus	\ominus
IId.	\ominus	\ominus	\ominus	\ominus
IIIa.	\oplus	\ominus	\oplus	\oplus
IIIb.	\ominus	\oplus	\oplus	\oplus
IIIc.	\oplus	\oplus	\oplus	\oplus
IIId.	\ominus	\ominus	\oplus	\oplus

Figure 7.1: Combinations of UV brane boundary conditions for the electroweak gaugino sector. The varieties without massless gaugino modes are marked in boldface. It is implied that the λ_2 components get the corresponding boundary conditions which make the variation of the boundary action vanish.

$$\text{IIa: } m_{\chi^0} \simeq m_{\chi^+} \simeq \sqrt{1 + \kappa} m_W \quad (7.3)$$

The former is appealing as the neutralino is naturally the LSP due to the mixing with the BLino of $U(1)_X$, while in the latter one would have to rely on radiative corrections or further localized terms to lift the degeneracy. It will also turn out that the “twisted gaugino” in Ib has suppressed couplings to the LSP and W which is favoured by observations.

7.1.2 Scalars

There is no reason why brane localized masses for the scalars from hypermultiplets should be at the TeV scale, and we therefore assign effective Dirac boundary conditions to them,

$$h_{Lf}(0) = h_{Lf}^c(0) = h_{Rf}(0) = h_{Rf}^c(0) = 0 \quad (7.4)$$

All sfermions in the model are now resonances, and the degeneracy between the “lefthanded” and “righthanded” sfermions is lifted. The same is assumed for the physical scalar partners of the gauge bosons,

$$\Sigma^L(0) = \Sigma^R(0) = \Sigma^X(0) = \Sigma^C(0) = 0 \quad (7.5)$$

This pushes the $SU(3)$ and $U(1)_X$ gauge scalars up to a mass²

$$m_{\Sigma C} = m_{\Sigma X} = z_0 k e^{-Rk\pi} \simeq z_0 \sqrt{Rk\pi(1+\kappa)} m_W \simeq \text{TeV} \quad (7.6)$$

where $z_0 \simeq 2.41$ is the first zero of the Bessel function $J_0(z)$. The sfermions lie in a similar mass range, depending on the localization parameter c of the multiplet. For a massless fermion we can approximate the tree level sfermion masses

$$m_{\tilde{f}} = z_0 k e^{-Rk\pi}, \quad (7.7)$$

where, if $c_L \neq 1/2, c_R \neq -1/2$, z_0 is the first positive root of $J_{c_L-1/2}$ for \tilde{f}_L , $J_{|c_R+1/2|}$ for \tilde{f}_R , $J_{|c_L-1/2|}$ for \tilde{f}_L^c and $J_{-c_R-1/2}$ for \tilde{f}_R^c . The situation is different for the scalars from gauge groups that are broken on the IR brane. These scalars receive smaller tree level masses

$$m_{\Sigma^0} = m_{\Sigma^+} \simeq \sqrt{\frac{2k}{R\pi}} e^{-Rk\pi} = \sqrt{2(1+\kappa)} m_W \quad (7.8)$$

which is very interesting from a phenomenological point of view. However, their tree level coupling to fermions is of the form $\Sigma\psi\psi^c$ and therefore suppressed with the fermion mass, vanishing altogether in the massless fermion limit where it is forbidden by the chiral symmetry. For a large range of parameters, the coupling to leptons and quarks is similar to the corresponding SM Higgs coupling. Note however that since it is not the vacuum expectation value of this scalar triplet that breaks electroweak symmetry, this similarity does not extend to the coupling to gauge bosons. Consequently, the processes corresponding to Higgsstrahlung and vector boson fusion in the SM are absent in our model at tree level. This provides an experimental signature for distinguishing our model from the MSSM at the upcoming LHC experiments.

7.1.3 Gravitinos

In some supersymmetric extensions of the SM, the gravitino poses a problem for cosmological observables, either because it is overabundant or so long-lived that its decay products spoil nucleosynthesis. So far we have not included supergravity in the bulk, and we want to give an argument that the inclusion of KK gravitons and gravitinos in the bulk is possible without losing the desired properties of the model. A holographic interpretation along the AdS/CFT correspondence where the energy momentum tensor and the supersymmetric currents are present on the CFT side also warrants the inclusion of supersymmetric gravity multiplets. Similarly to BC gauge symmetry breaking we adopt the philosophy that the simple picture with BCs is a description mimicking a full theory with symmetry breaking in a slice of AdS5 [47, 51]. By setting the appropriate BCs we obtain a heavy short-lived gravitino.

²This is accurate if further localized kinetic terms are absent. The values are given here for $k = \Lambda_{\text{Pl}}$.

Solving and KK expanding the (free) Rarita-Schwinger equations with “twisted” IR BCs $\psi_2^\mu(0) = \psi_1^\mu(\pi) = 0$, we obtain a very light gravitino [53],

$$\frac{J_1(\frac{m}{k})}{Y_1(\frac{m}{k})} - \frac{J_2(e^{Rk\pi}\frac{m}{k})}{Y_2(e^{Rk\pi}\frac{m}{k})} = 0 \quad \longrightarrow \quad m_0 \simeq \sqrt{8}ke^{-2Rk\pi},$$

However, twisting the BC on the UV brane yields the condition

$$\frac{J_2(\frac{m}{k})}{Y_2(\frac{m}{k})} - \frac{J_1(e^{Rk\pi}\frac{m}{k})}{Y_1(e^{Rk\pi}\frac{m}{k})} = 0 \quad \longrightarrow \quad m_n \simeq z_n ke^{-Rk\pi},$$

where z_n are the positive roots of J_1 . From $z_0 \approx 3.83$ we find a heavy gravitino solution at the scale of the lightest graviton KK mode ($\mathcal{O}(2 \text{ TeV})$ for $k = \Lambda_{\text{Pl}}$). Like the heavy gravitons, this gravitino does not have Planck suppressed interactions but rather a coupling $\lesssim \text{TeV}^{-1}$ depending on the localization parameters. To be more precise, let us calculate the coupling scales relevant for neutralino annihilation (and gravitino decay). The general solutions for the KK wave functions are (cf., e. g., [53, 51, 54])

$$\tilde{G}_1^{(n)}(y) = e^{2Rky} \left[\alpha J_2(m_n e^{Rky}/k) + \beta Y_2(m_n e^{Rky}/k) \right] \quad (7.9)$$

$$\tilde{G}_2^{(n)}(y) = e^{2Rky} \left[\alpha J_1(m_n e^{Rky}/k) + \beta Y_1(m_n e^{Rky}/k) \right] = \frac{e^{-Rky}}{Rm_n} \partial_y \tilde{G}_1^{(n)}, \quad (7.10)$$

with the canonical normalization condition

$$\int dy e^{-2Rky} G_i^2(y) = 1.$$

With these conventions, the coupling strength to a vector and a gaugino is

$$\langle \tilde{G}_i f_V f_{\chi_i} \rangle = \frac{1}{\Lambda_{\text{Pl}}} \sqrt{\frac{R}{2k}} \int dy e^{-3/2Rky} \tilde{G}_i f_V f_{\chi_i}. \quad (7.11)$$

The normalization is chosen such that a gravitino zero mode with unbroken SUSY would yield $\langle \tilde{G}_1^{(0)} f_V f_{\chi_1} \rangle = \Lambda_{\text{Pl}}^{-1}$, $\tilde{G}_2^{(0)} = 0$. For $\kappa = 0.4$ and $k = \Lambda_{\text{Pl}}$ we obtain

$$\langle \tilde{G}_1 f_Z f_{\chi_1}^{(1)} \rangle \approx (500 \text{ TeV})^{-1} \quad \langle \tilde{G}_2 f_Z f_{\chi_2}^{(1)} \rangle \approx (25 \text{ TeV})^{-1} \quad (7.12a)$$

$$\langle \tilde{G}_1 f_Z^{(2)} f_{\chi_1}^{(1)} \rangle \approx (10 \text{ TeV})^{-1} \quad \langle \tilde{G}_2 f_Z^{(2)} f_{\chi_2}^{(1)} \rangle \approx (80 \text{ TeV})^{-1} \quad (7.12b)$$

$$\langle \tilde{G}_1 f_Z^{(2)} f_{\chi_1}^{(2)} \rangle \approx (1 \text{ TeV})^{-1} \quad \langle \tilde{G}_2 f_Z^{(2)} f_{\chi_2}^{(2)} \rangle \approx (3 \text{ TeV})^{-1} \quad (7.12c)$$

Considering the usual holographic picture, this result is not surprising, because the heavy gravitino is interpreted as a bound state with TeV suppressed interactions to other bound states (7.12c), coupling less strongly to lighter, mostly elementary particles (7.12a) and (7.12b). With the result in (7.12a) for the SM couplings we can neglect neutralino annihilation with the gravitino in the t -channel in the following discussion. Still, such a gravitino couples strongly

$c_L(u, d)$	0.48	$c_L(e)$	0.48	κ	0.6
$c_L(c, s)$	0.48	$c_L(\mu)$	0.48	β	0
$c_L(t, b)$	1/3	$c_L(\tau)$	0.48	$\tan \theta$	0.6
$c_R(u, d)$	-0.48	$c_R(e)$	-0.48	k	10^{19} GeV
$c_R(c, s)$	-0.48	$c_R(\mu)$	-0.48	$ke^{-Rk\pi}$	622 GeV
$c_R(t, b)$	-0.4	$c_R(\tau)$	-0.48		

Table 7.1: A set of input parameters used in the following discussions

enough to essentially vanish immediately for a temperature of $T \ll \text{TeV}$, long before nucleosynthesis.

7.2 A Benchmark Point

The parameter space of our model is of course rather large. It is fortunate that important phenomenological aspects such as the DM relic density will turn out to depend weakly on most parameters and can be controlled by a few, in this case the neutralino mixing angle. For the following discussions of the model spectrum and collider phenomenology, we have to take into account the whole spectrum at least of the strongly interacting particle species. We therefore decide on a point in parameter space which will allow us to give numbers for explicit calculations and to run Monte Carlo simulations. We will mention when we encounter properties which depend strongly on our particular choice of parameters and are not stable under small variations. The values which we will assume in the following discussions are given by those in table 7.1 unless stated otherwise.

7.2.1 The Spectrum

We have developed a Fortran tool which is able to calculate all masses and coupling constants of the model automatically (E.1), and the following tree level quantities have largely been determined in this manner. There is one case in the scalar sector in which additional discussion is warranted. A typical tree level particle spectrum is shown in figure 7.2. The corresponding numbers are shown in table 7.2.

Spin	Tower	Light Mode(s)	First heavy Mode(s)			
1	Neutral	$\gamma(0)$ $Z(91)$	$Z^2(1503)$ $Z^3(1520)$			
1/2		$\chi_i^{0,1}(88)$	$\chi_i^{0,2}(1496)$	$\chi_i^{0,3}(1512)$		
0		- $\Sigma^0(145)$	$\Sigma_X^0(1522)$ $\Sigma^0(1522)$			
1	Charged	$W^\pm(80)$	$W^{\pm,2}(1504)$			
1/2		$\chi_i^{\pm,1}(102)$	$\chi_i^{\pm,2}(1509)$			
0		$\Sigma^\pm(145)$	$\Sigma^\pm(1522)$			
1	Gluons	$g(0)$	$g(1522)$			
1/2		- (-)	$\tilde{g}(1496)$			
0		-	$\Sigma^c(1522)$			
1/2	up	$u(0.003)$	$u^2(1489)$	$u^3(1527)$		
0		(-) (-)	$\tilde{u}_l^1(1477)$	$\tilde{u}_l^2(1527)$	$\tilde{u}_r^1(1477)$	$\tilde{u}_r^2(1527)$
1/2	down	$d(0.006)$	$d^2(1527)$ $d^3(1527)$			
0		(-) (-)	$\tilde{d}_l^1(1477)$	$\tilde{d}_l^2(1527)$	$\tilde{d}_r^1(1477)$	$\tilde{d}_r^2(1527)$
1/2	charm	$c(1.3)$	$c^2(1501)$ $c^3(1552)$			
0		(-) (-)	$\tilde{c}_l^1(1466)$	$\tilde{c}_l^2(1537)$	$\tilde{c}_r^1(1466)$	$\tilde{c}_r^2(1537)$
1/2	strange	$s(0.1)$	$s^2(1466)$ $s^3(1537)$			
0		(-) (-)	$\tilde{s}_l^1(1466)$	$\tilde{s}_l^2(1537)$	$\tilde{s}_r^1(1466)$	$\tilde{s}_r^2(1537)$
1/2	top	$t(175)$	$t^2(973)$ $t^3(2144)$			
0		(-) (-)	$\tilde{t}_l^1(878)$	$\tilde{t}_l^2(2038)$	$\tilde{t}_r^1(768)$	$\tilde{t}_r^2(1975)$
1/2	bottom	$b(4.5)$	$b^2(798)$ $b^3(1975)$			
0		(-) (-)	$\tilde{b}_l^1(878)$	$\tilde{b}_l^2(2038)$	$\tilde{b}_r^1(768)$	$\tilde{b}_r^2(1975)$
1/2	ν_e	$\nu_e(\approx 0)$	$\nu_e^2(1527)$ $\nu_e^3(1544)$			
0		(-) (-)	$\tilde{\nu}_{e_l}^1(1477)$	$\tilde{\nu}_{e_l}^2(1546)$	$\tilde{\nu}_{e_r}^1(1527)$	$\tilde{\nu}_{e_r}^2(1544)$
1/2	e	$e(0.0005)$	$e^2(1527)$ $e^3(1546)$			
0		(-) (-)	$\tilde{e}_l^1(1477)$	$\tilde{e}_l^2(1546)$	$\tilde{e}_r^1(1527)$	$\tilde{e}_r^2(1544)$
1/2	ν_μ	$\nu_\mu(\approx 0)$	$\nu_\mu^2(1523)$ $\nu_\mu^3(1548)$			
0		(-) (-)	$\tilde{\nu}_{\mu_l}^1(1476)$	$\tilde{\nu}_{\mu_l}^2(1547)$	$\tilde{\nu}_{\mu_r}^1(1523)$	$\tilde{\nu}_{\mu_r}^2(1548)$
1/2	μ	$\mu(0.1)$	$\mu^2(1523)$ $\mu^3(1549)$			
0		(-) (-)	$\tilde{\mu}_l^1(1476)$	$\tilde{\mu}_l^2(1547)$	$\tilde{\mu}_r^1(1523)$	$\tilde{\mu}_r^2(1548)$
1/2	ν_τ	$\nu_\tau(\approx 0)$	$\nu_\tau^2(1376)$ $\nu_\tau^3(1679)$			
0		(-) (-)	$\tilde{\nu}_{\tau_l}^1(1349)$	$\tilde{\nu}_{\tau_l}^2(1659)$	$\tilde{\nu}_{\tau_r}^1(1376)$	$\tilde{\nu}_{\tau_r}^2(1679)$
1/2	τ	$\tau(1.7)$	$\tau^2(1377)$ $\tau^3(1680)$			
0		(-) (-)	$\tilde{\tau}_l^1(1349)$	$\tilde{\tau}_l^2(1659)$	$\tilde{\tau}_r^1(1376)$	$\tilde{\tau}_r^2(1679)$

Table 7.2: The numbers corresponding to the sample spectrum shown in figure 7.2 (with fixed neutralino angle) including all Kaluza-Klein modes below 2500 GeV. A dash “-” indicates that no mode is present in the 4D $\mathcal{N} = 1$ supersymmetric spectrum, a dash in parentheses “(-)” indicates that a mode is projected out by boundary conditions.

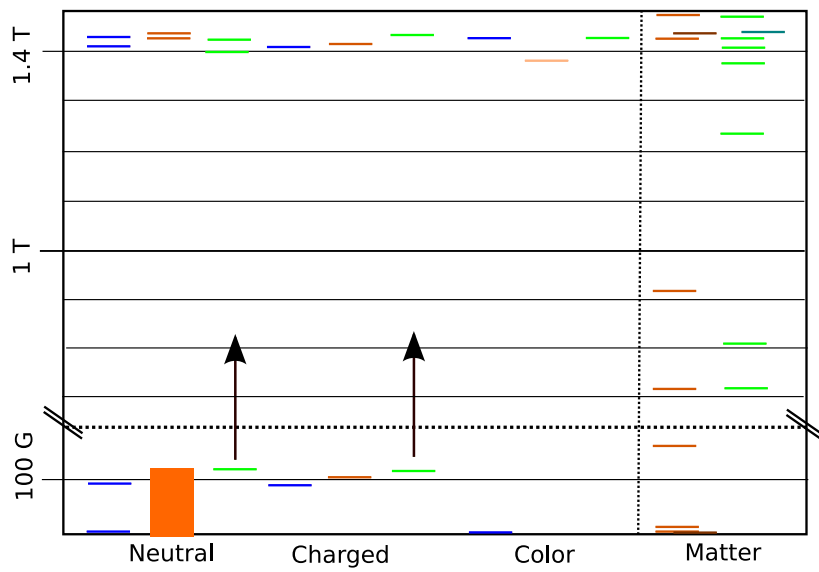


Figure 7.2: The tree level spectrum of the model . The arrows indicate that the scalar quasi-zeromodes receive large corrections from UV brane SUSY breaking. The neutralino mixing angle is left arbitrary leading to the mass range which is indicated by the solid rectangle.

Chapter 8

Phenomenology

La véritable physique consiste donc à bien déterminer tous les effets. Nous connaissons les causes premières quand nous serons des dieux. Il nous est donné de calculer, de peser, de mesurer, d'observer: voilà la philosophie naturelle; presque tout le reste est chimère.

- *Voltaire*

The phenomenological consequences of higgsless electroweak symmetry breaking, in warped models and in the context of deconstruction, have been studied in the literature. We therefore concentrate on the peculiarities that enter when such models are combined with SUSY in the EWSB sector.

8.1 General Features

There are some unique features which distinguish this model from the MSSM on one side and the basic warped higgsless models on the other. The model contains no fermions with negative R parity in the fundamental representation and there are thus no couplings of neutralinos with neutral gauge bosons at tree level,

$$\mathcal{L}[\chi_i^0, \chi_j^0, Z] \propto \epsilon^{333} = 0 \quad (8.1)$$

They are present in the MSSM due to the neutral Higgsinos. All gaugino gauge interactions at tree level are proportional to the $SU(N)$ structure constants and our neutralinos and charginos are by definition Wino and Bino mixings. This has important consequences for the phenomenology of the LSPs since potentially important annihilation and production channels are absent, for example coannihilation of the two (tree level) degenerate light neutralinos with a Z boson in the s channel.

Even the lightest sfermions in our model are without exception Kaluza-Klein resonances. They have, apart from the third quark generation, suppressed effective couplings to matter due to the wave function profile which is similar to that of the corresponding Kaluza-Klein matter fermions and thus almost orthogonal to the zero mode. At the same time, they are heavy with $m_{\tilde{f}} = 700 \dots 1500$ GeV. This

makes them harder to produce and detect, and were it not for the IR localization of the t and b quarks, the sfermion sector would be somewhat hidden from SM matter. The photon and gluon couplings to the sfermions are of course universal, but they have to produce them in pairs. These two properties together result in the rather low LHC production cross sections of neutralino pairs discussed in section 8.6.

Even though our SUSY extension does not modify directly the couplings within the “standard” higgsless particle spectrum, it can still drastically change their properties, namely through the introduction of new decay modes which increase the width of some of the Kaluza-Klein resonances. This will be discussed in more detail in section 8.5.

5D SYM theory necessarily contains scalar particles with special properties which will be reviewed in section 8.4. Again, the third generation coupling is strongest, but for different reasons.

8.2 Tree Level Contributions to Precision Observables

The calculations in this section are not per se tied to our supersymmetric extension, but concern the relationship between fermion localization and boundary kinetic terms of the gauge bosons and their combined impact on the Peskin-Takeuchi S parameter and the masses of Kaluza-Klein resonances. This has not been treated in the literature in detail, it is however relevant to our supersymmetric model because we use one of the kinetic terms to split the electroweak gauge supermultiplet. We follow the approach outlined in [17, 33] to calculate the tree level contributions to oblique corrections, but extend the analysis to account for the combined effect of an UV brane localized $SU(2)_L$ kinetic term, an IR brane localized $SU(2)_D$ diagonal kinetic term and bulk delocalized fermions. The calculation was done in the conformal coordinate frame. First of all, we introduce a second parameter β for the IR brane term and both together give us modified gauge boson boundary conditions,

$$\partial_z A_\mu^L + \kappa R\pi m^2 A_\mu^L = 0|_{z=1/k} \quad (8.2a)$$

$$(\partial_z A_\mu^L + \partial_z A_\mu^R) - \beta R\pi e^{Rk\pi} m^2 (A_\mu^L + A_\mu^R) = 0|_{z=e^{Rk\pi}/k} \quad (8.2b)$$

The procedure goes now as follows: the eigenvalue problem with these modified boundary conditions is now solved for the W and Z tower analytically, and we expand the resulting expressions for the lowest massive modes in $m/k \approx 10^{-17}$ and $me^{Rk\pi}/k \approx 0.2$, the latter of which is unfortunately not very small. We fix the ratio $Rk\pi$ and can thus invert the expressions for m_Z and m_W to calculate $R(m_W, \kappa, \alpha)^1$. We plug those back into the Kaluza-Klein wave functions which we also expand in the same small quantities to get an analytic expression for the normalization integral of the gauge bosons. We assume massless fermions which saves us the additional work of having to construct analytic expressions

¹We could now calculate \tilde{g}_{ew}/g_{ew} from m_W/m_Z , but this would lead to non-oblique deviations from the SM in the resulting gauge boson couplings to matter.

for massive fermion wave functions. This is justified as the IR Dirac mass of the light quarks and leptons ($m \ll \Lambda_{IR}$) only introduces a small deformation of the Kaluza-Klein wavefunction. The zero mode has the well-known shape

$$f_\psi^0 = N (kz)^{2-c_L} \quad (8.3)$$

and we demand canonical normalization

$$\int_{1/k}^{e^{Rk\pi}/k} dz (kz)^{-4} (f_\psi^0)^2 = N^2 \frac{1 - e^{(1-2c_L)Rk\pi}}{k(2c_L - 1)} = 1 \quad (8.4)$$

We can now build the analytic expressions for the coupling constants. The expression for the effective weak mixing angle from the Z coupling does not depend on the absolute values of \tilde{g}_{ew} and g_{ew} ,

$$\tan \theta_W = \sqrt{\frac{\tilde{g}_{ew} \langle \psi^0 \psi^0 B \rangle}{g_{ew} \langle \psi^0 \psi^0 A_L \rangle}} \quad (8.5)$$

However, the Kaluza-Klein wave functions f_B and f_L also depend on \tilde{g}_{ew}/g_{ew} . We can now solve for this ratio numerically, and together with the fine structure constant as an input parameter, we can determine the absolute values of \tilde{g}_{ew} and g_{ew} through the canonical normalization relation of the photon

$$\frac{g_{ew}}{\sqrt{4\pi\alpha}} = \sqrt{R\pi \left(\left(\frac{g_{ew}}{\tilde{g}_{ew}} \right)^2 + 2 + \kappa + 2\beta \right)} \quad (8.6)$$

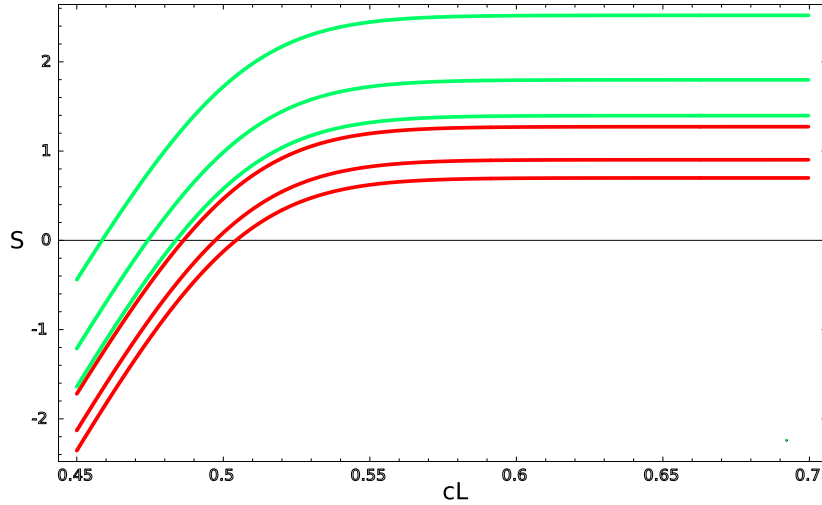
The point of this definition of g_{ew} and \tilde{g}_{ew} is that we can now compare the absolute size of the weak couplings to fermions to the SM value, and express the discrepancy as an effective BSM wave function renormalization of the gauge boson,

$$\Pi' \equiv \frac{2 \left(1 + \frac{g\sqrt{\cos \theta_w}}{g_{ew} \langle \psi^0 \psi^0 A_L \rangle} \right)}{g^2 + g'^2} \quad (8.7)$$

which can be used to determine the S parameter (which is simplified since our model does not produce tree level mixing $\Pi_{Z\gamma}$),

$$S = 16\pi\Pi' \quad (8.8)$$

Let us now plug in numbers to see how masses and couplings are affected. The result is shown in figure 8.1. The UV term raises the Kaluza-Klein scale relative to the W mass, shifting the W and Z resonances beyond the unitarity bound if the chargino is to escape detection at LEP and Tevatron. In return it lowers the S parameter somewhat. The IR term raises the S parameter again, but leads to much lighter gauge boson resonances. A combined IR and UV term gives us heavy charginos while the W and Z resonances stay below a TeV, and the S



κ	β	m_{χ^+}/GeV	$m_{W'}/\text{GeV}$
0	0.02	80	700
0.4	0.02	95	820
0.8	0.02	108	930
0	0	80	1189
0.4	0	95	1405
0.8	0	108	1590

Figure 8.1: The dependence of tree level contributions to the S parameter on κ , β and c_L for $e^{-Rk\pi} = 500 \cdot 10^{-19}$. The curves from top to bottom correspond to the values shown in the table in the same order. The two parameters have a tendency to counteract each other.

parameter again vanishes for almost delocalized fermions.

There is still the issue of the Zbb coupling which deviates significantly from the SM value and from the light quarks. The coupling becomes nonuniversal because the top mass is produced by a combination of IR localization and large IR boundary mass, which in turn makes a large splitting necessary. We do not address this weakness of the model in this work, and the ratio of couplings for $c_L = 0.4$, $c_R = -1/3$ indeed yields

$$g(Zb_l b_l)/g(Zd_l d_l) \approx 0.8 \quad (8.9)$$

For proposed solutions consider for example [34, 18]. It would be interesting to see how these mechanisms (in particular a second warped throat in [34]) could be used to implement soft SUSY breaking.

8.3 The LSP and its Relic Density

The calculation of the thermal relic density of stable DM candidates in beyond the SM-scenarios is by now a standard calculation which has been repeated for a wide range of models. As we do here, one often assumes a parity charge carried by some of the particles. If the Hamiltonian is even under this parity, the total parity of all particles participating in an interaction is always +1, rendering the lightest parity-odd particle of mass m_0 stable. If it participates for example in the weak interaction, it remains in thermal equilibrium with the other particle species present at early cosmological times as long as the temperature exceeds $T \gg m_0$. While the universe is cooling due to its expansion, less and less energy is available for production of heavy particles with $m \gg T$, and they begin to decouple from the other still effectively massless particle species which remain in thermal equilibrium relative to each other and the photons. From this time on, the number density per comoving volume can only decrease via annihilation with other parity-odd particles, and once the expansion rate of the universe exceeds the annihilation rate,

$$H \gg \Gamma \quad (8.10)$$

pairs of parity-odd particles hardly scatter any more and the number density per comoving volume remains constant (“freezes out”). The temperature at this point in time is called freezeout temperature $T_f = m_0/x_f$, and can be much smaller than the particle’s mass ($x_f > 20$ is a typical value for annihilation through the weak interaction). To obtain the density of the lightest stable particle at present times ($T = 2.7K$), one needs to solve the Boltzmann equations for the decoupling process,

$$\frac{dn}{dt} + 3Hn = -\langle\sigma v\rangle (n^2 - n_{eq}^2) \quad (8.11)$$

which describe the change in density n of a particle with annihilation cross section σ averaged over the velocity v . Fortunately, there are good approximative formulae for weakly interacting particles which can be used to give an estimate of relic densities without having to do the full numerical simulation. Once the relevant masses and cross sections are known, the only missing ingredient is the number of active (effectively massless) particle degrees of freedom g_* at times around the freezeout, where fermion d.o.f. are weighted with a relative factor of

$$\int_0^\infty d\epsilon \frac{\epsilon^3}{(e^{\epsilon\beta} + 1)} / \int_0^\infty d\epsilon \frac{\epsilon^3}{(e^{\epsilon\beta} - 1)} = 7/8. \quad (8.12)$$

accounting for the smaller energy density due to Fermi-Dirac statistics. The annihilation scattering crosssection is expanded in small velocities

$$\sigma v \approx a + v^2 b + \mathcal{O}(v^3) \quad (8.13)$$

and averaged thermally (in the nonrelativistic limit)

$$\langle\sigma v\rangle \approx a + 6\frac{T}{m_0}b = a + 6b/x \quad (8.14)$$

Based on this, the authors of [40] give the approximation for the relic density

$$\Omega h^2 = \frac{1.04 \cdot 10^9 \text{ GeV}^{-1}}{M_{pl}} \frac{x_f}{\sqrt{g_*}} \frac{1}{a + 3b/x_f} \quad (8.15)$$

At relevant energies $5 \text{ GeV} < E < 80 \text{ GeV}$ we assume $2 + 2 \times 8$ vector boson d.o.f. from γ and g , 3×2 neutrino d.o.f., 3×4 charged lepton d.o.f. and $5 \times 4 \times 3$ quark d.o.f., giving us $g_* \approx 86 1/4$. The relative freezeout temperature can in turn be determined by an iterative procedure [40],

$$x_{n+1} = \log \left(\frac{5}{4} \sqrt{\frac{45}{8}} \frac{g}{2\pi^3} \frac{m_0 M_{pl} (a + 6b/x_n)}{\sqrt{g_* x_n}} \right) \quad (8.16)$$

which involves some empirical factors from the matching to numerical integration. We have put in an estimate of x_f to obtain g_* , and the result for x_f determined in this manner should of course be self-consistent. Due to the log, the result turns out not to be very sensitive on σ . The number of degrees of freedom of the relic particle is $g = 4$ as will be explained later.

In our model with SUSY breaking on the UV brane, the scalar partners of quarks and gauge bosons receive large mass corrections. Therefore, the main contribution to neutralino annihilation is not into fermions via sfermion exchange, but into W pairs through chargino exchange. The third and fourth graph in figure 8.1 are only present if interactions with higher resonances of the gravity sector are taken into account. We have calculated the effective couplings in section 7.1.3 which indicate that spin 2 and 3/2 resonances do not play an important rôle in neutralino annihilation. Potential coannihilation partners are the NLSP charginos, and since we can assume $m(\text{NLSP}) - m(\text{LSP}) = m_{\chi^+} - m_{\chi^0} > 10 \text{ GeV}$ it seems justified to neglect the effect of coannihilation $\chi^0 \chi^+ \rightarrow X$ for simplicity. To give an estimate of the individual contributions $\chi_i^0 \chi_j^0 \rightarrow X$, it makes sense to add the inverse densities

$$1/\Omega h^2(x_f) = \sum_n \Omega h_n^2(x_f)^{-1} \propto \sum_n a_n + 3b_n/x_f \quad (8.17)$$

for a realistic fixed freezeout temperature, which depends only weakly on the cross section. The value currently favored by WMAP data is $1/\Omega h^2 \approx 9 \dots 11$ [55].

Now, let us calculate the effective coupling constants relevant for neutralino annihilation into W pairs. The corresponding piece of the Lagrangian is given in section 6.3.9. The effective coupling constants for the charged current are of the form

$$\langle W \lambda_i \lambda_j \rangle \equiv \int dy \sqrt{g} e^{Rky} f_W(y) f_{\lambda_i}(y) f_{\lambda_j}(y) \quad (8.18)$$

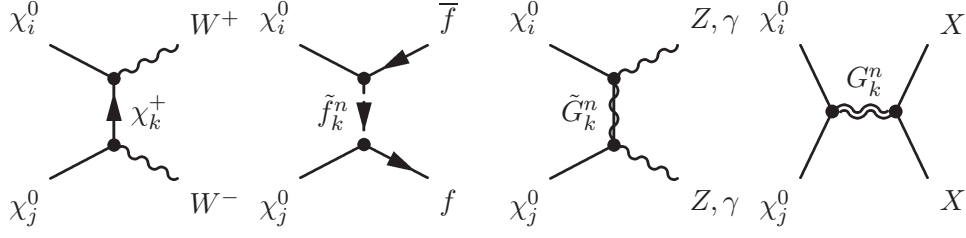


Table 8.1: The graphs which potentially contribute to Neutralino annihilation at tree level

They can be approximated analytically to leading order using $Rk\pi \gg 1$ and $m_W, m_\chi \ll ke^{-Rk\pi}$ as

$$\begin{aligned} \langle W^{L\pm} \lambda_2^{L\pm} \lambda_2^{L3} \rangle &\simeq -\frac{3}{8}C \\ \langle W^{R\pm} \lambda_2^{R\pm} \lambda_2^{R3} \rangle &\simeq -\frac{1}{8}C \end{aligned} \quad (8.19)$$

with

$$\begin{aligned} \langle W^{L\pm} \lambda_1^{L\pm} \lambda_1^{L3} \rangle &\simeq -C \\ \langle W^{R\pm} \lambda_1^{R\pm} \lambda_1^{R3} \rangle &\simeq -\frac{1}{48Rk\pi}C \end{aligned} \quad (8.20)$$

in scenario IIa and

$$\begin{aligned} \langle W^{L\pm} \lambda_1^{L\pm} \lambda_1^{L3} \rangle &\simeq -\frac{|\cos(\theta)|}{24Rk\pi}C \\ \langle W^{R\pm} \lambda_1^{R\pm} \lambda_1^{R3} \rangle &\simeq -\frac{7|\cos(\theta)|}{48Rk\pi}C \end{aligned} \quad (8.21)$$

in scenario Ib, respectively, where

$$C = \frac{1}{\sqrt{(\kappa + 1)R\pi}}. \quad (8.22)$$

They are accurate to about 5% for $Rk\pi > 30$ (cf. also Fig. 8.2 below). Note that the absolute size of the coupling is approximately independent of the free parameters,

$$g_{ew}C \simeq \frac{\sqrt{4\pi\alpha}}{\sin(\theta_W)}, \quad (8.23)$$

and the leading contributions are also independent of the neutralino mass. This is remarkable because it means that the annihilation cross section depends on the neutralino and chargino mass only which is governed by the kinetic term κ and the gaugino mixing angle θ . Since we have two lightest Majorana neutralinos

which are degenerate at tree level, we treat them as one particle with 4 degrees of freedom for our purposes. In terms of Majorana neutralinos there are four relevant annihilation processes

$$\chi_a \chi_a \rightarrow W^+ W^-, \quad \chi_b \chi_b \rightarrow W^+ W^-, \quad \chi_a \chi_b \rightarrow W^+ W^-, \quad \chi_b \chi_a \rightarrow W^+ W^- \quad (8.24)$$

We assume that both species χ_a and χ_b have the same density which seems reasonable since the cross sections σ_{aa} and σ_{bb} are equal. Four diagrams contribute to each of these processes, since there are two light charginos $\chi_{a,b}^\pm$ in either the t or u channel. We have implemented the relevant interaction (section 6.3.9) in FeynArts/FormCalc to compute the spin and neutralino flavor averaged analytic scattering cross section $\langle v\sigma \rangle = \langle v(\sigma_{aa} + \sigma_{bb} + 2\sigma_{ab})/4 \rangle$, which we have expanded to second order in v and performed the simple phase space integration over ϕ and t in Mathematica.

The coupling constants which result from scenario IIa are exactly of electroweak strength with

$$g_{ew} \langle W^{L\pm} \lambda_1^{L\pm} \lambda_1^{L3} \rangle \simeq -\frac{\sqrt{4\pi\alpha}}{\sin(\theta_W)}$$

which results in annihilation cross sections which are generally much too large. Incidentally, the “twisted gaugino” boundary conditions in scenario Ib which give us a light neutralino also suppresses the chargino component in λ_1^L sufficiently such that the corresponding coupling constants become very small and only the couplings to λ_2 contribute which are just about of the right size to lead to viable annihilation cross sections. Unfortunately, the appealing choice $\theta = \theta_{w5}$ which would implement the same mixing angle for gauge bosons and gauginos, leads to a neutralino with $m_\chi \approx 40$ GeV which, at tree level, only annihilates into fermions via sfermion resonance exchange. These channels are, despite the large number of quark and lepton final states, doubly suppressed. Due to the large KK mass of the sfermions around $-c_R, c_L \approx 0.2 \dots 0.7$ of $m_{\tilde{f}} > 2ke^{-Rk\pi}$, the cross sections $\chi^0 \chi^0 \rightarrow \bar{f}f$ will be suppressed relative to the annihilation to W pairs if $m_{\chi^0} > m_W$. We find that the couplings and cross section depend strongly on the localization of the fermion multiplets, but that a rather extreme localization towards the IR brane is necessary to make a significant contribution to the total annihilation cross section. This region of parameter space is ruled out due to FCNCs (unless an additional flavor symmetry is introduced to suppress them) and proton decay from higher dimensional operators. Therefore we conclude that in this scenario the tree level annihilation of neutralinos into fermions is negligible. For example, if one carries out the calculation for $k = \Lambda_{\text{Pl}}$, $\kappa = 0.4$, $x_f = 23$ the contribution of the charm quark stays below $1/\Omega h^2 < 0.3$ for $|c_{L,R}| > 0.25$ and even $1/\Omega h^2 < 0.02$ for $|c_{L,R}| > 0.5$. The electron which must be at $c_L \approx 0.5$ to get a realistic S parameter, contributes $1/\Omega h^2 < 0.01$. One uncertainty comes from the precise implementation of the third quark generation. The straightforward generation of m_b and m_t with boundary terms leads to problems with the $Zb\bar{b}$ coupling. Depending on how the b quark is realized, its coupling to the neutralino could be somewhat enhanced, but we can still expect that the channel $\chi_i^0 \chi_j^0 \rightarrow b\bar{b}$

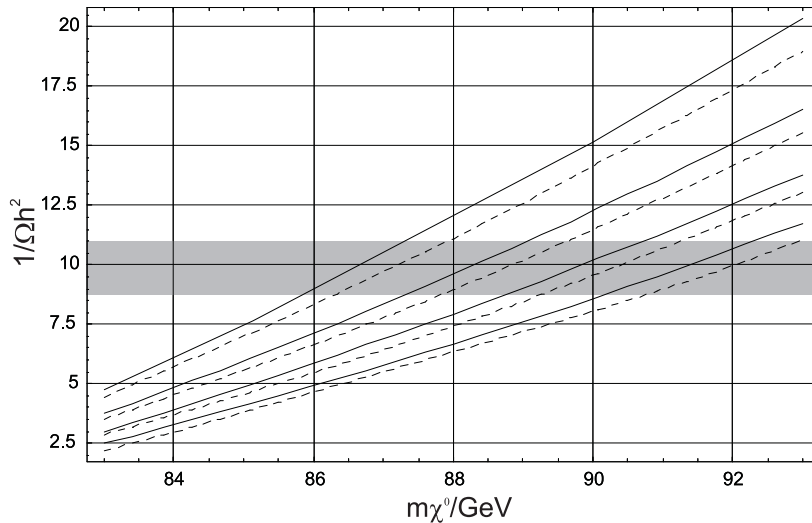


Figure 8.2: The m_{χ^0} -dependence of contributions to $1/\Omega h^2$ for annihilation into W pairs for $Rk\pi \simeq 37.5$, $k = \Lambda_{\text{Pl}}$. The parameter is (from topmost) $\kappa = 0.4, 0.6, 0.8, 1.0$, corresponding to $m_{\chi^+} = 95, 102, 108, 114$ GeV. For this process we use $\alpha = 1/128$. The dashed lines are obtained using the approximations in (8.19)-(8.23). The shaded area represents the region allowed by the WMAP three year data.

does not play a major role for LSP annihilation. This means that our neutralino must be heavy enough, $m_{\chi^0} > m_W$, to annihilate into W pairs efficiently. The resulting inverse density for Ib is shown in figure 8.2. We conclude that it is possible to reach realistic relic densities without the need for any fine tuning of parameters because our choice of twisted boundary conditions gives us sufficiently suppressed coupling constants relative to weak strength such that there is enough relic density from thermal production.

8.4 Properties of the Physical Scalars

Interestingly, there are physical scalars in higgsless warped SUSY models which result from the structure of the 5D vector supermultiplet. In the unbroken case they are degenerate with the massive gauge bosons. In our breaking scenario outlined in chapter 7, the tree level masses of the lightest modes in the electroweak triplet $\Sigma^{\pm 0}$ are shifted somewhat up to masses $m_\Sigma \gtrsim \sqrt{2}m_W$, while the color charged scalar Σ^c remains at $m_\Sigma = m_{\tilde{G}} \gtrsim \text{TeV}$. Let us now first investigate the properties of these scalars in the tree level approximation. We then consider the implications of our UV brane SUSY breaking scheme on the masses of the light electroweak scalars.

Particle	c_L	c_R	y_{eff}^0	m/y_{eff}^0
u	0.48	-0.48	$1.19 \cdot 10^{-5}$	253 GeV
d	0.48	-0.48	$2.35 \cdot 10^{-5}$	255 GeV
c	0.48	-0.48	$5.10 \cdot 10^{-3}$	255 GeV
s	0.48	-0.48	$4.36 \cdot 10^{-4}$	252 GeV
t	0.4	-1/3	0.53	338 GeV
b	0.4	-1/3	$1.53 \cdot 10^{-2}$	294 GeV

Table 8.2: The Yukawa couplings of the lightest neutral gauge scalar to quarks assuming the parameters given in table 7.1

8.4.1 Yukawa Couplings

Since our scalars do not have VEVs, the classic ‘‘Higgsstrahlung’’ production channel is absent and the corresponding LEP bounds are not relevant. There is, however, the interaction from \mathcal{L}_{18} (appendix B.2) which has an interesting property: Since massless fermion modes are localized entirely in the 5D fields ψ_L and ψ_R^c , this interaction vanishes exactly. Once we turn on the IR brane Dirac mass, the fields transforming under $SU(2)_L$ and $SU(2)_R$ mix and $\psi_R, \psi_L^c \neq 0$. Wouldn’t it be ironic if it turned out that this produces a Yukawa coupling which is approximately proportional to the fermion mass like the SM Higgs coupling? The effective coupling is given by

$$y_{\text{eff}}^0 = g_{ew} |T^3| \langle \psi_L \psi_L^c \Sigma_L^0 + \psi_R \psi_R^c \Sigma_R^0 \rangle \quad (8.25)$$

where $|T^3| = 1/2$ and

$$\langle \psi_i \psi_j \Sigma_k \rangle = \int dy \sqrt{g} f_{\psi_i} f_{\psi_j} f_{\Sigma_k} \quad (8.26)$$

We consider only the Kaluza-Klein wave functions of the lowest mode in each tower as they represent the SM fermions and the lightest scalar. The values for $k = 10^{19}$ GeV, $\kappa = 0.6$ are given in table 8.2.

The tree level mass of the scalars for this configuration is $m_\Sigma = 154$ GeV. The coupling strength is somewhat below the corresponding SM value of $m/y \simeq 246/\sqrt{2}$ GeV. This has consequence that the sneutralino Σ^0 might look Higgslike in some of the typical LHC production and decay channels such as gluon fusion to a top triangle. The same order of magnitude would hold for the charged scalar couplings

$$y_{\text{eff}}^\pm = g_{ew} |T^\pm| \langle \psi_{f1L} \psi_{f2L}^c \Sigma_L^\mp + \psi_{f1R} \psi_{f2R}^c \Sigma_R^\mp \rangle \quad (8.27)$$

which are however chiral, as shown in table 8.3. The situation is very different

Part. ($f1, f2$)	c_L	c_R	y_{eff}^+
ud	0.48	-0.48	$2.37 \cdot 10^{-5}$
du	0.48	-0.48	$1.17 \cdot 10^{-5}$
cs	0.48	-0.48	$4.31 \cdot 10^{-4}$
sc	0.48	-0.48	$5.15 \cdot 10^{-3}$
tb	0.4	-1/3	0.013
bt	0.4	-1/3	0.62

Table 8.3: The Yukawa couplings of the lightest charged gauge scalar to quarks assuming the parameters given in table 7.1

Particle	c_L	c_R	y_{eff}^c
u	0.48	-0.48	$< 10^{-6}$
d	0.48	-0.48	$< 10^{-6}$
c	0.48	-0.48	$< 10^{-6}$
s	0.48	-0.48	10^{-5}
t	0.4	-1/3	-0.1316
b	0.4	-1/3	$6.5 \cdot 10^{-3}$

Table 8.4: The Yukawa couplings of the color octet of gauge scalars to quarks assuming the parameters given in table 7.1

for the color charged gauge scalar Σ^c or “sgluino”, which couples to matter with

$$y_{\text{eff}}^c = g_{YM} \langle \psi_L \psi_L^c \Sigma^c + \psi_R \psi_R^c \Sigma^c \rangle \quad (8.28)$$

The electroweak scalars fulfil an IR boundary condition of the type

$$\Sigma_L^{\pm 0} = -\Sigma_R^{\pm 0} \Big|_{y=\pi}$$

and this sign flip compensates the relative sign flip of the matter fermion wave functions ψ_L/ψ_L^c to ψ_R/ψ_R^c . The color charged scalar however couples to both the $SU(2)_L$ transforming doublet as it does to the $SU(2)_R$ transforming doublet. If $c_L = -c_R$ and the UV brane fermion kinetic term is not large then $\psi_L \approx \psi_R$, $\psi_L^c \approx -\psi_R^c$ and the two contributions cancel! In our configurations, only the third generation quarks have a small coupling which can however still be neglected relative to the Kaluza-Klein gluon in most processes. The results are shown in table 8.4.

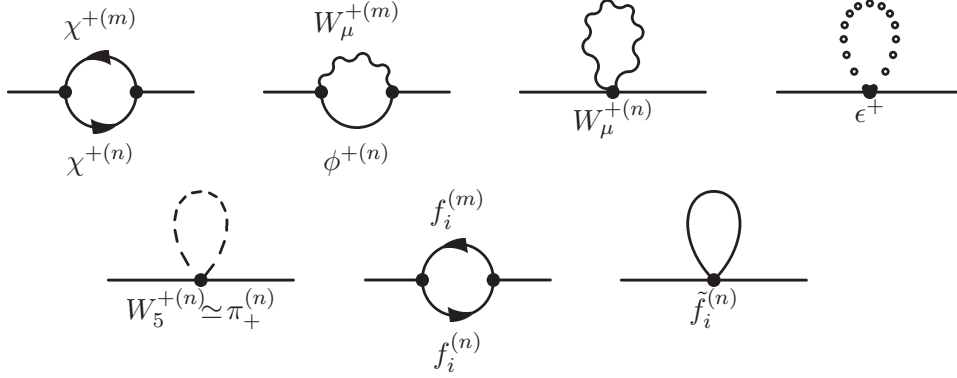


Figure 8.3: Quadratic contributions to the self energy of the neutral scalar.

8.4.2 Mass Corrections from UV Brane Breaking

The original Randall-Sundrum scenario addresses the hierarchy problem by placing the Higgs boson on what is now known as the infrared or TeV brane. We do not have to stabilize any Higgs masses, but it would be interesting if some of the scalars mentioned above remained light. Our IR sector is supersymmetric, and even though strongly IR localized states see the breaking on the UV brane and get masses at tree level, they can still get corrections through loops of UV localized particles. The quadratic corrections from the individual IR localized particles get very large, but they almost exactly cancel within supermultiplets. To obtain an estimate of how strongly our UV brane breaking in the matter- and gauge sector affects Σ^0 , we have evaluated the corresponding loops (figure 8.3) in the Kaluza-Klein picture and discuss the resulting effective couplings. We want to see how large the contributions from possible quadratic divergences will be. In massive regularization schemes like Pauli-Villars, we see the Λ scale dependence directly, but it breaks gauge invariance. There is however a general relationship between poles in dimensional regularization and quadratic and quartic divergences which has been discussed in detail in [56, 57]. It is important to note that quadratic divergences at the L loop level are associated with poles at

$$d = 4 - 2\epsilon = 4 - 2/L' \quad (8.29)$$

where $L' \leq L$ [56]. While there are poles associated to log divergences up to order ϵ^{-L} , the “leading” pole from higher divergences $1/(\epsilon - L)$ is simple. This is also true for the other poles except the one at $L' = 1$ which can be double from quadratically divergent subgraphs in quadratically divergent two loop graphs. The authors of [56, 57] follow the philosophy that the renormalized action should be finite for all $d \leq 4$, leading to generalized counterterms and renormalization group equations. In our case at one loop, if a quadratic divergence is present, there is a simple $\mu^2/(\epsilon - 1)$ pole alongside the $1/\epsilon$ pole in the self energy. We extract the quadratic divergences by going to $d \rightarrow 2$. Therefore we need the

contributions of the epsilon scalars which provide the missing two vector degrees of freedom. Consider the quadratic gauge contribution from the graphs in figure 8.3,

$$\Sigma^{lr} = \frac{1}{\epsilon - 1} \frac{ig_5^2 \mu^2}{2\pi} \sum_n \left[4 \sum_m \langle f_{\Sigma}^l f_{\chi_1}^m f_{\chi_2}^n \rangle \langle f_{\Sigma}^r f_{\chi_1}^m f_{\chi_2}^n \rangle + \xi \sum_m \langle f_{\Sigma}^l f_{W_{\mu}}^m f_{\Sigma^+}^n \rangle \langle f_{\Sigma}^r f_{W_{\mu}}^m f_{\Sigma^+}^n \rangle - \langle f_{\Sigma}^l f_{\Sigma}^r f_{W_5}^m f_{W_5}^m \rangle - (3 + \xi) \langle f_{\Sigma}^r f_{\Sigma}^l f_{W_{\mu}}^m f_{W_{\mu}}^m \rangle \right] + \mathcal{O}\left(\frac{1}{\epsilon} + \text{finite}\right)$$

It is implied that there are infinite sums over the Kaluza-Klein indices m and n . There is a ξ dependence, which we can get rid of by using the same types of sum rules which also ensure Ward identities and unitarity. We further identify the loop cutoff scale Λ^2 with the scale parameter $4\pi\mu^2$. It might appear a little strange that we have to take some sums to infinity to cancel the ξ dependence etc., but then have to cut the remaining sums off at our current cutoff scale. In a more comprehensive treatment, this can surely be avoided by introducing appropriate nonrenormalizable operators at the cutoff as they appear for example in deconstruction to restore gauge invariance using a finite particle content. We rewrite the self energy with sum rules in a manner such that ξ cancels and the quadratic divergences vanish manifestly in the unbroken case,

$$\Sigma_{quad}(\Lambda) = \frac{1}{\epsilon - 1} \frac{ig_5^2 \Lambda^2}{8\pi^2} \sum_{M_n < \Lambda} \left[\begin{aligned} &\langle f_{\Sigma}^l f_{\Sigma}^r f_{\chi_2}^n f_{\chi_2}^n \rangle - \langle f_{\Sigma}^l f_{\Sigma}^r f_{W_5}^n f_{W_5}^n \rangle \\ &\underbrace{+ 3 \langle f_{\Sigma}^r f_{\Sigma}^l f_{\chi_1}^n f_{\chi_1}^n \rangle - 3 \langle f_{\Sigma}^r f_{\Sigma}^l f_{W_{\mu}}^n f_{W_{\mu}}^n \rangle}_{=0 \text{ for unbroken SUSY}} \end{aligned} \right]$$

We then go to the 4D effective theory, and assuming an optimistic cutoff of $\Lambda_c \approx 10$ TeV we collect the corrections to the pole mass going from $m(\Lambda_c) \approx m_{KK}$ to $m(\Lambda) \approx \Lambda$, switching off contributions of particles in the loop with masses much larger than the current Λ . A general result is that the corrections to the scalar mass squared are positive and at the order of a few hundred GeV to 1.5 TeV. The largest contributions come from the lightest gauge sector modes and the top quark which has no light partner. The contributions from higher modes are almost supersymmetric and cancel. It is not clear how stable this procedure is since the effective couplings involved are rather large and we make the approximation that particles are either massless or integrated out, but we can draw the conclusion that in our class of models, the Higgslike scalars are shifted to heavier masses close to the Kaluza-Klein scale unless a softer SUSY breaking scheme is employed.

8.5 Decays of Heavy Resonances

In this section we will summarize the decay modes and widths of all color charged and some important weakly interacting Kaluza-Klein resonances below 2500 GeV insofar as they become relevant for our LHC simulations. Since all of them can decay to two onshell particles, we neglect processes with intermediate offshell

Squark	Mass	Width	Squark	Mass	Width
\tilde{u}^1	1477	1	\tilde{u}^2	1527	15
$\tilde{u}^{c,1}$	1477	0.2	$\tilde{u}^{c,2}$	1527	20
\tilde{d}^1	1477	0.1	\tilde{d}^2	1527	10
$\tilde{d}^{c,1}$	1477	0.5	$\tilde{d}^{c,2}$	1527	20
\tilde{c}^1	1466	4	\tilde{c}^2	1537	17
$\tilde{c}^{c,1}$	1466	2	$\tilde{c}^{c,2}$	1537	6
\tilde{s}^1	1466	3	\tilde{s}^2	1537	11
$\tilde{s}^{c,1}$	1466	4	$\tilde{s}^{c,2}$	1537	17
\tilde{t}^1	878	94	\tilde{t}^2	2038	> 500
$\tilde{t}^{c,1}$	798	21	$\tilde{t}^{c,2}$	1975	> 500
\tilde{b}^1	878	71	\tilde{b}^2	2038	> 500
$\tilde{b}^{c,1}$	798	66	$\tilde{b}^{c,2}$	1975	> 500

Figure 8.4: Masses and main contributions to tree level widths of the lightest and next-to lightest squark resonances.

Gaugino	Mass	Width	Boson	Mass	Width
$\chi_a^{0,2}, \chi_b^{0,2}$	1496	71	Z^2	1503	470
$\chi_a^{0,3}, \chi_b^{0,3}$	1512	133	Z^3	1520	385
$\chi_a^{+,2}$	1509	216	W^2	1504	595
$\chi_b^{+,2}$	1509	216	g^2	1522	333
$\tilde{g}_1^1, \tilde{g}_2^1$	1496	570	Σ^c	1522	96

Figure 8.5: Masses and main contributions to tree level widths of gauge sector resonances.

particles along with all other higher order contributions. In particular the small widths $\mathcal{O}(1 \text{ GeV})$ result from suppressed tree level couplings and will certainly receive large relative corrections at higher orders. We therefore give only one significant digit for widths below 1 GeV. Note that the branching ratios add up to 100% only together with the charge conjugate channels (where present).

Squarks

For our benchmark choice of parameters, the squark spectrum is given in figure 8.4. The Lagrangian relevant for these decays is given in Sections 6.3.1, 6.3.2 and 6.3.3. Both the lightest and next-to-lightest squark resonances can decay via

$$\tilde{q} \rightarrow q\chi^{0\pm} \quad (8.30)$$

The decay mode to a quark and the two lightest degenerate gluino resonances,

$$\tilde{q} \rightarrow q\tilde{g} \quad (8.31)$$

is only allowed for the next-to-lightest squark resonances. They are particularly heavy in the third generation and there can even decay to final states containing one Kaluza-Klein excitation,

$$\tilde{q}^2 \rightarrow q^2\chi^{0\pm}, q\chi^{0\pm,2} \quad (8.32)$$

Other Bosons

At tree level, the color charged gauge scalar Σ^c decays almost exclusively to pairs of one third generation quark and its lightest KK resonance,

$$\Sigma^c \rightarrow \bar{t}t^2(34\%), \bar{b}b^2(16\%) + c.c. \quad (8.33)$$

The relevant Lagrangian is given in section 6.3.4. The small partial width $\Gamma_{uu,dd,ss,cc}/\Gamma_{tot} < 1\%$ to zero mode quarks is due to a cancellation between the two 5D quark doublets (see section 8.4.1) and thus depends on the precise choice of quark bulk masses. The gluon resonance is rather broad because the decay to third generation quarks is enhanced compared to the other couplings which are suppressed because delocalized quark zero modes are nearly orthogonal to the heavier modes in the gluon Kaluza-Klein tower. While light quarks contribute $\Gamma_{uu,dd,ss,cc}/\Gamma_{tot} < 1\%$, the leading contribution is

$$g^2 \rightarrow \bar{t}t(33\%), \bar{b}b(15\%) \quad (8.34)$$

followed by decay into pairs of one third generation quark and its lightest KK resonance,

$$g^2 \rightarrow \bar{t}t^2(13\%), \bar{b}b^2(13\%) + c.c. \quad (8.35)$$

The relevant Lagrangian is given in section 6.3.8. The electroweak boson resonances are somewhat peculiar due to their strong decay mode to gauginos,

$$W^{+,2} \rightarrow \chi^+\chi^0(80\%) \quad Z^{2/3} \rightarrow \chi^+\chi^-(81/23\%) \quad (8.36)$$

which dominates for the first resonances W^2 , Z^2 and makes them unusually broad. The culprit is the large overlap of the wave functions belonging to the “righthanded” gaugino fields λ_2 with the first KK excitations of the gauge bosons which is of the order $g_{ew}\langle\lambda_2^{\pm 0}\lambda_2^{\pm}A'\rangle \gtrsim 3$. The relevant Lagrangian is given in Sections 6.3.9 and 6.3.10. At the same time, decays of gauge boson resonances to light gauge bosons do not contribute significantly.

Gauginos

The main contributions to gluino decay are

$$\tilde{g} \rightarrow \bar{t}\tilde{t}(34\%), \bar{b}\tilde{b}(16\%) + c.c. \quad (8.37)$$

The relevant Lagrangian is given in section 6.3.3. The corresponding couplings are enhanced by localization, making the gluinos very broad. In contrast the first and second generation quarks contribute less than 1 GeV at tree level. Similarly, the neutralinos decay almost exclusively via

$$\chi^{0,2} \rightarrow \bar{t}\tilde{t}(21\%), \bar{b}\tilde{b}(29\%) + c.c. \quad (8.38)$$

$$\chi^{0,3} \rightarrow \bar{t}\tilde{t}(40\%), \bar{b}\tilde{b}(10\%) + c.c. \quad (8.39)$$

while for the charginos

$$\chi_a^\pm \rightarrow \bar{t}\tilde{b}(76\%), \bar{b}\tilde{t}(24\%) \quad (8.40)$$

$$\chi_b^\pm \rightarrow \bar{t}\tilde{b}(42\%), \bar{b}\tilde{t}(58\%) \quad (8.41)$$

There are electroweak decays as well, namely

$$\chi^{0,2/3} \rightarrow \chi^\pm W^\mp \quad (8.42)$$

and

$$\chi^{\pm,2/3} \rightarrow \chi^\pm Z, \chi^0 W^\pm \quad (8.43)$$

but they couple two almost-zero modes to one gauge sector Kaluza-Klein mode which is approximately orthogonal to light modes, and therefore this effective coupling is suppressed relative to weak strength. One can state that generally, heavy gaugino resonances become broad mainly because of third generation IR localization and the large IR brane Dirac mass which splits the corresponding fermion and sfermion modes and pushes the light ones below the typical Kaluza-Klein scale.

Quarks

The quark resonances of the first and second generation are again very narrow compared to their mass (figure 8.6). They can only decay to a SM quark and a light massive gauge boson,

$$q^{2/3} \rightarrow qW, qZ \quad (8.44)$$

The relevant Lagrangian is given in section 6.3.7. The lightest third generation Kaluza-Klein resonances decay faster only because the heavy doublet has strong IR localization to generate the top mass on the IR brane, while couplings to the light almost delocalized quarks are again suppressed. There is just enough phase space for the light top resonance t^2 to decay to the light stop resonances and a neutralino,

$$t^2 \rightarrow \bar{t}^1 \chi^0 \quad (8.45)$$

Quark	Mass	Width	Quark	Mass	Width
u^2	1489	3	u^3	1527	5
d^2	1527	4	d^3	1527	4
c^2	1501	4	c^3	1552	3
s^2	1566	3	s^3	1537	4
t^2	973	25	t^3	2144	730
b^2	798	37	b^3	1975	650

Figure 8.6: Masses and main contributions to tree level widths of the lightest quark Kaluza-Klein resonances.

but these modes contribute only about 2%. The splitting of the third generation modes is however large enough to allow

$$f^3 \rightarrow f^2 Z, f^2 W, f g^2, f \Sigma, f W^2, f Z^{2/3}, \tilde{f}^1 \chi^{\pm 0} \quad (8.46)$$

which dominate because the couplings of two heavy modes to one light mode are not suppressed, and let those quark resonances become extremely broad.

8.6 Production of the LSP

8.6.1 Heavy Quarks and Missing Energy at the LHC

Stable neutralinos (and very likely any other DM candidates which are not yet ruled out by direct searches) are invisible to the detectors at collider experiments. This means that, even though our LSP might be produced copiously in processes of the type $q\bar{q} \rightarrow \chi^0 \chi^0$, the remainders of the protons go down the beam line, and since we lack information about the total cross-section, the process is entirely invisible. The standard approach is therefore to observe the associated production with other easily detectable objects such as leptons or hard jets, and to look for missing momentum in the direction transverse to the proton beams, \cancel{p}_T , which experiments are equipped to measure by balancing the visible momentum. One such process which we will however not pursue further is the electroweak production channel of neutralinos and charginos by VBF shown in figure 8.7. Instead we concentrate on another set of final states which is particularly favored in the model which we consider in this work, the production of third generation quarks in association with missing energy. In general, it can be an important process for discovering scenarios of WIMP DM such as SUSY with R parity. It is particularly interesting if a “partner” of heavy quarks exists which decays directly to a heavy quark (preferably the top) and invisible particles. In our scenario, this partner is the first stop mode \tilde{t} , and it is in a convenient mass range: it is still light enough to be pair produced copiously at the LHC at 14 TeV, and at the same time heavy enough ($m_{\tilde{t}} - m_\chi - m_t \gtrsim 400$ GeV) to produce a strong missing energy signal

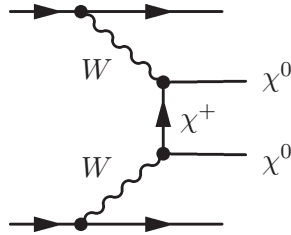


Figure 8.7: This vector boson fusion process is one of the electroweak LSP production channels at the LHC.

from the decay. Such a situation has been discussed in a generic way in [58]. The analysis carried out by the authors is valid for our \tilde{t} pair production contributions, but this is only one of the contributions to this class of final states in our model, where the production of heavy quark and gluon resonances proves to be important as well. Due to the size of the model, we rely on simulations with four particle final states, which means that we do not consider the possible decay modes of the t (hadronic, semileptonic, leptonic). When judging the results for the missing energy signal with t and b quarks in the final state, one therefore has to remember the following points: The t pair production itself does not introduce \cancel{p}_T , but the leptonic and semileptonic decay modes contain neutrinos, and considering the relative strength of t pair production, this can constitute an important background. In addition to this, there are SM processes with have final states distinguishable from our signal only by their kinematics, for example $pp \rightarrow b\bar{b}\nu l jj$ [58]. While the analysis of these contributions is beyond the scope of this thesis, there is a generic way to suppress these backgrounds: as becomes apparent in the following discussion, we can fortunately afford to place rather strong p_T and $\Delta\phi$ cuts without losing too much of our signal - this strategy would be futile if there was only a small mass gap between the t , neutralinos and the heavy partners. Let us therefore have a closer look at the model to see how the production of heavy quarks is suited for the discovery of our DM candidate via \cancel{p}_T .

The couplings of the neutralino itself are necessarily of weak strength, and considering the vertices in the model, the only production process at $\mathcal{O}(\alpha_s\alpha)$ is through squarks. Even though these are Kaluza-Klein in our version of UV brane symmetry breaking, they can be produced onshell and can only decay via

$$\tilde{q} \longrightarrow q\chi^0, q\chi^+ \quad (8.47)$$

due to the heavyness of the gluino, making this effectively an $\mathcal{O}(\alpha_s)$ process which can however be partly suppressed by the small coupling of Kaluza-Klein matter to matter and the large parton momentum fraction x needed to produce two onshell squarks. We can also obtain final states with two quarks and two LSPs by producing a heavy chargino or neutralino resonance which then decays to the LSP and two quarks through the decay chain shown in figure 8.8,

$$q\bar{q} \rightarrow \chi^0\chi^{0\pm,2/3}, \quad \chi^{0\pm,2/3} \rightarrow q\bar{q} \rightarrow \chi^0q\bar{q} + c.c \quad (8.48)$$

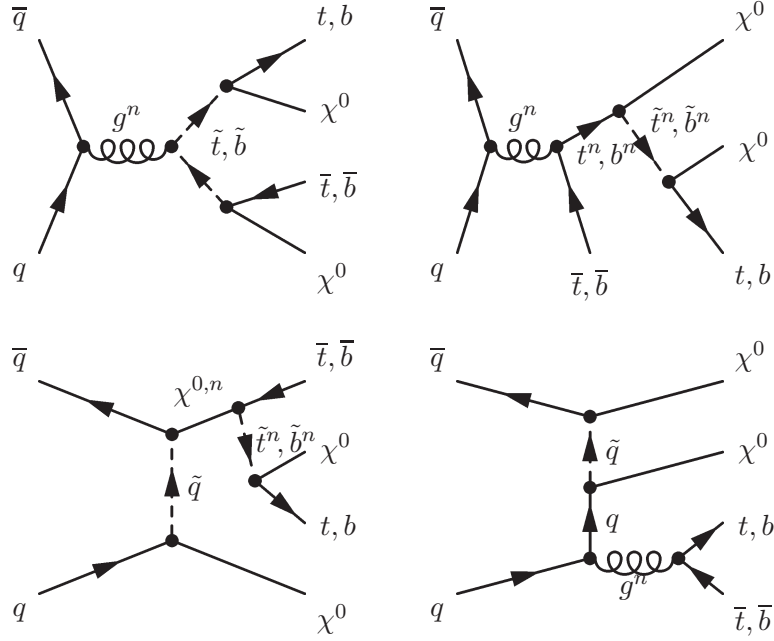


Figure 8.8: The relevant tree level contributions (up to charge conjugation and crossing) to associated heavy quark and LSP pair production with a $q\bar{q}$ initial state.

$$q\bar{q} \rightarrow \chi^0 \tilde{g}, \quad \tilde{g} \rightarrow \tilde{q}\bar{q} \rightarrow \chi^0 q\bar{q} + c.c. \quad (8.49)$$

but these channels are suppressed because of the small coupling of a light neutralino to squarks and light quarks and like for LSP annihilation they do not play a significant role. Kaluza-Klein top production and decay (figure 8.8) is not as suppressed because of the IR localization of the top quark, and we can thus have

$$q\bar{q} \rightarrow \bar{t}t^2 \quad t^2 \rightarrow \chi^0 \bar{t}^1 \rightarrow \chi^0 \chi^0 t \quad (8.50)$$

Considering the tree level 2 to 4 particle interactions for these processes we find that only the following vertices actually appear in $pp \rightarrow \chi^0 \chi^0 q_i \bar{q}_j$ (indices are implicit):

$$ggg \quad qqg \quad \tilde{q}\tilde{q}g \quad \tilde{q}\tilde{q}gg \quad q\tilde{q}\tilde{g} \quad qq\Sigma \quad \tilde{q}\tilde{q}\Sigma \quad \tilde{q}q\chi^0 \quad \tilde{q}q\chi^+ \quad (8.51)$$

For chargino production, we also have to include

$$WWZ, \gamma \quad qqW \quad qqZ, \gamma \quad \chi^+ \chi^- Z, \gamma \quad \chi^+ \chi^0 W^- \quad (8.52)$$

Due to the unbroken $U(1)_Q$ and $SU(3)_c$, the vertices involving only zero mode photons and gluons couple exactly with e , g_s and g_s^2 respectively. The strength of interactions between massive Kaluza-Klein modes as determined by the overlap of their bulk profiles may differ significantly from the strong or electroweak coupling of the lightest modes.

Clearly, the light third generation squarks will be most important at the LHC as

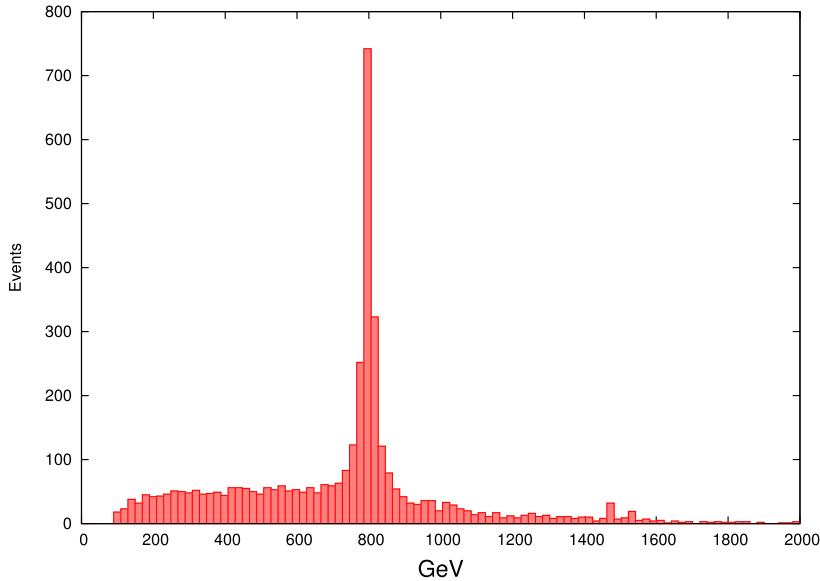


Figure 8.9: The invariant mass distribution of the quark and a neutralino in the process $gg \rightarrow q\bar{q}\chi^0\chi^0$ with a center of mass energy of $\sqrt{s} = 14$ TeV and $\int \mathcal{L} = 200 \text{ fb}^{-1}$ with PDFs and bin size 20 GeV. The lightest third generation squarks are clearly dominant, while heavier squark resonances are visible as well between 1400 . . . 1600 GeV.

they couple strongly (also to their quark partners) and are not too broad. This is illustrated by the (unobservable) production of neutralinos and squarks shown in figure 8.9.

8.6.2 Simulation of Warped Higgsless LSP Production at the LHC

We simulate the production of our LSP with O’Mega/WHIZARD, and all following statements refer to our implementation (section E.2) and, if not stated otherwise, hadronic cross sections using the *cteq6m.LHpdf* PDF sets from the LHAPDF library [59].

The SM cross section for $pp \rightarrow b\bar{b}, t\bar{t}$ at $\sqrt{s} = 14$ TeV is of course huge, at around $\sigma > 10^5$ fb for cuts $p_T(b) > 400$ GeV, $\eta(b) > 200$ GeV and “low x cuts” of $E > 20$ GeV of the incoming partons. One should avoid as much as possible misattributions of such processes, for example by cutting on angular distance of the jets. How well this works in each case depends on many experimental factors which are beyond the scope of this work. At the $2 \rightarrow 4$ particle level, the SM background from $pp \rightarrow q\bar{q}\nu\bar{\nu}$ is also large, and we want to separate it from our contributions with massive neutralinos. One efficient way to do this is by cutting on the transverse momentum of the quarks. For $p_T(q) > 300$ GeV the cross section is reduced down to ≈ 10 fb. The remaining neutrinos are dominantly produced from Z decays (figure 8.11). On the signal side, contributions from graphs like the last one in figure 8.8 would have a lot of recoil and large \cancel{E}_T

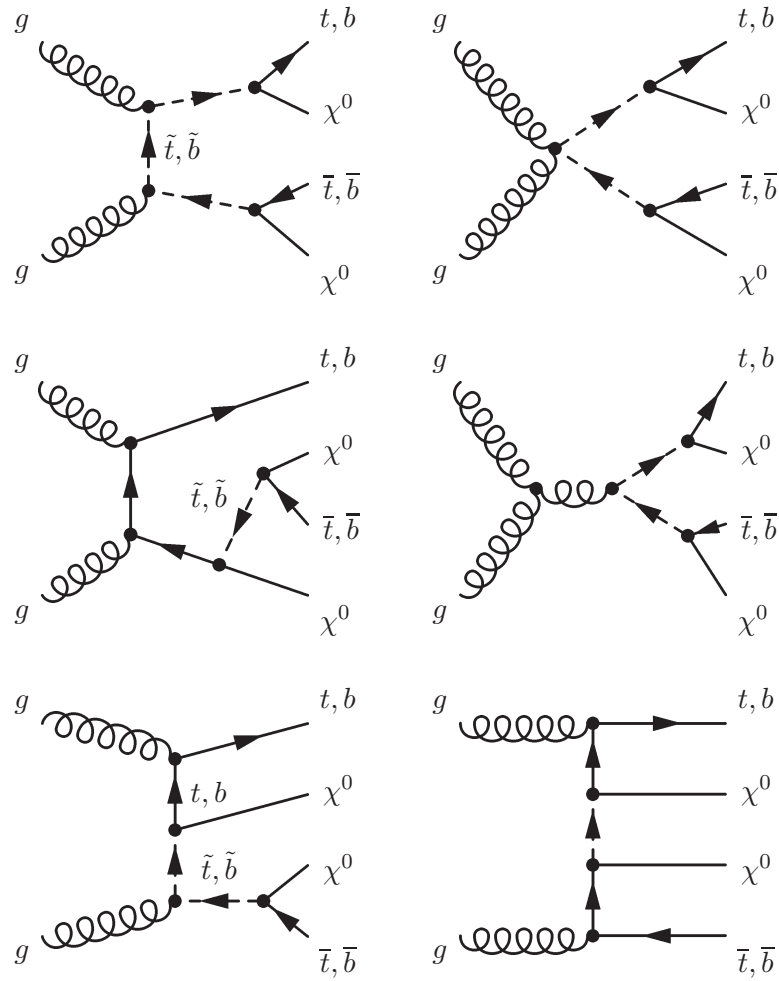


Figure 8.10: The relevant tree level contributions (up to charge conjugation and crossing) to associated heavy quark and LSP pair production with a gg initial state.

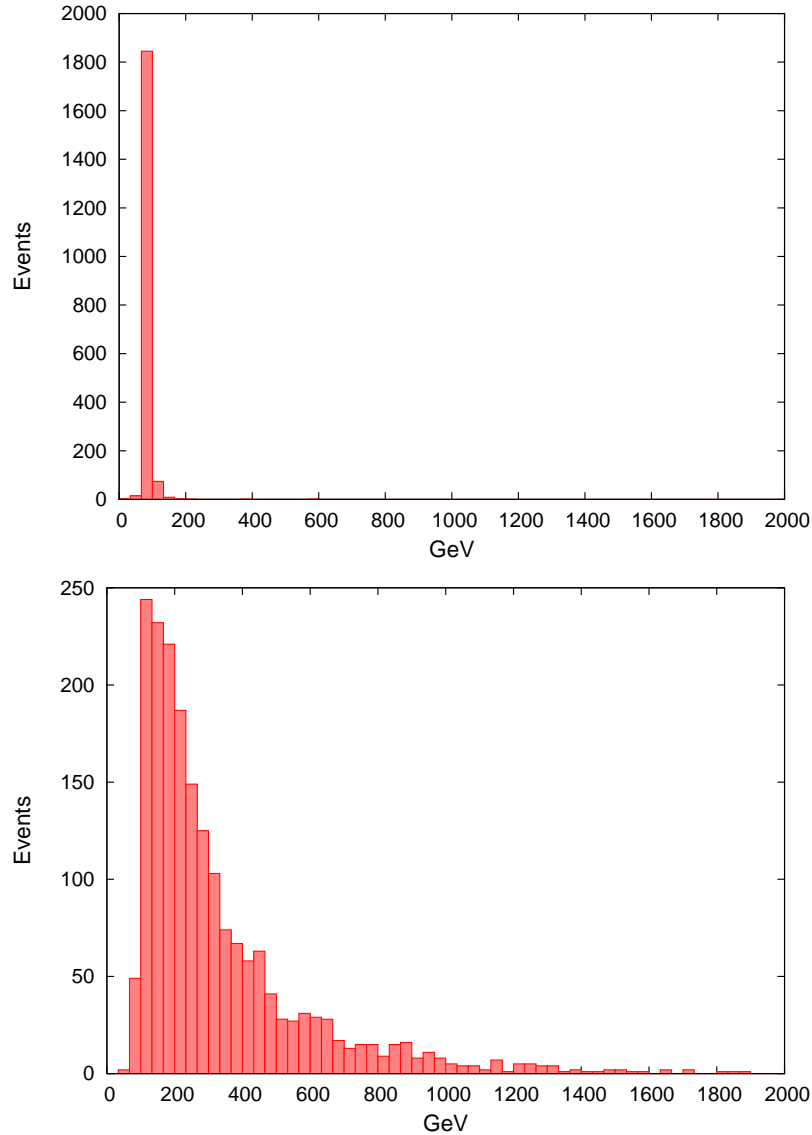


Figure 8.11: The invariant mass (above) and energy (below) of the neutrino pair in the SM background process $pp \rightarrow \nu\bar{\nu}t\bar{t}$ after the cut $p_T(t), p_T(\bar{t}) > 300$ GeV ($\int \mathcal{L} = 200 \text{ fb}^{-1}$, bin=33 GeV).

and produce $q\bar{q}$ and in particular $t\bar{t}$ pairs with $\Delta\phi < 180$ from heavy gluon decay. They are unfortunately strongly suppressed and do not play a significant role here. Important contributions which allow us to observe LSP neutralino production are the Kaluza-Klein top decay chain to a top and two LSPs, and the radiation of a top squark off a top, which in this form constitute a rather unique feature of warped SUSY models with UV brane SUSY breaking. It seems most straightforward to do an analysis of LSP production in association with t and b quark pairs as they are easy to detect and have fewer background processes.

Also, we have seen above that the third generation is favoured because it couples more strongly to the Kaluza-Klein sector. Let us look at the simulation results in detail. The integration error is below 1% for all simulations, but we give two digits only for small cross sections as some event samples are of the order of < 1000 events. Finally it should be noted that our enhanced particle spectrum can contribute to neutrino production as well. We neglect this background which does not change the nature of our predictions drastically.

8.6.3 Production of $t\bar{t} + \cancel{E}_T$

The SM background $pp \rightarrow \nu\bar{\nu}t\bar{t}$ is only moderately large. The classes of diagrams contributing to the signal at this order are shown in figure 8.8 for initial quarks and in figure 8.10 for initial gluons. We apply the following basic cuts:

cuts I	
Standard invariant mass cuts	$M(q, \bar{q}) \in [10, \infty]$ $M(\text{parton}, q), M(\text{parton}, \bar{q}) \in [-\infty, -10]$
Energy (“low x”)	$E(\text{parton}) > 20$
Pseudorapidity	$\eta(q), \eta(\bar{q}) \in [-5, 5]$

These are the default invariant mass cuts proposed by WHIZARD for the SM background process to exclude possible divergences which would make the integration unstable. We introduce cuts on energy and pseudorapidity of the quarks to improve convergence. To reduce the relative contributions of the SM background further, we add

cuts I.1	
cuts I	
Transverse momentum	$p_T(q), p_T(\bar{q}) > 100 \text{ GeV}$

and then a stronger one,

cuts I.2	
cuts I	
Transverse momentum	$p_T(q), p_T(\bar{q}) > 300 \text{ GeV}$

This results in the following total cross sections for the subprocesses:

Process	$\sigma_{\text{I}}/\text{fb}$	$\sigma_{\text{I.1}}/\text{fb}$	$\sigma_{\text{I.2}}/\text{fb}$
$q_i\bar{q}_j, \bar{q}_i q_j \rightarrow \nu_k \bar{\nu}_l t\bar{t}$	52	30	4.6
$gg \rightarrow \nu_k \bar{\nu}_l t\bar{t}$	100	53	5
$q_i\bar{q}_j, \bar{q}_i q_j \rightarrow \chi_k^0 \chi_l^0 t\bar{t}$	80	74	32
$gg \rightarrow \chi_k^0 \chi_l^0 t\bar{t}$	48	44	17
Signal/Background	0.84	1.4	5.1

Using these results we first generate events corresponding to an integrated luminosity of $\int \mathcal{L} = 200 \text{ fb}^{-1}$ (I.2) and $\int \mathcal{L} = 20 \text{ fb}^{-1}$ (I.I.1). These cross sections are however large enough to justify an analysis of lower integrated luminosities, and we choose $\int \mathcal{L} = 10 \text{ fb}^{-1}$ for (I.2).

The SM process has a \cancel{p}_T distribution which decreases quickly for large missing momentum. In contrast, if the two top quarks are almost collinear, we see a peak in our signal at around 600...700 GeV roughly corresponding to the intermediate resonance minus the neutralino energy. It moves towards 0 for larger azimuthal distance between the quarks, giving the distribution with $q\bar{q}$ initial state a rectangular shape. The resulting \cancel{p}_T distribution for cuts I.2 is shown in figure 8.28, the sum of all contributions is shown in figure 8.12 (I), figure 8.13 (I.1) and figure 8.14 (I.2). Since we get large contributions to LSP production with $\cancel{p}_T > 400 \text{ GeV}$, a clear signal can be seen at large \cancel{p}_T even for moderate cuts or only the basic cuts.

Let us now take a 10 fb^{-1} sample to discuss how well the missing energy signal could be observed after shorter observation times. The resulting \cancel{p}_T distribution is shown in figure 8.17. There are still plenty of events left, but it would require a more detailed investigation to determine how well these top jets can be detected and separated in a real detector.

In addition to cutting on the energy of the quarks, we can exploit the azimuthal distance distribution. They are shown in figure 8.15. We introduce a further set of cuts to exploit the larger contribution of top quarks from LSP production which are not back to back,

cuts I.3	
cuts I	
Transverse momentum	$p_T(q), p_T(\bar{q}) > 100 \text{ GeV}$
Azimuthal distance	$\Delta\phi(q, \bar{q}) < 140^\circ$

The resulting \cancel{p}_T distribution for $\int \mathcal{L} = 20 \text{ fb}^{-1}$ is shown in figure 8.16. These cuts might also be useful for excluding instrumental backgrounds, e.g. from hard t pair production without missing energy. The corresponding cross sections are

Process	$\sigma_{\text{I}}/\text{fb}$	$\sigma_{\text{I.3}}/\text{fb}$
$q_i\bar{q}_j, \bar{q}_i q_j \rightarrow \nu_k \bar{\nu}_l t\bar{t}$	52	1.6
$gg \rightarrow \nu_k \bar{\nu}_l t\bar{t}$	100	4.2
$q_i\bar{q}_j, \bar{q}_i q_j \rightarrow \chi_k^0 \chi_l^0 t\bar{t}$	80	18
$gg \rightarrow \chi_k^0 \chi_l^0 t\bar{t}$	48	12
Signal/Background	0.84	5.2

As one would expect, the low \cancel{p}_T contributions which can only come from almost back to back quarks, are reduced.

To gain some insight in the relevant underlying processes, let us look at the invariant mass spectra of subsets of the outgoing particles. This is only an academic

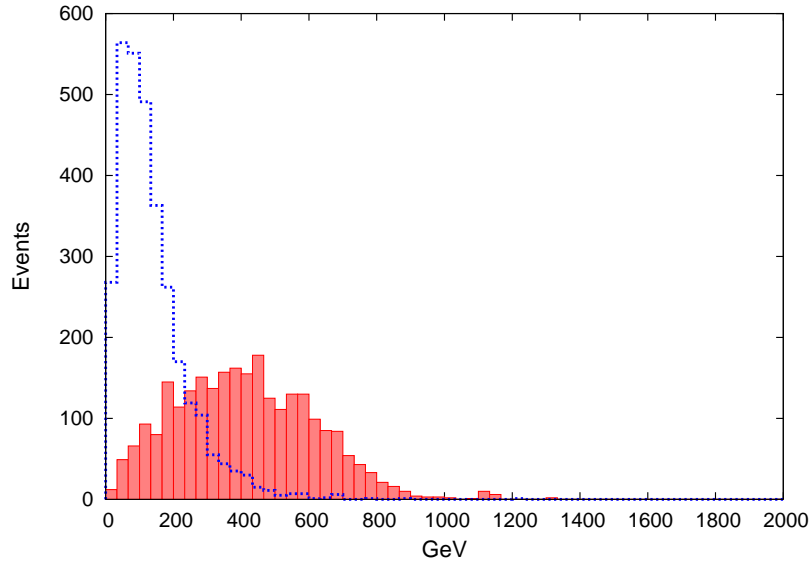


Figure 8.12: A histogram of the p_T distribution ($\int \mathcal{L} = 20 \text{ fb}^{-1}$, bin=33 GeV) after cuts I of the SM background (dashed, blue) and the signal (filled, red) for $pp \rightarrow xxt\bar{t}$.

exercise as they are not accessible experimentally. The histograms of $M(q, \chi)$ shown in Figures 8.24, 8.25 point to third generation squark decay as the primary source. The histogram of $M(q, \chi, \chi)$ in figure 8.23 indicates that diagrams involving decay cascades of the first top resonance t^2 into the LSPs and a top are important. The coupling of light quarks vanishes for ideal delocalization, but for our bulk mass value which gives us $S \approx 0$, there is a nonzero coupling of $\mathcal{O}(0.2)$ to the heavy gluon which is compensated by the $g^2 t^2 t$ coupling which is of $\mathcal{O}(2)$. The t^2 decays mainly to electroweak bosons and quarks, so the LSP production is certainly not the first sign of a warped extra dimension. The color charged gauge scalar Σ^c does not contribute because of the smallness of couplings.

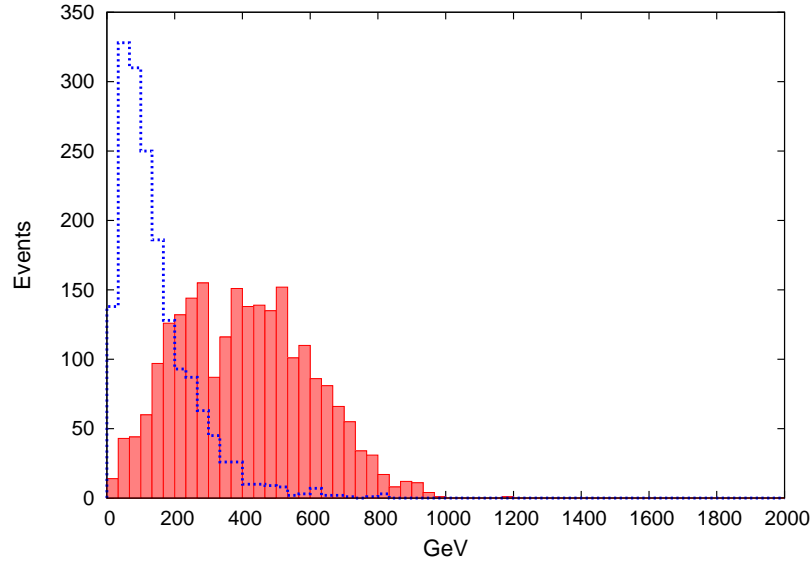


Figure 8.13: A histogram of the p_T distribution ($\int \mathcal{L} = 20 \text{ fb}^{-1}$, $\text{bin}=33 \text{ GeV}$) after cuts I.1 of the SM background (dashed, blue) and the signal (filled, red) for $pp \rightarrow xxt\bar{t}$.

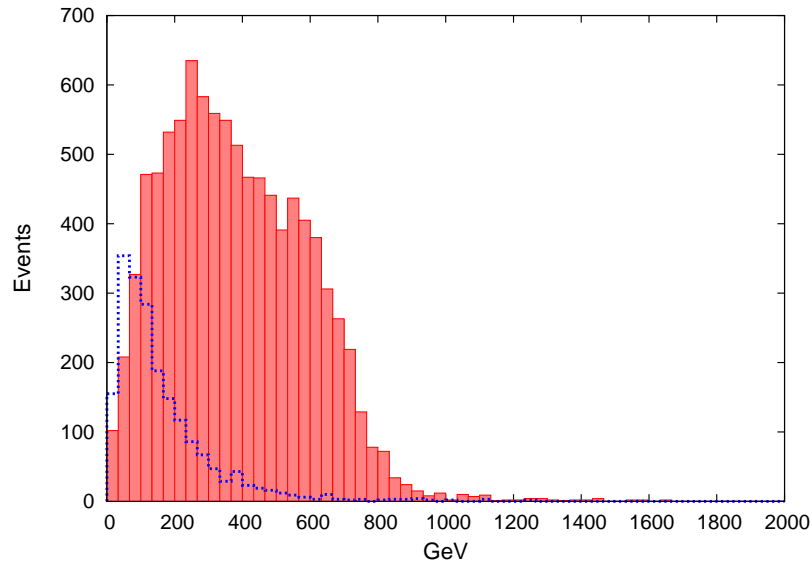


Figure 8.14: A histogram of the p_T distribution ($\int \mathcal{L} = 200 \text{ fb}^{-1}$, $\text{bin}=33 \text{ GeV}$) after cuts I.2 of the SM background (dashed, blue) and the signal (filled, red) for $pp \rightarrow xxt\bar{t}$.

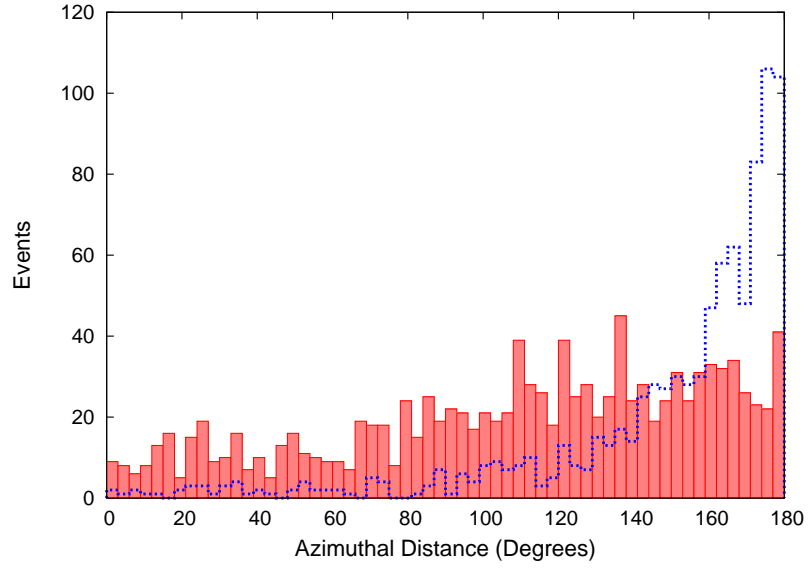


Figure 8.15: A histogram of the $\Delta\phi(t, \bar{t})$ distribution ($\int \mathcal{L} = 20 \text{ fb}^{-1}$, bin=33 GeV) after cuts I.1 of the SM background (dashed, blue) and the signal (solid, red) for $pp \rightarrow xt\bar{t}$.

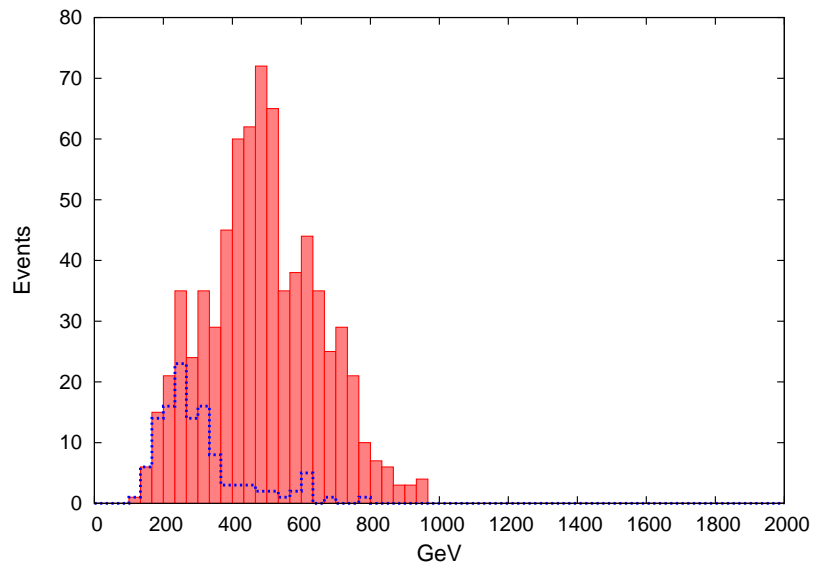


Figure 8.16: A histogram of the \cancel{p}_T distribution ($\int \mathcal{L} = 20 \text{ fb}^{-1}$, bin=33 GeV) after cuts I.3 of the SM background (dashed, blue) and the signal (solid, red) for $pp \rightarrow xt\bar{t}$.

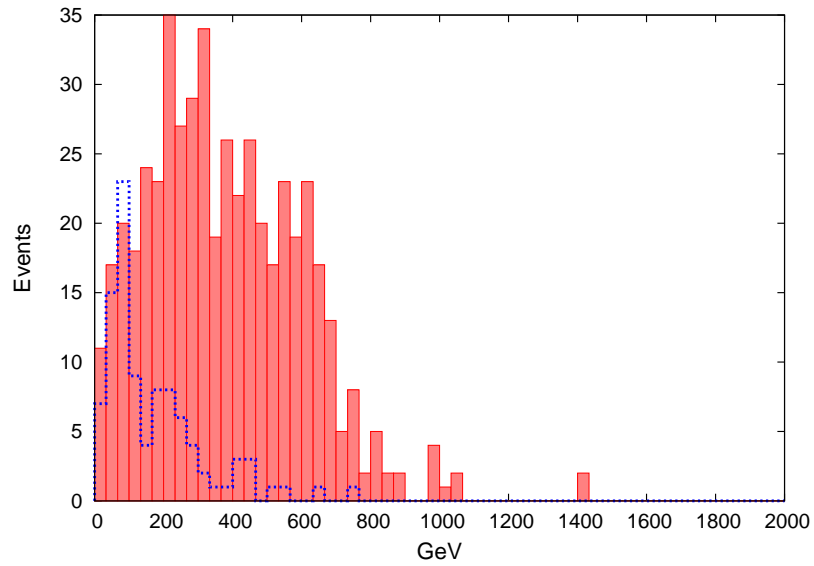


Figure 8.17: A histogram of the ϕ_T distribution ($\int \mathcal{L} = 10 \text{ fb}^{-1}$, bin=33 GeV) after cuts I.2 of the SM background (dashed, blue) and the signal (solid, red) for $pp \rightarrow xxt\bar{l}$.

8.6.4 Production of $b\bar{b} + \cancel{E}_T$

The SM background $pp \rightarrow \nu\bar{\nu}b\bar{b}$ is very large without the p_T cuts while our signal is much smaller than before. With the cuts given above, we get

Process	σ_I/fb	$\sigma_{I.1}/\text{fb}$	$\sigma_{I.2}/\text{fb}$
$q_i\bar{q}_j, \bar{q}_i q_j \rightarrow \nu_k\bar{\nu}_l b\bar{b}$	≈ 10000	100	6.9
$gg \rightarrow \nu_k\bar{\nu}_l b\bar{b}$	≈ 65000	320	7.6
$q_i\bar{q}_j, \bar{q}_i q_j \rightarrow \chi_k^0\chi_l^0 b\bar{b}$	6.4	6.4	2.5
$gg \rightarrow \chi_k^0\chi_l^0 b\bar{b}$	24	8.7	3.1
Signal/Background	0	0.035	0.39

The background is reduced efficiently by these cuts, but our signal never rises above the background contribution before the cross sections becomes too low to be observable with reasonable integrated luminosity. Yet, this becomes important as an additional background for the signatures discussed in the previous section if the reliability of t and b identification is limited. To improve the situation for the $\chi^0\chi^0 b\bar{b}$ signature itself we can try to exploit the fact that the \cancel{p}_T distribution of $pp \rightarrow \nu\bar{\nu}b\bar{b}$ falls off quickly, and try to look for very large \cancel{p}_T . We therefore employ

cuts II.1	
cuts I	
Transverse momentum	$p_T(q, \bar{q}) > 300 \text{ GeV}$

or

cuts II.2	
cuts I	
Transverse momentum	$p_T(q, \bar{q}) > 500 \text{ GeV}$

Since we now cut on the very quantity which we would like to observe, this is equivalent to a selection of the plot range. Doing so we can actually retain a larger percentage of signal events, but our signal is still almost drowned by SM b production.

Process	σ_I/fb	$\sigma_{II.1}/\text{fb}$	$\sigma_{II.2}/\text{fb}$
$q_i\bar{q}_j, \bar{q}_i q_j, gg \rightarrow \nu_k\bar{\nu}_l b\bar{b}$	≈ 10000	25	3.2
$q_i\bar{q}_j, \bar{q}_i q_j, gg \rightarrow \nu_k\bar{\nu}_l b\bar{b}$	≈ 65000	58	4.2
$q_i\bar{q}_j, \bar{q}_i q_j \rightarrow \chi_k^0\chi_l^0 b\bar{b}$	6.4	4.6	2.6
$gg \rightarrow \chi_k^0\chi_l^0 b\bar{b}$	24	10.6	4.0
Signal/Background	0	0.18	0.89

The production cross section drops below 10 fb, and the contribution from our LSPs which has the same basic shape is probably visible in the parton level simulation only (figure 8.18).

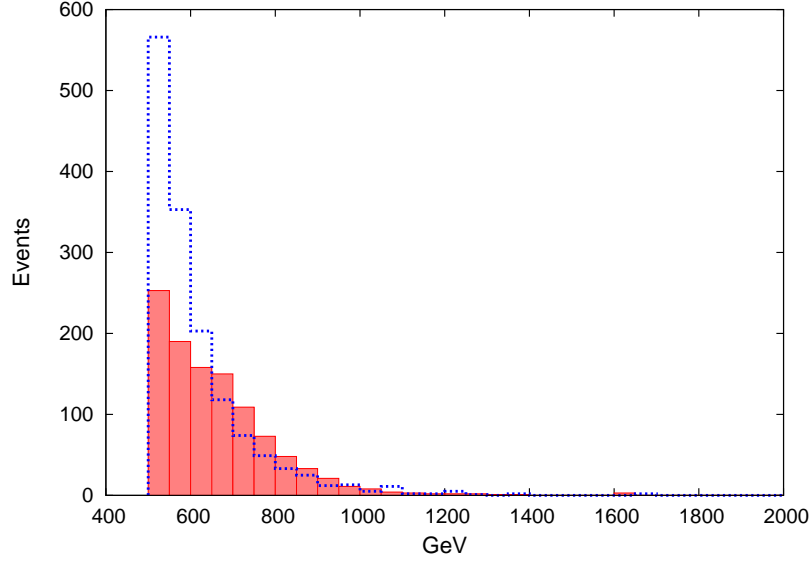


Figure 8.18: A histogram of the \cancel{p}_T distribution ($\int \mathcal{L} = 200 \text{ fb}^{-1}$, $\text{bin}=50 \text{ GeV}$) after cuts II.2 of the SM background (dashed, blue) and the signal (solid, red) for $pp \rightarrow xxb\bar{b}$.

8.6.5 Production of the NLSPs

In the previous sections we have considered the leading order contributions to neutralino pair production in association with third generation quarks. There is however another kind of events which might not be easily distinguishable from LSP production in an experiment, namely the production of chargino NLSPs or of one chargino NLSP and a neutralino LSP. Our charginos are close to the lower experimental exclusion bound and decay via $\chi^+ \rightarrow \chi^0 W^{+*} \rightarrow \chi^0 f_u \bar{f}_d$. They are very narrow ($\Gamma \approx 10^{-7} \text{ GeV}$) due to the offshell intermediate W , yet unlike in some models with light gravitino LSP, the corresponding lifetime is still negligible. The fermion pair has $\approx 10 \dots 20 \text{ GeV}$ in the chargino center of mass frame. Depending on how well such processes can be resolved in the experiments, this will be an important way to observe LSP or NLSP production. In the detector, one might see missing energy with one or two comparatively soft jets (few tens of GeVs) and two b or t jets, so chargino production events would look similar to the signal discussed above. We therefore close this section by studying the processes

$$pp \rightarrow \chi^+ \chi^- t \bar{t} \quad (8.53)$$

and

$$pp \rightarrow \chi^0 \chi^- t \bar{b} \quad pp \rightarrow \chi^0 \chi^+ \bar{t} b \quad (8.54)$$

to which the three point couplings $W^{+,n} \chi^- \chi^0$ and $Z^n \chi^+ \chi^-$ can make important contributions in contrast to neutralino pair production. We apply the cuts I.2 to the quarks. Now, the p_T of the b and t jets is not exactly equal to \cancel{p}_T any more, but only up to the p_T of the softer jet(s) from the chargino decay products. The

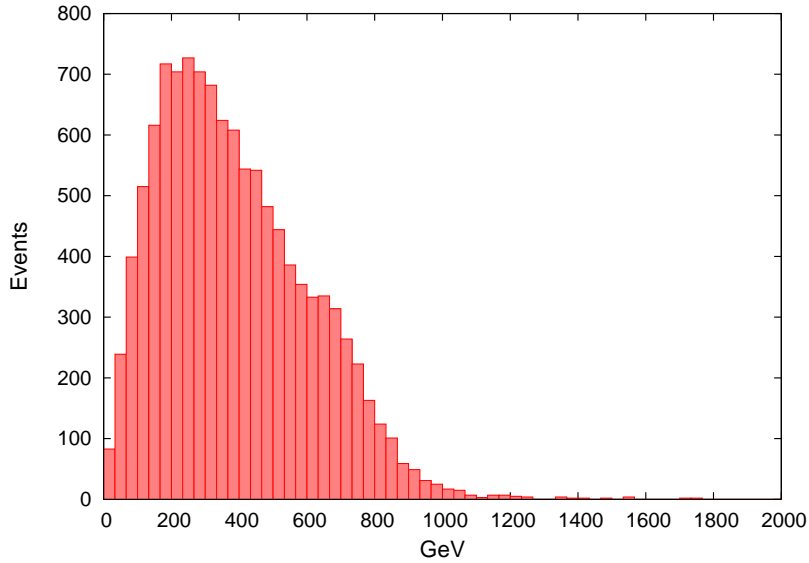


Figure 8.19: The p_T distribution of the quark pair in $pp \rightarrow \chi^+ \chi^- t \bar{t}$ ($\int \mathcal{L} = 200 \text{ fb}^{-1}$, $\text{bin}=33 \text{ GeV}$) after cuts I.2.

cross sections are

Process	$\sigma_{\text{I.2}}/\text{fb}$
$pp \rightarrow \chi^+ \chi^- t \bar{t}$	57
$pp \rightarrow \chi^0 \chi^- t \bar{b}$	25

The distribution of $p_T(q, \bar{q})$ is shown in figure 8.19. The boost distribution of the charginos can be used to infer how hard the jets from the chargino decay products are going to be (figure 8.20). The maximum is at around $\gamma(\chi^\pm) = E_\chi/m_\chi \approx 3$ leading to rather soft jets, but more than on third of the events can reach $\gamma(\chi^\pm) = E_\chi/m_\chi > 5$. The corresponding results for the production of one chargino are shown in figure 8.21 and figure 8.22. These cross sections are even larger than those for pure neutralino production, but it is subject of further study how well this type of events can be distinguished at the LHC. The proper treatment of the background to this type of processes would require production of 8 particles in the final state to account for the three body decays of two χ^\pm s via offshell W s, and possibly detector simulations which are beyond the scope of this thesis. In any case, NLSP production should give us an equally important source of missing energy.

8.7 Discussion and Further Issues

We have seen above that the production of third generation quark pairs in association with two neutralino LSPs gives us a clear missing energy signal with only

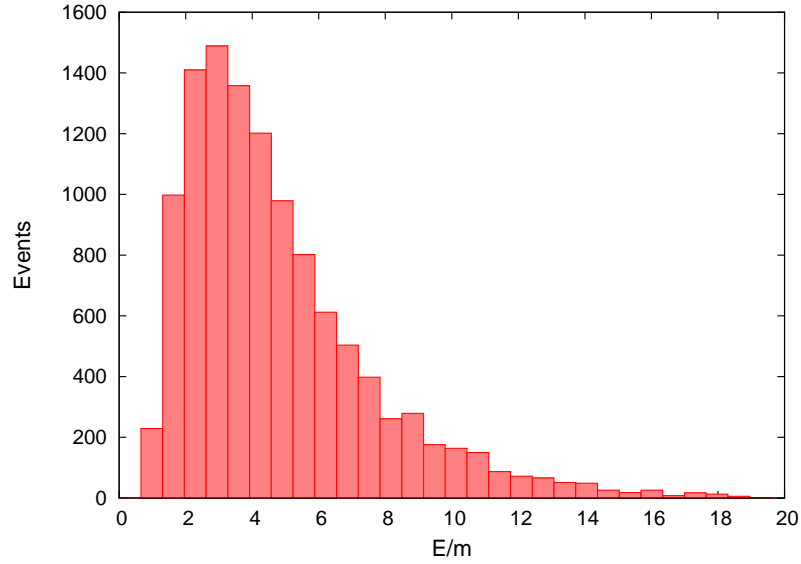


Figure 8.20: The boost $\gamma(\chi^+) = E_\chi/m_\chi$ of a chargino in $pp \rightarrow \chi^+\chi^-t\bar{t}$ ($\int \mathcal{L} = 200 \text{ fb}^{-1}$, bin=50 GeV) after cuts I.2.

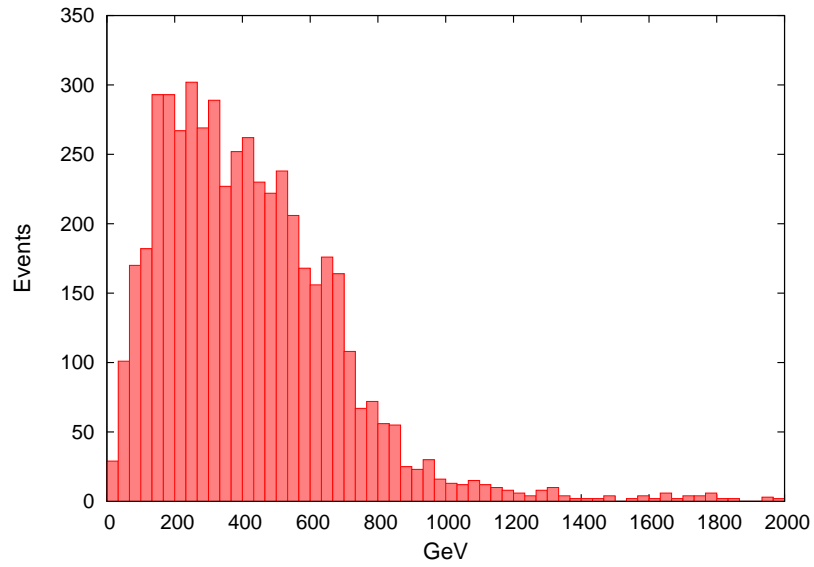


Figure 8.21: The p_T distribution of the quark pair in $pp \rightarrow \chi^0\chi^-t\bar{b}$ ($\int \mathcal{L} = 200 \text{ fb}^{-1}$, bin=33 GeV) after cuts I.2.

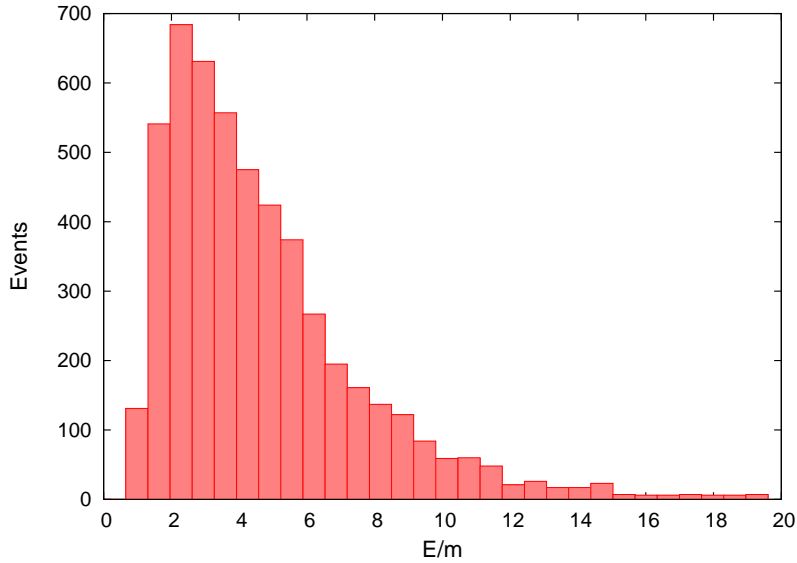


Figure 8.22: The boost $\gamma(\chi^+) = E_\chi/m_\chi$ of the chargino in $pp \rightarrow \chi^0 \chi^- t \bar{b}$ ($\int \mathcal{L} = 200 \text{ fb}^{-1}$, bin=50 GeV) after cuts I.2.

moderate backgrounds at the LHC, while the production of NLSPs in association with third generation quark pairs is even stronger but harder to interpret. These simulations with heavy quark final states give a first insight in the LHC phenomenology of the model, but have to be complemented by a more detailed analysis of final states, possibly including fragmentation and detector simulations to reliably gauge the potential of discovery and differentiation from other models at the LHC. Due to the structure of our SUSY breaking sector, production and annihilation channels involving squarks are suppressed, but we are nevertheless confident that our DM candidate will be visible at the LHC if models of this type are realized in nature. A realistic LSP density can be reached without extensive tuning of mixing angles. Many of the properties discussed in the previous sections are connected to the special rôle of the third generation in warped models. The IR localization of the top and bottom make them an important probe of the Kaluza-Klein sector in which for example the squark resonances reside. Many widths and cross sections are enhanced due to this effect, and the strong mixing of the Kaluza-Klein modes of third generation quarks and squarks on the IR brane gives us rather light resonances which are produced much more copiously at the LHC. In this context it would be interesting to investigate how alternative implementations of third generation quarks introduced to remedy the Zbb problem will affect the general phenomenology [18, 34]. If we do not limit ourselves to production of third generation quarks, there are LSP electroweak production channels which are much less Kaluza-Klein suppressed and will yield larger cross sections than the QCD ones discussed here, of course with much larger backgrounds to begin with. One such mode is shown in figure 8.7. Another interesting and challenging

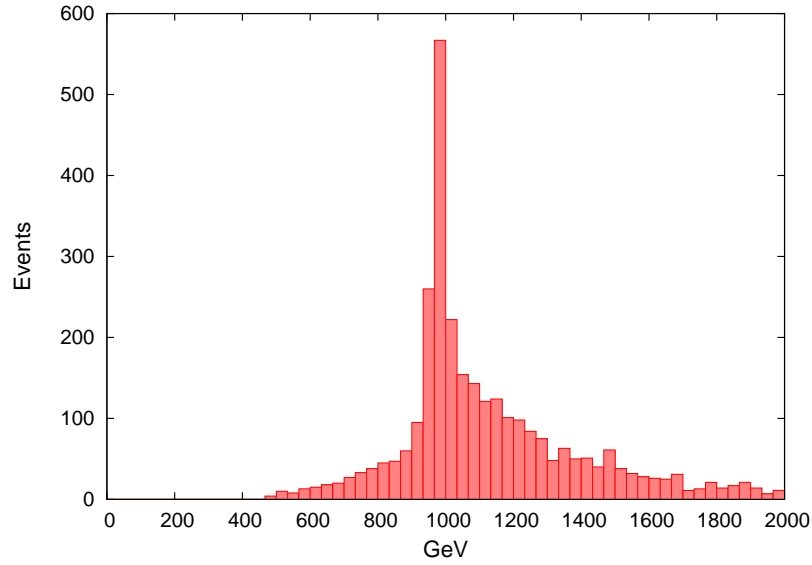


Figure 8.23: The invariant mass distribution of $\chi^0\chi^0t$ for initial state $\bar{q}q$ and cuts I.2 shows top resonance decay $t^2 \rightarrow \chi^0\chi^0t + c.c$ as a dominant production channel ($\int \mathcal{L} = 200 \text{ fb}^{-1}$, bin=33 GeV).

subject for further study which we have only hinted at in this thesis is the generation of flavour mixing in warped models in connection with supersymmetry, and the consequences for FCNCs and rare decays.

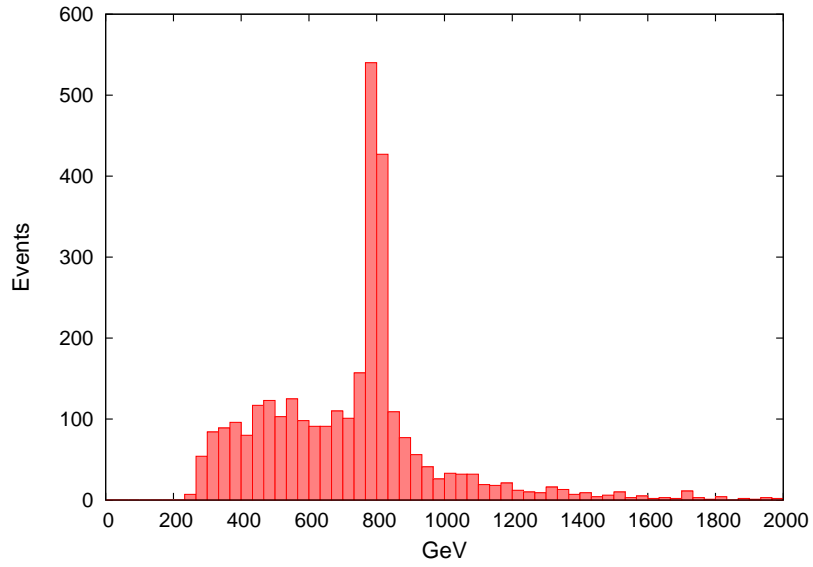


Figure 8.24: The invariant mass distribution of $\chi^0 t$ for initial state $\bar{q}q$ and cuts I.2 shows an intermediate stop resonance decaying as $\hat{t}_i^1 \rightarrow \chi^0 t + c.c$ ($\int \mathcal{L} = 200 \text{ fb}^{-1}$, bin=33 GeV).

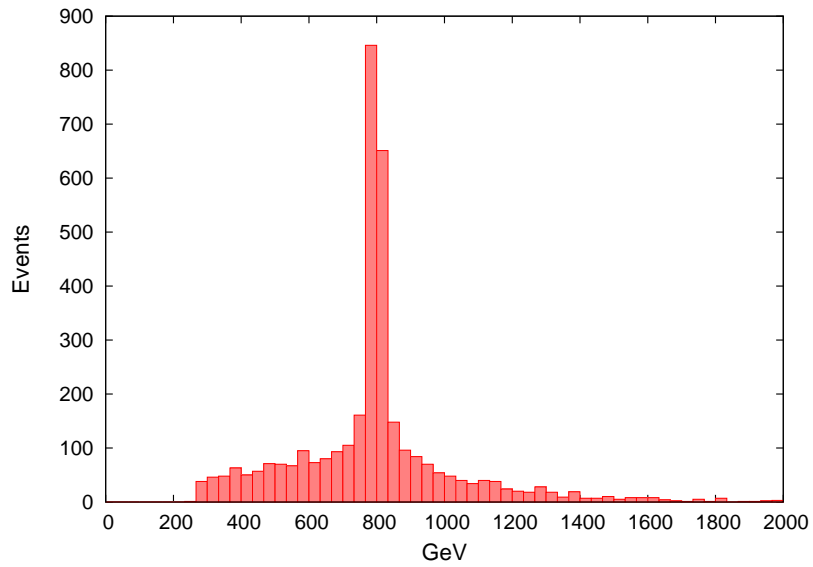


Figure 8.25: The invariant mass distribution of $\chi^0 t$ for initial state gg and cuts I.2 shows stop production and decay $\hat{t}_i^1 \rightarrow \chi^0 t + c.c$ as the dominant production channel ($\int \mathcal{L} = 200 \text{ fb}^{-1}$, bin=33 GeV).

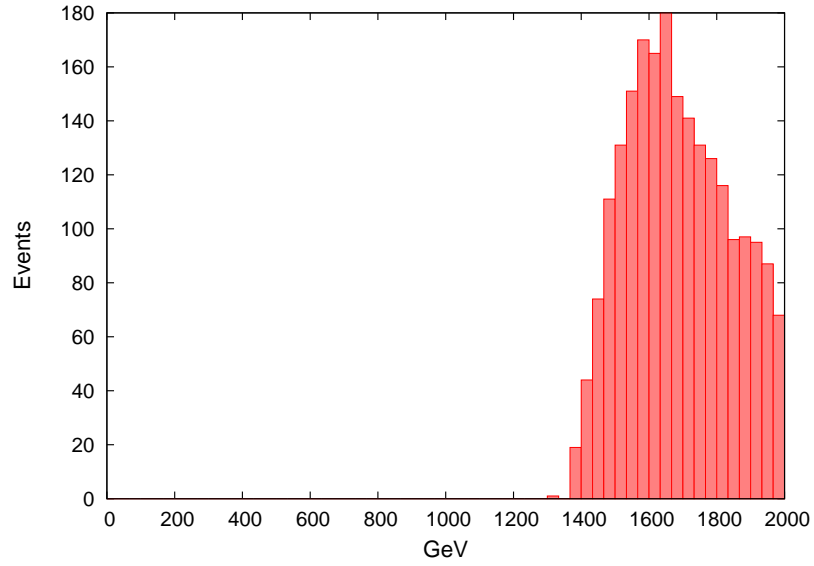


Figure 8.26: The total invariant mass distribution for the $q\bar{q}$ initial state and cuts I.2 ($\int \mathcal{L} = 200 \text{ fb}^{-1}$, $\text{bin}=33 \text{ GeV}$).

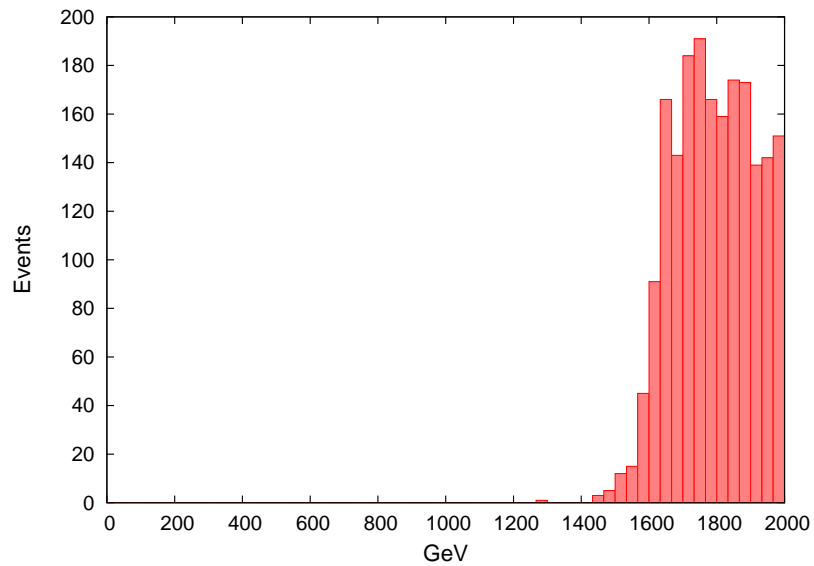


Figure 8.27: The total invariant mass for the gg initial state and cuts I.2 ($\int \mathcal{L} = 200 \text{ fb}^{-1}$, $\text{bin}=33 \text{ GeV}$).

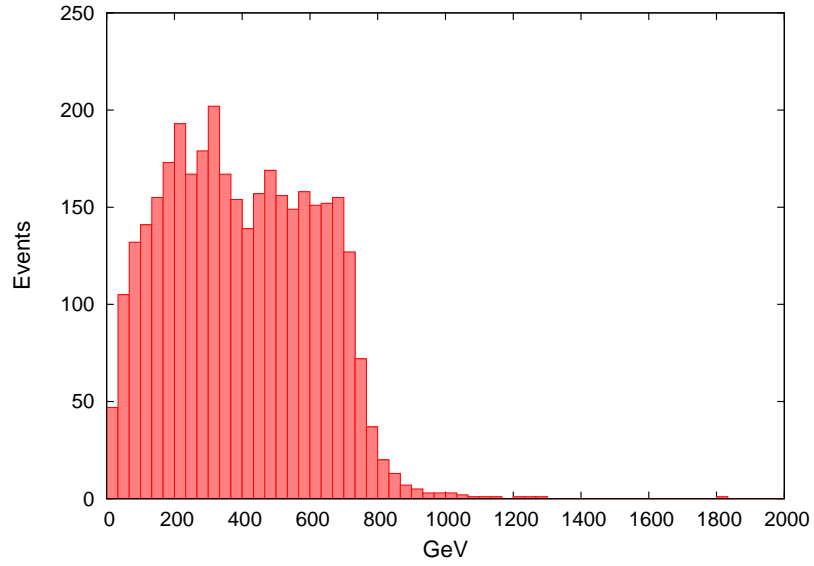


Figure 8.28: The p_T distribution of the signal $gg \rightarrow \chi^0 \chi^0 t \bar{t}$ after cuts I.2 ($\int \mathcal{L} = 200 \text{ fb}^{-1}$, $\text{bin}=33 \text{ GeV}$).

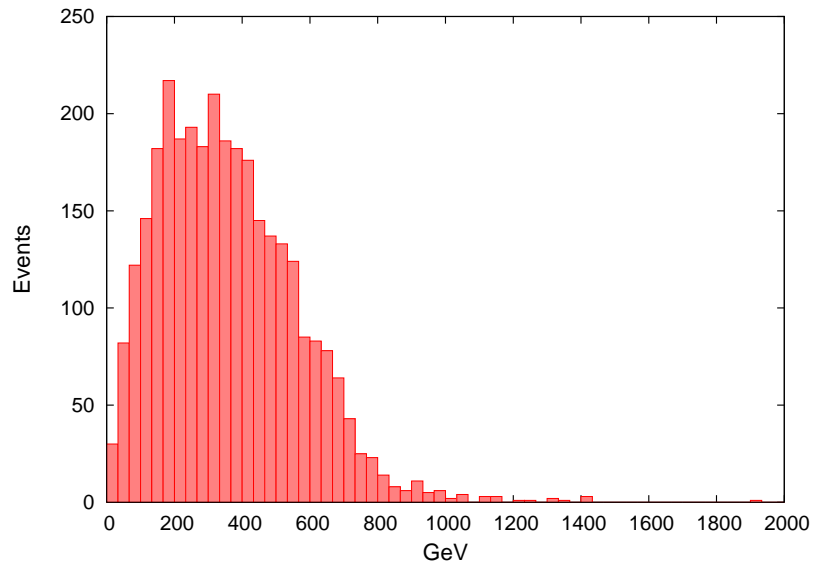


Figure 8.29: The p_T distribution of the signal $q\bar{q} \rightarrow \chi^0 \chi^0 t \bar{t}$ after cuts I.2. The same contribution comes from $\bar{q}q$ ($\int \mathcal{L} = 200 \text{ fb}^{-1}$, $\text{bin}=33 \text{ GeV}$).

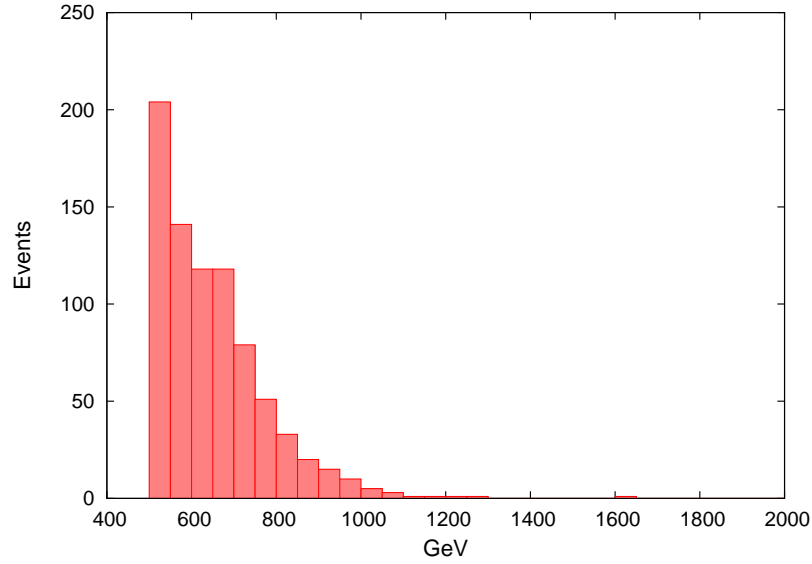


Figure 8.30: The \not{p}_T distribution of the signal $gg \rightarrow \chi^0 \chi^0 b \bar{b}$ after cuts I.2 ($\int \mathcal{L} = 200 \text{ fb}^{-1}$, bin=33 GeV).

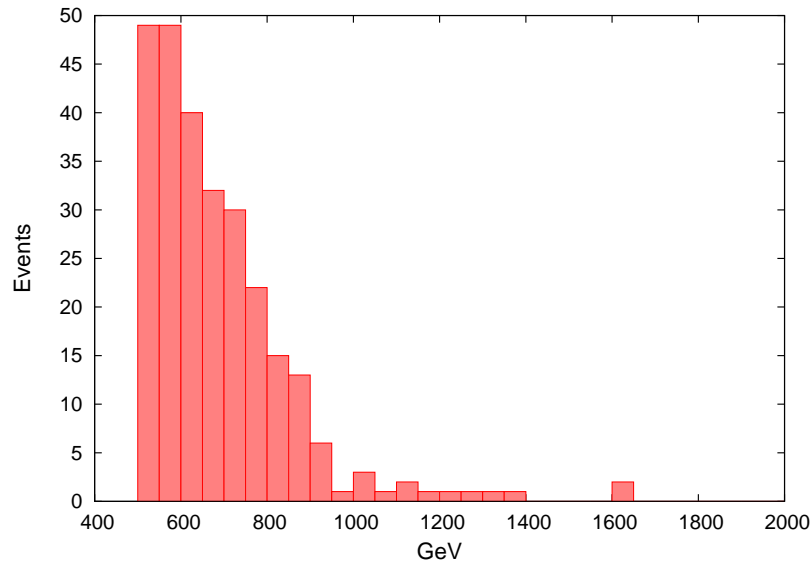


Figure 8.31: The \not{p}_T distribution of the signal $q\bar{q} \rightarrow \chi^0 \chi^0 b \bar{b}$ after cuts I.2. The same contribution comes from $\bar{q}q$ ($\int \mathcal{L} = 200 \text{ fb}^{-1}$, bin=33 GeV).

Chapter 9

Conclusions

Since its popularization due to Randall and Sundrum one decade ago, and in connection with the *AdS/CFT* correspondence in particular, 5D warped background spacetime has been one of the most fruitful new ideas in physics beyond the standard model, leading to new insights into symmetry breaking and the properties of strongly interacting theories inaccessible to direct perturbative calculations, while at the same time relating gravity to phenomenological model building. The nature of dark matter and electroweak symmetry breaking which are among the most prominent puzzles subject to experimental scrutiny at the Tevatron, direct search experiments, and in the near future at the LHC, invite us to speculate about possible solutions in the context of warped models.

In this thesis we have investigated phenomenological implications which arise for cosmology and collider physics when the electroweak symmetry breaking sector of warped higgsless models is extended to include warped supersymmetry with conserved R parity. The goal was to find the simplest supersymmetric extension of these models which still has a realistic light spectrum including a viable dark matter candidate. To accomplish this, we have used the same mechanism which is already at work for symmetry breaking in the electroweak sector to break supersymmetry as well, namely symmetry breaking by boundary conditions. While supersymmetry in five dimensions contains four supercharges and is therefore directly related to 4D $\mathcal{N} = 2$ supersymmetry, half of them are broken by the background leaving us with ordinary $\mathcal{N} = 1$ theory in the massless sector after Kaluza-Klein expansion. This is reflected in the fact that only one two-component Killing spinor with nontrivial dependence on the extradimensional coordinate remains. We thus use boundary conditions to model the effects of a breaking mechanism for the remaining two supercharges. The formulation of supersymmetric theories has been greatly simplified through the invention of the superfield formalism, and even though it can not be applied to higher dimensions or extended supersymmetry in a straightforward manner, there exists a hybrid approach for using superfields in $D > 4$ which we use to build our model. It exploits the fact that the field content of 5D vector- or hypermultiplets is equivalent to that of two 4D superfields which can each be furnished with the correct 5D dynamics by hand. Supersymmetry and gauge symmetry relate the boundary conditions

which have to be assigned to the fields within the extended supermultiplets, and the result is a Kaluza-Klein particle spectrum consisting of 4D $\mathcal{N} = 2$ multiplets. Even though they are degenerate in mass, the breaking of the extended supersymmetry divides them into two different classes of Kaluza-Klein wave functions each associated with one of two 4D $\mathcal{N} = 1$ superfields. It turns out that the infrared scale of the warped background, $\Lambda_{\text{IR}} = 200 \dots 600$ GeV which is related to the electroweak scale, is too low to account for all of the supersymmetry breaking necessary to achieve a realistic light spectrum. Since the strength with which fields couple to the IR brane is dictated by their localization, the masses of most superpartners remain below the allowed experimental exclusion bounds even for infinite IR brane masses. Since we do not have to worry about protecting Higgs scalars from quadratic corrections, the simplest scenario to investigate is a supersymmetric bulk and IR brane without supersymmetry on the UV brane. Even though parts of the light spectrum are effectively projected out by this mechanism, we retain the rich phenomenology of complete $\mathcal{N} = 2$ supermultiplets in the Kaluza-Klein sector. While the light supersymmetric spectrum consists of electroweak gauginos which get their $\mathcal{O}(100 \text{ GeV})$ masses from IR brane electroweak symmetry breaking, the light gluinos and squarks are projected out on the UV brane. After the implementation of UV Dirichlet boundary conditions for all physical scalars, further breaking is only governed by a few parameters consisting of localized kinetic terms and a mixing angle. The neutralinos, as mass eigenstates of the neutral bino-wino sector, are automatically the lightest gauginos, making them LSP dark matter candidates with a relic density that can be brought to agreement with WMAP measurements without extensive tuning of parameters. The coupling constants relevant for LSP annihilation are approximately independent of the neutralino mixing angle such that the cross section is mainly determined by the gaugino masses. For chargino masses close to the experimental lower bounds at around $m_{\chi^+} \approx 100 \dots 110$ GeV, the dark matter relic density points to LSP masses of around $m_{\chi} \approx 90$ GeV. Larger chargino masses are problematic since the corresponding rise in the Kaluza-Klein scale is at odds with unitarization by Kaluza-Klein modes, so light charginos are a prediction of this class of models.

At the LHC, the standard particle content of our model shares the key features of known warped higgsless models, with the exception of larger widths of resonances which can decay to superpartners such as W' and Z' . We have performed Monte Carlo simulations of warped higgsless LSP and NLSP production at a benchmark point using O'Mega/WHIZARD, concentrating on production in association with third generation quarks. After background reduction cuts on the quark momenta and angles, we get hadronic cross sections of $\sigma > 100$ fb with characteristic \cancel{p}_T spectra for $\chi\chi t\bar{t}$ final states, while the final states with $b\bar{b}$ pairs have much lower event rates and shapes which are hard to discern in experiments. Our results suggest that the discovery of warped higgsless LSP dark matter at the LHC via missing energy is within reach for the first $\mathcal{O}(10) \text{ fb}^{-1}$ if b and in particular t jet identification is reliable. More precise statements will require the inclusion of larger final states, fragmentation and detector simulations. Among the interesting

questions which were raised during this work, but are beyond the scope of this thesis, are the impact this particular extension has on flavour physics and related precision observables in higgsless models, the possibility of having scalars from warped space at the electroweak scale, and the embedding of the model in a UV completion including an underlying mechanism for supersymmetry breaking by boundary conditions consistent with supergravity. Whether in the context of higgsless models or related alternatives to the standard Higgs mechanism, these are intriguing questions for future research. As always, experimental observations will be the arbiter of which theoretical concepts, previously considered or hitherto unknown, best describe the physics that awaits us at the electroweak scale.

Appendix A

Conventions

A.1 Coordinate Systems and Lorentz Structure

Two coordinate systems are commonly used to parametrize a slice of AdS_5 . The “proper distance” coordinates have

$$x^M = (x^\mu, y), \quad y \in [0, \pi] \quad (\text{A.1})$$

They are related to the “conformal” coordinates with

$$x^M = (x^\mu, z), \quad z \in [k^{-1}, \Lambda_{\text{IR}}^{-1}] \quad (\text{A.2})$$

through

$$z = k^{-1} e^{Rky} \quad \Lambda_{\text{IR}} = k e^{-Rk\pi} \quad (\text{A.3})$$

We use lowercase greek letters $\mu, \nu \dots$ for 4D curved space Lorentz indices and uppercase letters $M, N \dots$ for 5D curved space Lorentz indices. In some instances, there appear flat 4D Lorentz indices which will be denoted by lowercase latin letters $a, b, n \dots$. We do not introduce 5D flat indices. There can be confusion between the use of “flat indices” and flat metrics with ordinary indices. Vectors with curved and flat indices are related by a vielbein, for example

$$V^\mu = e_a^\mu V^a \quad (\text{A.4})$$

Since $e_a^\mu = (e_\mu^a)^{-1}$, we get

$$V^\mu W_\mu = V^a W_a \quad (\text{A.5})$$

When doing a Kaluza-Klein expansion in warped space, we usually pull the space-time dependence out of the metric without making all vectors associated with it “flat index” vectors, for example

$$A_\mu A^\mu = g^{\mu\nu} A_\mu A_\nu = e^{2Rky} \eta^{\mu\nu} A_\mu A_\nu \quad (\text{A.6})$$

Compare this to

$$A_\mu A^\mu = g^{\mu\nu} A_\mu A_\nu = \eta^{mn} A_m A_n \quad (\text{A.7})$$

where the definition of the vector fields has changed to include an inverse vierbein factor. In this context it is important that we never raise or lower “curved” indices with the flat metric. (Covariant) derivatives and gauge fields with upper indices are always defined as $A^\mu = g^{\mu\nu} A_\nu$ and $F^{\mu\nu} = g^{\mu\rho} g^{\nu\omega} F_{\rho\omega}$. The flat dirac matrices are marked with a bar,

$$\gamma^\mu = e_a^\mu \bar{\gamma}^a \quad (\text{A.8})$$

but sometimes we use them with curved index

$$\bar{\gamma}^\mu = \delta_n^\mu \bar{\gamma}^n \quad (\text{A.9})$$

They are defined as

$$\{\bar{\gamma}^\mu, \bar{\gamma}^\nu\} = 2\eta^{\mu\nu} \quad \{\bar{\gamma}^m, \bar{\gamma}^n\} = 2\eta^{mn} \quad (\text{A.10})$$

Since the symbol $\bar{\sigma}$ is taken already, we define all appearances of the σ matrices in this work to be without spacetime dependence and with an upper index which can be flat or curved. We will not use curved σ matrices. Furthermore we use the flat metric sign convention

$$\eta = \text{diag}(+, -, -, -, -) \quad (\text{A.11})$$

and the corresponding Dirac matrices

$$\bar{\gamma}^m = - \begin{pmatrix} 0 & \sigma^m \\ \bar{\sigma}^m & 0 \end{pmatrix} \quad \bar{\gamma}^5 = \begin{pmatrix} i & 0 \\ 0 & -i \end{pmatrix} \quad (\text{A.12})$$

where $\sigma^0 = \bar{\sigma}^0 = -1$ and $-\bar{\sigma}^i = \sigma^i$ are the Pauli matrices. We define the projectors

$$P^+ = \frac{1}{2}(1 - i\bar{\gamma}^5) \quad P^- = \frac{1}{2}(1 + i\bar{\gamma}^5) \quad (\text{A.13})$$

on the 4D “left handed” and “right handed” component respectively. For Dirac spinors

$$\Psi^T = (\eta_\alpha, \bar{\chi}^{\dot{\alpha}}) \quad (\text{A.14})$$

we define

$$\bar{\Psi} = \Psi^\dagger \bar{\gamma}^0 = (\chi^\alpha, \bar{\eta}_{\dot{\alpha}}) \quad (\text{A.15})$$

The Dirac matrices read in proper distance coordinates

$$\gamma^\mu = -\delta_m^\mu e^{Rky} \begin{pmatrix} 0 & \sigma^m \\ \bar{\sigma}^m & 0 \end{pmatrix} \quad \gamma^5 = \frac{1}{R} \begin{pmatrix} i & 0 \\ 0 & -i \end{pmatrix} \quad (\text{A.16a})$$

$$\gamma_\mu = \eta_{\mu\nu} e^{-2Rky} \gamma^\nu \quad \gamma_5 = -R^2 \gamma^5 \quad (\text{A.16b})$$

and in conformal coordinates

$$\gamma^\mu = -\delta_m^\mu kz \begin{pmatrix} 0 & \sigma^m \\ \bar{\sigma}^m & 0 \end{pmatrix} \quad \gamma^5 = kz \begin{pmatrix} i & 0 \\ 0 & -i \end{pmatrix} \quad (\text{A.17a})$$

$$\gamma_\mu = \eta_{\mu\nu} \frac{1}{k^2 z^2} \gamma^\nu \quad \gamma_5 = -\frac{1}{k^2 z^2} \gamma^5 \quad (\text{A.17b})$$

A.2 Overlap Integrals for Effective Coupling Constants

We discuss in chapter D that the overlap integrals over the extra dimension as they appear in interaction terms, only come in a finite number of varieties which are determined by the spin of the fields. There are exceptions to the following rules in the case of some dimensionful couplings, and they are mentioned in the text explicitly.

Every interaction term contains one factor $\sqrt{g} = \det e = Re^{-4Rky}$. In addition to this, there are potential metric factors $g^{\mu\nu} = e^{2Rky} \eta^{\mu\nu}$ (from derivatives and vector fields) and vierbein factors (from Dirac/Weyl matrices) $e_a^\mu = \delta_a^\mu e^{Rky}$ in the Lagrangian. The most common cases throughout this work are the following:

Yukawa Type Couplings

This can be either the coupling of a scalar to two matter fermions, or the supersymmetric Yukawa interaction of one matter fermion, one gaugino and the sfermions. In either case, we have

$$S \propto \int \sqrt{g} \phi \psi \chi \quad (\text{A.18})$$

leading to

$$\langle \phi \psi \chi \rangle \equiv \int_0^\pi dy Re^{-4Rky} f_\phi f_\psi f_\chi \quad (\text{A.19})$$

Fermion Gauge Interactions

This applies to the standard 4D gauge interaction of matter in fundamental or abelian representations or gauginos with a vector boson. There is one vierbein,

$$S \propto \int \sqrt{g} e_n^\mu A_\mu \psi \sigma^n \bar{\chi} \quad (\text{A.20})$$

leading to

$$\langle A \psi \chi \rangle \equiv \int_0^\pi dy Re^{-3Rky} f_A f_\psi f_\chi \quad (\text{A.21})$$

Scalar Gauge Interactions

This applies to sfermion gauge interactions as well as to the scalars from the gauge supermultiplets. There is one metric factor,

$$S \propto \int \sqrt{g} g^{\mu\nu} A_\mu \phi_1 \partial_\nu \phi_2 \quad (\text{A.22})$$

or

$$S \propto \int \sqrt{g} g^{\mu\nu} A_\mu A_\nu \phi_1 \phi_2 \quad (\text{A.23})$$

leading to

$$\langle A \phi_1 \phi_2 \rangle \equiv \int_0^\pi dy R e^{-2Rky} f_A f_{\phi_1} f_{\phi_2} \quad (\text{A.24})$$

$$\langle A_1 A_2 \phi_1 \phi_2 \rangle \equiv \int_0^\pi dy R e^{-2Rky} f_{A_1} f_{A_2} f_{\phi_1} f_{\phi_2} \quad (\text{A.25})$$

Gauge Self Interactions

There are two metric factors,

$$S \propto \int \sqrt{g} g^{\mu\nu} g^{\omega\rho} F_{\mu\nu} F_{\omega\rho} \quad (\text{A.26})$$

leading to

$$\langle A_1 A_2 A_3 (A_4) \rangle \equiv \int_0^\pi dy R f_{A_1} f_{A_2} f_{A_3} (f_{A_4}) \quad (\text{A.27})$$

Appendix B

The Action of 5D SYM Coupled to Matter in 5D Component Fields

B.1 Derivation

The Gauge Multiplet

The 4D action of the gauge multiplet is the same as ordinary 4D SYM theory. The gauge boson part is given in the section on nonabelian gauge theory in warped space, and we will give the minimally coupled gaugino action later. First let us analyze the parts that are new in 5D, namely

$$\bar{\chi}e^{-V}\chi e^V + \sqrt{2}\partial_5 e^{-V}\chi e^V - \sqrt{2}\bar{\chi}e^{-V}\partial_5 e^V - \partial_5 e^{-V}\partial_5 e^V$$

They are equivalent (appendix E.4) to the component Lagrangian

$$\begin{aligned} S = & \text{4D-Part} \\ & + \int d^5x \frac{1}{4R g_{YM}^2} e^{-2Rky} \left\{ -i\lambda_2^a \sigma^\mu \partial_\mu \bar{\lambda}_2^a - \frac{1}{\sqrt{2}} f^{bda} \bar{\lambda}_2^a \bar{\lambda}_1^b A_1^d \right. \\ & - \frac{1}{\sqrt{2}} f^{dea} A_2^d \lambda_2^e \lambda_1^a + \frac{i}{2} f^{dea} A_2^a A_1^d D^e - \frac{1}{4} f^{dfg} f^{gea} A_2^a A_1^d A_\mu^e A_\mu^f - A_2^a \square A_1^a \\ & + \frac{1}{2} (f^{dea} A_2^a \partial_\mu A_1^d A_\mu^e + f^{bda} \partial_\mu A_2^a A_1^d A_\mu^b) + \frac{i}{2} f^{bda} A_\mu^b \lambda_2^d \sigma^\mu \bar{\lambda}_2^a + C^{\dagger a} C^a \\ & - i\lambda_2^a \partial_5 \lambda_1^a + i\bar{\lambda}_2^a \partial_5 \bar{\lambda}_1^a - \frac{1}{\sqrt{2}} (A_2 + A_1)^a \partial_5 D^a - \frac{i}{\sqrt{2}} \partial_\mu (A_2 - A_1)^a \partial_5 A_\mu^a \\ & \left. + \frac{1}{2} \partial_5 A_\mu^a \partial_5 A_\mu^a - \frac{i}{2} f^{bca} \frac{1}{\sqrt{2}} (A_2^c - A_1^c) A_\mu^b \partial_5 A_\mu^a \right\} \end{aligned}$$

where we have introduced $\frac{i}{\sqrt{2}}(A_2 - A_1) = A_5$, $\frac{1}{\sqrt{2}}(A_2 + A_1) = \Sigma$. Also, for simplicity $A_\mu A_\mu \equiv \eta^{\mu\nu} A_\mu A_\nu$ etc. The final form after all field redefinitions can be found in appendix B.2.

The Hypermultiplet

The first part of (4.34) is identical to 4D SUSY, but we present it here again for sake of completeness. Let us first turn to the expression $\overline{H}e^{-V}H|_{\theta^4}$ order by order in V . This is possible as in Wess-Zumino gauge, $V^3 = 0$.

$$\begin{aligned}
\int d^4\theta \operatorname{Re} e^{-2kRy} \overline{H}H &= \\
\operatorname{Re} e^{-2kRy} \left\{ -\frac{h^\dagger \square h}{4} - \frac{\square h^\dagger h}{4} + \frac{1}{2} \eta^{\mu\nu} (\partial_\mu h^\dagger) (\partial_\nu h) \right. \\
&\quad \left. - \frac{i}{2} \overline{\psi} \overline{\sigma}^\mu \partial_\mu \psi + \frac{i}{2} \partial_\mu \overline{\psi} \overline{\sigma}^\mu \psi + F^\dagger F \right\} \\
&= \operatorname{Re} e^{-2kRy} \left\{ -h^\dagger \square h - i \overline{\psi} \overline{\sigma}^\mu \partial_\mu \psi + F^\dagger F \right\} \tag{B.1}
\end{aligned}$$

$$\begin{aligned}
\int d^4\theta \operatorname{Re} e^{-2kRy} \overline{H}(-V^l T^l)H &= \\
-\operatorname{Re} e^{-2kRy} \left\{ -\frac{i}{2} \eta^{\mu\nu} A_\mu^l h^\dagger T^l \partial_\nu h + \frac{i}{2} \eta^{\mu\nu} A_\mu^l \partial_\nu h^\dagger T^l h \right. \\
&\quad \left. + \frac{i}{\sqrt{2}} \overline{\lambda}_1^l \overline{\psi} T^l h - \frac{i}{\sqrt{2}} h^\dagger T^l \psi \lambda_1^l + \frac{1}{2} A_\mu^l \overline{\psi} \overline{\sigma}^\mu T^l \psi + \frac{1}{2} D^l h^\dagger T^l h \right\} \tag{B.2}
\end{aligned}$$

$$\begin{aligned}
\int d^4\theta \operatorname{Re} e^{-2kRy} \overline{H} \frac{(-V^l T^l)^2}{2} H &= \\
\int d^4\theta \operatorname{Re} \frac{e^{-2kRy}}{2} \overline{H} (\theta \sigma^\mu \overline{\theta} A_\mu^l) (\theta \sigma^\nu \overline{\theta} A_\nu^k) T^l T^k H \\
&= +\frac{1}{4} \operatorname{Re} e^{-2kRy} \left\{ \eta^{\mu\nu} A_\mu^l A_\nu^k h^\dagger T^l T^k h \right\} \tag{B.3}
\end{aligned}$$

The corresponding expressions for $H^c e^V \overline{H}^c|_{\theta^4}$ are as follows:

$$\begin{aligned}
\int d^4\theta \operatorname{Re} e^{-2kRy} H^c \overline{H}^c &= \\
\operatorname{Re} e^{-2kRy} \left\{ -h^c \square h^{c\dagger} + F^c F^{c\dagger} + i \partial_\mu \psi^c \sigma^\mu \overline{\psi}^c \right\} \tag{B.4}
\end{aligned}$$

$$\begin{aligned}
\int d^4\theta \operatorname{Re} e^{-2kRy} H^c (V^l T^l) \overline{H}^c &= \\
\operatorname{Re} e^{-2kRy} \left\{ \frac{i}{2} \eta^{\mu\nu} A_\mu^l h^c T^l \partial_\nu h^{c\dagger} - \frac{i}{2} \eta^{\mu\nu} A_\nu^l \partial_\mu h^c T^l h^{c\dagger} + \frac{i}{\sqrt{2}} h^c T^l \overline{\psi}^c \overline{\lambda}_1^l \right. \\
&\quad \left. - \frac{i}{\sqrt{2}} \lambda_1^l \psi^c T^l h^{c\dagger} + \frac{1}{2} D^l h^c T^l h^{c\dagger} - \frac{1}{2} \psi^c T^l \sigma^\mu \overline{\psi}^c A_\mu^l \right\} \tag{B.5}
\end{aligned}$$

$$\int d^4\theta \operatorname{Re} e^{-2kRy} H^c \frac{(V^l T^l)^2}{2} \overline{H}^c =$$

$$\begin{aligned}
\int d^4\theta R \frac{e^{-2kRy}}{2} H^c (\theta\sigma^\mu\bar{\theta}A_\mu^l) (\theta\sigma^\nu\bar{\theta}A_\nu^k) T^l T^k \bar{H}^c \\
= \frac{1}{4} R e^{-2kRy} \left\{ \eta^{\mu\nu} A_\mu^l A_\nu^k h^c T^l T^k h^{c\dagger} \right\}
\end{aligned} \tag{B.6}$$

Now let us consider the 5D covariant action as given in the second part of (4.34). To simplify notation we define ‘‘covariant’’ derivatives of different orders in θ :

$$\begin{aligned}
\mathcal{D}_0 &= (\partial_y - (3/2 - c)Rk)\mathbb{1} - \frac{1}{2}(\Sigma^l + iA_5^l)T^l \\
\mathcal{D}_1 &= -\theta\lambda_2^l T^l \\
\mathcal{D}_2 &= -\frac{1}{\sqrt{2}}\theta\theta C^l T^l
\end{aligned}$$

Using those we find

$$\begin{aligned}
\int d^2\theta e^{-3Rky} H_L^c \mathcal{D}_0 H_L &= e^{-3Rky} \left\{ h_L^c \mathcal{D}_0 F_L - \psi_L^c \mathcal{D}_0 \psi_L + F_L^c \mathcal{D}_0 h_L \right\} \\
\int d^2\theta e^{-3Rky} H_L^c \mathcal{D}_1 H_L &= e^{-3Rky} \frac{1}{\sqrt{2}} \left\{ h_L^c T^l \psi \lambda_{2L}^l + \lambda_{2L}^l \psi^c T^l h_L \right\} \\
\int d^2\theta e^{-3Rky} H_L^c \mathcal{D}_2 H_L &= e^{-3Rky} \frac{1}{\sqrt{2}} \left\{ -h_L^c T^l h_L C^l \right\}
\end{aligned}$$

All of the above is of course before any field redefinitions, and the final form can again be found in the Appendix.

B.1.1 Integrating out the Auxiliary Fields

Let us first consider the general form of the action arising from integrating out auxiliary fields.

F Terms

The Lagrangian involving the auxiliary field of chiral multiplets can be cast in the form

$$\mathcal{L} = \alpha F^\dagger F + \beta(\Omega^\dagger F + F^\dagger \Omega) \tag{B.7}$$

Solving the algebraic equation of motion for F one finds

$$F + \frac{\beta}{\alpha}\Omega = 0 \Rightarrow F = -\frac{\beta}{\alpha}\Omega \tag{B.8}$$

So the onshell Lagrangian is

$$\mathcal{L} = -\frac{\beta^2}{\alpha}\Omega^\dagger \Omega \tag{B.9}$$

D Terms

For the real auxiliary field from the gauge multiplet,

$$\mathcal{L} = \alpha \frac{1}{2} D^2 + \beta (D\Omega) \quad (\text{B.10})$$

and the resulting equation of motion for D is

$$D + \frac{\beta}{\alpha} \Omega = 0 \Rightarrow D = -\frac{\beta}{\alpha} \Omega \quad (\text{B.11})$$

leading to an onshell Lagrangian

$$\mathcal{L} = -\frac{1}{2} \frac{\beta^2}{\alpha} \Omega^2 \quad (\text{B.12})$$

F Term from the Chiral Part of the Vector Multiplet

The F Term Lagrangian from the 5D gauge coupling to a matter hypermultiplet is

$$\mathcal{L} = \frac{e^{-2Rky}}{Rg^2} C^{\dagger a} C^a - \frac{e^{-3Rky}}{\sqrt{2}} \left(C^l (h^c T^l h) + C^{\dagger l} (h^c T^l h)^{\dagger} \right) \quad (\text{B.13})$$

So, using the above definitions

$$\Omega = (h^c T^l h)^{\dagger} \quad (\text{B.14})$$

$$-\frac{\beta^2}{\alpha} = -\frac{g^2}{2} R e^{-4Rky} = -\sqrt{g} \frac{g^2}{2} \quad (\text{B.15})$$

Therefore, the resulting onshell Lagrangian from the gauge F term is

$$\mathcal{L} = \sqrt{g} \left(-\frac{g^2}{2} \right) (h^c T^l h)^{\dagger} (h^c T^l h) \quad (\text{B.16})$$

D Term from the Vector Part of the Vector Multiplet

The coupling of a matter hypermultiplet to the vector superfield gives us a D term

$$\begin{aligned} \mathcal{L} &= \frac{R}{2g^2} D^2 + \frac{e^{-2Rky}}{Rg^2} \left[\frac{1}{4} f^{dea} (A_5^a \Sigma^d - \Sigma^a A_5^d) D^e - \Sigma^a \partial_5 D^a \right] \\ &\quad - R e^{-2Rky} \frac{1}{2} D^l h^{\dagger} T^l h + R e^{-2Rky} \frac{1}{2} D^l h^c T^l h^{c\dagger} \\ &= \frac{R}{2g^2} D^2 + \frac{e^{-2Rky}}{Rg^2} \left[\frac{1}{2} f^{dea} A_5^a \Sigma^d D^e - D^a (2Rk - \partial_5) \Sigma^a \right] \\ &\quad + \underbrace{\partial_5 \left[-\frac{e^{-2Rky}}{Rg^2} \Sigma^a D^a \right]}_{\text{Boundary } D \text{ term}} - R e^{-2Rky} \frac{1}{2} D^l h^{\dagger} T^l h + R e^{-2Rky} \frac{1}{2} D^l h^c T^l h^{c\dagger} \end{aligned}$$

So,

$$\begin{aligned}\Omega^e &= \left[\frac{1}{2} f^{dea} A_5^a \Sigma^d - (2Rk - \partial_5) \Sigma^e - R^2 g^2 \frac{1}{2} h^\dagger T^e h + R^2 g^2 \frac{1}{2} h^c T^e h^{c\dagger} \right] \\ \alpha &= \frac{R}{g^2} \quad \beta = \frac{e^{-2Rky}}{Rg^2}\end{aligned}\tag{B.17}$$

The resulting onshell Lagrangian is

$$\begin{aligned}\mathcal{L} &= -\frac{1}{2} \frac{e^{-4Rky}}{R^3 g^2} \left[\frac{1}{2} f^{adl} A_5^a \Sigma^d - (2Rk - \partial_5) \Sigma^l - R^2 g^2 \frac{1}{2} h^\dagger T^l h + R^2 g^2 \frac{1}{2} h^c T^l h^{c\dagger} \right]^2 \\ &= -\sqrt{g} \frac{1}{2g^2} \left[\frac{1}{2R^2} f^{adl} A_5^a \Sigma^d - \frac{2Rk - \partial_5}{R^2} \Sigma^l - g^2 \frac{1}{2} h^\dagger T^l h + g^2 \frac{1}{2} h^c T^l h^{c\dagger} \right]^2\end{aligned}$$

F Term from a Matter Hypermultiplet

$$\begin{aligned}e^{-3Rky} h^c \mathcal{D}F &= e^{-3Rky} \left[-(3/2 - c) R \sigma' \cdot h^c F - \frac{1}{2} (\Sigma^l + iA_5^l) h^c T^l F + h^c \partial_5 F \right] \\ &= e^{-3Rky} \left[-(3/2 - c) R \sigma' h^c F - \frac{1}{2} (\Sigma^l + iA_5^l) h^c T^l F + (-\partial_5 + 3Rk) h^c F \right] \\ &\quad + \partial_5 \left[e^{-3Rky} h^c F \right] \\ &\simeq e^{-3Rky} \left[-(3/2 - c) R \sigma' h^c - \frac{1}{2} (\Sigma^l + iA_5^l) h^c T^l + (-\partial_5 + 3Rk) h^c \right] \cdot F \\ &= e^{-3Rky} \Omega^\dagger F\end{aligned}$$

So, the onshell Lagrangian is

$$\begin{aligned}\mathcal{L} &= -\frac{e^{-4Rky}}{R} (\Omega^\dagger \Omega + \Omega^c \Omega^{c\dagger}) \\ &= -\frac{\sqrt{g}}{R^2} \left[-(3/2 - c) R \sigma' h^c - \frac{1}{2} (\Sigma + iA_5)^l h^c T^l + (3kR - \partial_5) h^c \right] \times \\ &\quad \left[-(3/2 - c) R \sigma' h^{c\dagger} - \frac{1}{2} (\Sigma - iA_5)^l T^l h^{c\dagger} + (3kR - \partial_5) h^{c\dagger} \right] \\ &\quad - \frac{\sqrt{g}}{R^2} \left[\partial_5 h^\dagger - (3/2 - c) R \sigma' h^\dagger - \frac{1}{2} (\Sigma - iA_5)^l h^\dagger T^l \right] \times \\ &\quad \left[\partial_5 h - (3/2 - c) R \sigma' h - \frac{1}{2} (\Sigma + iA_5)^l T^l h \right]\end{aligned}\tag{B.18}$$

B.1.2 Many Flavors

In all of these terms, we have only assumed there to be one $SU(N)$ gauge group and one flavour charged under it in the fundamental representation. Since each auxiliary field will couple to all flavours present in the model which are charged under it, the resulting interactions in the onshell Lagrangian will mix flavours.

B.2 Summary of the 5D Onshell Action

The following is the action of one hypermultiplet coupled to $SU(N)$ SYM in warped space, written in 5D component fields with the 5D gauge coupling constant g_{YM} . The convention is such that the correct density factors are already included in the expressions and

$$S = \int d^4x \int_0^\pi dy \sum_{i=0}^{31} \mathcal{L}_i \quad (\text{B.19})$$

For brevity we have again adopted a notation where $A_\mu A_\mu \equiv \eta^{\mu\nu} A_\mu A_\nu$ and $\nu, \mu = 0..3$. First, the 4D SYM Lagrangian (without the $RD^a D^a/2$ term which is already integrated out),

$$+Re^{-3Rky} \left[-i\lambda_1^a \sigma^\mu \partial_\mu \bar{\lambda}_1^a + ig_{YM} f^{bda} A_\mu^b \lambda_1^d \sigma^\mu \bar{\lambda}_1^a \right] - \frac{1}{4} R F_{\mu\nu}^a F_{\mu\nu}^a \quad (\text{L}_0)$$

B.2.1 Action from the Gauge Superfields

$$Re^{-2Rky} \left[-\frac{1}{2} \Sigma \square \Sigma - \frac{1}{2} A_5 \square A_5 \right] \quad (\text{L}_1)$$

$$Re^{-3Rky} (-i\lambda_2^a \sigma^\mu \partial_\mu \bar{\lambda}_2^a) \quad (\text{L}_2)$$

$$Re^{-4Rky} \left[-\lambda_2^a \frac{\partial_5 - 3/2Rk}{R} \lambda_1^a - \bar{\lambda}_2^a \frac{\partial_5 - 3/2Rk}{R} \bar{\lambda}_1^a \right] \quad (\text{L}_3)$$

$$Re^{-2Rky} \left[\frac{1}{2} \frac{\partial_5}{R} A_\mu \frac{\partial_5}{R} A_\mu \right] - Re^{-2Rky} \partial_\mu A_5 \frac{\partial_5}{R} A_\mu \quad (\text{L}_4)$$

$$Re^{-2Rky} g_{YM} f^{dea} \left[\Sigma^a \partial_\mu \Sigma^d A_\mu^e + A_5^a \partial_\mu A_5^d A_\mu^e \right] \quad (\text{L}_5)$$

$$Re^{-3Rky} ig_{YM} f^{bda} A_\mu^b \lambda_2^d \sigma^\mu \bar{\lambda}_2^a \quad (\text{L}_6)$$

$$Re^{-2Rky} g_{YM} \left[-f^{bca} A_5^c A_\mu^b \frac{\partial_5}{R} A_\mu^a \right] \quad (\text{L}_7)$$

$$Re^{-4Rky} g_{YM} \left[-if^{bda} \Sigma^d (\bar{\lambda}_2^a \bar{\lambda}_1^b - \lambda_2^a \lambda_1^b) + f^{bda} A_5^d (\bar{\lambda}_2^a \bar{\lambda}_1^b + \lambda_2^a \lambda_1^b) \right] \quad (\text{L}_8)$$

$$Re^{-2Rky} \frac{1}{2} g_{YM}^2 \left[-f^{dfg} f^{gea} (\Sigma^a \Sigma^d A_\mu^e A_\mu^f + A_5^a A_5^d A_\mu^e A_\mu^f) \right] \quad (\text{L}_9)$$

B.2.2 Interaction with Matter

$$Re^{-2Rky} \left[-h^\dagger \square h - h^c \square h^{c\dagger} \right] \quad (\text{L}_{10})$$

$$Re^{-3Rky} \left[i\partial_\mu \psi^c \sigma^\mu \bar{\psi}^c - i\bar{\psi} \sigma^\mu \partial_\mu \psi \right] \quad (\text{L}_{11})$$

$$Re^{-2Rky} ig_{YM} \left[A_\mu^l h^\dagger T^l \partial_\mu h - A_\mu^l \partial_\mu h^\dagger T^l h \right] \quad (\text{L}_{12})$$

$$Re^{-2Rky} i g_{YM} \left[A_\mu^l h^c T^l \partial_\mu h^{c\dagger} - A_\mu^l \partial_\mu h^c T^l h^{c\dagger} \right] \quad (\mathcal{L}_{13})$$

$$Re^{-2Rky} g_{YM}^2 \left[A_\mu^l A_\mu^k h^\dagger T^l T^k h + A_\mu^l A_\mu^k h^c T^l T^k h^{c\dagger} \right] \quad (\mathcal{L}_{14})$$

$$Re^{-3Rky} g_{YM} \left[-A_\mu^l \bar{\psi} \bar{\sigma}^\mu T^l \psi - \psi^c T^l \sigma^\mu \bar{\psi}^c A_\mu^l \right] \quad (\mathcal{L}_{15})$$

$$Re^{-4Rky} i g_{YM} \left[\sqrt{2} \bar{\lambda}_1^l \bar{\psi} T^l h - \sqrt{2} h^\dagger T^l \psi \lambda_1^l \right] \quad (\mathcal{L}_{16})$$

$$Re^{-4Rky} i g_{YM} \left[-\sqrt{2} h^c T^l \bar{\psi}^c \bar{\lambda}_1^l + \sqrt{2} \lambda_1^l \psi^c T^l h^{c\dagger} \right] \quad (\mathcal{L}_{17})$$

B.2.3 Matter Coupling to the Chiral Part of the Vector

$$Re^{-4Rky} \left[-\psi^c \left(\frac{\partial_5}{R} + (c-2)k \right) \psi + g_{YM} (\Sigma + iA_5)^l \psi^c T^l \psi \right] \quad (\mathcal{L}_{18})$$

$$Re^{-4Rky} i g_{YM} \left[-\sqrt{2} h^c T^l \psi \lambda_2^l - \sqrt{2} \lambda_2^l \psi^c T^l h \right] \quad (\mathcal{L}_{19})$$

$$Re^{-4Rky} \left[\left(-\frac{\partial_5 + (c-2)Rk}{R} \bar{\psi} \right) \bar{\psi}^c + g_{YM} (\Sigma - iA_5)^l \bar{\psi} T^l \bar{\psi}^c \right] \quad (\mathcal{L}_{20})$$

$$Re^{-4Rky} i g_{YM} \left[\sqrt{2} \bar{\lambda}_2^l \bar{\psi} T^l h^{c\dagger} + \sqrt{2} h^\dagger T^l \bar{\psi}^c \bar{\lambda}_2^l \right] \quad (\mathcal{L}_{21})$$

B.2.4 The F Term

$$\begin{aligned} & -Re^{-4Rky} \left[\frac{(3/2+c)kR - \partial_5}{R} \right] h^c \left[\frac{(3/2+c)kR - \partial_5}{R} \right] h^{c\dagger} \\ & -Re^{-4Rky} \left[\frac{\partial_5 - (3/2-c)Rk}{R} \right] h^\dagger \left[\frac{\partial_5 - (3/2-c)Rk}{R} \right] h \end{aligned} \quad (\mathcal{L}_{22})$$

$$\begin{aligned} & -Re^{-4Rky} g_{YM}^2 (\Sigma + iA_5)^l (\Sigma - iA_5)^m h^c T^l T^m h^{c\dagger} \\ & -Re^{-4Rky} g_{YM}^2 (\Sigma - iA_5)^l (\Sigma + iA_5)^m h^\dagger T^l T^m h \end{aligned} \quad (\mathcal{L}_{23})$$

$$\begin{aligned} & Re^{-4Rky} g_{YM} (\Sigma - iA_5)^l \left(\frac{(3/2+c)kR - \partial_5}{R} h^c \right) T^l h^{c\dagger} \\ & Re^{-4Rky} g_{YM} (\Sigma + iA_5)^l h^c T^l \left(\frac{(3/2+c)Rk - \partial_5}{R} h^{c\dagger} \right) \\ & Re^{-4Rky} g_{YM} (\Sigma + iA_5)^l \left(\frac{\partial_5 - (3/2-c)Rk}{R} h^\dagger \right) T^l h \\ & Re^{-4Rky} g_{YM} (\Sigma - iA_5)^l h^\dagger T^l \left(\frac{\partial_5 - (3/2-c)Rk}{R} h \right) \end{aligned} \quad (\mathcal{L}_{24})$$

B.2.5 The Vector F Term

$$Re^{-4Rky} (-2g_{YM}^2) (h^c T^l h)^\dagger (h^c T^l h) \quad (\mathcal{L}_{25})$$

B.2.6 The D Term

$$-Re^{-4Rky} \frac{1}{2} \left(\frac{\partial_5 - 2Rk}{R} \Sigma^l \right) \left(\frac{\partial_5 - 2Rk}{R} \Sigma^l \right) \quad (\mathcal{L}_{26})$$

$$-Re^{-4Rky} g_{YM}^2 \left(\frac{1}{2} f^{adl} f^{fgl} A_5^a \Sigma^d A_5^f \Sigma^g \right) \quad (\mathcal{L}_{27})$$

$$-Re^{-4Rky} g_{YM} f^{adl} A_5^a \Sigma^d \left(\frac{\partial_5 - 2Rk}{R} \Sigma^l \right) \quad (\mathcal{L}_{28})$$

$$-Re^{-4Rky} g_{YM}^2 \frac{1}{2} \left[(h^c T^l h^{c\dagger})(h^c T^l h^{c\dagger}) \right. \\ \left. + (h^\dagger T^l h)(h^\dagger T^l h) - 2(h^c T^l h^{c\dagger})(h^\dagger T^l h) \right] \quad (\mathcal{L}_{29})$$

$$-Re^{-4Rky} g_{YM}^2 f^{adl} \left[A_5^a \Sigma^d (h^c T^l h^{c\dagger} - h^\dagger T^l h) \right] \quad (\mathcal{L}_{30})$$

$$-Re^{-4Rky} g_{YM} \left(\frac{\partial_5 - 2Rk}{R} \Sigma^l \right) (h^c T^l h^{c\dagger} - h^\dagger T^l h) \quad (\mathcal{L}_{31})$$

Appendix C

Boundary Conditions and Linear Algebra

In this chapter we present the proof of the property (2.14) of the matrices defining the boundary conditions for a field on any of the two boundaries. We are looking for the most general matrices $N, D \in \mathbb{R}^{n \times n}$ which satisfy

$$\forall v, w \in \mathbb{R}^n : Dv + Nw = 0 \Rightarrow v^T w = 0 \quad (\text{C.1})$$

the latter being required for the boundary action to vanish. We proceed in several steps: first we recast (C.1) to a normal form, and then derive its properties. Let us first note that we are allowed to act with any regular $n \times n$ matrix from the left without changing the condition. Furthermore, we can do orthogonal basis transformations as long as we act on v and w simultaneously. As a first step we perform a SVD on D . For the SVD we choose the orthogonal matrices A, B such that

$$ADB^T = \begin{pmatrix} \sigma_1 & & & \\ & \ddots & & \\ & & \sigma_r & \\ & & & 0_{n-r \times n-r} \end{pmatrix} \quad (\text{C.2})$$

and define $v' = Bv$, $w' = Bw$. Here $r = \text{rk } D$ is the number of Dirichlet- or mixed boundary conditions. We obtain

$$Dv + Nw = A^T(ADB^T)Bv + Nw = 0 \Leftrightarrow (ADB^T)Bv + ANB^T Bw = 0 \quad (\text{C.3})$$

Furthermore we act from the left with $R = \text{diag}(\sigma_1^{-1}, \dots, \sigma_r^{-1}, 1, \dots, 1)$ and define $N' = RANB^T$. We now have

$$Dv + Nw = 0 \Leftrightarrow \text{diag}(1, \dots, 1, 0, \dots, 0)v' + N'w' = 0 \quad (\text{C.4})$$

We then split N' in submatrices,

$$Dv + Nw = 0 \Leftrightarrow \begin{pmatrix} I_{r \times r} & \\ & 0_{n-r \times n-r} \end{pmatrix} v' + \begin{pmatrix} W & X \\ Y & Z \end{pmatrix} w' \quad (\text{C.5})$$

Now we begin to determine the properties of W, X, Y, Z using (C.1).

i) $\text{rk } Z = n - r$:

Assume $\exists u \in \ker Z$. We choose

$$w' = \begin{pmatrix} 0 \\ u \end{pmatrix} \quad v' = \begin{pmatrix} -Xu \\ a \end{pmatrix} \quad (\text{C.6})$$

where a is arbitrary. This choice fulfils $D'v' + N'w' = 0$, but since $w'^T v' = u^T a$, it follows that $u = 0$. Thus $\dim \ker Z = 0$ \square

We use the fact that Z has full rank to act with another matrix R' from the left such that X is eliminated using row transformations. This changes W , but the matrix D' remains the same. We thus have, without loss of generality,

$$(Dv + Nw = 0 \Rightarrow v^T w = 0) \Leftrightarrow \begin{pmatrix} I_{r \times r} & \\ & 0_{n-r \times n-r} \end{pmatrix} v' + \underbrace{\begin{pmatrix} W' & 0 \\ Y & Z \end{pmatrix}}_{N''} w' \Rightarrow v^T w = 0 \quad (\text{C.7})$$

ii) $Y = 0$:

Assume $\exists u : Yu \neq 0$. We choose

$$w' = \begin{pmatrix} u \\ -Z^{-1}Yu \end{pmatrix} \quad v' = \begin{pmatrix} -W'u \\ a \end{pmatrix} \quad (\text{C.8})$$

which satisfies $D'v' + N''w' = 0$, but $Z^{-1}Yu \neq 0$ by assumption, and thus $w'^T v' = -u^T W'u - a^T Z^{-1}Yu$ can be made nonvanishing by choice of a . This is a contradiction, and $Y = 0$. \square

Therefore, without loss of generality, our problem is equivalent to

$$\begin{pmatrix} I_{r \times r} & \\ & 0_{n-r \times n-r} \end{pmatrix} v' + \begin{pmatrix} W' & 0 \\ 0 & Z \end{pmatrix} w' = 0 \Rightarrow v^T w = 0 \quad (\text{C.9})$$

iii) $W'^T = -W'$:

We choose

$$w' = \begin{pmatrix} a \\ 0 \end{pmatrix} \quad (\text{C.10})$$

To satisfy the LHS, we have to choose

$$v' = \begin{pmatrix} -W'a \\ * \end{pmatrix} \quad (\text{C.11})$$

We get

$$\forall a : v'^T w = -a^T W' a = 0 \Rightarrow W'^T = -W' \quad \square \quad (\text{C.12})$$

In a final step, we perform a basis change to bring W' to the (antisymmetric) real Jordan Normal Form, and to diagonalize Z . We then act with a regular matrix from the left to set the diagonal entries to unity. Both transformations do not change D' . We thus arrive at (2.14), up to an arbitrary regular matrix acting from the left.

Appendix D

Useful Properties of the Warped KK expansion

This chapter is in conformal coordinates because the results are relevant to the software implementation which works with this coordinate frame.

All effective n point coupling constants (including normalization conditions in the case of one field) can be written in the following form

$$\langle \phi_1 \dots \phi_n \rangle = \int_{r1}^{r2} dz k^\delta z^\gamma (a_1 J_{\alpha_1}(mz) + b_1 Y_{\alpha_1}(mz)) \times \dots \times (a_n J_{\alpha_n}(mz) + b_n Y_{\alpha_n}(mz)) \quad (\text{D.1})$$

where $r1 = 1/k$, $r2 = e^{Rk\pi}/k$ and z is the conformal coordinate. The Bessel functions for fermion modes always come with a $z^{5/2}$, for scalars with a z^2 and for gauge bosons with a z . This is compensated by the corresponding metric tensors and fünfbeins in such a way that in normalizations and nearly all interactions (4D gauge interactions and their “superpartners”), we get

$$\gamma = n - 1 \quad (\text{D.2})$$

For example, in a fermion gauge three point coupling,

$$\frac{1}{k^5 z^5} \psi \sigma^\mu A_\mu \bar{\psi} \propto \frac{1}{k^5 z^5} (z^{5/2} Y)(z \sigma^n)(z Y)(z^{5/2} Y) + \dots \propto z^2 \quad (\text{D.3})$$

while in a sfermion gauge four point coupling

$$\frac{1}{k^5 z^5} \phi^\dagger g^{\mu\nu} A_\mu A_\nu \phi \propto \frac{1}{k^5 z^5} (z^2 Y)(z^2 \eta^{mn})(z Y)(z Y)(z^2 Y) + \dots \propto z^3 \quad (\text{D.4})$$

The three scalar couplings such as the ones calculated in section 6.3.6 are an exception to this rule. The normalization conditions as well as some coupling constants receive corrections from boundary kinetic terms if they are present. In the case of coupling constants, we have no choice but to add them explicitly. In the case of normalization, there is a simpler way. Consider the recurrence

relations of Bessel functions $X_\alpha = J_\alpha, Y_\alpha$,

$$\frac{2\alpha}{x} X_\alpha(x) = X_{\alpha-1}(x) + X_{\alpha+1}(x) \quad (\text{D.5})$$

$$2\frac{d}{dx} X_\alpha(x) = X_{\alpha-1}(x) - X_{\alpha+1}(x) \quad (\text{D.6})$$

Taking the sum and difference, we get

$$\left(\frac{d}{dx} + \frac{\alpha}{x}\right) X_\alpha(x) = X_{\alpha-1}(x) \quad (\text{D.7})$$

$$\left(\frac{d}{dx} - \frac{\alpha}{x}\right) X_\alpha(x) = -X_{\alpha+1}(x) \quad (\text{D.8})$$

We exploit the fact that the modified derivatives in 5D kinetic terms always have the form (D.7) or (D.8), namely for any field

$$\phi = \phi^n(x) f^n(z) = \phi^n(x) z^r \left(a_n J_\alpha(m_n z) + b_n Y_\alpha(m_n z) \right) \quad (\text{D.9})$$

the combination

$$\tilde{\partial}_\delta^\alpha f = z^{r+\delta\alpha} \partial_z z^{-(r+\delta\alpha)} f \quad (\text{D.10})$$

appears which either raises ($\delta = 1$) or lowers ($\delta = -1$) the Bessel functions by one (which for $\alpha = 0$ is the same up to a relative sign), and which satisfies

$$\tilde{\partial}_\delta^\alpha \underbrace{z^r \left(a_n J_\alpha(m_n z) + b_n Y_\alpha(m_n z) \right)}_{\equiv f} = -m\delta \underbrace{z^r \left(a_n J_{\alpha+\delta}(m_n z) + b_n Y_{\alpha+\delta}(m_n z) \right)}_{\equiv g} \quad (\text{D.11})$$

so,

$$\tilde{\partial}_\delta^\alpha f = -m\delta g \quad \tilde{\partial}_{-\delta}^{\alpha+\delta} g = m\delta f \quad \tilde{\partial}_{-\delta}^{\alpha+\delta} \tilde{\partial}_\delta^\alpha f = -m^2 f \quad (\text{D.12})$$

The latter is the 5D kinetic operator which should be hermitian. This means that the scalar product in the action should satisfy

$$\int \widetilde{dz} B \tilde{\partial}_\delta^\alpha A = - \int \widetilde{dz} A \tilde{\partial}_{-\delta}^{\alpha+\delta} B + \text{bnd} \quad (\text{D.13})$$

which immediately gives us

$$\int \widetilde{dz} = \int dz z^{-2r+\delta^2} = \int dz z^{-2r+1} \quad (\text{D.14})$$

in accordance with (D.2) for $n = 2$. It only depends on spin and is proportional to \sqrt{g} times metric or fünfbein factors. If there are no localized kinetic terms, and iff the boundary problem is solved correctly, we can integrate by parts, and

$$\sum_i \int \widetilde{dz} f_i f_i = \sum_i \int \widetilde{dz} \frac{\tilde{\partial}_{-\delta}^{\alpha+\delta} g_i \tilde{\partial}_{-\delta}^{\alpha+\delta} g_i}{m^2} =$$

$$= - \sum_i \int \widetilde{dz} \frac{g_i \tilde{\partial}_\delta^\alpha \tilde{\partial}_{-\delta}^{\alpha+\delta} g_i}{m^2} + \text{bnd}_i = \sum_i \int \widetilde{dz} g_i g_i + \text{bnd}_i. \quad (\text{D.15})$$

which can be used as a consistency test. The sum over i covers all 5D fields which mix by boundary conditions to form one Kaluza-Klein tower. The boundary action does not necessarily vanish for each field individually, and therefore this relation only holds for the sum where $\sum_i \text{bnd}_i = 0$. Assume that ϕ satisfies a modified Neumann condition $\tilde{\partial}_\delta^\alpha \phi = 0$ on a boundary (and $g_\phi = 0$ there). If we switch on a boundary kinetic term for ϕ , above relation D.15 is not satisfied any more, but

$$\sum_i \int \widetilde{dz} f_i f_i + \text{B.K.T} = \sum_i \int \widetilde{dz} g_i g_i \quad (\text{D.16})$$

This can again be used as a consistency check, but more importantly, we can use the RHS to calculate our field normalizations without having to include boundary terms. The fields in our model when taken in conformal coordinates have the following assignments

Field $\phi =$	r	α	δ
A_μ	1	1	-1
λ_1	5/2	1	-1
ψ	5/2	$c + 1/2$	-1
h	2	$c + 1/2$	-1
A_5	1	0	1
Σ	2	0	1
λ_2	5/2	0	1
ψ^c	5/2	$c - 1/2$	1
h^c	2	$c - 1/2$	1

In the case of Dirac fermions with a boundary kinetic term in the 4D “righthanded” component, we can for example simply use the 4D “lefthanded” component to calculate the canonical normalization for both since they satisfy

$$g_\psi = \pm f_{\psi^c} \quad \Rightarrow \quad \tilde{\partial}_{-1}^{c+1/2} f_\psi = m g_\psi = \pm m f_{\psi^c} \quad (\text{D.17})$$

and thus a variation of (D.16) by virtue of the 5D Dirac equation.

D.1 Remarks about Majorana Spinors

There are no Majorana spinors in five dimensional space, simply because the reality condition $C\Psi = \Psi$ is incompatible with 5D Lorentz transformations of the form $\Psi \rightarrow \omega_{\mu 5} [\gamma^\mu, \gamma^5] \Psi$. However, after Kaluza-Klein decomposition we can always rewrite Dirac spinors as two Majorana spinors which are not necessarily charge eigenstates, but still degenerate mass eigenstates. Also, since 5D Lorentz invariance is broken on the branes, brane localized Majorana masses are allowed

which will split the degeneracy, leaving us with a pair of 4D Majorana spinors with different mass. How these Kaluza-Klein states are calculated in detail has not been treated all that extensively in the literature, and we will therefore use this as an excuse to present a compact approach using transport diffeomorphisms and some linear algebra to simultaneously obtain all modes and wave functions for an arbitrary number of fields coupled by boundary conditions. It is easy to miss half of the Majorana states if one solves the coupled eigenvalue problem in analogy to gauge bosons and scalars. The reason is as follows: As long as only Dirac masses appear, the relative sign convention of the dotted and undotted spinor Kaluza-Klein wave functions is inconsequential since it is equivalent to a redefinition of the 4D spinor. However, in the presence of Majorana masses, this amounts to flipping the sign of the boundary condition generated by the Majorana mass, essentially exchanging the two sets of solutions, for example the heavy and the light Neutrino with their respective KK towers. We will now consider the case of the electrically neutral spinor in the $SU(2)_L \times SU(2)_R \times U(1)_{B-L}$ gauge theory which is broken down to G_{SM} on the UV brane and $SU(2)_D \times U(1)_{B-L}$ on the IR brane as in the higgsless models with LR-symmetric Bulk gauge group. It consists of the following 5D fields in two component spinors (up to factors of $z = e^{Rky}/k$ which we consistently pull out of the KK wave functions for clarity)

$$\begin{aligned}
\chi_L(x, z) &= \chi_L^n(x) z^{5/2} f^{L,n}(z) \\
\psi_L(x, z) &= \psi_L^n(x) z^{5/2} g^{L,n}(z) \\
\chi_R(x, z) &= \chi_R^n(x) z^{5/2} f^{R,n}(z) \\
\psi_R(x, z) &= \psi_R^n(x) z^{5/2} g^{R,n}(z)
\end{aligned} \tag{D.18}$$

where

$$\begin{aligned}
f^{L,n}(z) &= a_{fL}^n J_{c_L+1/2}(m_n z) + b_{fL}^n Y_{c_L+1/2}(m_n z) \\
g^{L,n}(z) &= a_{gL}^n J_{c_L-1/2}(m_n z) + b_{gL}^n Y_{c_L-1/2}(m_n z) \\
f^{R,n}(z) &= a_{fR}^n J_{c_R+1/2}(m_n z) + b_{fR}^n Y_{c_R+1/2}(m_n z) \\
g^{R,n}(z) &= a_{gR}^n J_{c_R-1/2}(m_n z) + b_{gR}^n Y_{c_R-1/2}(m_n z)
\end{aligned} \tag{D.19}$$

They are related by the bulk equations of motion. Recall that

$$\partial_z(z^{1/2+c} J_{1/2+c}(mz)) = m(z^{1/2+c} J_{-1/2+c}(mz)) \tag{D.20}$$

$$\partial_z(z^{1/2-c} J_{-1/2+c}(mz)) = -m(z^{1/2-c} J_{1/2+c}(mz)) \tag{D.21}$$

and analogous for Y . The second order bulk equation then allows $a_{fi}^n = \pm a_{gi}^n$. This is the sign choice mentioned above, and both varieties will indeed appear automatically in the full treatment. It is therefore not sufficient to solve only for χ_{LR}, ψ_{LR} but we will have to include the derivatives. The vector of Kaluza-Klein wave functions and derivatives for which we solve is defined as

$$\vec{F} = (f_L, \tilde{\partial} f_L, f_R, \tilde{\partial} f_R, \tilde{\partial} g_L, g_L, \tilde{\partial} g_R, g_R)^T \tag{D.22}$$

where

$$\tilde{\partial}f \equiv z^{-1/2-c}\partial_z z^{1/2+c}f \quad (\text{D.23})$$

$$\tilde{\partial}g \equiv -z^{-1/2+c}\partial_z z^{1/2-c}g \quad (\text{D.24})$$

With these conventions, the transport diffeomorphism takes a particularly simple form for all components,

$$\vec{v}(a) = \underbrace{\begin{pmatrix} J_{c+1/2}(ma) & Y_{c+1/2}(ma) \\ J_{c-1/2}(ma) & Y_{c-1/2}(ma) \end{pmatrix} \begin{pmatrix} J_{c+1/2}(mb) & Y_{c+1/2}(mb) \\ J_{c-1/2}(mb) & Y_{c-1/2}(mb) \end{pmatrix}^{-1}}_{\equiv T(c, m)} \vec{v}(b) \quad (\text{D.25})$$

where now $\vec{v} = (f_i, \tilde{\partial}f_i)$ or $\vec{v} = (\tilde{\partial}g_i, g_i)$ [sic!]. The full transport diffeomorphism for \vec{F} is thus

$$T(m) = \begin{pmatrix} T(c_L, m) & 0 & 0 & 0 \\ 0 & T(c_R, m) & 0 & 0 \\ 0 & 0 & T(c_L, m) & 0 \\ 0 & 0 & 0 & T(c_R, m) \end{pmatrix} \quad (\text{D.26})$$

By putting a IR Dirac mass $\mu\chi_L\psi_R+h.c.$ and a UV Majorana mass $M\psi_R\psi_R+h.c.$, we generate effective boundary conditions

$$A\vec{F}(1/k) = 0 \quad B\vec{F}(e^{Rk\pi}/k) = 0 \quad (\text{D.27})$$

with

$$A = \begin{pmatrix} 0 & 1 & 0 & 0 & 0 & 0 & 0 & 0 \\ 0 & 0 & 1 & 0 & 0 & 0 & 0 & -M/k \\ 0 & 0 & 0 & 0 & 0 & 1 & 0 & 0 \\ 0 & 0 & 0 & -M/k & 0 & 0 & 1 & 0 \end{pmatrix} \quad (\text{D.28})$$

$$B = \begin{pmatrix} -\mu & 0 & 1 & 0 & 0 & 0 & 0 & 0 \\ 0 & 1 & 0 & \mu & 0 & 0 & 0 & 0 \\ 0 & 0 & 0 & 0 & -\mu & 0 & 1 & 0 \\ 0 & 0 & 0 & 0 & 0 & 1 & 0 & \mu \end{pmatrix} \quad (\text{D.29})$$

Now, to solve this system we proceed as follows: Choose a Matrix $K_B = (\vec{k}_1 \dots \vec{k}_4)$ where k_i span the Kernel of B. Now all allowed IR boundary configurations can be expressed as

$$\vec{F}(e^{Rk\pi}/k) = K_B\vec{a}, \quad \vec{a} \in \mathbb{R}^4 \quad (\text{D.30})$$

The corresponding UV boundary configurations are given by

$$\vec{F}(1/k) = T(m)K_B\vec{a} \quad (\text{D.31})$$

Those in turn have to satisfy

$$AT(m)K_B\vec{a} = 0 \quad (\text{D.32})$$

So, finally, a Kaluza-Klein mode of mass \tilde{m} exists iff

$$\det(AT(\tilde{m})K_B) = 0 \quad (\text{D.33})$$

and the corresponding mode(s) are uniquely determined by the initial conditions

$$\vec{F}_0(1/k) \in T(\tilde{m})K_B \ker(AT(\tilde{m})K_B) \quad (\text{D.34})$$

For $M = 0$, we will always have

$$\dim \ker(AT(\tilde{m})K_B) = 2$$

with the solutions corresponding to the two Majorana spinors which are equivalent to the Dirac fermion. Even if the degeneracy is lifted by M , this is the answer to the question where the second half of the states are in the Majorana case. Now, let us discuss the Kaluza-Klein expansion and orthonormality conditions for these modes. The Dirac mass relates pairs of fields χ_L and χ_R as well as ψ_L and ψ_R by the resulting boundary conditions and we have to choose $\chi_L^n(x) = \chi_R^n(x) \equiv \chi^n(x)$ and $\psi_L^n(x) = \psi_R^n(x) \equiv \psi^n(x)$ in order to satisfy them. We say that the corresponding pairs of 5D fields are part of the same Kaluza-Klein towers, and we are left with a tower of 4D Dirac fermions $\Psi^n(x) = (\chi^n, \bar{\psi}^n)$. Like in the gauge sector, the apparent loss of states is compensated by a Kaluza-Klein tower which is twice as dense. Since we want the 4D fields to have canonical normalization, we use a combined scalar product

$$\langle \chi^n, \chi^m \rangle \propto \int dz z^{-4} (\chi_L^n \chi_L^m + \chi_R^n \chi_R^m) \quad (\text{D.35})$$

with respect to which the KK solutions are indeed mutually orthogonal. As an aside, there is a nice consistency check analogous to the one for bosons:

$$\langle \chi^n, \chi^m \rangle = \langle \psi^n, \psi^m \rangle \propto N_n \delta^{mn} \quad (\text{D.36})$$

which is violated if the solutions are not compatible with the the variation of the boundary action, for example if there happen to be large numerical errors in m_n or the coefficients. It is again modified when brane kinetic terms are present, and if, as in the higgsless models, brane kinetic terms for ψ_R are introduced, it is simplest to use $\langle \chi, \chi \rangle$ as the scalar product because it is already the correct one without having to include further corrections from the boundary.

All this changes now when the Majorana mass term is introduced. It generates boundary conditions which relate χ and ψ , and suddenly, we have to choose $\chi_L^n(x) = \chi_R^n(x) = \psi_L^n(x) = \psi_R^n(x) \equiv \chi^n(x)$ in order to satisfy them. Now it looks as though we had again lost half of our degrees of freedom, since in 4D all we have are Majorana spinors $\Psi^n = (\chi^n, \bar{\chi}^n)$! For the reasons outlined above this is not

the case, since we have two solutions in each Kaluza-Klein level corresponding to the two sign choices. As we would hope, they are even orthogonal with respect to each other and to the other Kaluza-Klein levels, but only when we adopt the extended scalar product resulting naturally from the Kaluza-Klein reduced Lagrangian,

$$\langle \chi^n, \chi^m \rangle \propto \int dz z^{-4} (\chi_L^n \chi_L^m + \chi_R^n \chi_R^m + \psi_L^n \psi_L^m + \psi_R^n \psi_R^m) \quad (\text{D.37})$$

The example given in this section reproduces a Seesaw-like effect, with the $\tilde{\partial}f_i = mg_i$ solution giving a light Majorana neutrino and the $\tilde{\partial}f_i = -mg_i$ solution giving us the heavy Majorana neutrino which is pushed out of the spectrum as $m_{\nu 0} \rightarrow 0$. The Kaluza-Klein neutrino modes couple weakly to the UV brane and are therefore *pseudo-Dirac* in this scenario with a tiny mass shift $\Delta m^2 \ll m^2$ between the mass eigenstates. In the $m_{\nu 0} \rightarrow 0$ limit, we obtain for the light neutrino

$$f_R^0 = g_R^0 = g_L^0 = 0 \quad f_L^0 \propto z^{-c_L - 1/2} \quad (\text{D.38})$$

with the only nonvanishing wave function f_L^0 being identical to the $SU(2)_L$ transforming Weyl zero mode in the $\mu = M = 0$ case. Thus the resulting almost massless neutrino only contains a lefthanded component coupling to $SU(2)_L$.

Appendix E

Implementation of the Model

E.1 Fortran/Mathematica

We have implemented the entire model in a Fortran program which calculates all tree level masses and all desired coupling constants using only free parameters as inputs. The 16 input parameters are

Physical Parameters		#
Quark Masses	$m_u, m_d, m_c, m_s, m_t, m_b$	6
Lepton Masses	$m_{\nu e}, m_e, m_{\nu \mu}, m_\mu, m_{\nu \tau}, m_\tau$	6
Electroweak Masses	m_W, m_Z	2
finestructure constant	α	1
strong coupling	α_s	1

These are the free parameters which we introduce at this point

Free 5D parameters		#
RS curvature	k	1
Fermion bulk masses	$c_L(q1) \dots c_L(q3), c_L(l1) \dots c_L(l3)$	6
$SU(2)_L$ brane kinetic term	κ	1

There are more which we have not included in this implementation, such as brane kinetic terms for the other brane gauge groups and for the heavy fermion of each doublet. The 16 derived quantities are

Derived 5D Parameters		#
Radius	R	1
5D couplings	$g_{ew}, \tilde{g}_{ew}, g_s$	3
Fermion IR brane mass	$\mu(q1) \dots \mu(q3), \mu(l1) \dots \mu(l3)$	6
Fermion UV brane term	$\rho(q1) \dots \rho(q3), M(l1) \dots M(l3)$	6

The masses are calculated using a kind of shooting method in which all but one boundary condition are solved analytically, while the last boundary condition is

scanned as a function of the eigenvalue m . The roots of this function give us the mode masses¹. In order to get analytic expressions for the mass scan, the Kaluza-Klein wave function coefficients and the necessary dependent input parameters for a given set of particle masses, fermion bulk masses and gauge boson boundary terms, we let some Mathematica scripts generate the corresponding Fortran code which is then pasted to the appropriate places in the Fortran module using *#include*. The Bessel functions and integration routines are provided by the FGSL package. As an example, the analytic expressions for the gluino and neutralino towers are generated by the following code:

```
(* CreateAnalytics.m *)

myform = {BesselJ[a_, b_] -> jn[a, b], BesselY[a_, b_] -> yn[a, b],
          m -> mass, r1 -> "m_r1", r2 -> "m_r2", 0 -> "0d0",
          1 -> "1d0", 2 -> "2d0", 3 -> "3d0", 4 -> "4d0"};

Print["1b. the Gluino"];
f[z_] = z BesselJ[1, m z] + z par*BesselY[1, m z];
sol1 = Solve[(f[r1] == 0) // FullSimplify, par][[1]];
path=(prepath <> "analytics/gluino_prefactor_y1.analytic.pre");
Put[FortranForm[par /. sol1 //. myform], path];
action=f'[r2]/m/.sol1//FullSimplify;
path=(prepath <> "analytics/gluino_action.analytic.pre");
Put[FortranForm[action //. myform], path];
```

Here, the generic Kaluza-Klein wave function for the “lefthanded” Gluino is defined. We then solve for the prefactor of Y_1 using the UV (Dirichlet) boundary condition. The result is written to file for use in the Fortran module which calculates normalizations and coupling constants. The solution is substituted into the IR (Neumann) boundary condition which contains only m as a remaining free parameter and is also written to file for use in the module which determines the mass spectrum. In this simple case it looks like this:

```
m_r2*(jn(0d0, m_r2*mass) - &
      (jn(1d0, m_r1*mass)*yn(0d0, m_r2*mass))/yn(1d0, m_r1*mass))&
+0 !end of analytic
```

The case of the neutralino is a little more complicated because three 5D fields are involved, but the principle is the same.

```
Print["6. the Neutralino"];
zl[z_] = al z BesselJ[1, m z] + bl z BesselY[1, m z];
zr[z_] = ar z BesselJ[1, m z] + br z BesselY[1, m z];
zx[z_] = z BesselJ[1, m z] + bx z BesselY[1, m z];
sol1 = Solve[zx'[r2] == 0, bx][[1]] // FullSimplify;
path=(prepath <> "analytics/neux_prefactor_y.analytic.pre");
Put[FortranForm[bx /. sol1 //. myform], path];
sol2 = Solve[{zx[r1] - gneu zr[r1] == 0, zx'[r1] + 1/gneu zr'[r1] == 0}
            // sol1 // FullSimplify, {ar, br}][[1]] // FullSimplify;
path=(prepath <> "analytics/neur_prefactor_j.analytic.pre");
Put[FortranForm[SetPrecision[ar //. Join[sol1, sol2] //. myform,
                                   \[Infinity]]], path];
path=(prepath <> "analytics/neur_prefactor_y.analytic.pre");
Put[FortranForm[SetPrecision[br //. Join[sol1, sol2] //. myform,
                                   \[Infinity]]], path];
sol3 = Solve[{zl[r2] == zr[r2], zl'[r2] == -zr'[r2]} // Join[sol1, sol2]
```

¹This is similar to using the poles of the Holographic action, but simpler if boundary conditions do not mix more than two fields at once.

```

// FullSimplify, {a1, b1}][[1]] // FullSimplify;
path=(prepath <> "analytics/neul_prefactor_j.analytic.pre");
Put[FortranForm[SetPrecision[a1 // Join[sol3] // myform,
\[\Infinity]]], path];
path=(prepath <> "analytics/neul_prefactor_y.analytic.pre");
Put[FortranForm[SetPrecision[b1 // Join[sol3] // myform,
\[\Infinity]]], path];
rho=.;
cond = z1[r1] // sol3 // Together;
pcond = Numerator[cond] // FullSimplify;
path=(prepath <> "analytics/neu_action.analytic.pre");
Put[FortranForm[pcond // myform], path];

```

Note that we have $N - 1$ coefficients for N fields because we fix the normalization to an arbitrary value. Using this code, the gluino mass tower and canonical normalization constants are determined,

```

call rootify(m_bndaction, PART_GLUINO, 0, 10d0, maxmass, 1d-6, 1000, masslist)
call m_setparameters(PART_GLUINO, 0, masslist)
call m_normalizations(PART_GLUINO, 0)

```

All effective n point coupling constants (including normalization conditions in the case of one field) can be written in the following form

$$\langle \phi_1 \dots \phi_n \rangle = \int_{r1}^{r2} dz k^\delta z^\gamma (a_1 J_{\alpha_1}(mz) + b_1 Y_{\alpha_1}(mz)) \times \dots \times (a_n J_{\alpha_n}(mz) + b_n Y_{\alpha_n}(mz)) \quad (\text{E.1})$$

where $r1 = 1/k$, $r2 = e^{Rk\pi}/k$ and z is the conformal coordinate. This is implemented as (for the three point coupling)

```

m_wavefunction=m_prefactorj(which,mode)*jn(m_besselkindj(which,mode)+&
modifier,m_mass(which,mode)*x)+&
m_prefactory(which,mode)*yn(m_besselkindy(which,mode)+&
modifier,m_mass(which,mode)*x)
[...]
case(3)
multipoint=x**cmd_int_zweight * &
m_wavefunction(x,cmd_int_whichs(1),cmd_int_modes(1))*&
m_wavefunction(x,cmd_int_whichs(2),cmd_int_modes(2))*&
m_wavefunction(x,cmd_int_whichs(3),cmd_int_modes(3))

```

For normalizations we exploit the relation (D.16). This is done by setting $modifier = \pm 1$.

E.2 O'Mega/WHIZARD

E.2.1 O'Mega

The immediate implementation into O'Mega consists first of all of the O'Caml model and interface files *models7.ml*, *models7.mli* which contain the main functor *HLCDM'* ("HiggsLess Cold Dark Matter") and several auxiliary and option modules which are used to implement different model varieties. For each model variety there is an O'Caml file *f90_*_Col.ml* which tells O'Mega how the different modules are to be combined. The module definitions in the model files look like this:

```

(* models7.mli *)
module type HLCDM_options =
sig
val extended3 : bool

```



```

    val extended4 : bool
    val decays3 : bool
    val cdm3 : bool
    val cdm4 : bool
end

module HLCDM_Full : HLCDM_options
module HLCDM_Cdm : HLCDM_options
module HLCDM_Dec : HLCDM_options

module HLCDM_Full_export : Model.MyT
module HLCDM_Cdm_export : Model.MyT
module HLCDM_Dec_export : Model.MyT

module HLCDM_color : functor (Module_options : HLCDM_options) ->
    functor (F : Colorize.Flows) -> Model.T

(* models7.ml *)
module type HLCDM_options =
  sig
    val extended3 : bool
    val extended4 : bool
    val decays3 : bool
    val cdm3 : bool
    val cdm4 : bool
  end

module HLCDM_Full : HLCDM_options =
  struct
    let extended3 = true
    let extended4 = true
    let decays3 = true
    let cdm3 = true
    let cdm4 = true
  end

module HLCDM_Cdm : HLCDM_options =
  struct
    let extended3 = false
    let extended4 = false
    let decays3 = true
    let cdm3 = true
    let cdm4 = true
  end

module HLCDM_Dec : HLCDM_options =
  struct
    let extended3 = false
    let extended4 = false
    let decays3 = true
    let cdm3 = false
    let cdm4 = false
  end

module HLCDM' (Module_options : HLCDM_options) =
  struct

    <The Model Definition>

  end

module HLCDM_Full_export = (HLCDM' (HLCDM_Full))
module HLCDM_Cdm_export = (HLCDM' (HLCDM_Cdm))
module HLCDM_Dec_export = (HLCDM' (HLCDM_Dec))

```

```
module HLCDM_color (Options: HLCDM_options) (F: Colorize.Flows) =
  Colorize.It (F) (HLCDM' (Options))
```

The complete model including all resonances below 2500 GeV contains over 4000 vertices (without the four scalar vertices), which is a little too much for either O'Mega or WHIZARD to function efficiently. We have therefore introduced the module *HLCDM_Cdm* which contains a restricted set of particles and vertices necessary for neutralino and chargino production at the LHC without the factorizable SM backgrounds, and an even smaller set of interactions *HLCDM_Dec* necessary to integrate various decay widths. The functor *HLCDM_color* applies a model definition to the O'Mega Colorizer functor which implements the $SU(3)$ color flows. Whizard expects a model file **.mdl* defining particles, masses, widths and vertices which are used for phase space generation. The modules **_export* are of a module type derived from Model.T which provides additional information for the automatic generation of these WHIZARD model files.

```
(* model.mli *)
[... ]
module type MyT =
  sig
    include T
    val flavor_to_index: flavor -> int
    val flavor_of_index: int -> flavor
    val index_posneg: flavor -> int
    val index_weight: flavor -> int
  end
```

The files *f90-*_Col.ml* contain the following (here for the *HLCDM_Cdm* model)

```
module O = Omega.Make (Fusion.Mixed23_Majorana) (Targets.Fortran_Majorana)
  ( Models7.HLCDM_color (Models7.HLCDM_Cdm)
    ( struct let max_num = Config.ncf_max end ) )
```

Here it is defined that the final O'Mega module is obtained by giving *Omega.Make* our *HLCDM_color* functor which, as parameters, gets one of the modules containing the options corresponding to the desired model variety (in this case *HLCDM_Cdm*) and a module defining the maximal number of color flows.

The vertex definitions contain all relevant permutations of Kaluza-Klein states, where we exclude those which obviously vanish due to orthogonality, for example for the gluon squark interaction,

```
let perm_glu_sq=
  let perm_glu_sq_pre1 kk1 = (Kal0, kk1, kk1)
  in let perm_glu_sq_pre2 kk2 kk3 = (Kal1, kk2, kk3)
  in (loop_kk ([perm_glu_sq_pre1]))@(loop_kk (loop_kk ([perm_glu_sq_pre2])))

[... ]

let vertex_gluonKK_2sq =
let vertex_gluonKK_2sq_pre gen iso sf (kk1, kk2, kk3)=
  [( Gauge_Boson (GluonKK (kk1)),
    Scalar (Squark (Neg, sf, gen, iso, kk2)),
    Scalar (Squark (Pos, sf, gen, iso, kk3))),
    Vector_Scalar_Scalar (1),
    G_gluonKK_2sq (gen, iso, sf, kk1, kk2, kk3)]
in List.flatten (revmap2 (loop_sf (loop_iso (loop_gen
  [vertex_gluonKK_2sq_pre]))) perm_glu_sq)
```

E.2.2 WHIZARD

The WHIZARD model files themselves are generated by a short O'Caml script *HLCDM_automdl.ml* which reads the *vertices()* and *external_flavors()* lists and writes a valid model file template for each of the model varieties. The auxiliary function *index_weight* helps to sort the vertices by giving an estimate of the particles' masses.

```
(* HLCDM_automdl.ml *)

#load "models7.cmo"
module Writelt= struct
open Models7.#MODULENAME

let color_from_flavor = function x -> (match color(x) with
| Color.SUN 3 -> "color 3"^^"\n "
| Color.SUN (-3) -> "color 3"^^"\n "
| Color.AdjSUN 3 -> "color 8"^^"\n "
| _ -> "")

let spin_from_flavor = function x -> (match lorentz(x) with
| Coupling.Spinor -> "spin 1/2"^^"\n "
| Coupling.ConjSpinor -> "spin 1/2"^^"\n "
| Coupling.Vector -> "spin 1"^^"\n "
| Coupling.Massive_Vector -> "spin 1"^^"\n "
| Coupling.Majorana -> "spin 1/2"^^"\n "
| _ -> "spin 0"^^"\n ")

let ifgauge_from_flavor = function x -> (match lorentz(x) with
| Coupling.Vector -> "gauge"
| Coupling.Massive_Vector -> "gauge"
| _ -> "")
```

With those definitions, we can write a function which composes the particle descriptions including the name, mass and width variables, spin and color representation from the O'Mega flavor list,

```
let particle_from_flavor = function x -> (match index_posneg(x) with
| 1 -> ("\n\nparticle "^^"PART"^^string_of_int(flavor_to_index x)^
" "^^string_of_int(pdg x)^" "^^ifgauge_from_flavor(x)^^"\n "
^^spin_from_flavor(x)
^^color_from_flavor(x)
^^name "^^flavor_to_string(x)^^"\n "
^^anti_omega:"^^flavor_to_string(conjugate(x))^^"\n "
^^mass "^^mass"^(string_of_int(flavor_to_index x))^
", width width"^(string_of_int(flavor_to_index x))

| 0 -> ("\n\nparticle "^^"PART"^^string_of_int(flavor_to_index x)^
" "^^string_of_int(pdg x)^" "^^ifgauge_from_flavor(x)^^"\n "
^^spin_from_flavor(x)
^^color_from_flavor(x)
^^name "^^flavor_to_string(x)^^"\n "
^^mass "^^mass"^(string_of_int(flavor_to_index x))^
", width width"^(string_of_int(flavor_to_index x))

| -1 -> ""
| _ -> "hlcdm automdl: ERROR: index_posneg is not 10-1")
```

The functions which follow compose the lists of mass and width parameters corresponding to these particles. Since the numerical values are not yet known, we insert patterns $\#M(i)$ and $\#W(i)$.

```
let massparameter_from_flavor= function x -> (match index_posneg(x) with
```

```

| -1 -> ""
| - -> ("\nparameter " ^ "mass" ^ (string_of_int (flavor_to_index x))
^" #M(" ^ string_of_int (flavor_to_index x) ^")" ^" # particle name " ^
(flavor_to_string x))

let widthparameter_from_flavor = function x -> (match index_posneg(x) with
| -1 -> ""
| - -> ("\nparameter " ^ "width" ^ (string_of_int (flavor_to_index x))
^" 0#W(" ^ string_of_int (flavor_to_index x) ^")" ^" # particle name " ^
(flavor_to_string x))

```

The following functions generate the vertex lists and sort them according to the information given by *index_weight*,

```

let kksort = function liste -> List.sort (fun (x,-) (y,-) -> x - y) (liste)

let threeweight = function (a,b,c) -> index_weight(a)+index_weight(b)
+index_weight(c)
let fourweight = function (a,b,c,d) -> index_weight(a)+index_weight(b)
+index_weight(c)+index_weight(d)

let exverts3_pre = let filtern = function
| ((a,b,c),-,x) -> (threeweight(a,b,c)," vertex " ^ flavor_to_string(a) ^
" " ^ flavor_to_string(b) ^" " ^ flavor_to_string(c) ^
" # " ^ constant_symbol(x) ^ "\n")
in List.map filtern (match (vertices()) with (x,-,-) -> x)

let exverts4_pre = let filtern = function
| ((a,b,c,d),-,x) ->
(fourweight(a,b,c,d)," vertex " ^ flavor_to_string(a) ^
" " ^ flavor_to_string(b) ^" " ^ flavor_to_string(c) ^" " ^
flavor_to_string(d) ^" # " ^ constant_symbol(x) ^ "\n")
in List.map filtern (match (vertices()) with (-,x,-) -> x)

```

Now we call them one by one,

```

let massparam = let schreiben = function x ->
print_string (massparameter_from_flavor (x))
in let trennen = function (-,x) -> List.map schreiben x
in List.map trennen (external_flavors())

let widhparam = let schreiben = function x ->
print_string (widthparameter_from_flavor (x))
in let trennen = function (-,x) -> List.map schreiben x
in List.map trennen (external_flavors())

let flavs = let schreiben = function x ->
print_string (particle_from_flavor (x))
in let trennen = function (-,x) -> List.map schreiben x
in List.map trennen (external_flavors())

let exverts3 = let schreiben = function (wgt,x) ->
print_string (x)
in List.map schreiben (kksort(exverts3_pre))

let exverts4 = let schreiben = function (wgt,x) ->
print_string (x)
in List.map schreiben (kksort(exverts4_pre))
end

```

The output of this code looks like this,

```

#
# This file was created automatically using HLCDM_automdl.ml
#

```

```
#####
# Kinematic Parameters
parameter mass200 #M(200) # particle name nue_P_K00F
[...]
parameter width200 0#W(200) # particle name nue_P_K00F
[...]
#####
# Particle Content
particle PART200 12
  spin 1/2
  name nue_P_K00F
  anti omega:nue_M_K00F
  mass mass200, width width200
[...]
#####
# Three Point Vertices
vertex g_0_K00F g_0_K00F g_0_K00F #coup001_3glu(1)
[...]
#####
# Four Point Vertices
vertex g_0_K00F g_0_K00F SFL_u_M_K00F SFL_u_P_K00F
#coup021_2glu_2sq(1,1,1,1)
[...]
```

However, the O'Camel model file does not know the exact particle masses and widths. They are therefore read from file and inserted into the model file template by a Perl script *HLCDM_automdl.pl* using

$$s/\#M\(\$search2\)/\$value/g$$

$$s/0\#W\(\d{1,}\)/\$widthvalarray[$i]/g$$

The files containing the masses are written by the Fortran code discussed above, while the file containing the widths has to be provided by the user.

O'Mega generates Fortran code containing arrays for masses, widths and coupling constants. For each model variety, we have to provide a Fortran file *parameters.HLCDM_*.omega.f90* which contains the necessary declarations and a subroutine to read the data into the arrays from file.

E.3 FeynArts/FormCalc

The implementation into FeynArts [60] is not intended to be complete, but includes only the necessary interactions and particles to calculate the cross sections relevant for neutralino annihilation. The Following code was piggy-backed onto the existing MSSM implementation *MSSM.mod*. First the definition of fields,

```
M$ClassesDescription = {
[...]
(* Neutralinos *)
F[13] = {
  SelfConjugate -> True,
  Indices -> {},
  Mass -> MNeuA,
  PropagatorLabel -> ComposedChar["\\Lambda", "a", ""],
  PropagatorType -> Straight,
  PropagatorArrow -> None },
F[14] = {
  SelfConjugate -> True,
```

```

Indices -> {},
Mass -> MNeuB,
PropagatorLabel -> ComposedChar["\\Lambda", "b", ""],
PropagatorType -> Straight,
PropagatorArrow -> None },

(* Charginos *)
F[15] == {
  SelfConjugate -> False,
  Indices -> {},
  Mass -> MChA,
  PropagatorLabel -> ComposedChar["\\chi", "a", ""],
  PropagatorType -> Straight,
  PropagatorArrow -> Forward },
F[16] == {
  SelfConjugate -> False,
  Indices -> {},
  Mass -> MChB,
  PropagatorLabel -> ComposedChar["\\chi", "b", ""],
  PropagatorType -> Straight,
  PropagatorArrow -> Forward },

(* sneutrinos: Q = 0 *)
S[15] == {
  SelfConjugate -> False,
  Indices -> {Index[Sfermion], Index[Generation], Index[KK]},
  PropagatorLabel -> ComposedChar["\\nu", {Index[KK], Index[Sfermion]},
    Index[Generation], "\\tilde"],
  PropagatorType -> ScalarDash,
  PropagatorArrow -> Forward },

(* sleptons: Q = -1 *)
S[16] == {
  SelfConjugate -> False,
  Indices -> {Index[Sfermion], Index[Generation], Index[KK]},
  PropagatorLabel ->
    ComposedChar["e", Index[Generation], Index[Sfermion], "\\tilde"],
  PropagatorType -> ScalarDash,
  PropagatorArrow -> Forward },

(* squarks (u): Q = +2/3 *)
S[17] == {
  SelfConjugate -> False,
  Indices ->
    {Index[Sfermion], Index[Generation], Index[KK], Index[Colour]},
  PropagatorLabel ->
    ComposedChar["u", Index[Generation], Index[Sfermion], "\\tilde"],
  PropagatorType -> ScalarDash,
  PropagatorArrow -> Forward },

(* squarks (d): Q = -1/3 *)
S[18] == {
  SelfConjugate -> False,
  Indices ->
    {Index[Sfermion], Index[Generation], Index[KK], Index[Colour]},
  PropagatorLabel ->
    ComposedChar["d", Index[Generation], Index[Sfermion], "\\tilde"],
  PropagatorType -> ScalarDash,
  PropagatorArrow -> Forward }, [...] }

TheMass[ S[typ:15 | 16 | 17 | 18, {sf_, gen_, kk_, ___}] ] :=
MSf[sf, typ - 14, gen, kk]

```

```

TheLabel[ S[15, {sf_, 1, kk_}] ] :=
ComposedChar["\nu", "e", {IndexStyle[sf], IndexStyle[kk]}, "\tilde"];
TheLabel[ S[15, {sf_, 2, kk_}] ] :=
ComposedChar["\nu", "\mu", {IndexStyle[sf], IndexStyle[kk]}, "\tilde"];
TheLabel[ S[15, {sf_, 3, kk_}] ] :=
ComposedChar["\nu", "\tau", {IndexStyle[sf], IndexStyle[kk]}, "\tilde"];
TheLabel[ S[16, {sf_, 1, kk_}] ] :=
ComposedChar["e", Null, {IndexStyle[sf], IndexStyle[kk]}, "\tilde"];
TheLabel[ S[16, {sf_, 2, kk_}] ] :=
ComposedChar["\mu", Null, {IndexStyle[sf], IndexStyle[kk]}, "\tilde"];
TheLabel[ S[16, {sf_, 3, kk_}] ] :=
ComposedChar["\tau", Null, {IndexStyle[sf], IndexStyle[kk]}, "\tilde"];
TheLabel[ S[17, {sf_, 1, kk_, ___}] ] :=
ComposedChar["u", Null, {IndexStyle[sf], IndexStyle[kk]}, "\tilde"];
TheLabel[ S[17, {sf_, 2, kk_, ___}] ] :=
ComposedChar["c", Null, {IndexStyle[sf], IndexStyle[kk]}, "\tilde"];
TheLabel[ S[17, {sf_, 3, kk_, ___}] ] :=
ComposedChar["t", Null, {IndexStyle[sf], IndexStyle[kk]}, "\tilde"];
TheLabel[ S[18, {sf_, 1, kk_, ___}] ] :=
ComposedChar["d", Null, {IndexStyle[sf], IndexStyle[kk]}, "\tilde"];
TheLabel[ S[18, {sf_, 2, kk_, ___}] ] :=
ComposedChar["s", Null, {IndexStyle[sf], IndexStyle[kk]}, "\tilde"];
TheLabel[ S[18, {sf_, 3, kk_, ___}] ] :=
ComposedChar["b", Null, {IndexStyle[sf], IndexStyle[kk]}, "\tilde"]

```

The following code generates the vertices for $q\bar{q}\chi^0$, $W^\pm\chi^\mp\chi^0$, $\chi^\pm\chi^\mp\gamma$ and $\chi^\pm\chi^\mp Z$.

```

sfindices:=If[ifer<3,{s1,j2,k1},{s1,j2,k1,o2}];
findices:=If[ifer<3,{j1},{j1,o1}];
farbdelta:=If[ifer<3,1,IndexDelta[o1,o2]];

For[ifer=1,ifer<5,
  M$CouplingMatrices = Join[M$CouplingMatrices,
  {
    C[F[13], -F[ifer, findices], S[14+ifer, sfindices]] ==
      {{NFSL[ifer, j1, s1, k1, 1]*IndexDelta[j1, j2]*farbdelta},
      {NFSR[ifer, j1, s1, k1, 1]*IndexDelta[j1, j2]*farbdelta}},
    C[F[ifer, findices], F[13], -S[14+ifer, sfindices]] ==
      {{-NFSR[ifer, j1, s1, k1, 1]*IndexDelta[j1, j2]*farbdelta},
      {-NFSL[ifer, j1, s1, k1, 1]*IndexDelta[j1, j2]*farbdelta}},
    C[F[14], -F[ifer, findices], S[14+ifer, sfindices]] ==
      {{-I* NFSLi[ifer, j1, s1, k1, 2]*IndexDelta[j1, j2]*farbdelta},
      {-I* NFSRi[ifer, j1, s1, k1, 2]*IndexDelta[j1, j2]*farbdelta}},
    C[F[ifer, findices], F[14], -S[14+ifer, sfindices]] ==
      {{-I* NFSRi[ifer, j1, s1, k1, 2]*IndexDelta[j1, j2]*farbdelta},
      {-I* NFSLi[ifer, j1, s1, k1, 2]*IndexDelta[j1, j2]*farbdelta}}
  }];
  ifer++;
]

M$CouplingMatrices = Join[M$CouplingMatrices,
  {
    C[-F[15], F[13], -V[3]] ==
      {{ 1/Sqrt[2]*Re[NCWRL11]}, { 1/Sqrt[2]*Re[NCWRL22]}},
    C[F[13], F[15], V[3]] ==
      {{ 1/Sqrt[2]*Re[NCWRL11]}, { 1/Sqrt[2]*Re[NCWRL22]}},
    C[-F[16], F[14], -V[3]] ==
      {{-1/Sqrt[2]*Re[NCWRL22]}, {-1/Sqrt[2]*Re[NCWRL11]}},
    C[F[14], F[16], V[3]] ==
      {{ 1/Sqrt[2]*Re[NCWRL22]}, { 1/Sqrt[2]*Re[NCWRL11]}},
    C[-F[15], F[14], -V[3]] ==
      {{ 1/Sqrt[2]*Re[NCWRL11]}, { 1/Sqrt[2]*Re[NCWRL22]}},
    C[F[14], F[15], V[3]] ==
      {{-1/Sqrt[2]*Re[NCWRL11]}, {-1/Sqrt[2]*Re[NCWRL22]}}
  }

```

```

C[-F[16], F[13], -V[3]] ==
  {{ 1/Sqrt[2]*Re[NCWRL22]}, { 1/Sqrt[2]*Re[NCWRL11]}},
C[F[13], F[16], V[3]] ==
  {{ 1/Sqrt[2]*Re[NCWRL22]}, { 1/Sqrt[2]*Re[NCWRL11]}
  }];

M$CouplingMatrices = Join[M$CouplingMatrices,
  {
  C[-F[15], F[15], V[2]] == {{ I*(CCZ11)}, { I*(CCZ12)}},
  C[-F[16], F[16], V[2]] == {{ I*(CCZ21)}, { I*(CCZ22)}},
  C[-F[15], F[15], V[1]] == {{ I*(CCP11)}, { I*(CCP12)}},
  C[-F[16], F[16], V[1]] == {{ I*(CCP21)}, { I*(CCP22)}
  }];

```

E.4 FORM

The purpose of the FORM program presented in this section is to automatize the reduction of expressions involving Grassmann- and complex valued fields and derivatives carrying spinor-, lorentz and gauge indices to a standard form. In particular, it is suited to evaluate products of superfields to obtain expressions in terms of component fields which are of the form $\theta\theta X$ or $\theta\theta\theta\theta X$. It implements the two component spinor algebra with the conventions of Wess/Bagger [61].

Declarations

These are the necessary definitions for commutative and noncommutative fields, superspace coordinates, Lorentz- and spinor indices, differential operators as well as $\sigma_{\alpha\dot{\alpha}}^n$, $(\overline{\sigma}^m\sigma^n)_{\dot{\alpha}}^{\beta}$ and $\epsilon^{\alpha\beta}$, $\epsilon^{\dot{\alpha}\dot{\beta}}$. The 4D derivative is not treated as an object but is a fourvector valued argument of the object on which it acts.

```

* $Id:$
Off statistics;

AutoDeclare NFunction s; * Spinoren
AutoDeclare NFunction o; * Skalare
AutoDeclare NFunction v; * Vektoren
NFunction [tt];
NFunction [TT];
NFunction [ttTT];
NFunction Sigma;
NFunction SSigma;
NFunction thet;
NFunction foo;
NFunction goo;
NFunction roo;

NFunction y;
NFunction d5;

CFunction Y;
CFunction [tt_];
CFunction [TT_];
CFunction [ttTT_];
CFunction [TAG];
CFunction [DP];
CFunction [UP];

```



```

CFunction ep;
CFunction sigma;
CFunction cigma;
CFunction ssigma;
CFunction CCu;
CFunction CCd;
CFunction sqrt;
CFunction eta;

AutoDeclare Symbols i,k,n;
Symbols a,b,c,d,e,f;
Symbol BOX;
Symbol [BOX];
NFunction [!!DERIVATIVE!!];

set sdel:sD;
set spins:sPhi,sPhi1,...,sPhi20,sPsi,sPsi1,...,sPsi20,
      sChi,sChi1,...,sChi20,sLamb,sLamb1,...,sLamb20;
set scal:sA,oA1,...,oA10,oB,oB1,...,oB10,oC,oC1,...,oC10,
      oD,oD1,...,oD10,oF,oF1,...,oF10;
set vects:vA,vA1,...,vA10,vB,vB1,...,vB10,vG,vG1,...,vG10;
set udot:i1,...,i400,0; * undotted index
set dot:k1,...,k400,0; * dotted index
set lor:n1,...,n400; * Lorentz Index

#do bla=1,10
set udot{'bla'}:i{'bla'+1},...,i80;
set dot{'bla'}:k{'bla'+1},...,k80;
set lor{'bla'}:n{'bla'+1},...,n80;
#define udot{'bla'} "udot{'bla'}[ '~c']"
#define dot{'bla'} "dot{'bla'}[ '~c']"
#define lor{'bla'} "lor{'bla'}[ '~c']"
#define gaug "'a'"
#define gaug2 "'b'"
#enddo

```

Ordering for Spinors

The following procedure brings spinor valued fields and superspace coordinates in a standard order

```

#procedure checkthets
repeat;
  id thet(a?dot,b?dot)*foo?spins(?b)=-foo(?b)*thet(a,b);
  id thet(a?dot,b?dot)*thet(c?udot,d?udot)=-thet(c,d)*thet(a,b);
  id thet(a?dot,b?dot)*foo?scals(?b)=foo(?b)*thet(a,b);
  id thet(a?dot,b?dot)*foo?vects(?b)=foo(?b)*thet(a,b);
endrepeat;
id thet(a?dot,b?dot)*thet(c?dot,d?dot)*thet(e?dot,f?dot)=0;

repeat;
  id thet(a?udot,b?udot)*foo?spins(?b)=-foo(?b)*thet(a,b);
  id thet(a?udot,b?udot)*thet(c?dot,d?dot)=-thet(c,d)*thet(a,b);
  id thet(a?udot,b?udot)*foo?scals(?b)=foo(?b)*thet(a,b);
  id thet(a?udot,b?udot)*foo?vects(?b)=foo(?b)*thet(a,b);
endrepeat;
id thet(a?udot,b?udot)*thet(c?udot,d?udot)*thet(e?udot,f?udot)=0;
#endprocedure

```

Derivatives

The following procedure shifts superspace covariant derivatives D_α , $\overline{D}_{\dot{\alpha}}$ to the right using their Leibniz rule and sets them to zero after they have nothing left to act on. Then it does the same with the extra dimensional derivative ∂_y .

```
#procedure derivatives
#do cnt=100,200,3
repeat;

id sD(0,a?udot)*thet(0,b?udot)=-thet(0,b)*sD(0,a)-ep(0,a,0,b);
id sD(a?udot,0)*thet(b?udot,0)=-thet(b,0)*sD(a,0)+ep(a,0,b,0);

id sD(0,a?udot)*thet(b?udot,0)=-thet(b,0)*sD(0,a)+ep(0,a,b,0);
id sD(a?udot,0)*thet(0,b?udot)=-thet(0,b)*sD(a,0)-ep(a,0,0,b);

id sD(0,a?dot)*thet(0,b?dot)=-thet(0,b)*sD(0,a)+ep(0,a,0,b);
id sD(a?dot,0)*thet(b?dot,0)=-thet(b,0)*sD(a,0)-ep(a,0,b,0);

id sD(0,a?dot)*thet(b?dot,0)=-thet(b,0)*sD(0,a)-ep(0,a,b,0);
id sD(a?dot,0)*thet(0,b?dot)=-thet(0,b)*sD(a,0)+ep(a,0,0,b);

id sD(a?udot,b?udot)*thet(c?dot,d?dot)=-thet(c,d)*sD(a,b);
id sD(a?dot,b?dot)*thet(c?udot,d?udot)=-thet(c,d)*sD(a,b);

endrepeat;

id once sD(a?udot,b?udot)*foo?spins(?c)=
-foo(?c)*sD(a,b)+I_ * sigma(a,b,0,k{ 'cnt ' ,n' cnt ' })*
thet(k{ 'cnt ' ,0}*foo(?c,n' cnt ' );

id once sD(a?dot,b?dot)*foo?spins(?c)=
-foo(?c)*sD(a,b)-I_ * thet(i{ 'cnt ' ,0}*
sigma(0,i{ 'cnt ' ,a,b,n' cnt ' })*foo(?c,n' cnt ' );

id once sD(a?udot,b?udot)*foo?scals(?c)=
foo(?c)*sD(a,b)+I_ * sigma(a,b,0,k{ 'cnt '+1},n{ 'cnt '+1})*
thet(k{ 'cnt '+1},0)*foo(?c,n{ 'cnt '+1});

id once sD(a?dot,b?dot)*foo?scals(?c)=
foo(?c)*sD(a,b)-I_ * thet(i{ 'cnt '+1},0)*
sigma(0,i{ 'cnt '+1},a,b,n{ 'cnt '+1})*foo(?c,n{ 'cnt '+1});

id once sD(a?udot,b?udot)*foo?vects(?c)=
foo(?c)*sD(a,b)+I_ * sigma(a,b,0,k{ 'cnt '+2},n{ 'cnt '+2})*
thet(k{ 'cnt '+2},0)*foo(?c,n{ 'cnt '+2});

id once sD(a?dot,b?dot)*foo?vects(?c)=
foo(?c)*sD(a,b)-I_ * thet(i{ 'cnt '+2},0)*
sigma(0,i{ 'cnt '+2},a,b,n{ 'cnt '+2})*foo(?c,n{ 'cnt '+2});

id once sD(?a)*d5=d5*sD(?a);

#enddo

id sD(?b)=0;

repeat;
id d5*foo?scals(?c)=foo(?c,5)+foo(?c)*d5;
id d5*foo?spins(?c)=foo(?c,5)+foo(?c)*d5;
id d5*foo?vects(?c)=foo(?c,5)+foo(?c)*d5;
id d5*foo?{thet,[TT],[tt],[ttTT]}(?c)=foo(?c)*d5;

id d5*y(a?)=a*y(a-1)+y(a)*d5;
```

```

endrepeat ;

id y(a?)=Y(a);
#call collecty

id d5=0;
#endprocedure

```

The following procedure handles powers of the extra dimensional variable y and square roots.

```

#procedure collecty
repeat ;
id Y(a?)*Y(b?)=Y(a+b);
id Y(0)=1;
endrepeat ;
#endprocedure

#procedure sqrts
repeat ;
id sqrt(a?,b?)*sqrt(a?,c?)=sqrt(a,b+c);
id sqrt(a?,0)=1;
id sqrt(a?,-2)=1/a;
id sqrt(a?,2)=a;
endrepeat ;
#endprocedure

```

Superspace Coordinates

The following procedures perform substitutions of the form $\theta_\alpha\theta_\beta \rightarrow -\frac{1}{2}\theta^2\epsilon_{\alpha\beta}$. They then introduce θ^2 and θ^4 etc.. as commutative objects and delete higher powers of θ^2 and $\bar{\theta}^2$.

```

#procedure idthetas
repeat ;
id thet(a?udot,0)*thet(c?udot,0)=-1/2*[tt_]*ep(a,0,c,0);
id thet(0,b?dot)*thet(0,d?dot)=-1/2*[TT_]*ep(0,b,0,d);

id thet(0,a?udot)*thet(0,c?udot)=1/2*[tt_]*ep(0,a,0,c);
id thet(b?dot,0)*thet(d?dot,0)=1/2*[TT_]*ep(b,0,d,0);

id thet(a?udot,0)*thet(0,b?udot)=+1/2*[tt_]*ep(a,0,0,b);
id thet(0,a?udot)*thet(b?udot,0)=-1/2*[tt_]*ep(0,a,b,0);

id thet(a?dot,0)*thet(0,b?dot)=-1/2*[TT_]*ep(a,0,0,b);
id thet(0,a?dot)*thet(b?dot,0)=1/2*[TT_]*ep(0,a,b,0);

#call clearthet
endrepeat ;
#endprocedure

#procedure thetas
repeat ;
id thet(?i)*foo?spins(?a)=-foo(?a)*thet(?i);
id thet(?i)*foo?scals(?a)=foo(?a)*thet(?i);
id thet(?i)*foo?vects(?a)=foo(?a)*thet(?i);
repeat ;
id thet(c?udot,d?udot)*thet(a?dot,b?dot)=
      -thet(a,b)*thet(c,d);
endrepeat ;
endrepeat ;
repeat ;

```

```

#call idthetas
id once foo?spins(?a)*thet(?i)=-thet(?i)*foo(?a);
#call idthetas
id once foo?scals(?a)*thet(?i)=thet(?i)*foo(?a);
#call idthetas
id once foo?vects(?a)*thet(?i)=thet(?i)*foo(?a);
#call idthetas
id once thet(a?dot,b?dot)*thet(c?udot,d?udot)=
      -thet(c,d)*thet(a,b);
#call idthetas

endrepeat;
#endprocedure

#procedure clearthet

id [tt_] * [TT_] = [ttTT_];
id [TT_] * [tt_] = [ttTT_];

id [TT_] * thet(a?dot,b?dot) = 0;
id [tt_] * thet(a?udot,b?udot) = 0;

id [ttTT_] * thet(?c) = 0;

id [ttTT_] * [tt_] = 0;
id [ttTT_] * [TT_] = 0;

id [tt_] * [tt_] = 0;
id [TT_] * [TT_] = 0;

id [ttTT_] * [ttTT_] = 0;

#endprocedure

```

Renaming, Simplifications and Grouping of Spinors

The following procedures use the standard substitution rules to remove ϵ , $\eta_{\mu\nu}$ and Weyl chains $\sigma^\nu \bar{\sigma}^\mu \dots$ from the expression. They introduce commutative objects for $\xi \sigma^\mu \bar{\eta}$, $\xi \eta$, $\bar{\xi} \eta$ and perform a standard ordering.

```

#procedure contains(arg1,arg2,arg3)
.sort
Local 'arg3'=[TAG]*'arg1';
id [TAG]*'arg2'='arg2';
id [TAG]=0;
#endprocedure;

#procedure ridtheeps
repeat;
id ep(a?,0,b?,0)*ep(0,b?,0,c?)=ep(a,0,0,c);
id ep(a?,0,b?,0)*ep(0,c?,0,b?)=-ep(a,0,0,c);
endrepeat;

repeat;
id ep(a?,0,0,a?)=2;
id ep(0,a?,a?,0)=2;
id sigma(a?,0,?f)*ep(0,e?,0,a?)=sigma(0,e,?f);
id sigma(a?,b?,c?,0,?f)*ep(0,e?,0,c?)=sigma(a,b,0,e,?f);
id foo?(?a,f?,?c)*ep(f?,0,0,e?)=foo(?a,e,?c);
id foo?(?a,f?,?c)*ep(0,f?,e?,0)=foo(?a,e,?c);
id foo?(?a,f?,?c)*ep(e?,0,0,f?)=foo(?a,e,?c);
id foo?(?a,f?,?c)*ep(0,e?,f?,0)=foo(?a,e,?c);

```

```

id foo?(?a,f?,0,?c)*ep(0,e?,0,f?)=foo(?a,0,e,?c);
id foo?(?a,f?,0,?c)*ep(0,f?,0,e?)=-foo(?a,0,e,?c);
id foo?(?a,0,f?,?c)*ep(e?,0,f?,0)=foo(?a,e,0,?c);
id foo?(?a,0,f?,?c)*ep(f?,0,e?,0)=-foo(?a,e,0,?c);
endrepeat;
#endprocedure

```

Now, superfluous metric tensors are absorbed by renaming indices.

```

#procedure ridtheeta
repeat;
id eta(n1?,n2?)*foo?(?a,n1?,?b)=foo(?a,n2,?b);
id eta(n1?,n2?)*foo?(?a,n2?,?b)=foo(?a,n1,?b);
endrepeat;

id foo?scals(?e,n?lor,n?lor,?f)=foo(?e,?f,[BOX]);
id foo?spins(a?,b?,?e,n?lor,n?lor,?f)=foo(a,b,?e,?f,[BOX]);
id foo?vects(a?lor,?e,n?lor,n?lor,?f)=foo(a,?e,?f,[BOX]);
#endprocedure

```

The following lengthy procedure performs operations on the extended sigma matrices. First, mutually contracted matrices are converted to metric tensors using the completeness relation, and extra tensors are removed.

```

#procedure sigmas
repeat;
id sigma(0,a?,0,b?,n1?)*sigma(a?,0,b?,0,n2?)=-2*eta(n1,n2);
id sigma(a?,0,0,b?,n1?)*sigma(0,a?,b?,0,n2?)=2*eta(n1,n2);
endrepeat;
repeat;
id eta(n1?,n1?)=4;
id eta(n1?,n2?)*eta(n2?,n3?)=eta(n1,n3);
id eta(n1?,n2?)*eta(n3?,n2?)=eta(n1,n3);
endrepeat;

```

In the following, pairs of derivatives which are contracted with pairs of sigma matrices in the right fashion, are recast to d'Alembert operators. There are many different constellations in which this can occur.

```

repeat;
id sigma(i1?,0,k1?,0,n1?lor)*sigma(0,i4?,0,k1?,n2?lor)*
foo?spins(a?,b?,?c,n1?,?e,n2?,?f)=-ep(0,i4,i1,0)*foo(a,b,?c,?e,?f,[BOX]);
id sigma(0,i2?,k1?,0,n1?lor)*sigma(i3?,0,0,k1?,n2?lor)*
foo?spins(a?,b?,?c,n1?,?e,n2?,?f)=ep(0,i2,i3,0)*foo(a,b,?c,?e,?f,[BOX]);
id sigma(0,i1?,k1?,0,n1?lor)*sigma(0,i4?,0,k1?,n2?lor)*
foo?spins(a?,b?,?c,n1?,?e,n2?,?f)=-ep(0,i1,0,i4)*foo(a,b,?c,?e,?f,[BOX]);
id sigma(i2?,0,k1?,0,n1?lor)*sigma(i3?,0,0,k1?,n2?lor)*
foo?spins(a?,b?,?c,n1?,?e,n2?,?f)=ep(i2,0,i3,0)*foo(a,b,?c,?e,?f,[BOX]);

id sigma(i1?,0,k1?,0,n1?lor)*sigma(0,i1?,0,k2?,n2?lor)*
foo?spins(a?,b?,?c,n1?,?e,n2?,?f)=-ep(k1,0,0,k2)*foo(a,b,?c,?e,?f,[BOX]);
id sigma(i1?,0,0,k1?,n1?lor)*sigma(0,i1?,k2?,0,n2?lor)*
foo?spins(a?,b?,?c,n1?,?e,n2?,?f)=ep(k2,0,0,k1)*foo(a,b,?c,?e,?f,[BOX]);

id sigma(i1?,0,0,k1?,n1?lor)*sigma(0,i1?,0,k2?,n2?lor)*
foo?spins(a?,b?,?c,n1?,?e,n2?,?f)=-ep(0,k1,0,k2)*foo(a,b,?c,?e,?f,[BOX]);
id sigma(i1?,0,k1?,0,n1?lor)*sigma(0,i1?,k2?,0,n2?lor)*
foo?spins(a?,b?,?c,n1?,?e,n2?,?f)=ep(k1,0,k2,0)*foo(a,b,?c,?e,?f,[BOX]);

```

```

id sigma(i1?,0,k1?,0,n1?lor)*sigma(0,i1?,0,k2?,n2?lor)*
foo?spins(a?,b?,?c,n2?,?e,n1?,?f)=-ep(k1,0,0,k2)*foo(a,b,?c,?e,?f,[BOX]);
id sigma(i1?,0,0,k1?,n1?lor)*sigma(0,i1?,k2?,0,n2?lor)*
foo?spins(a?,b?,?c,n2?,?e,n1?,?f)=ep(k2,0,0,k1)*foo(a,b,?c,?e,?f,[BOX]);

id sigma(0,i1?,k1?,0,n1?lor)*sigma(0,i4?,0,k1?,n2?lor)*
foo?spins(a?,b?,?c,n2?,?e,n1?,?f)=-ep(0,i1,0,i4)*foo(a,b,?c,?e,?f,[BOX]);
id sigma(i2?,0,k1?,0,n1?lor)*sigma(i3?,0,0,k1?,n2?lor)*
foo?spins(a?,b?,?c,n2?,?e,n1?,?f)=ep(i2,0,i3,0)*foo(a,b,?c,?e,?f,[BOX]);

id sigma(i1?,0,k1?,0,n1?lor)*sigma(0,i4?,0,k1?,n2?lor)*
foo?spins(a?,b?,?c,n2?,?e,n1?,?f)=-ep(0,i4,i1,0)*foo(a,b,?c,?e,?f,[BOX]);
id sigma(0,i2?,k1?,0,n1?lor)*sigma(i3?,0,0,k1?,n2?lor)*
foo?spins(a?,b?,?c,n2?,?e,n1?,?f)=ep(0,i2,i3,0)*foo(a,b,?c,?e,?f,[BOX]);

id sigma(i1?,0,0,k1?,n1?lor)*sigma(0,i1?,0,k2?,n2?lor)*
foo?spins(a?,b?,?c,n2?,?e,n1?,?f)=-ep(0,k1,0,k2)*foo(a,b,?c,?e,?f,[BOX]);
id sigma(i1?,0,k1?,0,n1?lor)*sigma(0,i1?,k2?,0,n2?lor)*
foo?spins(a?,b?,?c,n2?,?e,n1?,?f)=ep(k1,0,k2,0)*foo(a,b,?c,?e,?f,[BOX]);
endrepeat;

repeat;
id sigma(i1?,0,k1?,0,n1?lor)*sigma(0,i4?,0,k1?,n2?lor)*
foo?vects(n10?lor,?c,n1?,?e,n2?,?f)=-ep(0,i4,i1,0)*foo(n10,?c,?e,?f,[BOX]);
id sigma(0,i2?,k1?,0,n1?lor)*sigma(i3?,0,0,k1?,n2?lor)*
foo?vects(n10?lor,?c,n1?,?e,n2?,?f)=ep(0,i2,i3,0)*foo(n10,?c,?e,?f,[BOX]);

id sigma(0,i1?,k1?,0,n1?lor)*sigma(0,i4?,0,k1?,n2?lor)*
foo?vects(n10?lor,?c,n1?,?e,n2?,?f)=-ep(0,i1,0,i4)*foo(n10,?c,?e,?f,[BOX]);
id sigma(i2?,0,k1?,0,n1?lor)*sigma(i3?,0,0,k1?,n2?lor)*
foo?vects(n10?lor,?c,n1?,?e,n2?,?f)=ep(i2,0,i3,0)*foo(n10,?c,?e,?f,[BOX]);

id sigma(i1?,0,k1?,0,n1?lor)*sigma(0,i1?,0,k2?,n2?lor)*
foo?vects(n10?lor,?c,n1?,?e,n2?,?f)=-ep(k1,0,0,k2)*foo(n10,?c,?e,?f,[BOX]);
id sigma(i1?,0,0,k1?,n1?lor)*sigma(0,i1?,k2?,0,n2?lor)*
foo?vects(n10?lor,?c,n1?,?e,n2?,?f)=ep(k2,0,0,k1)*foo(n10,?c,?e,?f,[BOX]);

id sigma(i1?,0,0,k1?,n1?lor)*sigma(0,i1?,0,k2?,n2?lor)*
foo?vects(n10?lor,?c,n1?,?e,n2?,?f)=-ep(0,k1,0,k2)*foo(n10,?c,?e,?f,[BOX]);
id sigma(i1?,0,k1?,0,n1?lor)*sigma(0,i1?,k2?,0,n2?lor)*
foo?vects(n10?lor,?c,n1?,?e,n2?,?f)=ep(k1,0,k2,0)*foo(n10,?c,?e,?f,[BOX]);

id sigma(i1?,0,k1?,0,n1?lor)*sigma(0,i1?,0,k2?,n2?lor)*
foo?vects(n10?lor,?c,n2?,?e,n1?,?f)=-ep(k1,0,0,k2)*foo(n10,?c,?e,?f,[BOX]);
id sigma(i1?,0,0,k1?,n1?lor)*sigma(0,i1?,k2?,0,n2?lor)*
foo?vects(n10?lor,?c,n2?,?e,n1?,?f)=ep(k2,0,0,k1)*foo(n10,?c,?e,?f,[BOX]);

id sigma(0,i1?,k1?,0,n1?lor)*sigma(0,i4?,0,k1?,n2?lor)*
foo?vects(n10?lor,?c,n2?,?e,n1?,?f)=-ep(0,i1,0,i4)*foo(n10,?c,?e,?f,[BOX]);
id sigma(i2?,0,k1?,0,n1?lor)*sigma(i3?,0,0,k1?,n2?lor)*
foo?vects(n10?lor,?c,n2?,?e,n1?,?f)=ep(i2,0,i3,0)*foo(n10,?c,?e,?f,[BOX]);

id sigma(i1?,0,k1?,0,n1?lor)*sigma(0,i4?,0,k1?,n2?lor)*
foo?vects(n10?lor,?c,n2?,?e,n1?,?f)=-ep(0,i4,i1,0)*foo(n10,?c,?e,?f,[BOX]);
id sigma(0,i2?,k1?,0,n1?lor)*sigma(i3?,0,0,k1?,n2?lor)*
foo?vects(n10?lor,?c,n2?,?e,n1?,?f)=ep(0,i2,i3,0)*foo(n10,?c,?e,?f,[BOX]);

id sigma(i1?,0,0,k1?,n1?lor)*sigma(0,i1?,0,k2?,n2?lor)*
foo?vects(n10?lor,?c,n2?,?e,n1?,?f)=-ep(0,k1,0,k2)*foo(n10,?c,?e,?f,[BOX]);
id sigma(i1?,0,k1?,0,n1?lor)*sigma(0,i1?,k2?,0,n2?lor)*
foo?vects(n10?lor,?c,n2?,?e,n1?,?f)=ep(k1,0,k2,0)*foo(n10,?c,?e,?f,[BOX]);

```

```

endrepeat ;

repeat ;
id sigma (i1?,0,k1?,0,n1?lor)*sigma(0,i4?,0,k1?,n2?lor)*
foo?scals(?c,n1?,?e,n2?,?f)=-ep(0,i4,i1,0)*foo(?c,?e,?f,[BOX]);
id sigma(0,i2?,k1?,0,n1?lor)*sigma(i3?,0,0,k1?,n2?lor)*
foo?scals(?c,n1?,?e,n2?,?f)=ep(0,i2,i3,0)*foo(?c,?e,?f,[BOX]);

id sigma(0,i1?,k1?,0,n1?lor)*sigma(0,i4?,0,k1?,n2?lor)*
foo?scals(?c,n1?,?e,n2?,?f)=-ep(0,i1,0,i4)*foo(?c,?e,?f,[BOX]);
id sigma(i2?,0,k1?,0,n1?lor)*sigma(i3?,0,0,k1?,n2?lor)*
foo?scals(?c,n1?,?e,n2?,?f)=ep(i2,0,i3,0)*foo(?c,?e,?f,[BOX]);

id sigma(i1?,0,k1?,0,n1?lor)*sigma(0,i1?,0,k2?,n2?lor)*
foo?scals(?c,n1?,?e,n2?,?f)=-ep(k1,0,0,k2)*foo(?c,?e,?f,[BOX]);
id sigma(i1?,0,0,k1?,n1?lor)*sigma(0,i1?,k2?,0,n2?lor)*
foo?scals(?c,n1?,?e,n2?,?f)=ep(k2,0,0,k1)*foo(?c,?e,?f,[BOX]);

id sigma(i1?,0,0,k1?,n1?lor)*sigma(0,i1?,0,k2?,n2?lor)*
foo?scals(?c,n1?,?e,n2?,?f)=-ep(0,k1,0,k2)*foo(?c,?e,?f,[BOX]);
id sigma(i1?,0,k1?,0,n1?lor)*sigma(0,i1?,k2?,0,n2?lor)*
foo?scals(?c,n1?,?e,n2?,?f)=ep(k1,0,k2,0)*foo(?c,?e,?f,[BOX]);

id sigma(i1?,0,k1?,0,n1?lor)*sigma(0,i1?,0,k2?,n2?lor)*
foo?scals(?c,n2?,?e,n1?,?f)=-ep(k1,0,0,k2)*foo(?c,?e,?f,[BOX]);
id sigma(i1?,0,0,k1?,n1?lor)*sigma(0,i1?,k2?,0,n2?lor)*
foo?scals(?c,n2?,?e,n1?,?f)=ep(k2,0,0,k1)*foo(?c,?e,?f,[BOX]);

id sigma(0,i1?,k1?,0,n1?lor)*sigma(0,i4?,0,k1?,n2?lor)*
foo?scals(?c,n2?,?e,n1?,?f)=-ep(0,i1,0,i4)*foo(?c,?e,?f,[BOX]);
id sigma(i2?,0,k1?,0,n1?lor)*sigma(i3?,0,0,k1?,n2?lor)*
foo?scals(?c,n2?,?e,n1?,?f)=ep(i2,0,i3,0)*foo(?c,?e,?f,[BOX]);

id sigma(i1?,0,k1?,0,n1?lor)*sigma(0,i4?,0,k1?,n2?lor)*
foo?scals(?c,n2?,?e,n1?,?f)=-ep(0,i4,i1,0)*foo(?c,?e,?f,[BOX]);
id sigma(0,i2?,k1?,0,n1?lor)*sigma(i3?,0,0,k1?,n2?lor)*
foo?scals(?c,n2?,?e,n1?,?f)=ep(0,i2,i3,0)*foo(?c,?e,?f,[BOX]);

id sigma(i1?,0,0,k1?,n1?lor)*sigma(0,i1?,0,k2?,n2?lor)*
foo?scals(?c,n2?,?e,n1?,?f)=-ep(0,k1,0,k2)*foo(?c,?e,?f,[BOX]);
id sigma(i1?,0,k1?,0,n1?lor)*sigma(0,i1?,k2?,0,n2?lor)*
foo?scals(?c,n2?,?e,n1?,?f)=ep(k1,0,k2,0)*foo(?c,?e,?f,[BOX]);
endrepeat ;

repeat ;
id ep(a?,0,0,b?)=ep(0,b,a,0);
endrepeat ;

```

A special name is introduced for chains of two sigma matrices.

```

id sigma(i1?udot,i2?udot,0,k1?dot,n1?)*
sigma(i3?udot,i4?udot,k1?dot,0,n2?)=ssigma(i1,i2,i3,i4,n1,n2);
id sigma(i1?udot,0,k1?dot,k2?dot,n1?)*
sigma(0,i1?udot,k3?dot,k4?dot,n2?)=ssigma(k1,k2,k3,k4,n1,n2);

#endprocedure

```

Compact names are introduced for sigma matrices which are contracted with a spinor.

```

#procedure contractSigma

```

```

id Sigma(f?,0,0,sbar2?(?c),?a)*foo?spins(0,f?,?b)=
  cigma(0,foo(?b),0,sbar2(?c),?a);
id Sigma(0,f?,0,sbar2?(?c),?a)*foo?spins(f?,0,?b)=
  -cigma(0,foo(?b),0,sbar2(?c),?a);

id Sigma(0,sbar2?(?c),f?,0,?a)*foo?spins(0,f?,?b)=
  -cigma(0,sbar2(?c),0,foo(?b),?a);
id Sigma(0,sbar2?(?c),0,f?,?a)*foo?spins(f?,0,?b)=
  cigma(0,sbar2(?c),0,foo(?b),?a);

id Sigma(f?,0,0,sbar2?(?c),?a)*foo?{thet}(0,f?,?b)=
  cigma(0,foo(?b),0,sbar2(?c),?a);
id Sigma(0,f?,0,sbar2?(?c),?a)*foo?{thet}(f?,0,?b)=
  -cigma(0,foo(?b),0,sbar2(?c),?a);

id Sigma(0,sbar2?(?c),f?,0,?a)*foo?{thet}(0,f?,?b)=
  -cigma(0,sbar2(?c),0,foo(?b),?a);
id Sigma(0,sbar2?(?c),0,f?,?a)*foo?{thet}(f?,0,?b)=
  cigma(0,sbar2(?c),0,foo(?b),?a);

#endprocedure

#procedure contractSSigma

id SSigma(f?,0,0,sbar2?(?c),?a)*foo?spins(0,f?udot,?b)=
  CCu(0,foo(?b),0,sbar2(?c),?a);
id SSigma(0,f?,0,sbar2?(?c),?a)*foo?spins(f?udot,0,?b)=
  -CCu(0,foo(?b),0,sbar2(?c),?a);
id SSigma(0,sbar2?(?c),f?,0,?a)*foo?spins(0,f?udot,?b)=
  -CCu(0,sbar2(?c),0,foo(?b),?a);
id SSigma(0,sbar2?(?c),0,f?,?a)*foo?spins(f?udot,0,?b)=
  CCu(0,sbar2(?c),0,foo(?b),?a);

id SSigma(f?,0,0,sbar2?(?c),?a)*foo?{thet}(0,f?udot,?b)=
  CCu(0,foo(?b),0,sbar2(?c),?a);
id SSigma(0,f?,0,sbar2?(?c),?a)*foo?{thet}(f?udot,0,?b)=
  -CCu(0,foo(?b),0,sbar2(?c),?a);

id SSigma(0,sbar2?(?c),f?,0,?a)*foo?{thet}(0,f?udot,?b)=
  -CCu(0,sbar2(?c),0,foo(?b),?a);
id SSigma(0,sbar2?(?c),0,f?,?a)*foo?{thet}(f?udot,0,?b)=
  CCu(0,sbar2(?c),0,foo(?b),?a);

id SSigma(f?,0,0,sbar2?(?c),?a)*foo?spins(0,f?dot,?b)=
  CCd(0,foo(?b),0,sbar2(?c),?a);
id SSigma(0,f?,0,sbar2?(?c),?a)*foo?spins(f?dot,0,?b)=
  -CCd(0,foo(?b),0,sbar2(?c),?a);
id SSigma(0,sbar2?(?c),f?,0,?a)*foo?spins(0,f?dot,?b)=
  -CCd(0,sbar2(?c),0,foo(?b),?a);
id SSigma(0,sbar2?(?c),0,f?,?a)*foo?spins(f?dot,0,?b)=
  CCd(0,sbar2(?c),0,foo(?b),?a);

id SSigma(f?,0,0,sbar2?(?c),?a)*foo?{thet}(0,f?dot,?b)=
  CCd(0,foo(?b),0,sbar2(?c),?a);
id SSigma(0,f?,0,sbar2?(?c),?a)*foo?{thet}(f?dot,0,?b)=
  -CCd(0,foo(?b),0,sbar2(?c),?a);

id SSigma(0,sbar2?(?c),f?,0,?a)*foo?{thet}(0,f?dot,?b)=
  -CCd(0,sbar2(?c),0,foo(?b),?a);
id SSigma(0,sbar2?(?c),0,f?,?a)*foo?{thet}(f?dot,0,?b)=
  CCd(0,sbar2(?c),0,foo(?b),?a);

#endprocedure

```



```

#procedure dummysator
repeat ;
id foo?spins (k1?dot ,0 ,?c)* thet (0 ,k1?dot)=-[DP]( foo (?c) , thet );
id thet (k1?dot ,0)* foo?spins (0 ,k1?dot ,?c)=-[DP]( foo (?c) , thet );

id foo?spins (0 ,k1?dot ,?c)* thet (k1? ,0)=[DP]( foo (?c) , thet );
id thet (0 ,k1?dot)* foo?spins (k1?dot ,0 ,?c)=[DP]( foo (?c) , thet );
endrepeat ;

repeat ;
id foo?spins (i1?udot ,0 ,?c)* thet (0 ,i1?udot)=[UP]( foo (?c) , thet );
id thet (i1?udot ,0)* foo?spins (0 ,i1?udot ,?c)=[UP]( foo (?c) , thet );

id foo?spins (0 ,i1?udot ,?c)* thet (i1?udot ,0)=-[UP]( foo (?c) , thet );
id thet (0 ,i1?udot)* foo?spins (i1?udot ,0 ,?c)=-[UP]( foo (?c) , thet );
endrepeat ;

id sigma (a? ,b? ,c? ,d? ,n?)* thet (d? ,0)=Sigma (a ,b ,0 , thet , n);
id sigma (a? ,b? ,c? ,d? ,n?)* thet (0 ,c?)=-Sigma (a ,b ,0 , thet , n);

id sigma (a? ,b? ,c? ,d? ,n?)* thet (b? ,0)=Sigma (0 , thet , c ,d ,n);
id sigma (a? ,b? ,c? ,d? ,n?)* thet (0 ,a?)=-Sigma (0 , thet , c ,d ,n);

id sigma (a? ,b? ,c? ,d? ,n?)* foo?spins (d? ,0 ,?f)=Sigma (a ,b ,0 , foo (?f) , n);
id sigma (a? ,b? ,c? ,d? ,n?)* foo?spins (0 ,c? ,?f)=-Sigma (a ,b ,0 , foo (?f) , n);

id sigma (a? ,b? ,c? ,d? ,n?)* foo?spins (b? ,0 ,?f)=Sigma (0 , foo (?f) , c ,d ,n);
id sigma (a? ,b? ,c? ,d? ,n?)* foo?spins (0 ,a? ,?f)=-Sigma (0 , foo (?f) , c ,d ,n);

id ssigma (a? ,b? ,c? ,d? ,n1? ,n2?)* thet (d? ,0)=SSigma (a ,b ,0 , thet , n1 ,n2);
id ssigma (a? ,b? ,c? ,d? ,n1? ,n2?)* thet (0 ,c?)=-SSigma (a ,b ,0 , thet , n1 ,n2);
id ssigma (a? ,b? ,c? ,d? ,n1? ,n2?)* thet (b? ,0)=SSigma (0 , thet , c ,d ,n1 ,n2);
id ssigma (a? ,b? ,c? ,d? ,n1? ,n2?)* thet (0 ,a?)=-SSigma (0 , thet , c ,d ,n1 ,n2);
id ssigma (a? ,b? ,c? ,d? ,n1? ,n2?)* foo?spins (d? ,0 ,?f)=
SSigma (a ,b ,0 , foo (?f) , n1 ,n2);
id ssigma (a? ,b? ,c? ,d? ,n1? ,n2?)* foo?spins (0 ,c? ,?f)=
-SSigma (a ,b ,0 , foo (?f) , n1 ,n2);
id ssigma (a? ,b? ,c? ,d? ,n1? ,n2?)* foo?spins (b? ,0 ,?f)=
SSigma (0 , foo (?f) , c ,d ,n1 ,n2);
id ssigma (a? ,b? ,c? ,d? ,n1? ,n2?)* foo?spins (0 ,a? ,?f)=
-SSigma (0 , foo (?f) , c ,d ,n1 ,n2);

repeat ;
id Sigma (?a)* foo?spins (?b)=-foo (?b)* Sigma (?a);
id Sigma (?a)* foo?scals (?b)=foo (?b)* Sigma (?a);
id Sigma (?a)* foo?vects (?b)=foo (?b)* Sigma (?a);
id Sigma (?a)* foo?{[TT] , [tt] , [ttTT]} (?b)=foo (?b)* Sigma (?a);
id Sigma (?a)* foo?{ thet } (?b)=-foo (?b)* Sigma (?a);
endrepeat ;

repeat ;
id foo?spins (?b)* Sigma (?a)=-Sigma (?a)* foo (?b);

#call contractSigma

id foo?{ thet } (?b)* Sigma (?a)=-Sigma (?a)* foo (?b);

#call contractSigma

id foo?scals (?b)* Sigma (?a)=Sigma (?a)* foo (?b);
id foo?vects (?b)* Sigma (?a)=Sigma (?a)* foo (?b);
id foo?{[TT] , [tt] , [ttTT]} (?b)* Sigma (?a)=Sigma (?a)* foo (?b);
endrepeat ;

```

```

repeat ;
id SSigma(?a)*foo?spins(?b)=-foo(?b)*SSigma(?a);
id SSigma(?a)*foo?scals(?b)=foo(?b)*SSigma(?a);
id SSigma(?a)*foo?vects(?b)=foo(?b)*SSigma(?a);
id SSigma(?a)*foo?{[TT],[tt],[ttTT]}(?b)=foo(?b)*SSigma(?a);
id SSigma(?a)*foo?{thet}(?b)=-foo(?b)*SSigma(?a);
endrepeat ;

repeat ;
id foo?spins(?b)*SSigma(?a)=-SSigma(?a)*foo(?b);

#call contractSSigma

id foo?{thet}(?b)*SSigma(?a)=-SSigma(?a)*foo(?b);

#call contractSSigma

id foo?scals(?b)*SSigma(?a)=SSigma(?a)*foo(?b);
id foo?vects(?b)*SSigma(?a)=SSigma(?a)*foo(?b);
id foo?{[TT],[tt],[ttTT]}(?b)*SSigma(?a)=SSigma(?a)*foo(?b);
endrepeat ;
#endprocedure

```

Main Program

Those were the procedures that make up the bulk of the program. Now it remains to define the superfields and to call the procedures that do the simplification. The example given here evaluates $\bar{\chi}e^{-V}\chi e^V$

```

#procedure part1
  #call derivatives
  #call ridtheeps
#endprocedure

#procedure part2
  #call thetas
  repeat ;
  #call ridtheeta
  #call ridtheeps
  #call sigmas
  endrepeat ;
  #call sqrts
  #call dummynator
#endprocedure

#define chi(c,a) "(
  oA1('gaug')
  +i_*thet('udot1',0)*sigma(0,'udot1',0,'dot1','lor1')*
  oA1('lor1','gaug')*thet('dot1',0)+1/4*thet('udot1',0)*
  thet(0,'udot1')*thet(0,'dot1')*thet('dot1',0)*
  oA1('lor1','lor1','gaug')+sqrt(2,1)*thet('udot1',0)*
  sPsi1(0,'udot1','gaug')-i_*sqrt(2,-1)*thet('udot1',0)*
  thet(0,'udot1')*sPsi1('udot2',0,'lor1','gaug')*
  sigma(0,'udot2',0,'dot2','lor1')*thet('dot2',0)
  +thet('udot1',0)*thet(0,'udot1')*oF1('gaug')
)"

#define chibar(c,a) "(
  oA2('gaug')
  -i_*thet('udot1',0)*sigma(0,'udot1',0,'dot1','lor1')*
  oA2('lor1','gaug')*thet('dot1',0)+1/4*thet('udot1',0)*

```

```

    thet(0,'udot1')*thet(0,'dot1')*thet('dot1',0)*
    oA2('lor1','lor1','gaug')+sqrt(2,1)*thet(0,'dot1')*
    sPsi2('dot1',0,'gaug')+i_*sqrt(2,-1)*thet(0,'dot1')*
    thet('dot1',0)*thet('udot1',0)*sigma(0,'udot1',0,'dot2','lor1')*
    sPsi2('dot2',0,'lor1','gaug')
    +thet(0,'dot1')*thet('dot1',0)*oF2(,'gaug')
    )"

#define eV(c,a,b) "(
1
- thet('udot1',0)*sigma(0,'udot1',0,'dot1','lor1')*
thet('dot1',0)*vA('lor1','gaug')-i_*thet('udot1',0)*
thet(0,'udot1')*thet(0,'dot1')*(sLamb2('dot1',0,'gaug'))
+i_*thet(0,'dot1')*thet('dot1',0)*thet('udot1',0)*
(sLamb1(0,'udot1','gaug'))+1/2*thet(0,'dot1')*
thet('dot1',0)*thet('udot1',0)*thet(0,'udot1')*(oD('gaug'))
-1/4*thet(0,'dot1')*thet('dot1',0)*thet('udot1',0)*
thet(0,'udot1')*vA('lor1','gaug')*vA('lor1','gaug2')
)"

#define emV(c,a,b) "(
1
+ thet('udot1',0)*sigma(0,'udot1',0,'dot1','lor1')*
thet('dot1',0)*vA('lor1','gaug')+i_*thet('udot1',0)*
thet(0,'udot1')*thet(0,'dot1')*(sLamb2('dot1',0,'gaug'))
-i_*thet(0,'dot1')*thet('dot1',0)*thet('udot1',0)*
(sLamb1(0,'udot1','gaug'))-1/2*thet(0,'dot1')*thet('dot1',0)*
thet('udot1',0)*thet(0,'udot1')*(oD('gaug'))
-1/4*thet(0,'dot1')*thet('dot1',0)*thet('udot1',0)*
thet(0,'udot1')*vA('lor1','gaug')*vA('lor1','gaug2')
)"

Local action1='chibar(10,a)*emV(20,b,c)*chi(30,d)*eV(40,e,f)';
* Local action2=sqrt(2,1)*emV(20,b,c)*chi(20,d)*d5*emV(10,a,b)';
* Local action3='chibar(10,a)*emV(20,b,c)*chi(30,d)*eV(40,e,f)';
* Local action4='chibar(10,a)*emV(20,b,c)*chi(30,d)*eV(40,e,f)';
* .sort

#call part1
#call part2

#call contains(action1,[ttTT_],output1);

Print +s;
.end

```

Bibliography

- [1] Theodor Kaluza. On the Problem of Unity in Physics. *Sitzungsber. Preuss. Akad. Wiss. Berlin (Math. Phys.)*, 1921:966–972, 1921.
- [2] O. Klein. Quantum theory and five-dimensional theory of relativity. *Z. Phys.*, 37:895–906, 1926.
- [3] Lisa Randall and Raman Sundrum. An alternative to compactification. *Phys. Rev. Lett.*, 83:4690–4693, 1999.
- [4] Nima Arkani-Hamed, Savas Dimopoulos, and G. R. Dvali. The hierarchy problem and new dimensions at a millimeter. *Phys. Lett.*, B429:263–272, 1998.
- [5] Ignatios Antoniadis, Nima Arkani-Hamed, Savas Dimopoulos, and G. R. Dvali. New dimensions at a millimeter to a Fermi and superstrings at a TeV. *Phys. Lett.*, B436:257–263, 1998.
- [6] Howard Georgi. Deconstruction and new approaches to electroweak symmetry breaking. Contributed to 30th SLAC Summer Institute on Particle Physics: Secrets of the B Meson (SSI 2002), SLAC, Menlo Park, California, 5-16 Aug 2002.
- [7] Lisa Randall and Raman Sundrum. A large mass hierarchy from a small extra dimension. *Phys. Rev. Lett.*, 83:3370–3373, 1999.
- [8] Joseph Polchinski. Renormalization and Effective Lagrangians. *Nucl. Phys.*, B231:269–295, 1984.
- [9] Juan Martin Maldacena. The large N limit of superconformal field theories and supergravity. *Adv. Theor. Math. Phys.*, 2:231–252, 1998.
- [10] Csaba Csaki, Christophe Grojean, Jay Hubisz, Yuri Shirman, and John Terning. Fermions on an interval: Quark and lepton masses without a Higgs. *Phys. Rev.*, D70:015012, 2004.
- [11] Tony Gherghetta. An introduction to warped dimensions and holography. *PoS*, STRINGSLHC:006, 2006.
- [12] Nima Arkani-Hamed, Massimo Porrati, and Lisa Randall. Holography and phenomenology. *JHEP*, 08:017, 2001.

-
- [13] Steven Weinberg. Implications of Dynamical Symmetry Breaking. *Phys. Rev.*, D13:974–996, 1976.
- [14] Csaba Csaki, Christophe Grojean, Hitoshi Murayama, Luigi Pilo, and John Terning. Gauge theories on an interval: Unitarity without a Higgs. *Phys. Rev.*, D69:055006, 2004.
- [15] Csaba Csaki, Christophe Grojean, Luigi Pilo, and John Terning. Towards a realistic model of Higgsless electroweak symmetry breaking. *Phys. Rev. Lett.*, 92:101802, 2004.
- [16] H. Davoudiasl, J. L. Hewett, B. Lillie, and T. G. Rizzo. Warped Higgsless models with IR-brane kinetic terms. *JHEP*, 05:015, 2004.
- [17] Giacomo Cacciapaglia, Csaba Csaki, Christophe Grojean, and John Terning. Curing the ills of Higgsless models: The S parameter and unitarity. *Phys. Rev.*, D71:035015, 2005.
- [18] Giacomo Cacciapaglia, Csaba Csaki, Guido Marandella, and John Terning. A new custodian for a realistic Higgsless model. *Phys. Rev.*, D75:015003, 2007.
- [19] E. C. G. Stueckelberg. Interaction energy in electrodynamics and in the field theory of nuclear forces. *Helv. Phys. Acta*, 11:225–244, 1938.
- [20] Robert Delbourgo, S. Twisk, and George Thompson. Massive Yang-Mills Theory: Renormalizability Versus Unitarity. *Int. J. Mod. Phys.*, A3:435, 1988.
- [21] Marcel Froissart. Asymptotic behavior and subtractions in the Mandelstam representation. *Phys. Rev.*, 123:1053–1057, 1961.
- [22] Benjamin W. Lee, C. Quigg, and H. B. Thacker. Weak Interactions at Very High-Energies: The Role of the Higgs Boson Mass. *Phys. Rev.*, D16:1519, 1977.
- [23] John M. Cornwall, David N. Levin, and George Tiktopoulos. Derivation of Gauge Invariance from High-Energy Unitarity Bounds on the s Matrix. *Phys. Rev.*, D10:1145, 1974.
- [24] Loyal Durand, James M. Johnson, and Jorge L. Lopez. Perturbative unitarity and high-energy $W(L)_{+-}$, $Z(L)$, H scattering. One loop corrections and the Higgs boson coupling. *Phys. Rev.*, D45:3112–3127, 1992.
- [25] Alexander Knochel. Electroweak symmetry breaking and perturbative unitarity in higher-dimensional field theories (masters thesis). 2005.
- [26] Thorsten Ohl and Christian Schwinn. Unitarity, BRST symmetry and Ward identities in orbifold gauge theories. *Phys. Rev.*, D70:045019, 2004.

-
- [27] R. Sekhar Chivukula et al. A three site higgsless model. *Phys. Rev.*, D74:075011, 2006.
- [28] Riccardo Barbieri, Alex Pomarol, and Riccardo Rattazzi. Weakly coupled Higgsless theories and precision electroweak tests. *Phys. Lett.*, B591:141–149, 2004.
- [29] H. Davoudiasl, J. L. Hewett, B. Lillie, and T. G. Rizzo. Higgsless electroweak symmetry breaking in warped backgrounds: Constraints and signatures. *Phys. Rev.*, D70:015006, 2004.
- [30] Gustavo Burdman and Yasunori Nomura. Holographic theories of electroweak symmetry breaking without a Higgs boson. *Phys. Rev.*, D69:115013, 2004.
- [31] Riccardo Barbieri, Alex Pomarol, Riccardo Rattazzi, and Alessandro Strumia. Electroweak symmetry breaking after LEP1 and LEP2. *Nucl. Phys.*, B703:127–146, 2004.
- [32] J. L. Hewett, B. Lillie, and T. G. Rizzo. Monte Carlo exploration of warped Higgsless models. *JHEP*, 10:014, 2004.
- [33] Giacomo Cacciapaglia, Csaba Csaki, Christophe Grojean, and John Terning. Oblique corrections from Higgsless models in warped space. *Phys. Rev.*, D70:075014, 2004.
- [34] Giacomo Cacciapaglia, Csaba Csaki, Christophe Grojean, Matthew Reece, and John Terning. Top and bottom: A brane of their own. *Phys. Rev.*, D72:095018, 2005.
- [35] Kaustubh Agashe, Roberto Contino, Leandro Da Rold, and Alex Pomarol. A custodial symmetry for Z b anti- b . *Phys. Lett.*, B641:62–66, 2006.
- [36] Kaustubh Agashe, Gilad Perez, and Amarjit Soni. Flavor structure of warped extra dimension models. *Phys. Rev.*, D71:016002, 2005.
- [37] Csaba Csaki, Adam Falkowski, and Andreas Weiler. A Simple Flavor Protection for RS. 2008.
- [38] Csaba Csaki, Cedric Delaunay, Christophe Grojean, and Yuval Grossman. A Model of Lepton Masses from a Warped Extra Dimension. *JHEP*, 10:055, 2008.
- [39] S. Casagrande, F. Goertz, U. Haisch, M. Neubert, and T. Pfoh. Flavor Physics in the Randall-Sundrum Model: I. Theoretical Setup and Electroweak Precision Tests. *JHEP*, 10:094, 2008.
- [40] Geraldine Servant and Timothy M. P. Tait. Is the lightest Kaluza-Klein particle a viable dark matter candidate? *Nucl. Phys.*, B650:391–419, 2003.

-
- [41] Alexander Knochel and Thorsten Ohl. Supersymmetric Extensions and Dark Matter in Models of Warped Higgsless EWSB. *Phys. Rev.*, D78:045016, 2008.
- [42] Giuliano Panico, Eduardo Ponton, Jose Santiago, and Marco Serone. Dark Matter and Electroweak Symmetry Breaking in Models with Warped Extra Dimensions. *Phys. Rev.*, D77:115012, 2008.
- [43] Kaustubh Agashe and Geraldine Servant. Baryon number in warped GUTs: Model building and (dark matter related) phenomenology. *JCAP*, 0502:002, 2005.
- [44] Kaustubh Agashe, Adam Falkowski, Ian Low, and Geraldine Servant. KK Parity in Warped Extra Dimension. *JHEP*, 04:027, 2008.
- [45] Alex Pomarol and Andrea Wulzer. Stable skyrmions from extra dimensions. *JHEP*, 03:051–051, 2008.
- [46] M. F. Sohnius. Introducing Supersymmetry. *Phys. Rept.*, 128:39–204, 1985.
- [47] Lawrence J. Hall, Yasunori Nomura, Takemichi Okui, and Steven J. Oliver. Explicit supersymmetry breaking on boundaries of warped extra dimensions. *Nucl. Phys.*, B677:87–114, 2004.
- [48] Neil Marcus, Augusto Sagnotti, and Warren Siegel. Ten-Dimensional Supersymmetric Yang-Mills Theory in Terms of Four-Dimensional Superfields. *Nucl. Phys.*, B224:159, 1983.
- [49] Nima Arkani-Hamed, Thomas Gregoire, and Jay G. Wacker. Higher dimensional supersymmetry in 4D superspace. *JHEP*, 03:055, 2002.
- [50] Daniel Marti and Alex Pomarol. Supersymmetric theories with compact extra dimensions in $N = 1$ superfields. *Phys. Rev.*, D64:105025, 2001.
- [51] Tony Gherghetta and Alex Pomarol. A Stueckelberg formalism for the gravitino from warped extra dimensions. *Phys. Lett.*, B536:277–282, 2002.
- [52] Tony Gherghetta and Alex Pomarol. The standard model partly supersymmetric. *Phys. Rev.*, D67:085018, 2003.
- [53] Tony Gherghetta and Alex Pomarol. A warped supersymmetric standard model. *Nucl. Phys.*, B602:3–22, 2001.
- [54] H. Davoudiasl, J. L. Hewett, and T. G. Rizzo. Experimental probes of localized gravity: On and off the wall. *Phys. Rev.*, D63:075004, 2001.
- [55] D. N. Spergel et al. Wilkinson Microwave Anisotropy Probe (WMAP) three year results: Implications for cosmology. *Astrophys. J. Suppl.*, 170:377, 2007.
- [56] M. S. Al-Sarhi, D. R. T. Jones, and I. Jack. Quadratic divergences and dimensional regularization in two-dimensions and four-dimensions. *Nucl. Phys.*, B345:431–444, 1990.

- [57] M. S. Al-sarhi, I. Jack, and D. R. T. Jones. Quadratic divergences in gauge theories. *Z. Phys.*, C55:283–288, 1992.
- [58] Tao Han, Rakhi Mahbubani, Devin G. E. Walker, and Lian-Tao Wang. Top Quark Pair plus Large Missing Energy at the LHC. 2008.
- [59] M. R. Whalley, D. Bourilkov, and R. C. Group. The Les Houches Accord PDFs (LHAPDF) and Lhaglu. 2005.
- [60] T. Hahn. Generating and calculating one-loop Feynman diagrams with FeynArts, FormCalc, and LoopTools. 1999.
- [61] J. Wess and J. Bagger. Supersymmetry and supergravity. Princeton, USA: Univ. Pr. (1992) 259 p.

Dank

An dieser Stelle möchte ich mich bei allen bedanken, die zum Gelingen dieser Arbeit beigetragen haben. Insbesondere gilt mein Dank:

- PD Dr. Thorsten Ohl, für die Betreuung, die Bereitschaft, jederzeit meine Fragen anzuhören und zu diskutieren, sowie unzählige Gespräche über Physik und darüber hinaus.
- Prof. Dr. R. Rückl für die Möglichkeit, dieses interessante Thema an seinem Lehrstuhl zu bearbeiten, und die Unterstützung und Beratung während meiner Zeit als Doktorand.
- Prof. Dr. K. Mannheim für das Mitwirken in meiner Betreuungskommission und hilfreiche Diskussionen zu meiner Arbeit.
- dem GK1147, das durch das Stipendium die Anfertigung dieser Arbeit und darüber hinaus durch finanzielle Unterstützung die Teilnahme an Schulen, Konferenzen und Workshops sowie einen Auslandsaufenthalt ermöglicht hat.
- Alex Pomarol und dem IFAE Barcelona für die Gastfreundschaft während meines Aufenthaltes.
- Brigitte Wehner, für ihre Hilfe in Verwaltungs- und Organisationsangelegenheiten und so manchen guten Ratschlag, der mich vor unnötigen Komplikationen bewahrt hat.
- Den lieben Kollegen im GK1147 und am Lehrstuhl TP2 für bereichernde Diskussionen und die gute Arbeitsatmosphäre, insbesondere:
- Christian Speckner für lange, aufschlussreiche Diskussionen, gelegentliche Linux-Notfallbetreuung und wertvolle Tips, ohne die der Einstieg in O'Mega und Whizard wesentlich steiniger gewesen wäre.
- Laslo Reichert und Karoline Köpp, die nützliche Hinweise zu meiner Arbeit gegeben und meine Sicht der Dinge durch viele schwierige Fragen bereichert haben.
- Dominik Elsässer für wertvolle Diskussionen zur Dunkelmaterie.
- meinen Eltern für die unermüdliche Unterstützung in allen Belangen.
- meinen Schwiegereltern für alle Hilfe und Versorgung, das rege Interesse am Fortschritt meiner Arbeit, und Robert dafür, dass er mein Interesse an der Astronomie geweckt hat.
- und natürlich Lisa, für Rückhalt und unablässige Ermunterung in allen Lebenslagen, die konstruktiven Vorschläge zur Arbeit, Diskussionen zu allen Zeiten und Unzeiten, und für Einblicke in physikalische Themen die mir sonst entgangen wären.

Lebenslauf

Persönliche Daten

Alexander Karl Knochel

* 03. Juni 1979 in Ludwigshafen am Rhein

Familienstand: Verheiratet (05.12.08), keine Kinder

Staatsangehörigkeit: Deutsch

Ausbildung

1986 - 1990 Grundschule Landau-Nussdorf

1990 - 1997 Otto-Hahn-Gymnasium Landau (Pfalz)

1997 - 1998 Greenwood High School, Greenwood TX (USA)

Mai 1998 High School Diploma

1998-2000 Otto-Hahn-Gymnasium Landau (Pfalz)

Juni 2000 Abitur (Allgemeine Hochschulreife)

August 2000 Zivildienst

WS 2001/02 Beginn des Studiums der Physik und Mathematik (Diplom)
an der Julius-Maximilians-Universität Würzburg

2003 Vordiplom Physik

Vordiplom Mathematik

August 2004 Beginn des Auslandsstudiums an der State University of
New York in Stony Brook, NY (USA)

August 2005 Abschluss "Master of Arts in Physics" mit Thesis

seit Oktober 2005 Doktorand, Aufnahme als Stipendiat des Graduiertenkollegs GK1147
"Theoretische Astrophysik und Teilchenphysik" in Würzburg.